The HPV E6 oncoprotein as tool to study the ubiquitin ligase UBE3A/E6AP

Doctoral thesis

for obtaining the academic degree

Doctor of Natural Sciences (Dr. rer. nat.)

submitted by

Daniela Eichbichler

at the

Faculty of Sciences

Department of Biology

Konstanz, 2023

Date of the oral examination: 20.10.2023

1st reviewer: Prof. Dr. Martin Scheffner

2nd reviewer: Prof. Dr. Florian Stengel

This work was prepared from 2019 to 2023 in the group of Prof. Dr. Martin Scheffner (Cellular Biochemistry) at the University of Konstanz. MS/MS data was obtained in collaboration with Jasmin Jansen from the group of Prof. Dr. Florian Stengel (Laboratory of Biochemistry and Mass Spectrometry) at the University of Konstanz. AlphaFold predictions were obtained in collaboration with Maite Mißun from the group of Prof. Dr. Andreas Marx (Organic and Cellular Chemistry). The work was supported by the Konstanz Research School Chemical Biology (KoRS-CB) and the SFB 969.

Parts of this work are published in:

Ebner F. A., Sailer C., Eichbichler D., Jansen J., Sladewska-Marquardt A., Stengel F., Scheffner M. A ubiquitin variant-based affinity approach selectively identifies substrates of the ubiquitin ligase E6AP in complex with HPV-11 E6 or HPV16-E6 (JBC, 2020)

Several students have contributed to this work:

‘Investigating the potential interaction of RhoA and UBE3A’ bachelor thesis of Nadja Eulich, University of Konstanz, 2021

‘Charakterisierung der RhoA Interaktion mit E6AP’ bachelor thesis of Julia Küpfer, University of Konstanz 2022

‘Analysis of the RhoA-E6AP complex’ master thesis of Sarah Lott, University of Konstanz 2023

‘Investigation of E6AP allosteric activators’ bachelor thesis of Daniel Lingott, University of Konstanz 2023

Table of contents

Zusammenfassung

Die E3-Ubiquitin-Ligase E6AP spielt eine entscheidende Rolle für die menschliche Gesundheit, da ihre Deregulierung an mehreren Krankheiten beteiligt ist. Die Auswirkungen von E6AP reichen von den frühen Stadien der neuronalen Entwicklung bis hin zum möglichen Fortschreiten von Gebärmutterhalskrebs nach einer Infektion mit humanen Papillomviren (HPV). Ein gründliches Verständnis der E6AP-Interaktoren, -Regulatoren und -Substrate in Abwesenheit und Anwesenheit des HPV-E6-Onkoproteins ist daher von großer Bedeutung. Es ist bekannt, dass high-risk E6-Proteine E6AP allosterisch aktivieren und gleichzeitig sein Substratspektrum erweitern. Im Rahmen biochemischer Experimente kann das E6-Protein auch genutzt werden, um die Effekte von E6AP zu verstärken und damit deren Nachweis und Visualisierung zu vereinfachen.

Im Rahmen dieser Studie konnten mehrere potenzielle Zielproteine von high-risk E6 sowie von low-risk E6-Proteinen im Komplex mit E6AP nachgewiesen werden. Die vielversprechendsten Ergebnisse wurden für Mitglieder der RhoA-Unterfamilie der kleinen GTPasen erzielt: RhoA, RhoB und RhoC. Rho-GTPasen wechseln zwischen einem inaktiven, GDP-gebundenen und einem aktiven, GTP-gebundenen Zustand. Aktives RhoA ist in der Lage, mit verschiedenen nachgeschalteten Effektoren zu interagieren und diese zu stimulieren. Wir zeigen, dass bevorzugt GTP-gebundenes RhoA an seinem C Terminus durch E6AP im Komplex mit high-risk HPV 16 E6 effizient ubiquitiniert wird. In Zellen führt dies zum proteasomalen Abbau von RhoA. In Abwesenheit des E6-Proteins stimuliert E6AP hauptsächlich die Monoubiquitinierung von RhoA. Der ternäre RhoA-16 E6-E6AP-Komplex wird ebenfalls bevorzugt mit aktivem RhoA gebildet. Außerdem ist RhoA in der Lage, die stimulierende Wirkung von 16 E6 auf E6AP zu blockieren. Diese hemmende Wirkung ist ein allgemeines Phänomen, das nicht von der Identität des Substratproteins abhängt und auch für die Autobiquitierung von E6AP gilt. Das prominenteste Substrat des durch high-risk E6-E6AP vermittelten Abbaus ist der Tumorsuppressor p53. RhoA konkurriert nicht mit p53 um die Bindung von E6-E6AP, da alle vier Proteine in einem quaternären Komplex vorhanden sind. Diese Ergebnisse deuten auf ein komplexes Netzwerk zwischen Rho-GTPase-Signalwegen und der E3-Ligase E6AP sowohl in einem HPV-abhängigen als auch in einem HPV-unabhängigen Kontext hin.

Abstract

The E3 ubiquitin ligase E6AP plays a crucial role in human health, as its deregulation is involved in several diseases. The impact of E6AP reaches from the early stages of neuronal development to the potential progression of cervical cancer following an infection with human papillomaviruses (HPV). A thorough understanding of E6AP interactors, regulators, and substrate proteins, in absence and presence of the HPV E6 oncoprotein, is therefore of great importance. High-risk E6 proteins are known to allosterically activate E6AP, while at the same time broadening its substrate spectrum. In the context of biochemical experiments, the E6 protein can also be exploited to enhance E6AP effects, thereby simplifying their detection and visualisation.

Within this study, we were able to verify multiple potential target proteins of high-risk E6, as well as low-risk E6 proteins in complex with E6AP. The most promising results were obtained for members of the RhoA subfamily of small GTPases: RhoA, RhoB, and RhoC. Rho GTPases cycle between an inactive GDP-bound and an active GTP-bound state. Active RhoA is able to interact with and stimulate distinct downstream effectors. We show that preferentially GTP-bound RhoA is efficiently ubiquitinated at its C terminus by E6AP in complex with the high-risk HPV 16 E6 protein. In cells, this leads to the proteasomal degradation of RhoA. In the absence of the E6 protein, E6AP catalyses mostly RhoA monoubiquitination. The ternary RhoA-16 E6-E6AP complex is also preferentially formed with active RhoA. Additionally, RhoA is able to block the stimulatory effect of 16 E6 on E6AP. This inhibitory effect is a general phenomenon, does not depend on the identity of the substrate protein and also applies to E6AP autoubiquitination. The most prominent target of high-risk E6-E6AP-mediated degradation is the tumour suppressor p53. RhoA does not compete with p53 for 16 E6-E6AP binding, as all four proteins are present in one quaternary complex. These results imply an intricate network between Rho GTPase signalling and the E3 ligase E6AP in both an HPV-dependent and HPV-independent context.

Abbreviations

Å	Ångström
16 E6	HPV type 16 early protein 6
AA	Amino acid
A/L	Aprotinin/Leupeptin
AMP	Adenosine monophosphate
AS	Angelman syndrome
ASD	Autism spectrum disorder
ATP	Adenosine triphosphate
AZUL	Amino-terminal Zinc-finger of UBE3A
BCA	Bicinchoninic acid
BRET	Bioluminescence resonance energy transfer
CFTR	Cystic fibrosis transmembrane conductance regulator
CUL	Cullin E3 ligase
DDR	DNA damage response
DDX3X	DEAD box protein 3 X-chromosomal
DOCK	Dedicator of cytokinesis
DSS	Disuccinimidyl suberate
DTT	Dithiothreitol
E1	Ubiquitin-activating enzyme (in this study: UBA1)
E2	Ubiquitin-conjugating enzyme (in this study: UbcH5b/ UbcH7)
E3	Ubiquitin ligase
E6AP	E6-associated protein/ UBE3A E3 ligase
EDTA	Ethylenediaminetetraacetic acid
ERM	ezrin, radixin, and moesin
GAP	GTPase activating protein
GDI	Guanine nucleotide dissociation inhibitor
GDP	Guanosine diphosphate
GEF	Guanine nucleotide exchange factor
GSH	Glutathione
GST	Glutathione S-Transferase
GTP	Guanosine triphosphate
HECT	Homologous to E6AP C terminus
HERC	HECT and Rcc1-like domain containing protein

HPV	Human papillomavirus
I/Ile	Isoleucine
K/Lys	Lysine
kDa	Kilo Dalton
L/Leu	Leucine
ld-score	Linear discriminator score
MBP	Maltose-binding protein
miRNA	Micro RNA
NEB	New England Biolabs
NHS	N-hydroxysuccinimidyl
OTUD5	OTU domain-containing protein 5
POI	Protein of interest
PTM	Post-translational modification
qXL-MS	quantitative cross-linking mass-spectrometry
R/Arg	Arginine
RBR	Ring between Ring E3 ligase
RCC1	Regulator of chromosome condensation 1
RING	Really interesting new gene E3 ligase
RL	Reticulocyte lysate
RLD	RCC1-like domain
SDS-PAGE	Sodium dodecyl sulphate-polyacrylamide gel electrophoresis
SEC	Size-exclusion chromatography
S/Ser	Serine
T/Thr	Threonine
TKT	Transketolase
Y/Tyr	Tyrosine
Ub	Ubiquitin
Ub LIA	Ubiquitin with the L8A and I44A hydrophobic patch mutations
V/Val	Valine
WG	Wheat germ extract
WT	Wildtype

1. Introduction

1.1 The ubiquitin-proteasome system

At any given moment, under stress as well as during steady-state conditions, cells are required to remove damaged, misfolded, or excessive proteins rapidly and in a specific manner. To this end, proteins are labelled with a certain type of ubiquitin chains and targeted for proteasomal degradation (reviewed in Hershko and Ciechanover (1998)). The oligopeptides generated and the resulting free ubiquitin moieties can be further processed to free amino acids and recycled, respectively, and can eventually be reused for protein synthesis (Ciechanover and Schwartz 1998).

1.1.1 Ubiquitin and ubiquitin modifications

Ubiquitin comprises 76 amino acids (aa), resulting in an 8.5 kDa globular protein. As the name suggests, it is highly conserved in eukaryotes and present in most, if not all tissues (Goldstein et al. 1975; Vijay-Kumar, Bugg, and Cook 1987; Ciehanover, Hod, and Hershko 1978). It can be covalently attached to target proteins in a reversible process by the formation of an isopeptide bond between the C-terminal carboxyl group of ubiquitin and the ε-amino group of a lysine (Lys, K) residue of the target protein (Hershko and Ciechanover 1992) (reviewed in Hershko and Ciechanover (1998)). Ubiquitin can also serve as its own substrate, resulting in ubiquitin chain formation. Its seven lysine residues (K6, K11, K27, K29, K33, K48, K63) (Peng et al. 2003; Mattiroli and Sixma 2014) and the α-amino group of the N-terminal methionine (M) can serve as ubiquitin acceptors (Kirisako et al. 2006; Ciechanover and Ben-Saadon 2004). In contrast to the ubiquitination of the N-terminal methionine of a protein, chain formation via the ε-amino group of lysines is regarded as ‘canonical’. The attachment of single ubiquitin moieties (monoubiquitination, multi-mono-ubiquitination) and/or ubiquitin chains (polyubiquitination) of different topologies (e.g. differently linked chains, branched chains) results in a multitude of different signals, termed the ubiquitin code, that determine the actual fate of the protein modified (reviewed in Komander and Rape (2012)). In addition to proteasomal degradation, ubiquitin modifications can signal for e.g. cellular trafficking and endocytosis (Yuan et al. 2014), DNA-repair mechanisms (Gatti et al. 2015), NF-ʁB activation (M1) (Iwai, Fujita, and Sasaki 2014), and regulation of the cell cycle (Wickliffe et al. 2009).

Ubiquitin itself can be further post-translationally modified by phosphorylation (Wauer et al. 2015) and acetylation (Kienle et al. 2022), enabling even more complex signals. This affects the structure of ubiquitin and therefore its interaction with ubiquitin-binding domain (UBD)-containing proteins, ubiquitin ligases, and deubiquitinating enzymes (Mendes, Fougeras, and Dittmar 2020; Swaney, Rodríguez-Mias, and Villén 2015). All its serine (3) and threonine residues (7) as well as one tyrosine residue can be phosphorylated (Swatek and Komander 2016). The phosphorylation of serine 65 was shown to play a crucial role in the removal of damaged mitochondria by mitophagy (Fiesel and Springer 2015; Ordureau et al. 2015). Acetylation, on the other hand, can

presumably occur on any lysine residue and the acetylation at K6 and K48 was shown to inhibit chain formation via K11, K48, and K63 (Ohtake et al. 2015).

Four different genes encode for ubiquitin in mammals. The product of the stress-regulated genes *UBB* and *UBC* is a 'polyubiquitin' protein, which is further processed to single ubiquitin moieties resulting in increased ubiquitin concentrations to allow the efficient degradation of damaged or misfolded proteins (Wiborg et al. 1985). *UBA52* and *RPS27A* produce ubiquitin fused to ribosomal proteins under steady-state conditions (Redman and Rechsteiner 1989; Webb et al. 1994). With the help of deubiquitinating enzymes (DUBs), the ubiquitin precursors are cleaved into separate ubiquitin moieties (Grou et al. 2015).

1.1.2 The ubiquitin transfer cascade and ubiquitin recognition

The attachment of ubiquitin to target proteins is facilitated by the concerted actions of three to four different enzyme classes (reviewed in Hershko and Ciechanover (1998)). In a first ATP-dependent step, a ubiquitin adenylate between the C-terminal carboxyl group of ubiquitin and AMP is formed by the ubiquitin-activating enzyme (E1) (Haas, Warms, and Rose 1983). This activated intermediate is transferred to the active site cysteine of the E1 enzyme, forming a thioester bond and releasing AMP. Then, a ternary complex is formed with an additional ubiquitin adenylate on the E1 enzyme (Haas, Warms, and Rose 1983). Next, via transthiolation, the ubiquitin is transferred to a ubiquitin-conjugating enzyme (E2) (Stewart et al. 2016). Finally, a ubiquitin-protein ligase (E3) mediates substrate recognition and the transfer of ubiquitin to the substrate protein under the formation of an isopeptide linkage between the carboxyl group of the C-terminal glycine of ubiquitin and the ε-amino group of a lysine on the target protein (Hershko and Ciechanover 1998; Komander and Rape 2012). E3 ligases can operate as scaffolding proteins, in which case the E2 enzyme and the substrate are brought into close proximity by the E3 ligase, with the E2 enzyme catalysing the actual transfer of the ubiquitin to the substrate protein (Really interesting new gene (RING) E3 ligases (Deshaies and Joazeiro 2009)). Alternatively, the E3 ligase undergoes an additional transthiolation reaction, resulting in the attachment of ubiquitin to its own active site cysteine (Homologous to E6AP C terminus (HECT) E3 ligases (Scheffner and Kumar 2014) and Ring Between Ring (RBR) E3 ligases (Dove and Klevit 2012)) and transfers the ubiquitin to the target protein, again under the formation of an isopeptide bond (reviewed in Hershko and Ciechanover (1998)) (**Figure 1**).

An extensive number of enzymes is involved the ubiquitination process. In humans, two genes encode for E1 enzymes (*UBA1*, UBA6), and roughly 40 genes encode for E2 enzymes (in this study, UbcH5B (*UBE2D2*) and UbcH7 (*UBE2L3*) were used) (Ye and Rape 2009; Husnjak and Dikic 2012). Specificity is achieved by the large number of genes encoding E3 ligases (more than 600) and the possibility of different E2 enzymes interacting with multiple E3 ligases (Pickart and Eddins 2004). For some substrates, an additional class of enzymes is required for the formation of polyubiquitin chains. These so-called E4 enzymes collaborate with the E1/E2/E3 machinery to facilitate chain elongation (Koegl et al. 1999). A prominent example is the histone acetyltransferase p300, which was shown to function together with Mdm2, a RING

ligase known to ubiquitinate the tumour suppressor p53. p300 recognises monoubiquitinated p53 and catalyses the ubiquitin chain elongation thereof (Grossman et al. 2003). Analogous to the process of ubiquitination, ubiquitin-like proteins (e.g. SUMO, Nedd8) can be post-translationally and reversibly attached to target proteins (reviewed in Taherbhoy, Schulman, and Kaiser (2012)). Their removal is mediated by ubiquitin-like proteases (ULPs) (Ha and Kim 2008; Mukhopadhyay and Dasso 2007).

The process of ubiquitination can be reversed by DUBs, which recognize either the length of a ubiquitin chain, the linkage type, post-translational modifications (PTMs) of the chain, or the substrate-ubiquitin linkage (Reyes-Turcu and Wilkinson 2009; Komander, Clague, and Urbé 2009). DUBs can be divided into four classes of cysteine-proteases, comprising ubiquitin specific proteases (USPs), ovarian tumour proteases (OTUs), ubiquitin C-terminal hydrolases (UCHs), and Josephins. The zinc-dependent metalloproteases of the JAB1/MPN/MOV34 (JAMM) family form a fifth class (reviewed in Amerik and Hochstrasser (2004); Komander, Clague, and Urbé (2009)).

The isoleucine 44 (I44) hydrophobic patch on the surface of ubiquitin is crucial for the recognition of ubiquitin by many UBD-containing proteins (Hicke, Schubert, and Hill 2005), the 26S proteasome (Beal et al. 1998), and ligases such as E6AP (Mortensen et al. 2015). This characteristic patch is comprised of I44, leucine 8 (L8), and valine 70 (V70). A second hydrophobic patch is located around I36 (I36, L71, L73) (Winget and Mayor 2010) and implicated in the recognition by certain DUBs (Komander and Rape 2012).

1.1.3 The 26S proteasome

The 26S proteasome is a multi-subunit protein complex responsible for the ATP-dependent degradation of target proteins, which are sequentially deubiquitinated, unfolded and proteolytically cleaved into oligopeptides (reviewed in Finley (2009); Rousseau and Bertolotti (2018)). Aminopeptidases further process the oligopeptides into single amino acids (Saric, Graef, and Goldberg 2004). The free amino acids, as well as the free ubiquitin moieties can be reused for protein synthesis and a new round of ubiquitination, respectively (Suraweera et al. 2012; Hershko and Rose 1987). The barrel-shaped 20S core particle (CP) of the proteasome represents the proteolytic chamber with the proteolytic activities inside of the cylinder and is capped on either side by a 19S regulatory particle (RP) (Coux, Tanaka, and Goldberg 1996). The RP is comprised of a lid and a base. The three lid subunit proteins Rpn1, Rpn10, and Rpn13 mediate the recognition of substrates targeted for degradation, mainly by K48-linked chains of at least four ubiquitin moieties (Deveraux et al. 1994; Husnjak et al. 2008; Schreiner et al. 2008). The proteins are subsequently deubiquitinated by Rpn11 in the lid subunit (Verma et al. 2002).

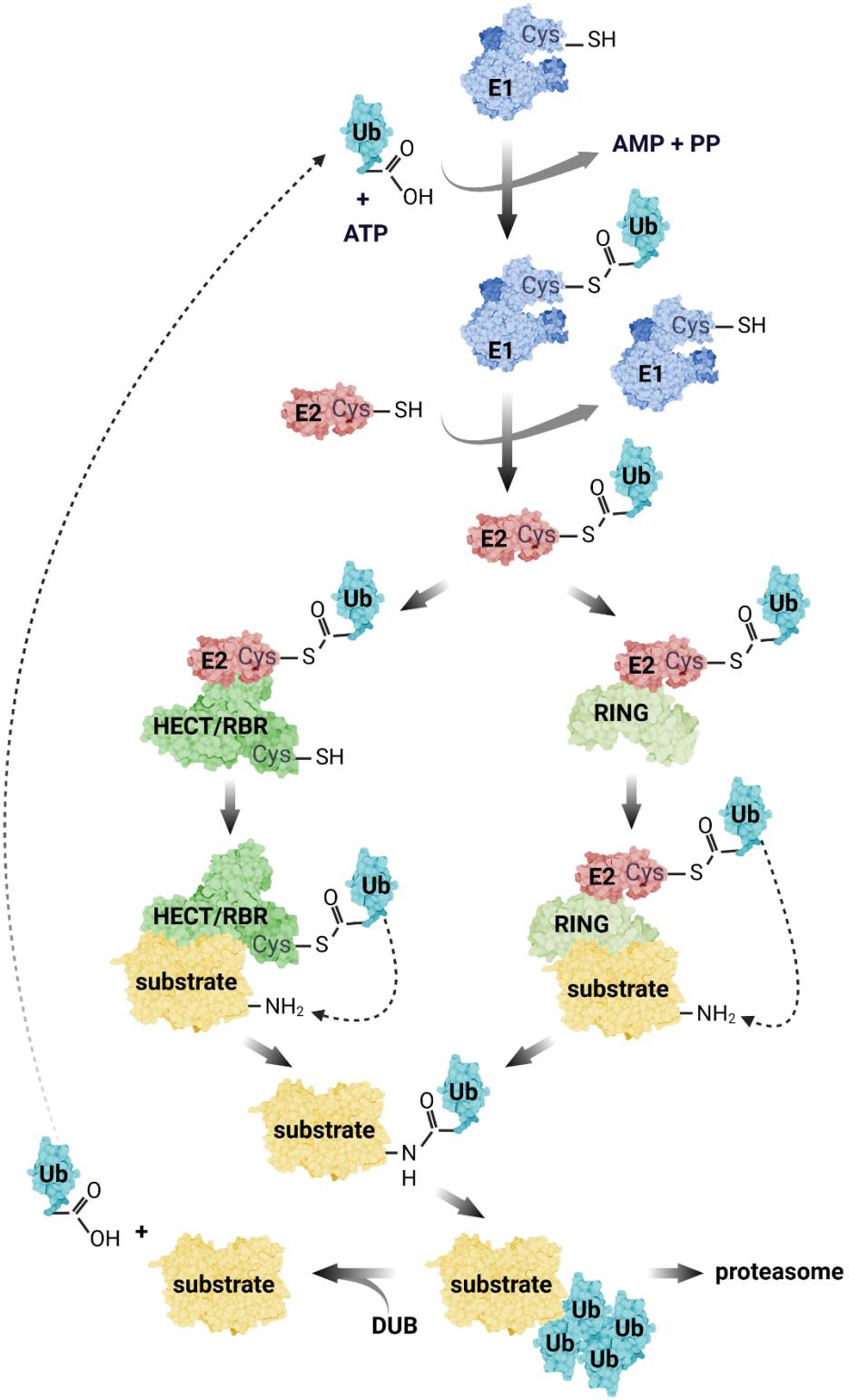

Figure 1: The ubiquitination cascade. In a first ATP-dependent step, ubiquitin is activated and bound by the E1 enzyme. This ubiquitin adenylate is transferred to the active site cysteine of an E2 enzyme under the formation of a thioester bond. Depending on the type of E3 ligase, ubiquitin is either directly transferred to the substrate protein (RING E3) or conferred to an active site cysteine of the E3 ligase (HECT and RBR E3s). In this case, the HECT and RBR E3 ligases catalyse the attachment of ubiquitin to the substrate via the formation of an isopeptide bond. Repeating ubiquitination cycles lead to ubiquitin chain formation. Chains of four or more K48-linked ubiquitin moieties signal for the proteasomal degradation of the targeted protein. The process of ubiquitination can be reversed by deubiquitinating enzymes (DUBs). For further details, see text. Created with BioRender.com

The base subunit contains a ring of six ATPases required for the unfolding of the protein and its subsequent translocation into the CP (Walz et al. 1998). The cylinder of the CP is composed of four stacked heptameric rings (Groll et al. 1997), of which some subunits function to prevent uncontrolled access of proteins to its interior (Groll et al. 2000), while others exhibit the proteolytic activity required to cleave the proteins (Arendt and Hochstrasser 1997).

The exchange of certain proteolytic subunits for immune-specific subunits give rise to the so-called immunoproteasome, which is particularly involved in the generation of peptides for antigen presentation (Heink et al. 2005; Griffin et al. 1998).

1.1.4 Ubiquitin ligases

As mentioned above, there are three classes of E3 ligases in humans, which deploy two different general ubiquitin-transfer mechanisms (reviewed in Yang et al. (2021)). The largest group, the RING ligases, comprises roughly 600 putative members. Their RING domain coordinates two zinc ions to form a binding platform for the E2 enzyme (Borden and Freemont 1996). Canonical RING ligases do not contain an active site cysteine of their own and therefore do not enzymatically participate in the transfer of ubiquitin. They act as allosteric activators for the E2 enzyme as well as scaffolding proteins to co-localise the ubiquitin-bound E2 enzyme with the substrate protein (reviewed in Deshaies and Joazeiro (2009); Metzger et al. (2014)). RBR ligases (14 members in humans) harbour two RING domains: one facilitates the binding of the E2 enzyme, the second harbours an active site cysteine which is used to form an E3-ubiquitin intermediate via a thioester bond (Marín and Ferrús 2002; Spratt, Walden, and Shaw 2014). RBR ligases are therefore considered as hybrids of RING and HECT ligases.

1.2 HECT ligases – E6AP

As indicated by the name, E6AP is the founding member of the HECT (Homologous to E6AP C Terminus) ligase family (Huibregtse et al. 1995), which in humans comprises 27 members in addition to E6AP (Rotin and Kumar 2009). Their common denominator is the C-terminal HECT domain, but they vary greatly in their N-terminal extensions (Huibregtse et al. 1995). This variety presumably enables the specific interaction with a multitude of different target proteins (Scheffner and Staub 2007) as well as the localisation of the HECT E3 to different cellular compartments (reviewed in Lorenz (2018)). According to distinct domains in their N-termini, HECT ligases are further divided into the NEDD4/NEDD4-like family, the HERC family, and ‘other’ HECT E3 ligases (reviewed in Rotin and Kumar (2009)).

E6AP is known to mainly catalyse the formation of K48-linked ubiquitin chains, resulting in proteasomal degradation of the target protein (Wang and Pickart 2005; Kim and Huibregtse 2009). As a result of alternative splicing, the *UBE3A* gene encodes three isoforms. In comparison to E6AP isoform 1 with 852 amino acids (in this study, ‘E6AP’ stands for isoform 1 unless stated otherwise), isoforms 2 and 3 contain 20 and 23 amino acids long N-terminal extensions, respectively (Yamamoto, Huibregtse, and Howley 1997). The functional relevance of these extensions has yet to be uncovered.

E6AP is expressed in all tissues and cell types, with apparent differential isoform expression in subcellular compartments (Avagliano Trezza et al. 2019).

1.2.1 Structural characteristics of E6AP

At the very N terminus of E6AP, the AZUL domain (Amino-terminal Zn-finger of UBE3A Ligase), a C4 type zinc finger, coordinates a zinc and is required for the interaction of E6AP with the RAZUL domain of the proteasomal RP subunit Rpn10 (Lemak et al. 2011; Kühnle et al. 2018). The AZUL domain (residues 1-64) ensures the nuclear localisation of E6AP isoform 1, which is in contrast to isoform 2 and isoform 3 not re-exported into the cytoplasm (Avagliano Trezza et al. 2019). HERC2, a HECT ligase itself, is known to bind to E6AP between residues 150 and 200 and acts as an allosteric activator (Kühnle et al. 2011). In addition to HERC2, the E6 oncoprotein of the human papillomavirus (HPV) type 16 (16 E6) is another known allosteric activator of E6AP (Mortensen et al. 2015). The E6 binding site is located between residues 378 and 395 (Huibregtse, Scheffner, and Howley 1993b; Zanier et al. 2013). The C-terminal HECT domain (residues 495-852) is composed of a larger N-lobe connected to a smaller C-lobe via a flexible linker (Huang et al. 1999) (**Figure 2A**).

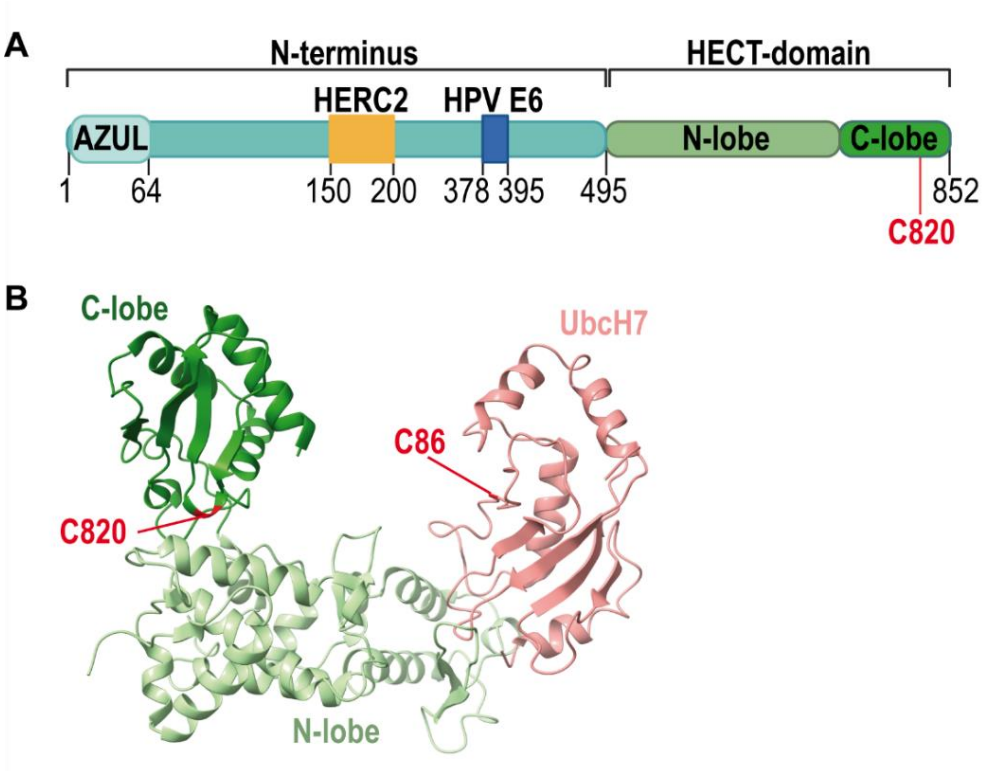

Figure 2: Schematic of E6AP. A| Schematic of E6AP domains and the binding sites for HERC2 (residues 150-200) and the HPV E6 oncoprotein (residues 378-395). The N-terminal AZUL domain comprises the residues 1-64 and the HECT domain ranges from residue 495 to 852. The numbering is according to E6AP isoform 1. Created with BioRender.com **B**| Crystal structure of the E6AP HECT domain in complex with UbcH7 (PDB 1C4Z). The catalytic cysteines of E6AP (C820) and UbcH7 (C86), as well as the E6AP N-lobe and C-lobe are indicated. The structure was modified with UCSF ChimeraX (Goddard et al. 2018).

Members of the UbcH5 and UbcH7 families are cognate E2 enzymes for E6AP that have been described (Eletr and Kuhlman 2007; Kamadurai et al. 2009). In this study, UbcH5b and UbcH7 were used. Thus far, crystallization attempts of full-length E6AP have failed, but the structure of the E6AP HECT domain in complex with the E2 enzyme UbcH7 has provided valuable insights (Huang et al. 1999) (**Figure 2B**).

1.2.2 E6AP regulation, interaction partners, and substrate proteins

Via a process called auto-ubiquitination, E6AP is able to target itself for proteasomal degradation and thereby regulate its own levels in a negative feedback loop (de Bie and Ciechanover 2011; Nuber, Schwarz, and Scheffner 1998). This is mainly achieved by one E6AP molecule targeting another E6AP (*trans* ubiquitination). It is also possible for E6AP to target itself by transferring ubiquitin from its active site cysteine to a lysine residue on the same E6AP molecule (*cis* ubiquitination) (Nuber, Schwarz, and Scheffner 1998). 16 E6 is known to impair *trans* and promote *cis* ubiquitination of E6AP (Kao et al. 2000). The presence of a substrate protein shifts the E6AP activity from auto-ubiquitination to substrate ubiquitination (Nuber, Schwarz, and Scheffner 1998). Auto-ubiquitination is a common regulatory feature of E3 ligases and not exclusively of proteolytic nature. For example, the auto-ubiquitination of the RING ligase TRAF6 leads to the recruitment of substrate proteins (Lamothe et al. 2007), while an increase in ligase activity is achieved upon auto-ubiquitination of the RING ligase Ring1b (Ben-Saadon et al. 2006).

Ring1b is also a known substrate protein of E6AP (Zaaroor-Regev et al. 2010) and, in our laboratory, a catalytically inactive mutant of Ring1b (Ring1b I53S) is commonly used in *in vitro* ubiquitination assays. Ring1b is part of the polycomb group repressive complex (PRC), which causes translation repression via the modification of histones in the nucleosome (Eskeland et al. 2010). The human homologs of yeast Rad23 (HHR23A and HHR23B) have been shown to interact with E6AP and act as substrates of E6AP (Kumar, Talis, and Howley 1999). Both proteins are involved in DNA repair processes and cell cycle regulation (Miller, Prakash, and Prakash 1982; Masutani et al. 1994). The RhoA guanine nucleotide exchange factor (GEF) Ephexin5 (Margolis et al. 2010) and the transketolase TKT (Pandya et al. 2022) are additional potential E6AP substrates, to name just a few. E6AP has also been reported to interact with and stimulate the transcriptional activity of nuclear hormone receptors like the glucocorticoid receptor, the estrogen receptor α and β, the androgen receptor, and the progesterone receptor (Nawaz et al. 1999). The E6-dependent degradation of the tumour suppressor p53 will be discussed in detail in 1.3.3 ‘The E6 oncoprotein’. Taken together, proteins that interact with E6AP can either be substrates of its ligase activity or function as potential regulators or adaptor proteins.

Previously, E6AP has been suggested to be active as a trimer (Ronchi et al. 2014); however, these findings have been contradicted by other groups (Lorenz 2018) and we ourselves have also not been able to experimentally verify that statement. Several mechanisms regulating E6AP activity have been reported. It may be a substrate for other E3s like the HECT ligase UBR5 (Tomaic et al. 2011). Its activity, as mentioned above, is stimulated by the interaction with the allosteric activators 16 E6 (Mortensen

et al. 2015) and HERC2 (Kühnle et al. 2011) which cause structural rearrangements within E6AP. Cross-linking coupled to mass spectrometry experiments indicated a closer proximity of the E6AP N- and C terminus upon binding to 16 E6 (Sailer et al. 2018). E6AP is phosphorylated at tyrosine 636 (Y636) and threonine 485 (T485) by c-Abl (Chan et al. 2013) and PKA (Yi et al. 2015), respectively. Both phosphorylations cause a reduced ligase activity of E6AP.

1.2.3 Involvement of E6AP in human diseases

E6AP has been linked to several human diseases including cancer and neurodevelopmental disorders. The role of E6AP in the development of cervical cancer is discussed together with the HPV E6 oncoprotein in 1.3.3 ‘The E6 oncoprotein’. Besides cervical cancer, E6AP has been reported to be involved in multiple other cancers, including breast cancer, non-small cell lung cancer (NSCLC), prostate cancer, and Burkitt’s lymphoma (reviewed in Owais, Mishra, and Kiyokawa (2020)). While the role of E6AP regarding cancer development is primarily based on deregulation of its E3 activity, the underlying cause in neurodevelopmental disorders are genetic aberrations. E6AP is encoded by the *UBE3A* gene on chromosome 15q11-q13 (Sutcliffe et al. 1997), and the presence of repetitive DNA fragments renders this region susceptible to rearrangements (Donlon et al. 1986; Buiting et al. 1992). While E6AP is expressed biallelic in non-neuronal tissues, expression of E6AP is regulated epigenetically by imprinting of the paternal allele in neuronal cells, i.e. E6AP is almost exclusively expressed from the maternal allele (Sahoo et al. 2007; Rougeulle, Glatt, and Lalande 1997). Therefore, genetic alterations of the maternal allele cannot be compensated by the paternal allele. The restriction to maternal expression occurs in certain brain tissues, namely the hippocampus, the olfactory bulb, the hypothalamus, the cerebral cortex, and the cerebellum (reviewed in Khatri and Man (2019)).

Deletion or duplication of the 15q11-q13 region on the maternal allele is causally associated with the rare neurodevelopmental disorders Angelman syndrome (AS) and the Dup15q syndrome, respectively (reviewed in Kalsner and Chamberlain (2015)). Besides deletion of the 15q11-q13 region and therefore loss of functional E6AP, which accounts for roughly two thirds of all AS cases, AS can also be caused by paternal uniparental disomy, imprinting defects, or point mutations within the maternal allele (reviewed in Margolis et al. (2015)). More than 100 different missense mutations have been found in AS patients, which are distributed in clusters over the entire E6AP coding region and result in loss of E6AP function (Buiting, Williams, and Horsthemke 2016; Sadikovic et al. 2014; Yi et al. 2015). While E6AP is known to play a crucial role in AS development, the exact mechanism and targets of E6AP remain elusive. AS is named after the pediatrician Harry Angelman, who first described children with the characteristic symptoms of developmental delay, mental retardation, absence of speech, ataxia, and an overall happy demeanour (Angelman 1965). Treatment options are so far limited to the alleviation of symptoms and AS patients have a slightly reduced life expectancy (Larson et al. 2015).

The genetic mechanism underlying the autism spectrum disorder (ASD) Dup15q is the duplication of the *UBE3A* containing 15q11-q13 region, which results in

overexpression of E6AP (reviewed in Lopez, Segal, and LaSalle (2018)). Other genes that are potentially involved are coding for HERC2 and multiple $GABA_A$ receptor subunits (Urraca et al. 2018; Lusk et al. 1993). So far, no gene of this region could be identified as solely causative. Patients show an overall ASD-like phenotype, including impaired social interest, decreased communication, as well as cognitive and intellectual disabilities, hyperactivity, and motor delays (LaSalle, Reiter, and Chamberlain 2015). The same region on chromosome 15 is affected in patients with the Prader-Willi syndrome (PWS) (reviewed in Driscoll et al. (1993)), but in this case the maternal allele is epigenetically silenced by imprinting (Knoll et al. 1989). PWS is caused by deletions within the 15q11-q13 region of the paternal allele and the resulting loss of the *SNRPN* (encoding for small nuclear ribonucleoprotein-associated protein N) and *NDN* (encoding for the protein necdin) genes and its development is independent of E6AP (Wevrick and Francke 1996; Runte et al. 2001; Zanella et al. 2008).

1.3 Human Papillomaviruses (HPVs)

HPVs comprise a group of small non-enveloped viruses with a double-stranded encapsulated circular genome (DNA), which infect the basal layer of stratified squamous epithelia. HPV infections can cause multiple diseases, ranging from benign lesions to malignant tumours (reviewed in zur Hausen (2002)). So far, more than 150 different types have been identified and they are subdivided according to their capability to infect cutaneous or mucosal epithelia (Bzhalava et al. 2013). While they are mainly associated with the formation of warts, some cutaneous HPV types (5 and 8) have been reported to be involved in the formation of nonmelanoma skin cancer (NMSC) (Hasche et al. 2017). The more prominent and more extensively discussed types regarding human disease belong to the alpha-papillomavirus genus, which preferentially infect the genital mucosa and are mainly sexually transmitted (Mistry, Wibom, and Evander 2008). They are further divided into low-risk and high-risk types, according to their propensity to progress lesions to malignancy. Low-risk HPVs (e.g. type 6 and 11) are associated with the formation of benign genital warts (Pfister and Ter Schegget 1997), while high-risk HPVs have been causally linked to cancer formation (Walboomers et al. 1999), most notably to cervical cancer. HPVs of the high-risk group are present in 99% of all cervical squamous cell cancers worldwide (Walboomers et al. 1999) and type 16 and 18 alone are responsible for roughly 70% of them (Braaten and Laufer 2008). Even though more than two-thirds of all women worldwide encounter HPVs in their life, only a small fraction of infections progresses to forms of low-grade (CIN1) or high-grade (CIN3) cervical intraepithelial neoplasia (CIN 1-3), due to clearance by the immune system (Chesson et al. 2014; Kim et al. 2012). In addition, high-risk types are also known to play a role in the development of some head and neck squamous cell carcinomas (HNSCC) (Gillison et al. 2000).

As preventive measurements, routine check-ups of the cervix by a Pap smear (Papanicolaou test) and vaccination against the most common HPV types are performed (Braaten and Laufer 2008). Currently, multiple vaccines are available and designed to prevent infections with either two (Cervarix: 16 and 18), four (Gardasil: 6,

11, 16, and 18), or nine (Gardasil: 6, 11, 16, 18, 31, 33, 45, 52, and 58) different HPV types. All of them include protection against the high-risk HPV types 16 and 18. By Pap smear, cells of the cervix are collected to check for pre-cancerous or cancerous abnormalities. Besides the standard treatment plans like surgery and chemotherapy, there are no other options for women already infected with HPV and suffering from cervical cancer. Ongoing research is working towards drug-based therapies, which either target the expression of the HPV oncogenes E6 and E7 or try to prevent the interaction between viral and host proteins that are required for cancer progression (NIH, HPV vaccines, 02/2023).

1.3.1 The viral genome and life cycle

The HPV genome can be divided into the non-coding upstream regulatory region (URR), which is also called the long control region (LCR), and genes of the early (E) and the late (L) region, which are named according to their time of expression during the viral life cycle (reviewed in Graham (2010)). The LCR harbours the origin of DNA replication, promoter regions, and binding sites for transcription factors and regulatory proteins. The replication of the HPV genome is dependent on the replication machinery of the host cell. The early proteins E1, E2, E4, E5, E6, and E7 are required for replication and transcription of the viral DNA and the viral life cycle, and contribute to the transformation of host cells (E5-E7). The two proteins encoded by the late region are the major capsid protein L1 and the minor capsid protein L2 (reviewed in Kajitani et al. (2012)) (**Figure 3A**).

In general, HPVs infect the basal primary keratinocytes of stratified squamous epithelia mainly through micro-lesions (Egawa 2003; Grayson et al. 2002). After the virus has gained access, it is uncoated in the cytoplasm and the DNA is imported into the nucleus. There, the viral DNA is kept in low copy numbers as episomes, extra-chromosomal plasmids which are not integrated into the host DNA but replicate as part of the human genome (reviewed in Doorbar (2006)). During this time, the early proteins E1 and E2 are expressed at low levels. The viral life cycle is closely linked to the differentiation state of the host cell. The productive phase of the viral life cycle is triggered by the entrance of an HPV-infected cell into the differentiating compartment to eventually become a fully differentiated keratinocyte (reviewed in Doorbar (2005)). The increasing expression of the viral E6 and E7 oncoproteins causes differentiated cells to re-enter S phase, which enables the replication of viral DNA. Finally, the structural proteins L1 and L2 are expressed in the top epithelial layers, where the virion is subsequently assembled and released (Bedell et al. 1991; Ozbun and Meyers 1998) (**Figure 3B**).

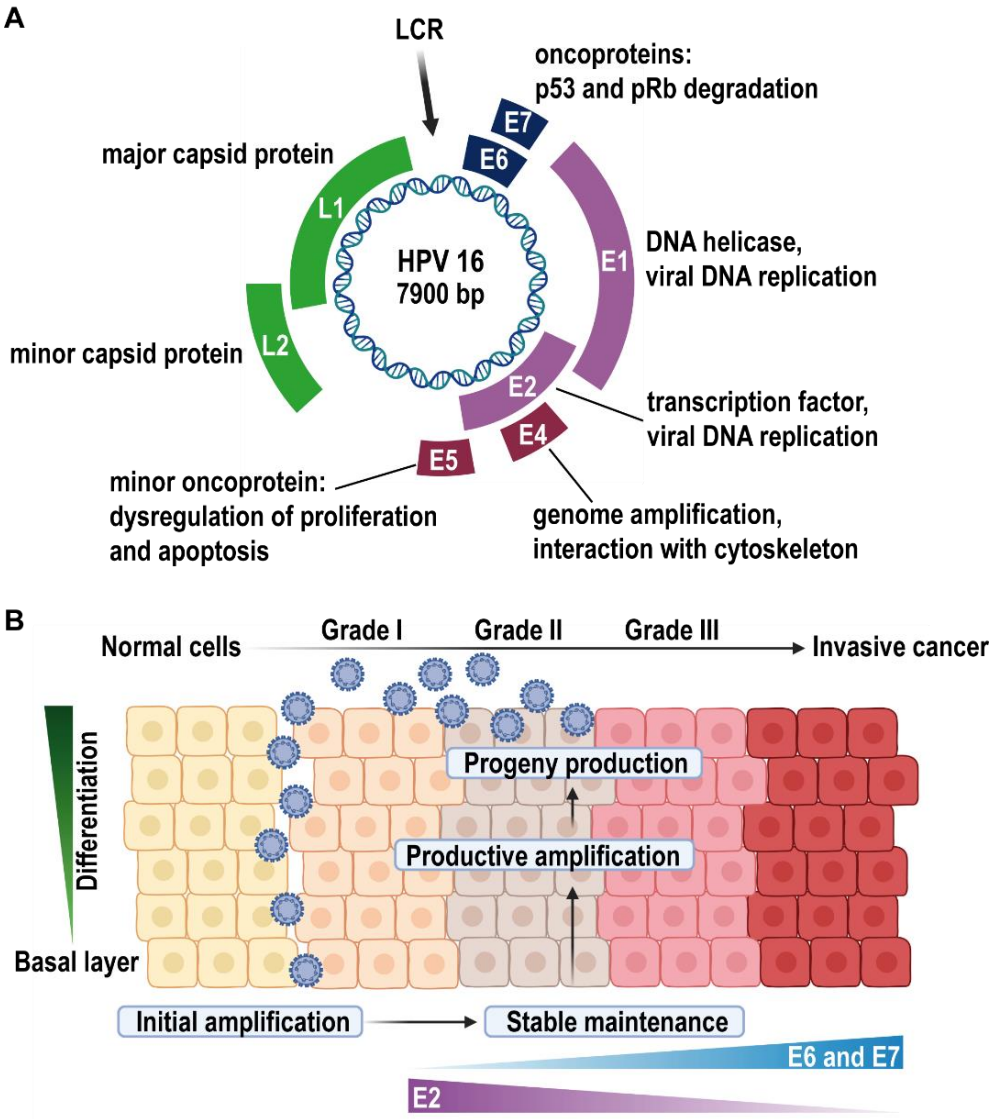

Figure 3: High-risk HPV genome and infection stages. A| Organisation of the alpha HPV type 16 genome. Indicated are the LCR, and the early and late genes with their respective usage during an HPV infection. **B**| Life cycle of high-risk HPV from productive infection to invasive cancer formation. Modified from (Nakahara and Kiyono 2016) and created with BioRender.com

The E1 and E2 proteins are required for viral transcription and DNA replication and have been suggested to be required for stable episome maintenance. First, the dimeric E2 interacts with the E2 binding site (E2BS), a palindromic motif in the LCR, which triggers the recruitment of E1 to the viral origin and the subsequent release of the E2 (Hines et al. 1998; Sanders and Stenlund 1998). The E1 multimerizes to a ring-like structure to exhibit its helicase activity and recruits the cellular replication machinery for viral DNA replication (Sedman and Stenlund 1998). E2 is further required for the correct segregation of viral genomes during host cell division of undifferentiated cells (Lehman and Botchan 1998). Additionally, E2 can act as a transcription factor (Cripe et al. 1987; Phelps and Howley 1987).

Early gene expression is stimulated upon binding of host cell transcription factors to the LCR and can be further regulated by the differential binding of E2 to different E2BS.

The regulation occurs in a concentration dependent manner, with high amounts of E2 causing transcriptional inhibition (Steger and Corbach 1997; Bouvard et al. 1994). Integration of viral episomes into the host genome often leads to the disruption of the E2 open reading frame (ORF), thereby abrogating the E2 mediated repression. This, in turn, results in an increase in E6 and E7 expression and therefore elevated proliferation (Bernard et al. 1989; Schwarz et al. 1985; Romanczuk and Howley 1992). The E4 and E5 early proteins are less well characterized and do not seem to play a direct role during the viral life cycle. The E5 ORF is characteristic for members of the alpha-HPV group and was shown to exhibit oncogenic properties, which were first described in bovine papillomaviruses (BPV) (reviewed in Venuti et al. (2011)). The E5 protein of HPV 16 is able to dysregulate proliferation and inhibit apoptosis by stimulating the epidermal growth factor receptor (EGFR) (Pedroza-Saavedra et al. 2010) and by triggering the degradation of Fas receptors (Kabsch and Alonso 2002). Expression of the main viral oncoproteins, E6 and E7, is required for the carcinogenic progression of HPV infected cells (Hawley-Nelson et al. 1989). They act together in order to immortalize keratinocytes by degrading the tumour suppressor proteins p53 and pRb (retinoblastoma protein), thus achieving continuous cell cycle progression (reviewed in Moody and Laimins (2010)).

1.3.2 The E7 oncoprotein

The E7 protein is comprised of roughly 100 amino acids and contains a C-terminal zinc finger domain (McIntyre et al. 1993). E7 is crucial in the deregulation of the host cell cycle, which results in the re-entry of differentiated keratinocytes into S phase that is required for the replication of viral DNA. The main targets of E7 are members of the so-called pocket protein family which regulate cell cycle phase transitions (G0-S and G1-S) by interacting with transcription factors of the E2F family (Banks, Barnett, and Crook 1990; Dyson 1998). The pocket protein family is comprised of pRb, p107 (retinoblastoma-like protein 1), and p130 (retinoblastoma-like protein 2) (Cobrinik 2005). pRb is phosphorylated by cyclin-dependent kinases (CDKs), which results in its dissociation from the transcription factor E2F and allows the cell to enter S phase (Mittnacht 1998). In HPV infected cells, E7 disrupts the E2F-pRB complex by competing with E2F for pRb binding, resulting in continuous S phase entry and uncontrolled proliferation (Stevaux and Dyson 2002). Additionally, E7 targets all members of the pocket protein family for proteasomal degradation (Zhang, Chen, and Roman 2006). High-risk HPV 16 E7 was shown to recruit an active cullin 2 ligase complex to ubiquitinate pRb which leads to its subsequent degradation (Huh et al. 2007). On the other hand, E7 proteins of low-risk HPVs were shown to interact with pRb with a lower affinity than high-risk E7 proteins (Münger et al. 1989) and are unable to promote pRb degradation.

1.3.3 The E6 oncoprotein

The 18 kDa HPV E6 protein consists of roughly 150 amino acids with two conserved zinc finger domains which are comprised of four C−X−X−C motifs and are connected via a helical linker (36 aa) (**Figure 4A**). This results in a binding pocket for proteins

with a characteristic acidic leucine-rich motif (L−X−X−L−L; L−Q−E−L−L for E6AP, **Figure 4B-D**) (Huibregtse, Scheffner, and Howley 1993b). The mutation of the leucine residue at position 50 of HPV 16 E6 to a glutamate (L50E) renders E6 unable to interact with E6AP (Zanier et al. 2013). At the very C terminus, a PDZ-binding motif (ETQL) mediates the interaction with PDZ domain-containing proteins. The PDZ domain is named according to the first three proteins discovered to contain it: Psd95, Dlg, ZO-I. Via this motif, high-risk E6 is known to interact with the human proteins disks large homolog 1 (hDlg1) (Kiyono et al. 1997; Gardiol et al. 1999), protein scribble homolog (hScrib) (Nakagawa and Huibregtse 2000), and membrane-associated guanylate kinase, WW and PDZ domain-containing protein 1 (MAGI1) (Glaunsinger et al. 2000), which are members of the MAGUK protein superfamily (membrane-associated guanylate kinase).

In addition to the E6AP-associated disorders introduced in 1.2.3 ‘Involvement of E6AP in human diseases’, E6AP plays a crucial role in the malignant progression of high-risk HPV-infected cells to cervical cancer, which is strongly dependent on the degradation of the tumour suppressor p53 (Talis, Huibregtse, and Howley 1998). The transcription factor p53 is known as the ‘guardian of the genome’ and is activated upon cellular stresses such as DNA damage or oxidative stress, resulting in cell cycle arrest and potentially subsequent apoptosis (reviewed in Vousden and Prives (2009)). The cellular ubiquitin ligase E6AP in complex with the high-risk E6 oncoprotein was shown to target p53 for ubiquitination (**Figure 4B**) and subsequent proteasomal degradation (Huibregtse, Scheffner, and Howley 1993a; Scheffner et al. 1993). Notably, in the absence of high-risk E6 or in complex with low-risk E6, E6AP is unable target p53 (Scheffner et al. 1990; Scheffner et al. 1993). Also, low-risk E6 only weakly binds to E6AP (Brimer, Lyons, and Vande Pol 2007). The interaction between E6 and p53 is independent of the PDZ-binding motif but has been shown to involve residues at the very N terminus of high-risk E6. A mutant 16 E6 protein with the point mutations F2E, R8S, P9A, and R10T (ESAT) is unable to interact with p53 (Foster et al. 1994) (**Figure 4A and D**). Recently, a structural model as to how E6 targets p53 for E6AP-mediated ubiquitination has been proposed. In this model E6 localizes adjacent to the HECT domain, thereby bringing the catalytic cysteine of E6AP and p53 into close proximity for the transfer of ubiquitin to p53 (Sailer et al. 2018). While it is commonly accepted that E6-mediated degradation plays a prominent role in HPV-induced carcinogenesis, it is presumably also important for the viral life cycle, insofar as p53 degradation is required to counteract the p53 activation resulting from E7-mediated pRb degradation (Moody and Laimins 2010).

Contributing to its oncogenic potential, in addition to targeting p53, E6 also mediates the degradation of members of the aforementioned MAGUK protein superfamily (Kuballa, Matentzoglu, and Scheffner 2007). They are localised e.g. at tight-junctions in epithelial cells and are responsible for cell-cell contacts (González-Mariscal, Betanzos, and Avila-Flores 2000). Additionally, high-risk E6 increases telomerase activity by transcriptionally upregulating the human telomerase reverse transcriptase (hTERT) gene (Klingelhutz, Foster, and McDougall 1996). This is further enhanced in the presence of E7. hTERT, the catalytic subunit of telomerase, together with the

telomerase RNA (TR), is responsible for the maintenance of telomere repeats at chromosomal ends. This process is often deregulated in cancers to enable unlimited cell division (Maciejowski and de Lange 2017).

In contrast to high-risk E6, low-risk E6 lacks the C-terminal PDZ-binding motif and is therefore unable to interact with and cause the degradation of members of the MAGUK protein superfamily. With mutant chimeric low-risk E6 proteins, in which the C terminus is exchanged by the high-risk E6 C terminus containing the PDZ-binding motif, the high-risk abilities are restored (Kuballa, Matentzoglu, and Scheffner 2007).

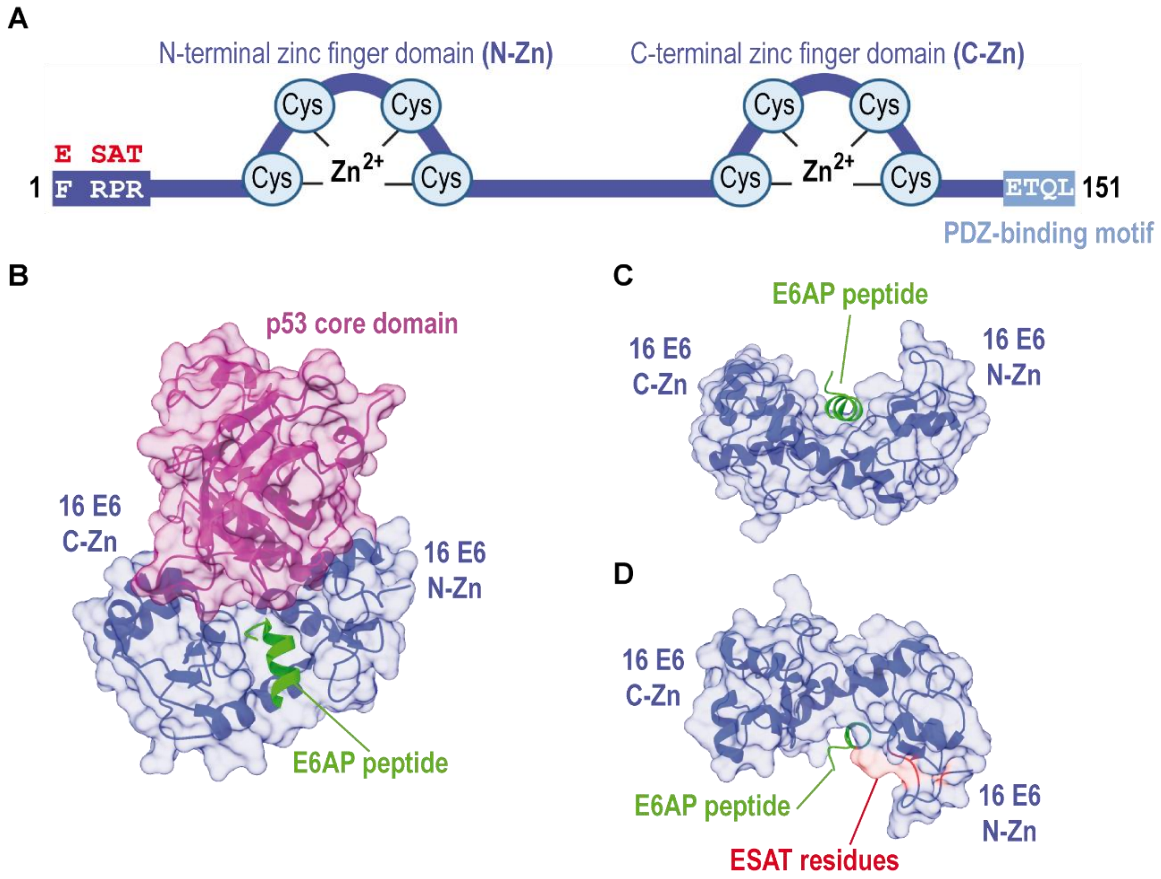

Figure 4: The HPV 16 E6- E6AP- p53 complex. A| Structural representation of the high-risk HPV 16 E6 protein. The N-terminal ESAT mutations (F2E, R8S, P9A, R10T), the N-terminal (N-Zn) and the C-terminal (C-Zn) zinc finger domains, and the PDZ-binding motif (ETQL) at the very C terminus are indicated. A 16 E6 variant with the ESAT mutations is unable to bind to p53. Created with BioRender.com **B-D**| Crystal structure (PDB 4XR8) of 16 E6 (blue) in complex with the extended peptide of E6AP (Martinez-Zapien et al. 2016) that is required for the formation of the ternary complex (ELT-LQELL-GEER, light green) and **B**| the p53 core domain (pink). **C**| The structure is rotated to display the 'LxxLL pocket' of 16 E6. **D**| The structure is further rotated to highlight the ESAT mutations adjacent to the 'LxxLL pocket'. The structure was modified with UCSF ChimeraX (Goddard et al. 2018).

1.4 Rho GTPases – the RhoA subfamily

The Ras superfamily of small (~21 kDa) GTPases is composed of more than 150 members and is subdivided into several families which in turn are further divided into subfamilies (**Figure 5**). One of these is the RhoA subfamily, comprising the proteins RhoA, RhoB, and RhoC, which are ubiquitously expressed. The RhoA subfamily is part of the Rho (Ras homologous) family of GTPases. All GTPases function as molecular switches (**Figure 6**) and share considerable structural and biochemical similarities. Active GTPases interact with a multitude of distinct downstream effectors and control many essential cellular processes or pathways (reviewed in Hodge and Ridley (2016); Brakebusch (2021); Bar-Sagi and Hall (2000)).

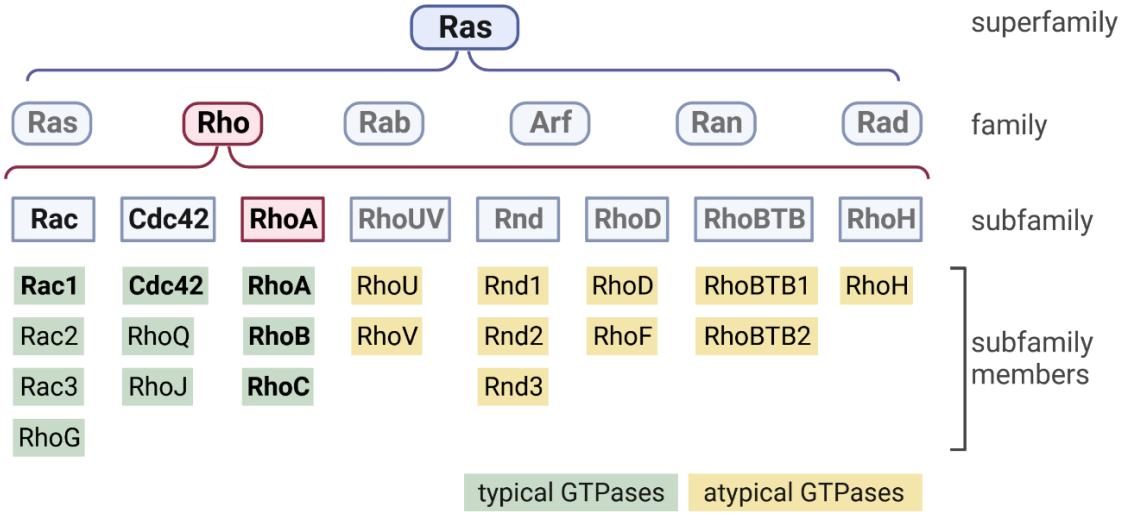

Figure 5. The Ras superfamily of GTPases. Overview of the Ras superfamily of GTPases with a detailed list of the Rho family members, including the subfamilies and their members. The GTPases relevant for this thesis are highlighted (bold). Modified from (Shutes and Der 2004) and created with BioRender.com

1.4.1 Mode of action and regulation

Rho GTPases belong to the typical GTPases, i.e. they cycle between an inactive guanosine diphosphate (GDP)-bound state and an active guanosine triphosphate (GTP)-bound state and this switch is accompanied by a conformational change (Wennerberg and Der 2004; Hakoshima, Shimizu, and Maesaki 2003). Atypical GTPases predominantly exist in a GTP-bound form and are regulated by different means (Soundararajan and Eswaran 2012). The activation state of typical GTPases is directly regulated by guanine nucleotide exchange factors (GEFs) and GTPase activating enzymes (GAPs) (van Buul, Geerts, and Huveneers 2014) (**Figure 6B**). The high cytosolic concentration of Mg^{2+} prevents a spontaneous guanine nucleotide exchange, as the Mg^{2+} stabilizes guanine nucleotide binding (Zhang et al. 2000). Mainly extracellular stimuli signal for the activation of Rho GTPases via surface receptors like G-protein-coupled receptors (GPCRs), cytokine receptors, or receptor tyrosine kinases (Buchsbaum 2007). In humans, 85 GEFs and 66 GAPs manage the

regulation of the 20 known Rho GTPases, which allows for a high level of control (Mosaddeghzadeh and Ahmadian 2021).

1.4.1.1 GEFs, GAPs, and GDIs

GEFs stimulate the mainly cytosolic inactive Rho proteins to release GDP. This is achieved by structural alterations of the nucleotide binding pocket, while leaving it solvent exposed. Then, due to a higher intracellular concentration, GTP is bound. GEFs are released from Rho proteins in the GTP-bound state and free to activate the next GDP-Rho. Active GTP-Rho is then predominantly localised to its effector proteins at cellular membranes. GEFs can either be specific for a certain Rho or be able to activate multiple different Rho proteins (reviewed in Rossman, Der, and Sondek (2005)). The largest Rho GEF family (~ 70 members) is structurally characterised by diffuse B-cell lymphoma (Dbl)-homology (DH) domains often together with a pleckstrin-homology (PH) domain resulting in a DH/PH combination (Snyder et al. 2002). Dbl GEFs, including their respective specificities, are reviewed in Cook, Rossman, and Der (2014). To sense the nucleotide loading state, the GEF DH domain interacts with the switch I and II regions of Rho (see also **Figure 7**) (Hoffman and Cerione 2002). Due to the high structural similarities of Rho proteins (see 1.4.3 ‘Structural details – RhoA, RhoB, and RhoC’), many GEFs activate all three members of the RhoA subfamily (Rossman, Der, and Sondek 2005; van Buul, Geerts, and Huveneers 2014).

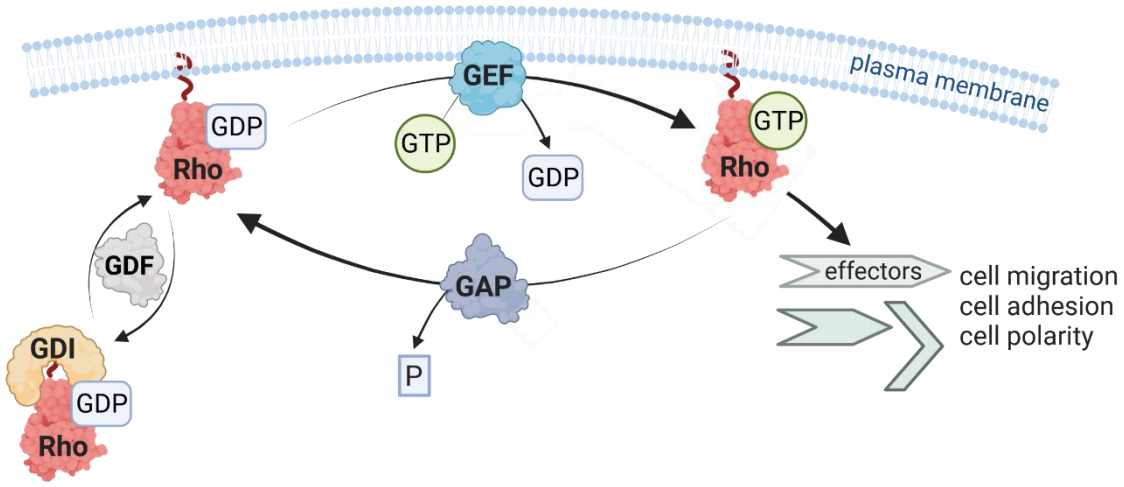

Figure 6: The Rho GTPase cycle. Schematic of the regulation of typical Rho GTPases. The activation of downstream effectors leads to cell migration, cell adhesion, or cell polarity, depending on the specific effector protein. GEF: guanine nucleotide exchange factor; GAP: GTPase activating protein; GDI: guanine nucleotide dissociation inhibitor; GDF: guanine dissociation factor. Modified from (Etienne-Manneville and Hall 2002) and created with BioRender.com

ARHGEF10 was initially identified as RhoA GEF (Matsushita et al. 2009), but was recently shown to specifically activate only RhoB (Khan et al. 2021). For the nuclear fractions of RhoA and RhoB, Net1 has been described as a specific GEF in response to DNA damage (Dubash et al. 2011; Srougi and Burridge 2011). The second and atypical GEF family is comprised of eleven dedicator of cytokinesis (DOCK) proteins, which contain a catalytic and a membrane-associated domain but lack the classical

DH domain (reviewed in Laurin and Côté (2014)). The DOCK GEFs only activate Rac1 and/or Cdc42 GTPases and are unable to activate any Rho GTPases (Côté and Vuori 2002, 2006).

GAPs stimulate the intrinsically low GTPase activity of Rho by several orders of magnitude, causing the hydrolysis of GTP to GDP. This results in inactive Rho and termination of the signal transduction (van Buul, Geerts, and Huveneers 2014). Of the 66 known human GAPs, 57 contain a common catalytic domain with a conserved arginine residue (‘arginine finger’), which stabilizes the GTPase reaction (Graham, Eccleston, and Lowe 1999). The charge distribution between the β- and γ-phosphate of GTP is altered by the ‘arginine finger’ and a conserved lysine residue in the P-loop of Rho. This promotes the nucleophilic attack of water at the γ-phosphate resulting in GTP hydrolysis (reviewed in Li and Zhang (2004); Gerwert, Mann, and Kötting (2017)). Substrate specificity is achieved by other GAP domains and the exact mechanism remains to be investigated. A list of Rho GAPs and their domains is provided in (Amin et al. 2016).

A third layer of regulation is provided by Rho guanine nucleotide dissociation inhibitors (GDIs). GDIs are able to sequester inactive GDP-Rho in the cytoplasm by preventing the dissociation of GDP (Ohga et al. 1989), while others also bind to active GTP-Rho thereby completely blocking (intrinsic and GAP-stimulated) GTP hydrolysis (Hart et al. 1992). In both cases, the GTPases are rendered unable to stimulate effector proteins. Additionally, GDIs mediate the shuttling of Rho GTPases between cellular membranes and the cytosol (reviewed in Takai et al. (1993)). Of the three human Rho GDIs (RhoGDI1, RhoGDI2/GDID4, RhoGDI3), only RhoGDI1 is expressed ubiquitously (Fukumoto et al. 1990; Ueda et al. 1990). GDI1 and GDI2 are cytosolic, with GDI2 being specific for hematopoietic cells (Lelias et al. 1993; Scherle, Behrens, and Staudt 1993). GDI3 is localised to vesicular membranes in the lung, brain, and testis and is specific for RhoB and RhoG (Zalcman et al. 1996; Adra et al. 1997). GDI dissociation factors (GDF) enable GDP-Rho to be released from the GDI and to be activated by GEFs. An overview of the interactions between different Rho proteins and their GDIs is provided in (DerMardirossian and Bokoch 2005).

In addition to these ‘conventional’ modes of regulation, Rho GTPases are additionally regulated by microRNAs (miRNAs). For this, the miRNA either directly interferes post-transcriptionally with the Rho mRNA or targets Rho GEFs, GAPs, and GDIs, thereby regulating Rho activity (reviewed in Liu et al. (2012); Humphries, Wang, and Yang (2020)).

1.4.1.2 Post-translational modifications

Like other members of the Ras superfamily, Rho GTPases are post-translationally and irreversibly modified with either farnesyl (C12 chain, 15-carbon) or geranylgeranyl (C16 chain, 20-carbon) isoprenoids at a conserved cysteine residue (Hancock et al. 1989). These lipid moieties are required for the membrane anchorage of active GTP-Rho and therefore its correct sub-cellular localisation (Moissoglu and Schwartz 2014). The GDIs bind to and mask the lipid anchor to prevent reactivation. In a three-step mechanism,

the cysteine in the C-terminal ‘CAAX box’ (A = aliphatic aa; X = any aa) is prenylated via a thioether bond in the cytoplasm, followed by the proteolytic removal of the C-terminal tripeptide (‘AAX’) and the subsequent carboxyl-methylation of the cysteine on the ER surface (reviewed in Zhang and Casey (1996); Cox and Der (1992)). Depending on the type of lipid, the prenylation is catalysed by either farnesyltransferase (FTase) or geranylgeranyl transferase type I (GGTase-I). The endo-proteolytic cleavage is catalysed by Ras converting enzyme I (RceI). In the last step, carboxyl methylation is mediated by the isoprenylcysteine-carboxyl methyltransferase (Icmt). The fully processed GTPase is then trafficked to its target membrane (Taylor et al. 2003). Besides members of the Ras superfamily, nuclear lamins, some kinases and phosphatases, and intracellular membrane proteins contain the CAAX box (Gao, Liao, and Yang 2009). As a rule of thumb, the ‘X’ within the CAAX-box determines the type of isoprenoid. Serine (S), methionine (M), or glutamine (Q) result in the recognition by FTase (Ras and nuclear lamins) (Reiss et al. 1990), while leucine (L), isoleucine (I), and phenylalanine (F) signal for recognition by GGTase-I and therefore modification with a geranylgeranyl moiety (Casey, Thissen, and Moomaw 1991; Yokoyama et al. 1991) (RhoA: CLVL; RhoB: CKVL; RhoC: CPIL; Rac1: CLLL). RhoB marks an exemption, as it can be both farnesylated and geranylgeranylated by GGTase-I, with farnesylation being more efficient (Armstrong et al. 1995). In addition to this, the cysteines at position 189 and 192 of RhoB, which are just upstream of the CAAX box are palmitoylated. Palmitoylation is a reversible process important for the correct subcellular localisation of certain proteins (Dietrich and Ungermann 2004). For RhoB, the palmitoylated cysteine at position 192 together with the prenylated cysteine at position 193 were shown to be responsible for the anti-proliferative and pro-apoptotic properties of RhoB (Wang and Sebti 2005).

In addition to lipidation, Rho GTPases can also be modified by various other PTMs like phosphorylation, methylation, ubiquitination, oxidation and sumoylation (summarized in Hodge and Ridley (2016), Olson (2018), and Hurst, McGarry, and Olson (2022)). Ser188 of RhoA is phosphorylated by PKA and PKG, which exhibits an inhibitory effect by enhancing the interaction between RhoA and RhoGDI (Tkachenko et al. 2011) and potentially decreasing the interaction with the downstream effector Rho-associated coiled-coil-containing kinase (ROCK) (Nusser et al. 2006).

RhoA has been described to be ubiquitinated by three different E3 ligase complexes. The SKP1-CUL1-F-box (SCF)^{FBXL19} complex targets RhoA at K135 after RhoA phosphorylation by Erk2 (Wei et al. 2013). The SMAD-specific E3 ubiquitin protein ligase 1 (SMURF1) preferentially targets active GTP-RhoA at K6 and K7 for proteasomal degradation (Ozdamar et al. 2005; Wang et al. 2003). The BACURD-CUL3-RING complex, on the other hand, ubiquitinates inactive GDP-RhoA, and no specific lysine residues of RhoA have been identified to be targeted by this ligase complex (Chen et al. 2009; Ibeawuchi et al. 2015). RhoC, but not RhoA, is ubiquitinated in a regulatory manner by the RING ligase LNX1 (Kholmanskikh, Singh, and Ross 2022). RhoC was shown to be targeted for degradation by the RING ligases RNF180 (Wu et al. 2020) and RNF168 (Xu et al. 2021). RhoB is targeted for proteasomal degradation by SMURF1 at K6 and K7 (Wang et al. 2014), as well as by the CUL3-

TNFAIP1 complex in inflammatory responses (Liu et al. 2021). In comparison to RhoA and RhoC, degradation of RhoB is faster, resulting in a short half-life of roughly 30 minutes and low RhoB steady-state levels (Zalcman et al. 1995). To target RhoB to lysosomes, it is polyubiquitinated at K162 and K181 by the CUL3-Rbx1-KCTD10 RING ligase complex (Kovačević et al. 2018).

1.4.2 Biological functions

Rho GTPases are key players in the regulation of the actin-cytoskeleton, cell polarity, cell-cell and cell-matrix adhesion, membrane transport, and transcription factors. This enables concerted and fast spatiotemporal cellular changes in different compartments after the activation of a single GTPase. Changes in expression levels or in PTMs of Rho itself or its regulators, as well as alternative splicing and changes in miRNA patterns, form the basis for Rho deregulation (reviewed in Porter, Papaioannou, and Malliri (2016b)). Deregulated Rho GTPases are potentially oncogenic and can lead to malignant transformation (reviewed in Orgaz, Herraiz, and Sanz-Moreno (2014); Svensmark and Brakebusch (2019)).

For Rho GTPases, more than 60 different effector proteins have been described (reviewed in Bishop and Hall (2000)). Effector stimulation can occur via recruitment to the membrane or induction of a conformational change. RhoA family members bind to effector proteins like Rhotekin (RTKN), mammalian diaphanous homolog 1 and 2 (mDia), ROCK I and II, or PKN via their Rho-binding-domain (RBD) (Fujisawa et al. 1996; Reid et al. 1996; Rose et al. 2005; Maesaki et al. 1999). Two of these downstream effectors, ROCK and mDia, are responsible for the modulation of actomyosin-mediated cell contractility and cell shape (Watanabe et al. 1999). Active RhoA stimulates the kinases ROCK I and II, which subsequently phosphorylate the myosin light chain (MLC) (Kimura et al. 1996; Amano et al. 1996) and inhibit the corresponding MLC phosphatase at the regulatory subunit 1 (MYPT1) (Feng et al. 1999). This results in overall increased MLC phosphorylation and therefore myosin II filament generation by increasing the ATPase activity of myosin (Chrzanowska-Wodnicka and Burridge 1996). In addition to MLC phosphorylation and with the help of ROCK inhibitor Y27632, the RhoA-ROCK axis was shown to play crucial roles in smooth muscle contraction (Uehata et al. 1997), tumour invasions (Itoh et al. 1999) and cell motility (Niggli 1999). For the precise regulation of cell migration, the spatio-temporal organization of RhoA and Rac1 is indispensable (reviewed in Nguyen, Kholodenko, and von Kriegsheim (2018)).

1.4.2.1 Role in cancer development

The involvement of Rho GTPases in cancer progression has been described in detail in (Orgaz, Herraiz, and Sanz-Moreno 2014; Porter, Papaioannou, and Malliri 2016a; Clayton and Ridley 2020; Vega and Ridley 2008; Ridley 2013). For this work, mainly the different oncogenic or tumour suppressive properties of members of the RhoA subfamily are of interest. At a first glance, Rho GTPases appear as classical oncogenes, as constitutively active forms promote uncontrolled cell growth (Avraham and Weinberg 1989). In astrocytic tumours of grades II to IV, RhoA and RhoB protein

levels were shown to be inversely correlated to the different stages of malignancy (Forget et al. 2002). Conversely, RhoB has been described to additionally exhibit anti-proliferative and therefore tumour-suppressive functions (Liu et al. 2001; Huang and Prendergast 2006; Wang and Sebti 2005). RhoB, but not RhoA or RhoC, has been found to be localised in endosomes, multi vesicular bodies, and the nucleus besides the plasma membrane. This subcellular localisation of RhoB is suggested as the basis for its differential properties regarding cancer development (reviewed in Zaoui and Duhamel (2023)). In an attempt to determine the basis for the tumour suppressive properties of RhoB, the 25 RhoB residues that deviate from the RhoA sequence were mutated to the corresponding RhoA residues. Mutation of the two cysteine residues 192 and 193 was shown to abolish the anti-apoptotic properties of RhoB. As mentioned above, the combination of palmitoylation (C192) and prenylation (C193) is required for RhoB to exhibit its unique functions (Wang and Sebti 2005).

1.4.2.2 Role in neuronal processes

Considering their general role in cytoskeleton organisation, the importance of Rho GTPases in proper brain development and neuronal maintenance is not surprising. During neuronal development, RhoA was shown to regulate the initiation of neuronal polarisation and axon outgrowth by preventing microtubule protrusions towards the leading edge of the neuron (Dupraz et al. 2019). RhoA expression shows an overall low tissue specificity, which also applies to the brain (RhoA entry in the protein atlas, accessed May 2023). However, research on rat brains showed elevated RhoA and Cdc42 protein levels in the hippocampus, the cerebellum, the neocortex, and the thalamus in comparison to other brain regions (Olenik et al. 1997). While Rac1 and Cdc42 stimulate lamellipodia and filopodia formation, members of the Rho GTPase family prevent neurite outgrowth and promote the retraction of neurites. This actin cytoskeleton antagonism is indispensable for synaptic plasticity (reviewed in Govek, Newey, and Van Aelst (2005)). Activated RhoA and Rac1 were shown to directly counteract each other in neurons and their precise antagonistic regulation determines changes in neuronal morphology (Kozma et al. 1997; Moorman et al. 1999; Li, Aizenman, and Cline 2002). As part of this crosstalk, Rac1 activation by its GEF Tiam1 promotes Rac1-dependent neurite outgrowth, while at the same time inhibiting RhoA signalling (Leeuwen et al. 1997). The RhoA GEF Ephexin5 was indicated to restrain the development of excitatory synapses via the activation of RhoA and therefore the E6AP-mediated degradation of phosphorylated Ephexin5 was suggested to reinstate synapse development (Margolis et al. 2010). In addition to neurodevelopmental processes, Rho GTPases also play pivotal roles in neurodegenerative diseases. This has been extensively reviewed in DeGeer and Lamarche-Vane (2013); Arrazola Sastre et al. (2020); Schmidt et al. (2022).

1.4.3 Structural details – RhoA, RhoB, and RhoC

RhoA was first described as a homolog of the Ras GTPase, which gave rise to its name: Ras homolog A (Madaule and Axel 1985). The *RhoA* gene is located on chromosome 3, while the genes for *RhoB* and *RhoC* are located on chromosome 2 and 1, respectively (Cannizzaro et al. 1990; Morris et al. 1993). The *RhoB* and *RhoC*

genes contain less exons and introns and are thought to have evolved by reverse transcription or incomplete duplication from the *RhoA* gene, respectively. In comparison to the amino acid sequence of RhoA, RhoB is to 83% and RhoC to 91% identical (reviewed in Wheeler and Ridley (2004)). These high similarities result in structural homology between the three proteins. The main differences are at the C terminus, where the hypervariable region (HVR) is located. In addition to the HVR, Rho proteins contain a guanine nucleotide binding domain (G-domain) and an insert region.

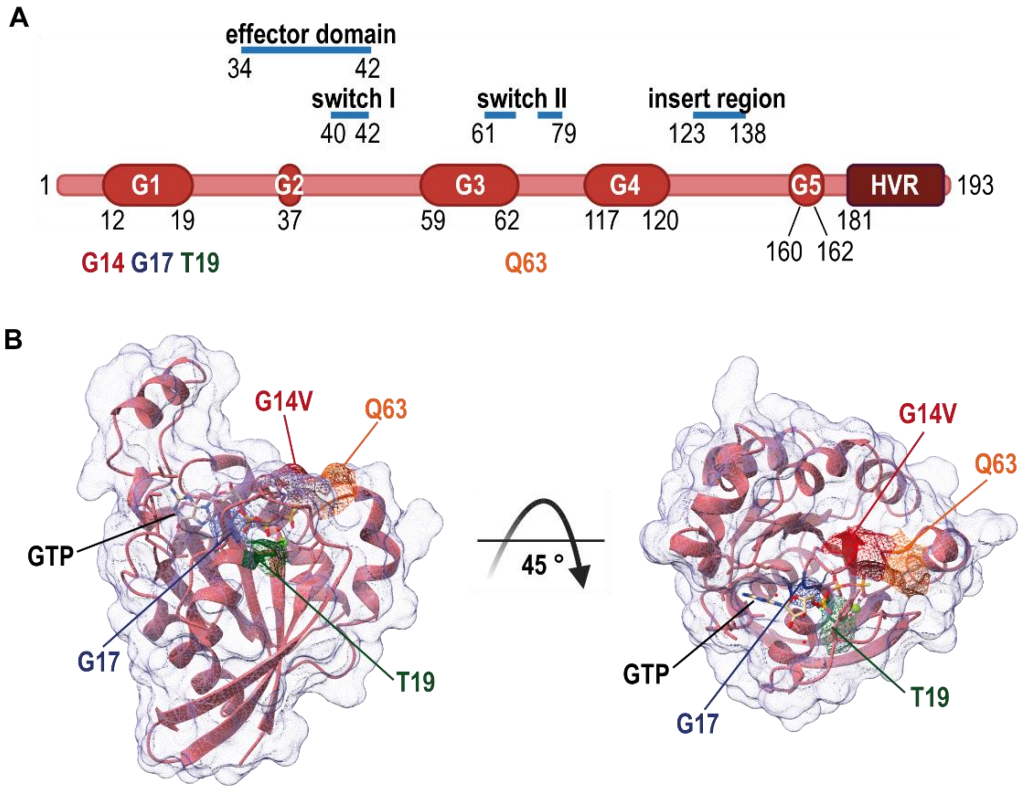

Figure 7: Structural insights into RhoA. A| Schematic of the RhoA domains. The effector domain, the switch I and II regions, the insert region, the hypervariable region (HVR), and the positions of G14, G17, T19 and Q63 within the five different G-motifs (G1-5) are indicated with the respective amino acid numbering. Modified from (Lou et al. 2021) and created with BioRender.com **B**| Crystal structure of RhoA G14V in complex with GTPγS (PDB 1A2B). The locations of the point mutations resulting in aberrant guanine nucleotide binding and the GTPγS (GTP) are indicated. The structure was modified with UCSF ChimeraX (Goddard et al. 2018).

Nucleotide binding as well as conformational changes are mediated by the five conserved motifs (G1-G5) that form the G-domain (reviewed in Wittinghofer and Vetter (2011)) (**Figure 7A**). The β- and γ-phosphates of the guanine nucleotide are bound by G1, a motif that is also known as the P-loop (phosphate binding loop; residues 12-19 of RhoA) (Kozlova et al. 2022). The presence of Mg^{2+} causes a reduction in on- and off-rates of the guanine nucleotides, resulting in stabilization of the binding. The interaction of GEFs with Rho proteins results in the exclusion of Mg^{2+} from the binding pocket, thereby enabling the release of GDP (Zhang et al. 2000). The nucleobase of GTP/GDP is bound by the G4 and G5 motif. The switch I (residues 32-42 of RhoA) and switch II (residues 61-78 of RhoA) regions comprise the G2 and G3 motif, respectively,

and are responsible for the conformational change upon binding of the different nucleotides. The release of the γ-phosphate leads to a relaxation of the two switch regions in the GDP-bound state that is known as the characteristic ‘loaded-spring’ mechanism (reviewed in Vetter and Wittinghofer (2001)). This conformational change is the basis for the activation state of the GTPase and can be detected by regulatory proteins. Effector proteins and regulators can additionally bind to the HVR at the C terminus and the insert domain, which is located between G4 and G5 (Wittinghofer and Vetter 2011). As the name suggests, the HVR is the region of highest variability and confers specificity among the RhoA subfamily. The CAAX box is located at the very C terminus and post-translationally modified by prenylation (discussed in detail in 1.4.1.2 ‘Post-translational modifications’).

1.4.4 Frequently used Rho mutants

The mutation of glycine at position 14 to valine (G14V) and the mutation of glutamine 63 to leucine (Q63L) each turn the Rho GTPase into a dominantly active form (Chen et al. 2022). The mutations abolish both the intrinsic and stimulated GTPase activity mainly by altering the dynamics of the switch regions. This was first described by determining the crystal structure of RhoA G14V in complex with a non-hydrolysable analogue of GTP (GTPγS) (Ihara et al. 1998). The crystal structure of RhoA Q63L confirmed a highly similar structure of the two mutants (Longenecker et al. 2003). While Q63L mainly affects the switch I region, the G14V mutation alters the conformation of both switch regions (**Figure 7B**). The overall more closed structure facilitates a decreased solvent exposure and thereby excludes water molecules which are required for hydrolysis (Chen et al. 2022). In cellular studies, the two mutations elicit contradictory effects, like differential cellular morphology (Mayer et al. 1999), subcellular localisation, or GDI-binding affinities (Michaelson et al. 2001). Mutation of phenylalanine 30 to leucine (F30L) results in increased intrinsic GTP/GDP exchange activity, while still being able to hydrolyse GTP. Due to the higher cellular concentrations of GTP, this also results in a net increase of active RhoA (Lin, Cerione, and Manor 1999).

The concept of a dominant-negative GTPase mutant was initially described for Ras (S17N) but is also applicable to other members of the Ras superfamily (Feig and Cooper 1988a). The mutation of threonine at position 19 to asparagine (Rho T19N) stabilizes an inactive state of RhoA as its affinity for GDP is higher than for GTP. Yet, in cells, the dominant-negative mutants are still able to bind GTP, but even when GTP-bound they are unable to interact with downstream effectors (Farnsworth and Feig 1991). They were also suggested to bind GEFs with a higher affinity and to compete with wild-type (WT) Rho proteins for GEF binding. Since the affinity of 19N mutants for GTP is reduced, the displacement of GEFs from the mutant Rho protein is less likely (Feig and Cooper 1988b). The mutation of glycine 17 to alanine (G17A) renders the GTPase unable to bind any guanine nucleotide. This GTP/GDP binding deficient mutant can serve as a mimic for the intermediate GEF-bound state of Rho (García-Mata et al. 2006).

2. Objectives

The involvement of the HECT E3 ligase E6AP in several human diseases (**Figure 8**) emphasizes the importance to further our knowledge regarding its direct substrates, its interaction partners, and its regulators.

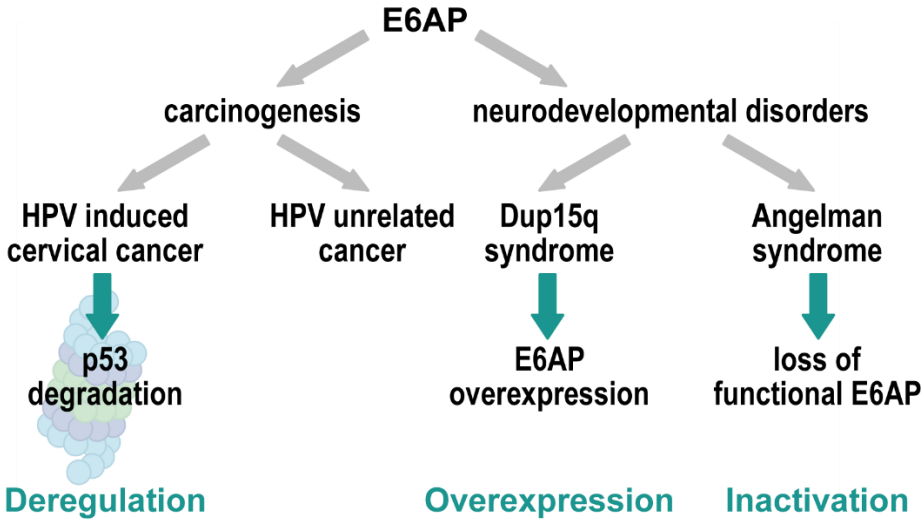

Figure 8. E6AP in human diseases. Overview of E6AP deregulation and its implications for human health. Created with BioRender.com

The E6 oncoprotein of high-risk HPV types (e.g. 16 E6) is a known allosteric activator of E6AP and has been proposed to not only stimulate its ligase activity, but also to broaden the substrate spectrum of E6AP (Mortensen et al. 2015). This means that on the one hand, 16 E6 is able to enhance the activity of E6AP regarding proteins that are substrates of E6AP also in the absence of E6, and on the other hand, cause the ubiquitination and subsequent proteasomal degradation of proteins that are not targeted by E6AP in the absence of 16 E6. For instance, only in presence of the E6 protein, E6AP is able to target the tumour suppressor p53 for proteasomal degradation (Huibregtse, Scheffner, and Howley 1993a; Scheffner et al. 1993). Furthermore, E6 proteins of low-risk HPV types, while able to interact with E6AP, cannot cause p53 degradation (Brimer, Lyons, and Vande Pol 2007; Scheffner et al. 1990). Despite this profound difference, the expression pattern and the structure of the E6 proteins are highly similar, as are the viral life cycles of high- and low-risk HPV types (reviewed in Howie, Katzenellenbogen, and Galloway (2009); Doorbar et al. (2012)). The characterisation of additional substrates of the E6-E6AP complex and their biological relevance during the viral infection might therefore provide the missing pieces to unravel the underlying mechanisms of cancer formation versus the formation of benign lesions.

In addition to carcinogenesis, E6AP plays a significant role in neurodevelopmental disorders (reviewed in Kalsner and Chamberlain (2015)). Alterations of the *UBE3A* gene resulting in loss of E6AP expression or the expression of ligase-impaired E6AP variants (Buiting, Williams, and Horsthemke 2016; Sadikovic et al. 2014; Yi et al. 2015)

are the cause of Angelman syndrome (AS). The amplification of the chromosomal region containing the *UBE3A* gene (15q11-13) resulting in overexpression of E6AP, has been linked to the autism spectrum disorder Dup15q syndrome. Overall, this highlights the severe consequences of dysregulated ubiquitination in human diseases. Several proteins have been reported as substrates of E6AP in absence of 16 E6, e.g. HR23A (Kumar, Talis, and Howley 1999), the E3 ligase Ring1b (Zaaroor-Regev et al. 2010), the RhoA GEF Ephexin5 (Margolis et al. 2010), and TKT (Pandya et al. 2022), yet their relevance regarding AS or Dup15q development remains elusive. Despite the critical role of E6AP in the neurodevelopmental disorders AS and Dup15q syndrome, the disease-relevant proteins affected by E6AP overexpression or by the loss of functional E6AP, and therefore the mechanisms underlying the development of these diseases remain elusive. This reinforces the need for E6AP substrates or interactors in a neuronal and HPV-independent context.

In this study, we initially employed the stimulating properties of 16 E6 for the discovery of substrates and/or interaction partners of E6AP, which otherwise are potentially difficult to detect with available methods.

3. Results and Discussion

An approach to analyse the substrate spectrum, the so-called 'ubiquitome', of high-risk (16 E6) and low-risk (11 E6) HPV types was recently developed in our laboratory (Ebner et al. 2020). By this, over 190 proteins were identified to be ubiquitinated in the presence of either of the HPV E6 proteins and E6AP. For this thesis, several were cherry-picked (**Table 1**) for further validation and analysis. Proteins were chosen based on their involvement in pathways that could be impaired during HPV infections or could be important during neuronal development. The known E6-E6AP substrate proteins p53 (Huibregtse, Scheffner, and Howley 1993a; Scheffner et al. 1993), NHERF1 (Drews, Case, and Vande Pol 2019), and Dlg1 (Kiyono et al. 1997; Gardiol et al. 1999) served as positive controls for the method development and were also identified in the ubiquitome approach by Ebner et al. (2020) (see **Table 1**).

Table 1. Results of the MS/MS evaluation of newly identified E6-E6AP substrate proteins. List of proteins that were identified as potential substrates of the 16 E6-E6AP or 11 E6-E6AP complex by Ebner et al. (2020) and were cherry-picked to be further investigated in this study. In total, approximately 190 potential substrates were identified. The results for p53, NHERF1, and Dlg1 are listed as control values. [%] = percentage of the protein sequence covered by peptides; peptide spectrum matches (PSM): number of peptides found for the protein with 16 E6 or 11 E6; diGly: peptides found with a Gly-Gly motif indicating a modification with ubiquitin; peptides 16 or 11: number of peptides found for the protein in the presence of 16 E6 or 11 E6, respectively.

Protein	Uniprot ID	[%]	PSM 16 E6	PSM 11 E6	diGly 16 E6	diGly 11 E6	peptides 16 E6	peptides 11 E6
Transforming protein **RhoA**	P61586	79	295	64	+	-	18	14
Rho-related GTP-binding protein **RhoC**	Q5JR08	73	42	-	+		15	
RelA-associated inhibitor **iASPP**	Q8WUF5	53	335	478	+	+	40	42
Double-strand break repair protein **MRE11**	P49959	26	51	18	+	+	20	11
Na^+/H^+ exchange regulatory factor **NHERF1**	O14745	74	430	500	+	+	33	33
Disks large homolog 1 **Dlg1**	A0A0C4DFT3	59	201	-	+		45	
Cellular tumour antigen **p53**	P04637	30	66	-	-		11	

In general, trypsin specifically cleaves after arginine (Arg, R) and lysine (Lys, K) residues (Olsen, Ong, and Mann 2004), which results in distinct peptide patterns for each protein. The approach implemented by Ebner et al. (2020) makes use of the three C-terminal amino acid residues Arg-Gly-Gly of ubiquitin. Upon tryptic digest of ubiquitinated proteins for subsequent MS/MS analysis, ubiquitin is cleaved after the Arg, with the diGly (Gly-Gly) remaining covalently attached on the ubiquitinated lysine residue (Olsen, Ong, and Mann 2004). Furthermore, trypsin is unable to recognise and/or cleave after diGly-modified lysine residues. For this reason, the presence of diGly motifs on lysines in the digested peptides indicates the modification of the respective protein with ubiquitin. Nevertheless, the detection of diGly motifs may fail in some cases, due to e.g. insufficient amounts of ubiquitinated protein, peptides of unfavourable length that are either too short or too long to be detected in the mass spectrometer, or peptides with unfavourable ionisation properties.

3.1 iASPP and ASPP2 as potential substrates of E6-E6AP

The ASPP protein family comprises three members (ASPP1, ASPP2, iASPP), which are all known to interact with wild-type p53 (Iwabuchi et al. 1994) and the p53 family members p63 and p73 (Robinson et al. 2008). As a result of their interaction, p53-dependent apoptosis signals are altered, while cell cycle regulation is not affected (Samuels-Lev et al. 2001). ASPP1 and ASPP2, which are also known as tumour suppressor p53 binding protein 1 (53BP1) and 2 (53BP2), respectively, exhibit stimulatory functions on p53 (Iwabuchi et al. 1994). iASPP, on the other hand, acts as an inhibitor of p53 (Bergamaschi et al. 2003) and was first described to bind to the NF-κB subunit RelA (an alternative name of iASPP is RelA-associated inhibitor) thereby inhibiting the transcriptional activity of NF-κB (Nuclear factor NF-kappa-B p150 subunit) (Yang et al. 1999). The three members of the ASPP family show structural similarities at their C-termini with Ankyrin repeats, an SH3 domain and a proline rich region. All known interaction partners, e.g. p53, Bcl-2, RelA, and YAP1, bind in this region (reviewed in Sullivan and Lu (2007)). Due to their role in p53 regulation and the fact that iASPP was found to be a potential target of E6-E6AP by Ebner et al. (2020), while ASPP2 was suggested as an E6AP substrate by Martínez-Noël et al. (2018), both proteins were further investigated in this study.

3.1.1 *in vitro* experiments with ASPP proteins

As indicated in **Table 1**, iASPP can be found with diGly modifications in the presence of both 11 E6 and 16 E6. Therefore, all validation experiments were performed with 11 E6-E6AP and 16 E6-E6AP. In a first step, to confirm iASPP as substrate protein, a ubiquitination assay (5.2.4.1) with *in vitro* translated, radiolabelled iASPP (5.2.2.7) was performed in the presence of UBA1, UbcH7, and E6AP as well as the E6 proteins. To focus solely on the E6 effect, the ubiquitin hydrophobic patch mutant LIA (L8A and I44A, ub LIA) was used in this experiment. E6AP-mediated ubiquitination is strongly impaired with ub LIA, but the E6 proteins are able to rescue this deficit (Mortensen et al. 2015). After incubation for 90 min at 30°C, whole reaction mixtures were analysed by SDS-PAGE (5.2.3.1) followed by fluorography (5.2.4.1).

This shows that iASPP is ubiquitinated by 16 E6-E6AP and 11 E6-E6AP, as indicated by the appearance of a smear (asterisk, **Figure 9A**) representing polyubiquitinated forms of iASPP and the concomitant loss of unmodified iASPP (**Figure 9A**). The effect of 16 E6 is slightly stronger than that of 11 E6.

In a parallel GST coprecipitation experiment (for details, see 5.2.4.2 in the Methods section), GST-tagged E6 variants or GST alone were immobilized on GSH beads and incubated with *in vitro* translated, radiolabelled iASPP for 90 min at 4°C. Unbound proteins were removed in three subsequent washing steps, before analysing the interaction via SDS-PAGE followed by Coomassie staining and fluorography. The Coomassie readout enables the visualization of GST input levels used in the coprecipitation and the fluorographic readout reveals potential binding of the *in vitro* translated protein. Here, iASPP shows an interaction with GST-16 E6 and GST-11 E6 but not with GST alone (**Figure 9B**).

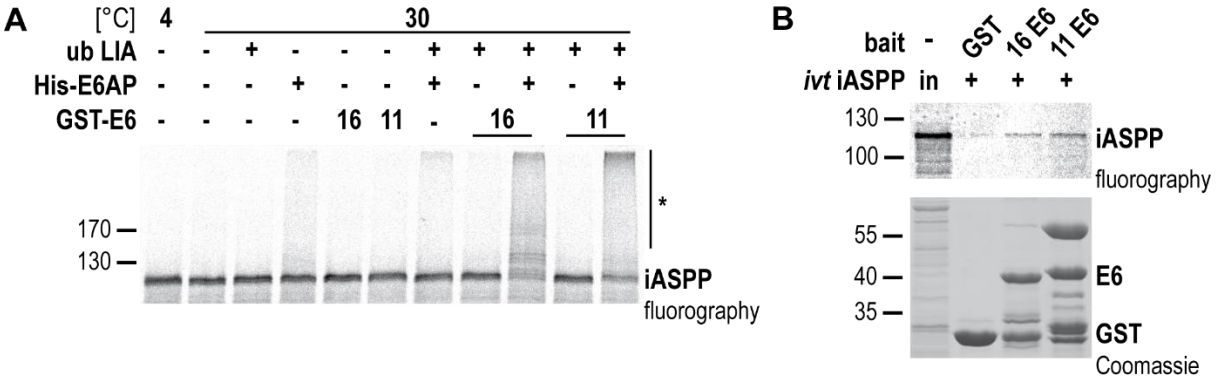

Figure 9. iASPP is a substrate of 11 E6-E6AP and 16 E6-E6AP *in vitro*. A⎪ *in vitro* translated, radiolabelled iASPP was incubated with UBA1 and UbcH7 in the presence and absence of His-E6AP, GST-tagged E6 proteins, and the ubiquitin hydrophobic patch mutant LIA (ub LIA) for 90 min at 30°C as indicated. E6AP is unable to use ub LIA for ubiquitination without the stimulation of E6 proteins. The reactions were stopped with Laemmli buffer (see 0) and the samples were analysed by SDS-PAGE followed fluorography. The running positions of the unmodified form (iASPP) and polyubiquitinated forms (*) are indicated. **B**⎪ The GST-E6 fusion proteins or GST alone bound to GSH beads were incubated with *in vitro* translated, radiolabelled iASPP for 90 min at 4°C. Beads were washed after the binding reaction and the eluates were analysed by SDS-PAGE followed by Coomassie staining (GST bait input detection, lower panel) and fluorography (binding reaction, upper panel). The running positions of the molecular mass markers (in kDa), the GST-tagged proteins, and iASPP are indicated. in⎪ 10% of the iASPP used in the binding reaction.

As discussed above, ASPP2 was not found in the study of Ebner et al. (2020), but as a potential substrate protein of E6AP (Martínez-Noël et al. 2018). ASPP2 ubiquitination was therefore investigated in the presence of 11 E6-E6AP and 16 E6-E6AP essentially as described above for iASPP with the difference that ubiquitin WT was used. ASPP2 is ubiquitinated to a certain extent by E6AP alone, and this ubiquitination is further stimulated by 16 E6. 11 E6 does not seem to be able to enhance the E6AP-mediated ubiquitination of ASPP2 (**Figure 10**). However, for a better readout regarding 11 E6, the ubiquitination assay should be repeated with the ubiquitin mutant LIA instead of ubiquitin WT.

In GST coprecipitation experiments, the *in vitro* translated ASPP2 shows strong background binding to GST alone or to empty glutathione beads (data not shown). It is therefore not possible to distinguish between background binding and E6-mediated binding. Additional bead-binding controls with empty Q-Sepharose and Ni-NTA beads show comparable unspecific background binding of *in vitro* translated ASPP2 (data not shown). A switch to differently tagged E6 proteins would therefore have been inconclusive as well.

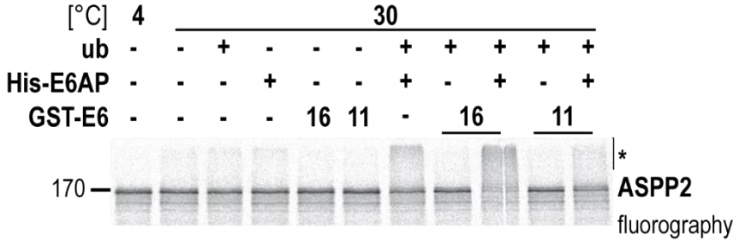

Figure 10. ASPP2 is a substrate of 16 E6-E6AP. *In vitro* translated, radiolabelled ASPP2 was incubated with UBA1 and UbcH7 in the presence and absence of His-E6AP, GST-tagged E6 proteins, and ubiquitin (ub) for 90 min at 30°C as indicated. The reactions were stopped with laemmli buffer (see 0) and the samples were analysed by SDS-PAGE followed by fluorography. The running positions of the molecular mass marker (in kDa), the unmodified form (ASPP2) and polyubiquitinated forms (*) are indicated.

3.1.2 Degradation of ASPP proteins *in cellula*

To verify the data obtained in the *in vitro* assays, degradation of the ASPP proteins was investigated in transient transfection experiments in different cell lines (see 5.1.5 ‘Mammalian cell lines’ for details). Expression constructs encoding N-terminally HA-tagged variants of the respective proteins were used for western blot analysis with an αHA.11 antibody. Degradation was studied in the non-small cell lung carcinoma cell line H1299 (which does not express endogenous p53), an H1299 E6APi cell line (containing a stable RNAi-mediated E6AP knockdown, **Supplementary Figure 1**), and the human embryonic kidney cell line HEK293T. Levels of ectopically expressed iASPP are strongly reduced in the presence of 11 E6-E6AP in H1299 (**Figure 11A**) and HEK293T (**Figure 11B**) cells. In the presence of 16 E6-E6AP, iASPP levels are not reduced in either cell line. Generally, the expression of the 11 E6 protein is stronger than the expression of 16 E6, even though four times more plasmid encoding 16 E6 was transfected. Based on this, it could be argued that iASPP is not degraded by 16 E6 due to its lower levels. However, previous experiments with different substrate proteins show that even very low and in western blot analysis undetectable 16 E6 levels are sufficient for near complete degradation of known substrate proteins (data not shown).

In H1299 E6APi cells, iASPP degradation was also tested in presence of a catalytically inactive E6AP mutant (E6AP C820A), which shows that 11 E6 in complex with E6AP C820A is not able to stimulate iASPP degradation (**Figure 11C**). Thus, this confirms that the reduction of iASPP levels and therefore the 11 E6-mediated iASPP degradation is indeed E6AP dependent.

Tandem ubiquitin binding entities (TUBEs) were used to further validate the notion that iASPP is degraded by the 26S proteasome as a result of E6AP-mediated polyubiquitination. TUBEs selectively and specifically bind to ubiquitin chains, thereby protecting them from recognition by the proteasome (Hjerpe et al. 2009). TUBEs are comprised of four ubiquitin-associated (UBA) domains, separated by flexible linkers (in this study the UBA domains of the human homolog of RAD23A, HR23A, were used). Indeed, co-expression of HA-HR23A-TUBEs stabilises the levels of iASPP in presence of 11 E6-E6AP in H1299 cells, indicating the prevention of proteasomal degradation of iASPP (**Figure 11D**). While iASPP can be found with diGly motifs in presence of 16 E6 and 11 E6, and it is ubiquitinated *in vitro* by both E6 proteins, it is only effectively degraded by the 11 E6-E6AP complex in cells. This tendency may also be reflected in the GST coprecipitation assay, as iASPP shows a stronger interaction with 11 E6 than with 16 E6.

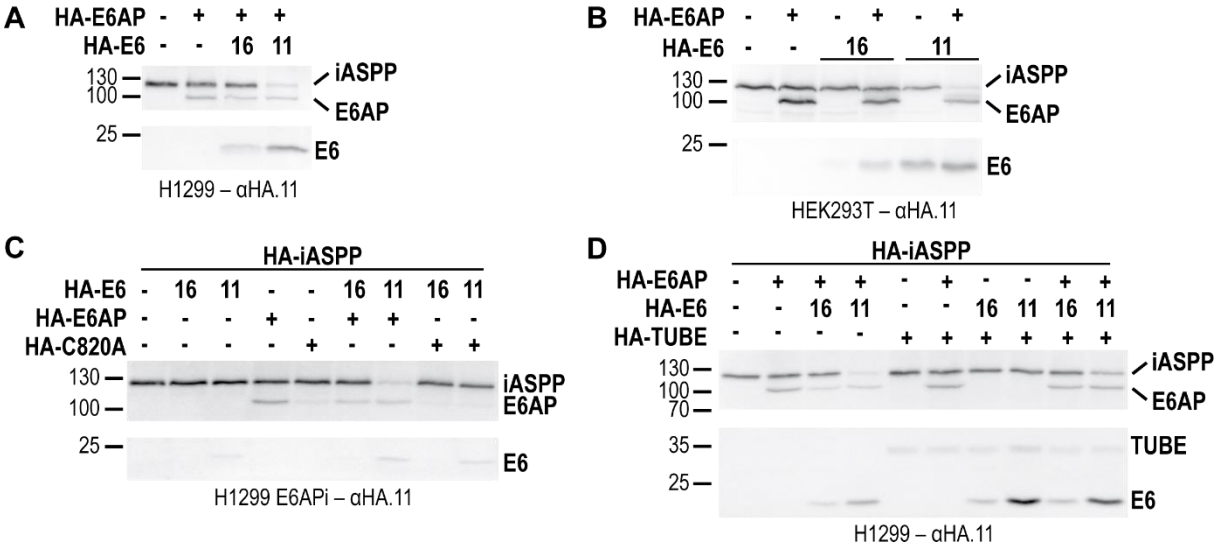

Figure 11. Ectopic iASPP is degraded by the 11 E6-E6AP complex. H1299 **A**│**D**│, HEK293T **B**│, or H1299 E6APi (stable downregulation of E6AP by RNAi) **C**│ cells were transfected with expression constructs encoding for HA-tagged proteins as indicated. 24 h post-transfection, the lysates were prepared and adjusted according to the transfection efficiency (β-galactosidase activity). Samples were analysed by SDS-PAGE followed by western blot analysis and proteins were detected using an αHA.11 antibody. iASPP is degraded only in the presence of 11 E6 and E6AP, but not by 16 E6 and E6AP in **A**│ H1299 and **B**│ HEK293T cells. **C**│ 11 E6 in complex with the catalytically inactive E6AP mutant (C820A) is unable to degrade iASPP, suggesting an 11 E6-E6AP dependent degradation of iASPP. **D**│ The expression of tandem ubiquitin binding entities (TUBEs) stabilises iASPP levels, indicating that iASPP is ubiquitinated by 11 E6-E6AP and therefore targeted for proteasomal degradation. The running positions of the molecular mass markers (in kDa) and the HA-tagged proteins are indicated.

Overall, iASPP could be confirmed as substrate of E6-E6AP. Of all the potential substrate proteins that were identified in Ebner et al. (2020) and verified in ubiquitination and degradation assays, it is the only one to be specifically targeted by 11 E6-E6AP in cellular degradation assays.

Degradation of ASPP2 was tested in H1299 E6APi (**Figure 12A**) and HEK293T (**Figure 12B**) cells. In contrast to iASPP, ASPP2 is completely degraded by 16 E6-E6AP as well as by 11 E6-E6AP. ASPP2 was originally described as a substrate of

E6AP alone (Martínez-Noël et al. 2018), and while this can be confirmed in the *in vitro* ubiquitination assay, E6AP alone has no effect on ASPP2 levels in the cellular degradation assays in either cell line.

In conclusion, even though the degradation of p53 regulators by HPV E6 oncoproteins appears intriguing, future experiments need to address the paradox as to why both an activator (ASPP2) and an inhibitor (iASPP) are targeted by 11 E6 at the same time.

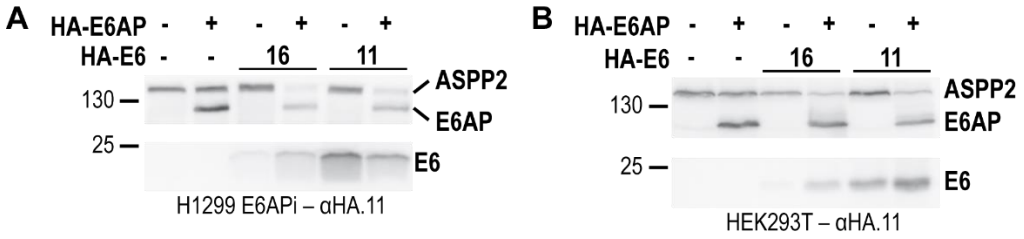

Figure 12. Degradation of ectopic ASPP2 by both 11 E6-E6AP and 16 E6-E6AP. H1299 E6APi (stable downregulation of E6AP by RNAi) **A**⎪ and HEK293T **B**⎪ cells were transfected with expression constructs encoding for HA-tagged proteins as indicated. 24 h post-transfection, the lysates were prepared and adjusted according to the transfection efficiency (β-galactosidase activity). Samples were analysed by SDS-PAGE followed by western blot analysis and proteins were detected using an αHA.11 antibody. ASPP2 is degraded in the presence of the 11 E6-E6AP complex as well as the 16 E6-E6AP complex in **A**⎪ H1299 E6APi and **B**⎪ HEK293T cells. The running positions of the molecular mass markers (in kDa) and the HA-tagged proteins are indicated.

3.2 MRE11 as potential E6-E6AP substrates

Genomic instability presumably favours the malignant transformation of cells (Schiffman et al. 2007) and 16 E6 was shown to be able to induce DNA damage, resulting in the upregulation of DNA damage response (DDR) proteins (Duensing and Münger 2002). Additionally, at a certain stage during an HPV infection, the virus requires proteins involved in the DDR system for the amplification of the viral genome (Sakakibara, Mitra, and McBride 2011).

The double-strand break repair protein MRE11 is part of the MRN (MRE11-Rad50,NBS1) complex, which is known to initiate DDR (Williams, Williams, and Tainer 2007) and HPV-positive cells were shown to upregulate the expression of DDR proteins like MRE11 (Johnson, Aloor, and Moody 2017). Since MRE11 was found with both 11 E6 and 16 E6 (**Table 1**), it was chosen as one of the candidates to be further investigated. The results of Ebner et al. (2020) suggest MRE11 as a potential substrate of the E6-E6AP complex, which would lead to its proteasomal degradation, thereby reducing MRE11 levels and contradicting previous findings regarding MRE11 levels in presence of HPV. However, E6AP-dependent MRE11 regulation in presence of E6 may take place in a timely defined manner, e.g. to get rid of increased levels of MRE11 after viral DNA amplification has occurred in order to subsequently enable uncontrolled cell growth.

The following results are published in the supplementary part of Ebner et al. (2020). The ubiquitination assay with *in vitro* translated MRE11 in the presence of UBA1, UbcH7, and ub LIA shows a stimulation of E6AP-mediated ubiquitination in the

presence of 16 E6 and 11 E6. This is indicated by the smear representing polyubiquitinated forms of MRE11 (**Figure 13A**, asterisk) and the concomitant reduction of unmodified MRE11. The effect of 16 E6 is slightly stronger than that of 11 E6. In GST coprecipitation experiments, MRE11 shows no background binding to GST alone and an interaction of comparable intensity with GST-16 E6 and GST-11 E6 (**Figure 13B**). In cotransfection experiments with H1299 E6APi cells, MRE11 is degraded by 16 E6-E6AP and 11 E6-E6AP, but not with the catalytically inactive E6AP mutant (C820A) (**Figure 13C**). MRE11 degradation is therefore dependent on the presence of active E6AP.

In conclusion, the results obtained for MRE11 and iASPP confirm the validity of the approach established by Ebner et al. (2020) to identify bona fide substrate proteins of the E6 proteins in complex with E6AP.

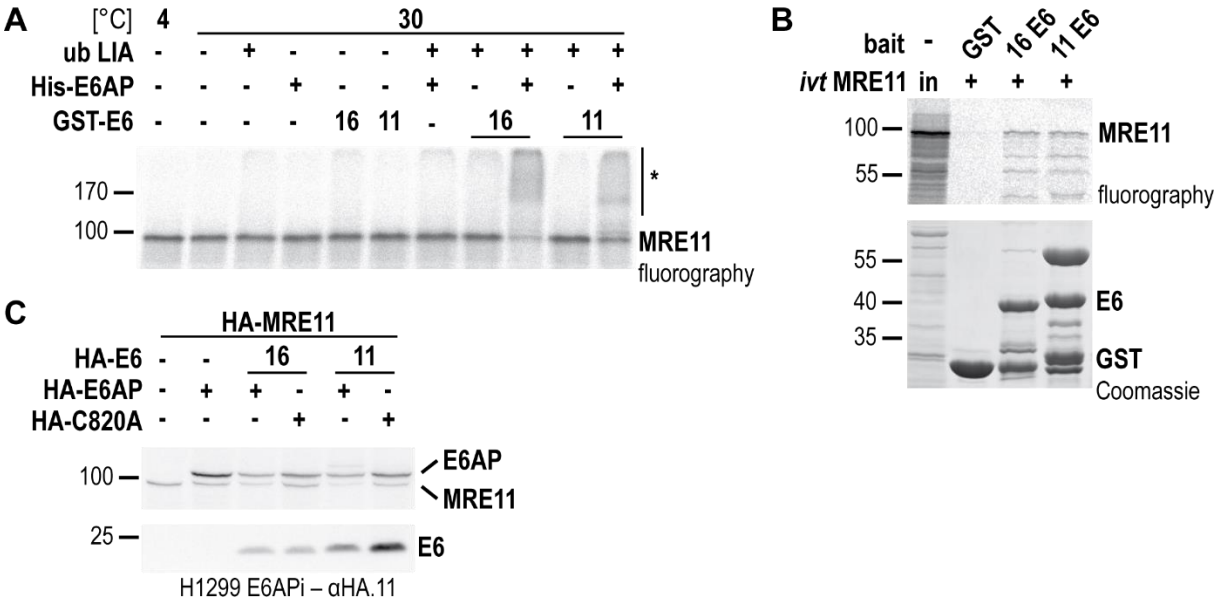

Figure 13. MRE11 serves as substrate for 11 E6-E6AP and 16 E6-E6AP *in vitro* and *in cellula*. A│*in vitro* translated, radiolabelled MRE11 was incubated with UBA1 and UbcH7 in the presence and absence of His-E6AP, GST-tagged E6 proteins, and the ubiquitin hydrophobic patch mutant LIA (ub LIA) for 90 min at 30°C as indicated. E6AP is unable to use ub LIA for ubiquitination without the stimulation of E6 proteins. The reactions were stopped with Laemmli buffer (see 0) and the samples were analysed by SDS-PAGE followed by fluorography. The running positions of the unmodified form (MRE11) and polyubiquitinated forms (*) are indicated. **B**│GST-E6 fusion proteins or GST alone bound to GSH beads were incubated with *in vitro* translated, radiolabelled MRE11 for 90 min at 4°C. Beads were washed after the binding reaction and eluates analysed by SDS-PAGE followed by Coomassie staining (GST bait input detection, lower panel) and fluorography (binding reaction, upper panel). The running positions of the molecular mass markers (in kDa), the GST-tagged proteins, and MRE11 are indicated. in│ 10% of the MRE11 used in the binding reaction. **C**│ H1299 E6APi (stable downregulation of E6AP by RNAi) cells were transfected with expression constructs encoding for HA-tagged proteins as indicated. 24 h post-transfection, the lysates were prepared and adjusted according to the transfection efficiency (β-galactosidase activity). Samples were analysed by SDS-PAGE followed by western blot analysis and proteins were detected using an αHA.11 antibody. The E6 proteins in complex with the catalytically inactive E6AP mutant (C820A) are unable to degrade MRE11, suggesting an E6-E6AP dependent degradation of MRE11. The running positions of the molecular mass markers (in kDa) and the HA-tagged proteins are indicated.

3.3 The RhoA GTPase family and the E6-E6AP ligase complex

Of the RhoA subfamily of small GTPases, RhoA and RhoC were identified by Ebner et al. (2020) as potential substrate proteins of 11 E6-E6AP (RhoA) and 16 E6-E6AP (RhoA and RhoC) (**Table 1**). RhoB was not identified, which may be due to the notions that it is indeed not a substrate or that its endogenous levels are too low in HaCaT cells, the cell line used by Ebner et al. (2020). Indeed, basal RhoB levels are reported to be very low in HaCaT cells compared to the other Rho proteins (Canguilhem et al. 2005). Additionally, RhoB is more rapidly degraded than RhoA and RhoC by the proteasome, resulting in an overall shorter half-life (Zalcman et al. 1995).

Due to the high similarity between RhoA and RhoC (**Figure 14A**), RhoA was chosen to be investigated in initial experiments, while RhoC was included later on for reasons of completeness. While it was not identified by Ebner et al. (2020), RhoB was also included to cover the whole RhoA subfamily of GTPases. To determine if E6-E6AP specifically target RhoA subfamily members, Rac1 and Cdc42 were included as prominent members of other Rho GTPase subfamilies (**Figure 5**, **Figure 14B**). Overall, the five tested Rho family GTPases share high sequence similarity, with deviations mainly in the C-terminal region (**Figure 14A**).

As described in chapter 1.4.2.1 ‘Role in cancer development’, Rho GTPases are presumably of high relevance in an HPV-positive context with respect to the development of cervical cancer. This is the reason for investigating the interaction of RhoA and RhoA subfamily members with the HPV E6-E6AP complex in more detail. Moreover, the importance of undisturbed RhoA regulation in neurons is highlighted in chapter 1.4.2.2 ‘Role in neuronal processes’. Thus, RhoA family members may represent highly interesting potential interactors or substrate proteins of E6AP alone as well.

3.3.1 RhoA as potential substrate of E6AP or 16 E6-E6AP

3.3.1.1 Ubiquitination of *in vitro* translated RhoA

To determine if RhoA is a substrate protein of E6AP alone, 11 E6-E6AP and/or 16 E6-E6AP, a ubiquitination assay with *in vitro* translated, radiolabelled RhoA was performed in the presence of UBA1, UbcH7, and His-E6AP as well as the GST-E6 proteins for 90 min at 30°C. In the presence of E6AP alone, RhoA is mainly monoubiquitinated (**Figure 15A**, arrow). Ubiquitination is strongly increased in the presence of 16 E6. The 16 E6-E6AP complex leads to RhoA polyubiquitination, which is visualized by the loss of the unmodified form of RhoA and by the smear to higher molecular mass species representing polyubiquitinated forms of RhoA in the fluorographic readout (**Figure 15A**, asterisk). The presence of 11 E6 in addition to E6AP has hardly any effect on RhoA ubiquitination. Since the purification of active GST-11 E6 protein preparations has proven to be complicated in the past (unpublished observation), ubiquitination of *in vitro* translated RhoA was tested with multiple GST-11 E6 protein preparations.

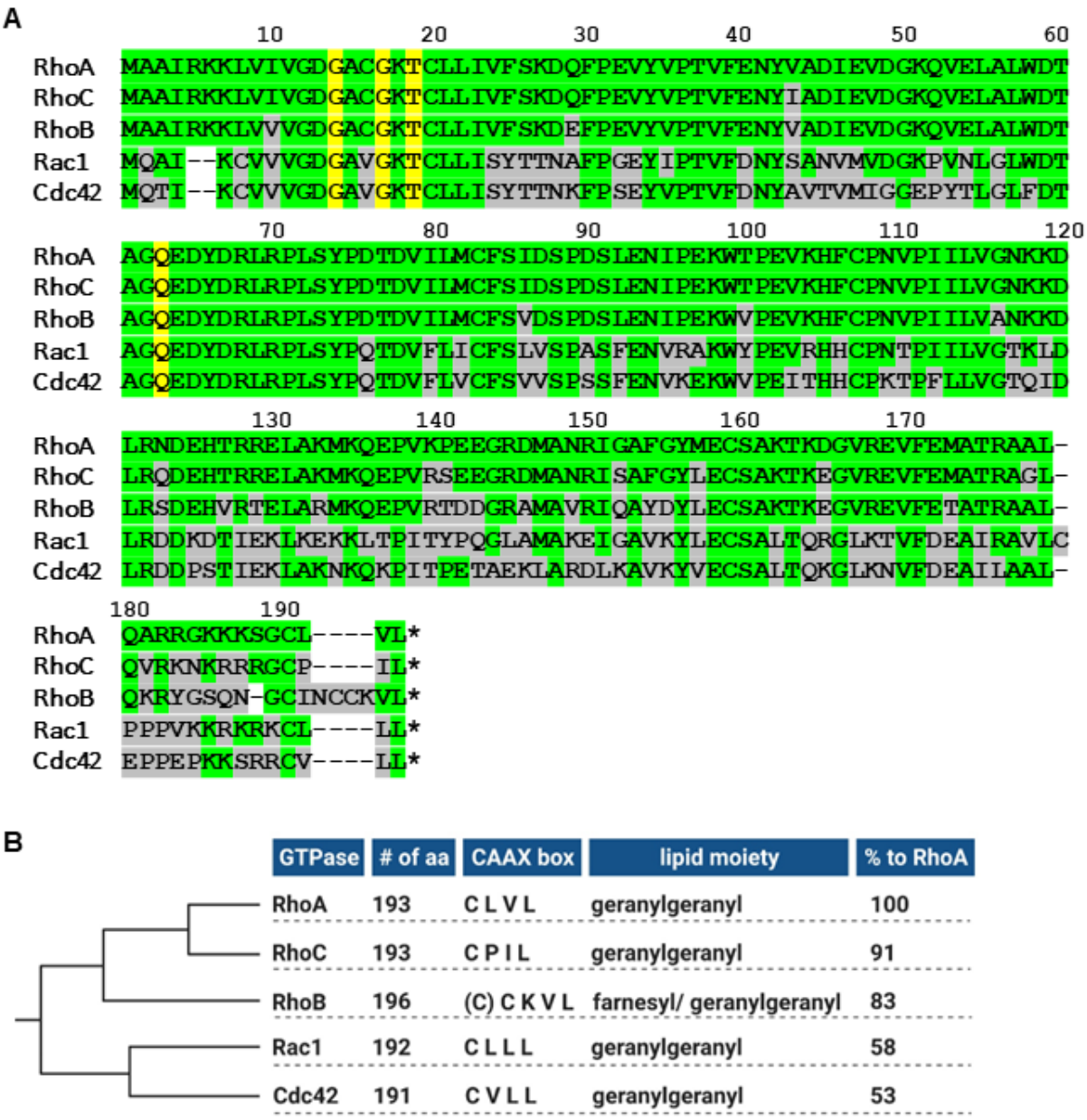

Figure 14: Comparative analysis of relevant GTPases. A| Sequence alignment of RhoA, RhoC, RhoB, Rac1, and Cdc42. Identical amino acids are highlighted in green, amino acids diverging from the RhoA sequence are highlighted in grey. The residues which are involved in GTP/GDP-binding and of which alanine point mutations were created (G14, G17, T19, and Q63) are highlighted in yellow and are conserved between the five different GTPases. The numbering is according to RhoA. (*) represents the stop codon. **B**| Detailed information on protein length, the CAAX box, the type of lipidation and the sequence percentage of a given GTPase that is identical to RhoA. The simplified phylogenetic tree on the left indicates the evolutionary relationship between the GTPases in respect to RhoA.

These were simultaneously used for ubiquitination assays of other proteins, like iASPP, where a stimulatory effect mediated by 11 E6 could be observed. This indicates that RhoA is at least *in vitro* not a substrate of the 11 E6-E6AP complex, yet this is not in line with the original data obtained in the mass spectrometric analysis (**Table 1** and Ebner et al. (2020)). GST-16 E6, on the other hand, is able to stimulate some polyubiquitination of RhoA even in the absence of recombinant E6AP and to a lesser extent even without additional ubiquitin and E6AP. This indicates that the levels of

endogenous E6AP and ubiquitin present in the reticulocyte lysate (Huibregtse, Scheffner, and Howley 1991) used for *in vitro* translation of RhoA, are already sufficient to promote 16 E6-mediated RhoA ubiquitination.

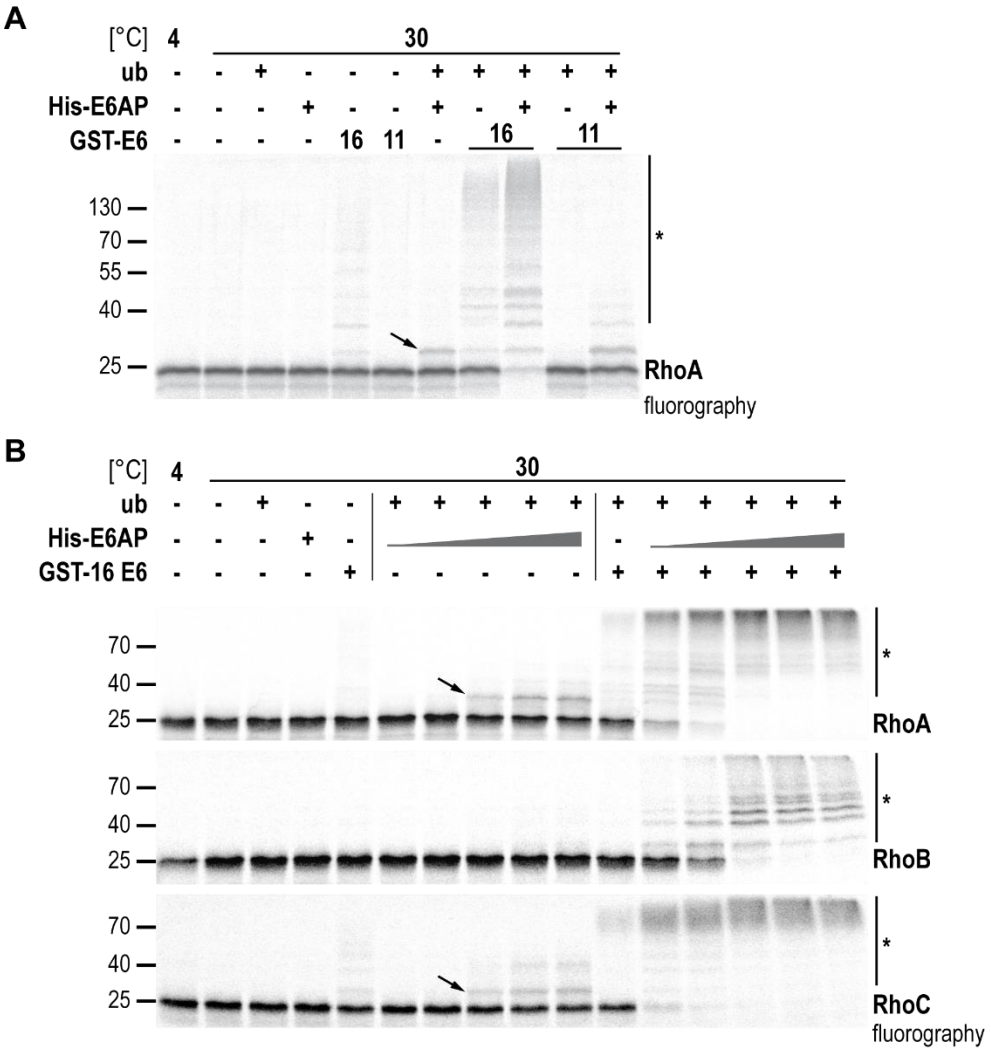

Figure 15. All RhoA subfamily members are substrates of 16 E6-E6AP. A| *In vitro* translated, radiolabelled RhoA was incubated with UBA1 and UbcH7 in the presence and absence of His-E6AP, GST-tagged E6 proteins, and ubiquitin (ub) for 90 min at 30°C as indicated. The reactions were stopped with Laemmli buffer (see 0) and the samples were analysed by SDS-PAGE followed by fluorography. The running positions of the molecular mass markers (in kDa), the unmodified form (RhoA), the monoubiquitinated form (arrow), and polyubiquitinated forms (*) are indicated. **B**| *In vitro* translated, radiolabelled RhoA, RhoB, and RhoC were incubated with UBA1 and UbcH7 in the presence and absence of increasing amounts of His-E6AP, GST-tagged 16 E6, and ubiquitin (ub) for 90 min at 30°C as indicated. The reactions were stopped with Laemmli buffer (see 0) and the samples were analysed by SDS-PAGE followed by fluorography. The running positions of the molecular mass markers (in kDa), the respective unmodified forms (RhoA, RhoB, RhoC), polyubiquitinated forms (*), and E6AP-mediated monoubiquitination (arrow) are indicated.

Next, *in vitro* translated RhoA, RhoB, and RhoC were compared in a ubiquitination assay with increasing amounts of E6AP in the presence and absence of GST-16 E6 (**Figure 15B**). Overall, the RhoA and RhoC ubiquitination patterns look very similar, while RhoB seems to be less well accepted as substrate protein by the 16 E6-E6AP

complex, as higher amounts of E6AP are required for unmodified RhoB to disappear and the polyubiquitination smear (asterisk) is less pronounced.

Similarly, E6AP alone is able to catalyse monoubiquitination of RhoA and RhoC (**Figure 15B**, arrows), but not of RhoB. In the presence of ubiquitin, 16 E6 stimulates some RhoA and RhoC polyubiquitination with only the endogenous reticulocyte lysate E6AP present. With different E6AP and GST-16 E6 protein preparations the tendency of RhoA and RhoC showing stronger ubiquitination than RhoB was consistently observed (data not shown).

3.3.1.2 Ubiquitination of bacterially expressed GST-RhoA

In vitro translated proteins are produced in a cell-free eukaryotic system that is also capable of posttranslationally modifying the protein of interest (POI), while bacterially expressed proteins do not bear PTMs observed in eukaryotes. Therefore, in addition to *in vitro* translated RhoA, ubiquitination experiments were performed with bacterially expressed GST-tagged RhoA. To this end, a time course ubiquitination assay (0-120 min) was performed under standard ubiquitination conditions (see 5.2.4.1 'Ubiquitination assays'). Whole reaction mixtures were analysed by SDS-PAGE followed by Coomassie staining. In line with the data obtained with *in vitro* translated RhoA (**Figure 15A**), GST-RhoA is primarily monoubiquitinated by E6AP in the absence of 16 E6 (**Figure 16A**, arrow). The presence of 16 E6-E6AP causes a distinct ubiquitination ladder (asterisk), which represents probably multi-monoubiquitinated forms of GST-RhoA. This was also observed in the ubiquitination of *in vitro* translated RhoA, but to a lesser extent (**Figure 15A**). Evaluation of potential GST-RhoA polyubiquitination is impeded in Coomassie stained gels, as polyubiquitinated forms of RhoA cannot be distinguished from polyubiquitinated E6AP resulting from E6AP auto-ubiquitination (**Figure 16A** and **C**, double asterisk). Nonetheless, the presence of GST-16 E6 enhances E6AP-mediated GST-RhoA ubiquitination, as is indicated by the reduction in levels of unmodified GST-RhoA. While ubiquitination of RhoA is increased in the presence of 16 E6-E6AP over time, less ubiquitin appears to be consumed in the presence of E6 over time (**Figure 16A** and **B**). This unexpected observation was confirmed by quantification of ubiquitin levels relative to the ubiquitin input (**Figure 16B**). Comparison of lanes 5-6 (in absence of 16 E6) to 12-13 (in presence of 16 E6) shows that more ubiquitin remains at later time points in the samples with 16 E6.

Ubiquitination assays with GST-RhoA and increasing amounts of E6AP in presence and in absence of GST-16 E6 show similar tendencies (**Figure 16C**). E6AP-mediated monoubiquitination of GST-RhoA (**Figure 16C**, arrow) is stimulated by GST-16 E6, while ubiquitin consumption is decreased in the presence of GST-16 E6 (**Figure 16C** and **D**). Comparison of lanes 2-3 (in absence of 16 E6) to 9-10 (in presence of 16 E6) shows more remaining ubiquitin with increasing E6AP amounts in the samples with GST-16 E6. This unexpected phenomenon is further investigated and discussed in chapter 3.3.5 'Inhibitory effect on 16 E6 stimulation'.

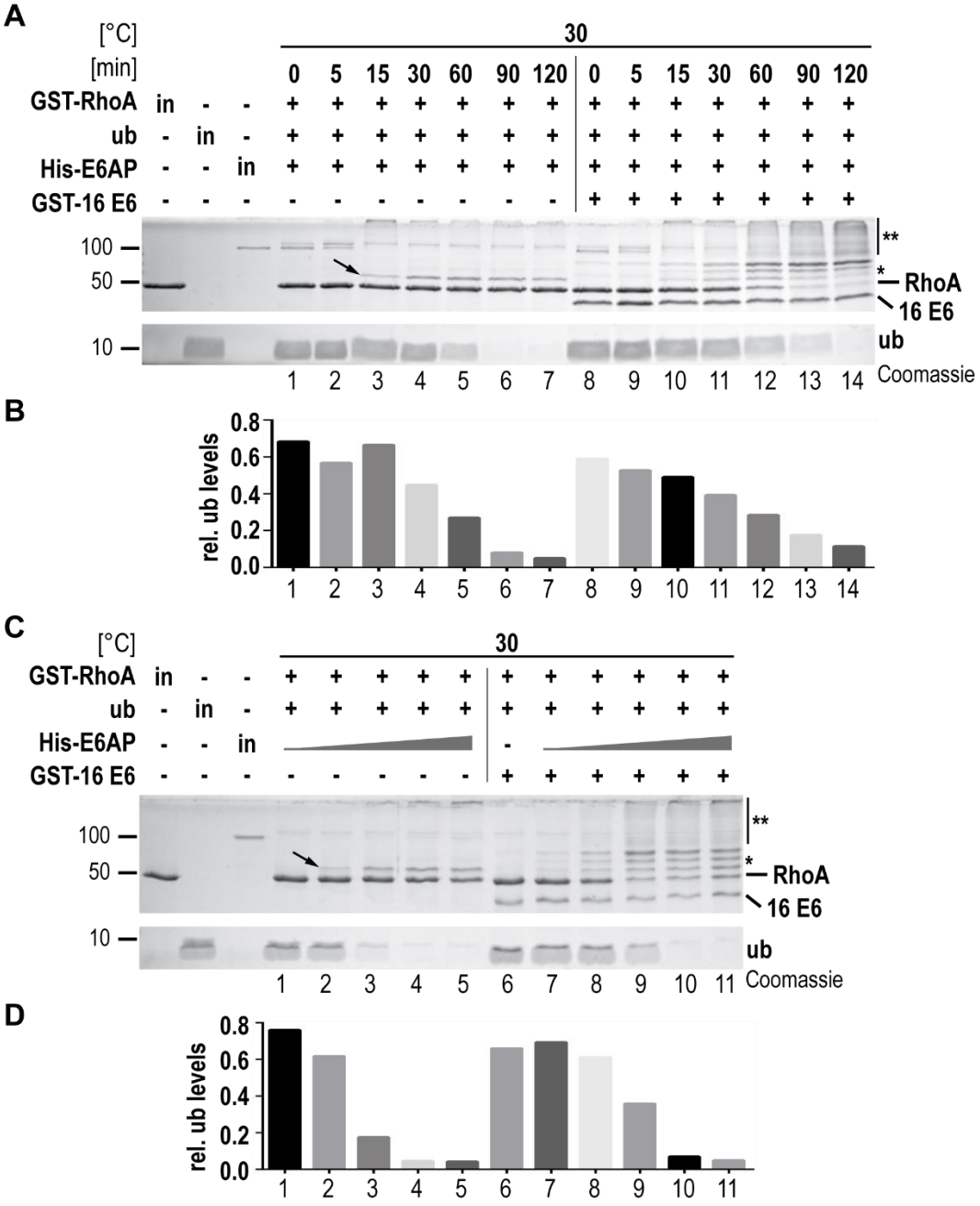

Figure 16. HPV 16 E6 in complex with E6AP stimulates GST-RhoA multi-mono-ubiquitination and polyubiquitination. A| GST-tagged RhoA (RhoA) was incubated with UBA1 and UbcH7 in the presence and absence of His-E6AP, GST-tagged 16 E6 (16 E6), and ubiquitin (ub) at 30°C as indicated. The reactions were stopped at different timepoints with Laemmli buffer (see 0) and the samples were analysed by SDS-PAGE followed by Coomassie staining. The running positions of the molecular mass markers (in kDa), the unmodified form (RhoA), mono-/ multi-monoubiquitinated RhoA (*), polyubiquitinated proteins (**), 16 E6, and ub are indicated. **B**| Quantification of the relative ub levels of (**A**) in reference to the ub input level. **C**| GST-tagged RhoA (RhoA) was incubated with UBA1 and UbcH7 in the presence and absence of GST-tagged 16 E6 (16 E6), ubiquitin (ub), and increasing amounts of His-E6AP at 30°C as indicated. The reactions were stopped and the samples were analysed by SDS-PAGE followed by Coomassie staining. The running positions of the molecular mass markers (in kDa), the unmodified form (RhoA), mono-/ multi-monoubiquitinated RhoA (*), polyubiquitinated proteins (**), 16 E6, and ub are indicated. **D**| Quantification of the relative ubiquitin (ub) levels of (**C**) in reference to the ub input level.

Ubiquitination assays with GST-RhoA were also performed with UbcH5b instead of UbcH7, but this did not render different results (data not shown). Both E2 enzymes are known to support E6AP-mediated ubiquitination (Nuber et al. 1996; Scheffner, Huibregtse, and Howley 1994), but in contrast to UbcH5b, UbcH7 is unable to catalyse the formation of isopeptide bonds (Huang et al. 1999; Houben et al. 2004).

To determine, if RhoA ubiquitination is specific for E6AP, RhoA ubiquitination assays were performed with another HECT E3 ligase, HECT-H9, also known as HECT, UBA and WWE domain-containing protein 1 (HUWE1). Due to its large size (~480 kDa), an N-terminally truncated GST-tagged version of HECT-H9 was used (amino acids 3474-4374, including the HECT domain). HECT-H9 targets a number of proteins for degradation, including the Myc oncoprotein (Zhao et al. 2008; Adhikary et al. 2005). Analogous to E6AP, HECT-H9 has also been implicated in neurodevelopmental disorders (Froyen et al. 2008) and is therefore an ideal control for our experiments. HECT-H9 is unable to ubiquitinate GST-RhoA or *in vitro* translated RhoA with either UbcH5b or UbcH7, while its activity was confirmed in autoubiquitination assays (data not shown). This implies that RhoA is not ubiquitinated by HECT E3 ligases per se, but rather the effect may be at least partly specific for E6AP.

3.3.1.3 Which RhoA lysine residues are targeted for ubiquitination by 16 E6-E6AP *in vitro*?

The appearance of the distinct ladder of ubiquitinated forms of RhoA (*in vitro* translated: **Figure 15A**; GST-tagged: **Figure 16A** and **C**, asterisks) in presence of 16 E6-E6AP as well as the prominent monoubiquitination of RhoA mediated by E6AP alone (**Figure 15A**, **Figure 16A** and **C**, arrows) gave rise to the question, whether RhoA is ubiquitinated at defined lysine residues and whether different lysine residues are targeted by E6AP alone and by the 16 E6-E6AP complex. To determine which of the 17 lysine residues of RhoA serve as ubiquitin acceptors in E6AP-mediated and 16 E6-E6AP-mediated ubiquitination, a collaboration with Jasmin Jansen from the AG Stengel was started. As in the previous chapter, a ubiquitination assay with GST-RhoA WT was performed with E6AP in the absence and presence of GST-16 E6 (**Figure 17A)**. The experiment was performed in technical duplicates (two different ubiquitination assays) and the Coomassie stained gel shown in **Figure 17A** is representative for both. Upon staining of the SDS-PA gel with colloidal Coomassie blue the bands labelled 1 to 8 were excised from the gel and each subjected to in-gel digestion (5.2.3.6 'In-gel digestion for mass spectrometric analysis'). Band 3 is relevant for the lysines targeted by E6AP alone, while bands 5-8 represent the 'ubiquitination ladder' in presence of 16 E6-E6AP. The samples were further processed, analysed by mass spectrometry, and screened for RhoA peptides with diGly motifs by J. Jansen. The results are summarized in **Figure 17B**; a detailed list of the results is provided in **Supplementary Table 1** for replicate (a) and in **Supplementary Table 2** for replicate (b). Surprisingly, in samples 1, 2, and 4, which should represent unmodified RhoA, also lysine residues with a diGly motif can be found. This might be due to cross-contamination during sample preparation, e.g. while cutting bands in close proximity on the SDS-PA gel, or during LC-MS/MS measurements. Of the 17 RhoA lysine

residues potentially ubiquitinated, 8 are found with high confidence (dark blue), 4 lysine residues are found with low abundant PSMs (light blue), and 5 are not found (yellow) (**Figure 17B**). The identified potential ubiquitination sites were mapped on the RhoA structure (**Figure 17C**). They do not cluster to a distinct 'surface patch' but appear to be randomly distributed over the whole protein. As a next step, all identified lysine (K) residues were each mutated to an arginine (R). Unlike lysine residues, arginine residues cannot be ubiquitinated; yet due to similar physicochemical properties (i.e. positive charge), the stability and function of RhoA should not or only mildly be affected. The lysine residues, which were not found with a diGly motif (marked in yellow in **Figure 17B** and **C**), were not mutated.

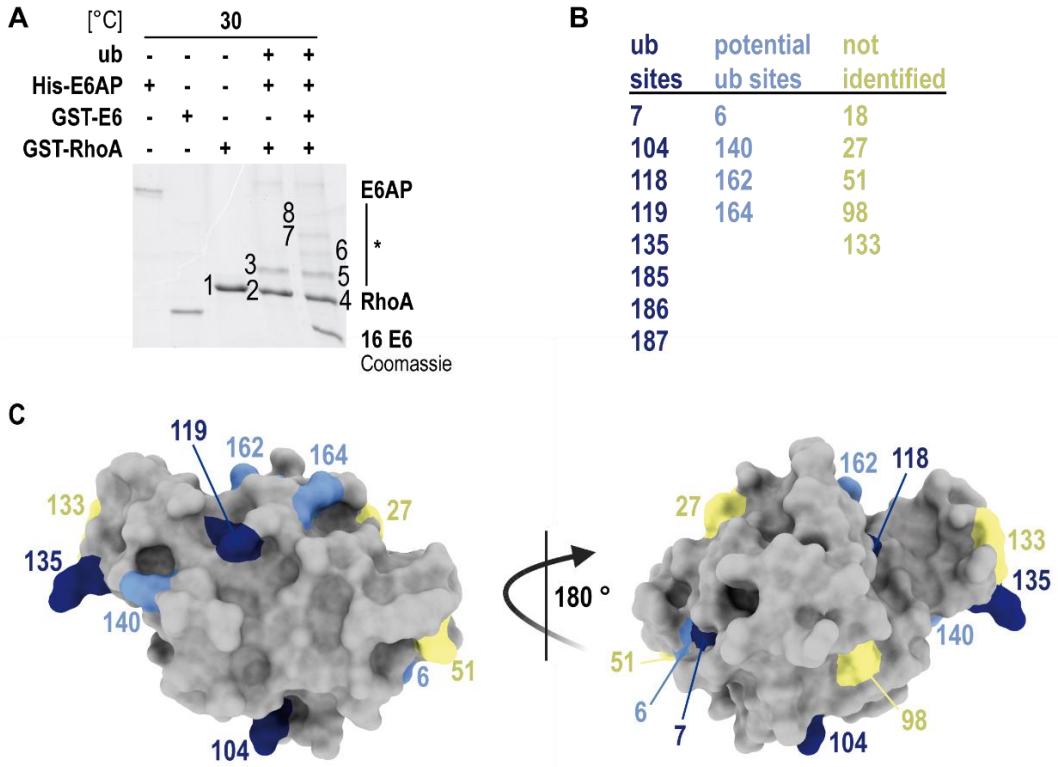

Figure 17. Multiple lysine residues of RhoA are potential targets for ubiquitination by 16 E6-E6AP. A⎪ The ubiquitination assay of GST-tagged RhoA (RhoA) with UBA1 and UbcH7 in the presence and absence of His-E6AP, GST-tagged 16 E6 (16 E6), and ubiquitin (ub) was incubated at 30°C as indicated. The reactions were stopped with Laemmli buffer (see 0) and the samples were analysed by SDS-PAGE followed by colloidal Coomassie staining. The running positions of the unmodified form (RhoA), ubiquitinated forms (*), E6AP, and 16 E6 are indicated. Bands of ubiquitinated RhoA forms (1-8) were each cut from the gel and destained. In biological duplicates, an in-gel digestion of each band was performed and the samples subsequently subjected to mass spectrometric analysis. **B**⎪ Of the 17 lysine residues in total of RhoA, eight were found with diGly motifs as ubiquitination sites (ub sites) with high confidence (dark blue), four lysine residues were identified with low abundance as potential ub sites (light blue), and five lysine residues were not identified in the MS/MS analysis (yellow). **C**⎪ Indicated are the lysine residues mentioned in **B**⎪ on the RhoA surface structure (grey) (PDB 1A2B) with the same colour code. The structure was modified with UCSF ChimeraX (Goddard et al. 2018). Of note: K185, K186 and K187 were identified as ub sites with high confidence but are not present in the PDB structure. K18 is mostly hidden from the surface.

To reduce the amount of cloning, several double or triple lysine to arginine (KR) mutants were created in the beginning. With the mutants K6/7R, K118/119R, K162/164R, and K185-187R, more than one position could be investigated simultaneously. With these constructs as basis, RhoA variants with multiple KR mutations at different positions were also created. Moreover, the KR mutant constructs were initially generated in the context of the RhoA variant containing the G14V mutation, which results in a predominantly GTP-bound RhoA protein (Chen et al. 2022). Later, the KR mutations identified to be of importance were also introduced into RhoA WT.

The mutant constructs were *in vitro* translated and investigated in various ubiquitination assays in the presence and absence of E6AP and GST-16 E6 (**Figure 18A** and **B**). A comparison with RhoA WT reveals that the G14V mutation does not affect the behaviour of the KR mutants (data not shown). A selection of the generated RhoA KR mutants is shown in **Figure 18A** and **B** and the results obtained demonstrate that ubiquitination of RhoA is strongly impaired whenever K185-K187 are mutated. The mutation of each single lysine residue at the RhoA C terminus (K185, K186, K187) and the double KR mutants (K185/186R, K185/187R, K186/187R) reveal that 16 E6-E6AP is unable to distinguish between these residues and only mutation of all three lysine residues strongly impairs RhoA ubiquitination (data not shown). The mutation of any other lysine residue does not have an impact on the ubiquitination of RhoA by E6AP alone or by 16 E6-E6AP. Since RhoA has been described to be ubiquitinated at K135 by the SCF^{FBXL19} complex and by SMURF1 at K6 and K7 (Ozdamar et al. 2005; Wang et al. 2003), these residues were also mutated. RhoA K6/7/135R is ubiquitinated as efficiently as RhoA WT by 16 E6-E6AP (**Figure 18B**).

Due to their high similarities, it was hypothesized that the other RhoA subfamily members, RhoB and RhoC, as well as Rac1 are also targeted for ubiquitination by 16 E6-E6AP at their C terminus. An overview of the C-terminal amino acids of the relevant proteins is shown in **Figure 19A**. The lysine residues of each protein are highlighted and the respective KR mutants were created for RhoB (K181R and K194R), RhoC (K183R, K185R, and K183/185R), and Rac1 (K183/184/186/188R). For RhoB, the K162/164R mutation was created additionally, since RhoB is known to be polyubiquitinated at K162 and K181 by the CUL3-CTD10 RING ligase complex (Kovačević et al. 2018) and since these residues were identified for RhoA in the original mass spectrometric analysis (**Figure 17B**). Even though RhoC is known to be ubiquitinated by multiple ligases (Kholmanskikh, Singh, and Ross 2022; Wu et al. 2020; Xu et al. 2021), no specific target lysine residues have been identified so far. For this reason, no additional control RhoC KR mutants were created.

In line with the data obtained for RhoA, 16 E6-E6AP-mediated ubiquitination of RhoB (**Figure 18C**), RhoC (**Figure 18D**), and Rac1 (**Figure 18E**) is impaired for the C-terminal KR mutants. For RhoB, it has to be considered that the K194 residue lies within its CAAX box (C<u>K</u>VL) and is therefore not present in the active and processed protein. The mutation of RhoB K181R alone has no effect on RhoB ubiquitination (**Figure 18C**). This may imply that RhoB can only be affected by 16 E6-E6AP mediated ubiquitination before it is processed and the KVL residues are proteolytically removed.

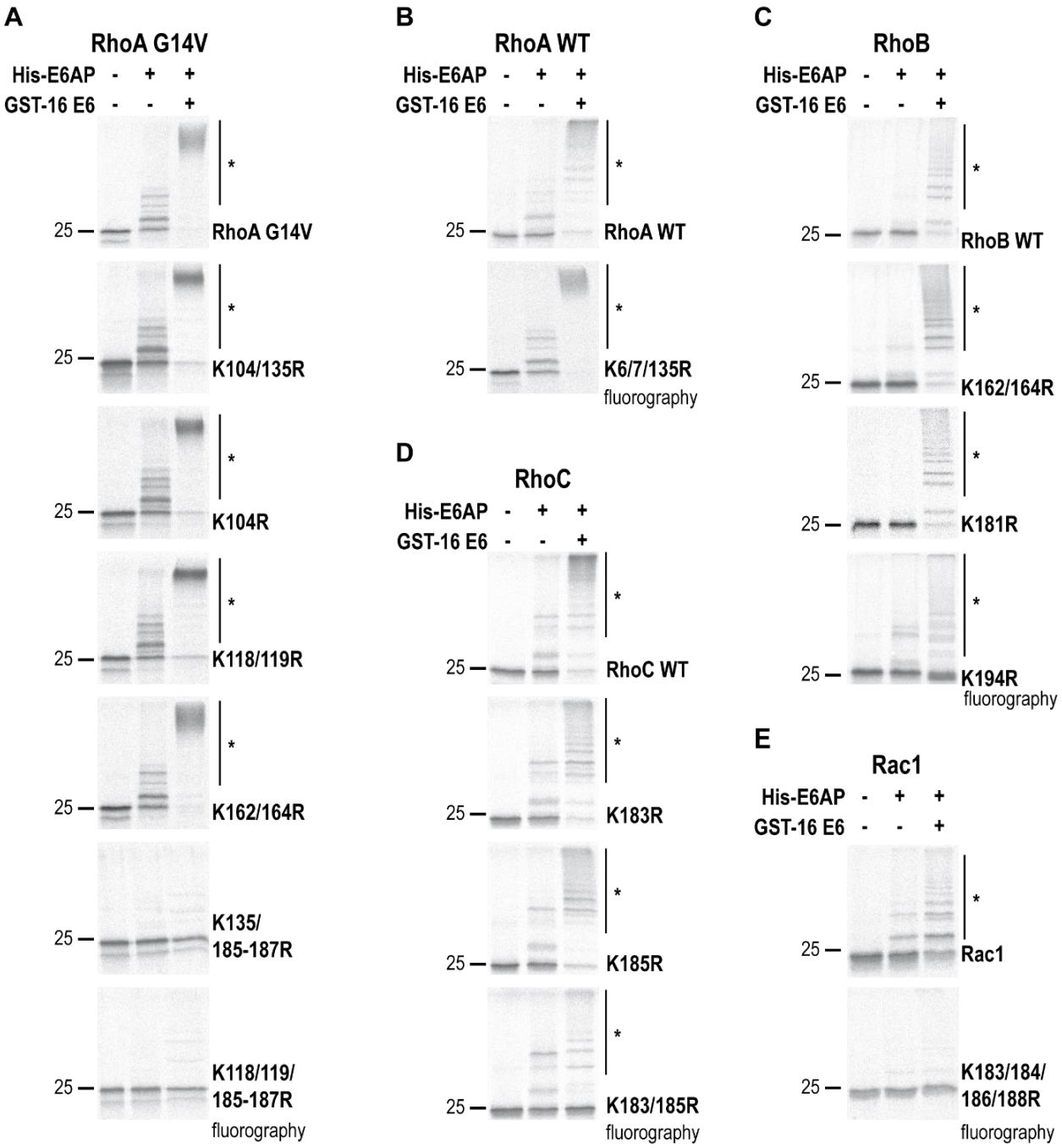

Figure 18. RhoA family members are primarily ubiquitinated at their C terminus by 16 E6-E6AP. *In vitro* translated, radiolabelled Rho proteins were incubated with UBA1, UbcH7, and ubiquitin in the presence and absence of His-E6AP and GST-tagged 16 E6 for 90 min at 30°C as indicated. The reactions were stopped with Laemmli buffer (see 0) and the samples were analysed by SDS-PAGE followed by fluorography. The running positions of the molecular mass marker (in kDa), the respective unmodified forms and the polyubiquitinated forms (*) are indicated. The ubiquitination assays of **A**| RhoA G14V Lys to Arg (KR) mutants, **B**| RhoA WT KR mutants, **C**| RhoB KR mutants, **D**| RhoC KR mutants and **E**| the Rac1 KR mutant show a specific ubiquitination of Rho proteins at their C terminus by 16 E6-E6AP. The ubiquitination assays of RhoA G14V K104R, K118/119R, K162/164R, K135/185-187R, and K118/119/185-187R were performed by Theresia Eich during the VTK 2022 under my supervision.

Mutation of K183 and K185 to R in RhoC abolishes RhoC ubiquitination almost completely (**Figure 18D**). While the levels of unmodified RhoC remain similar to those in the input, some polyubiquitinated species (**Figure 18D**, asterisk) can still be observed. This also applies for RhoB K194R and to a lesser extent for RhoA K185-187R and suggests that, although the C-terminal residues are the primary target of 16 E6-E6AP, other lysine residues can also be ubiquitinated though with little efficiency. In contrast to RhoA K185-187R, the E6AP-mediated mono- or multi-monoubiquitination of RhoC is not impaired with the RhoC K183/185R mutation (**Figure 18D**), and in line with the data obtained for RhoA, 16 E6-E6AP is unable to distinguish between K183 and K185 of RhoC (**Figure 18D**).

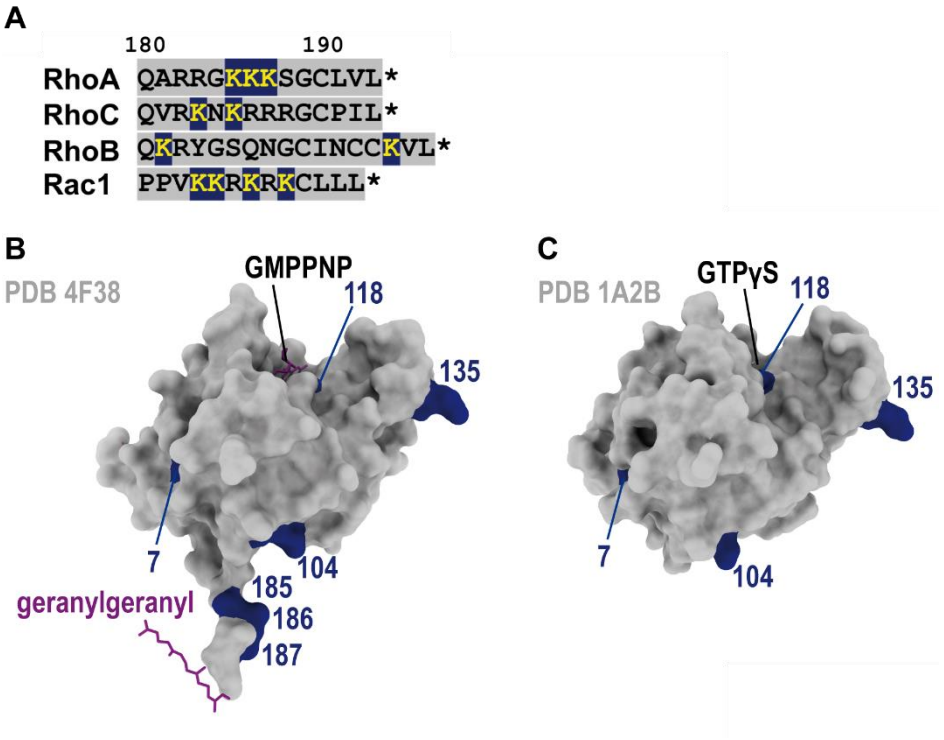

Figure 19. Detailed insights into Rho GTPase C-termini. A| Sequence alignment of RhoA, RhoC, RhoB, and Rac1. The C-terminal lysine residues are highlighted in yellow on dark blue background: RhoA K185, K186, K187; RhoC K183, K185; RhoB K181, K194 (located in the CAAX box); Rac1 K183, K184, K186, K188. The numbering is applicable to all listed Rho proteins. (*) represents the stop codon. **B**| Surface structure of RhoA according to PDB 4F30 and **C**| PDB 1A2B. Indicated are the lysine residues that were found with diGly motifs as potential ubiquitination sites with high confidence (dark blue). **B**| The geranylgeranylated (purple) RhoA (mus musculus) was complexed with the non-hydrolysable fluorescent GTP analogue GMPPNP. **C**| Structure of RhoA (homo sapiens) complexed with the non-hydrolysable GTP analogue GTPγS. The structures were modified with UCSF ChimeraX (Goddard et al. 2018).

The three C-terminal lysine residues of RhoA are not included in the crystal structure (PDB 1A2B, RhoA complexed with GTPγS, Ihara et al. (1998), **Figure 19C**) used to highlight the lysine residues on the RhoA surface in **Figure 17C**. So far, several different RhoA crystal structures have been published, for example in complex with GDP (e.g. PDB 1FTN, Wei et al. (1997)), in complex with the GEF Net1 (e.g. PDB 4XH9, Petit et al. (2018)), or in complex with downstream effector proteins (e.g. PDB 1S1C, complexed with ROCK, Dvorsky et al. (2004)). Neither of these structures

contains the very C terminus of RhoA, with all of them terminating roughly at position 180. This indicates a high structural variability in this region, possibly a flexible protrusion, which could therefore be readily accessible for the 16 E6-E6AP complex.

The geranylgeranylated form of Mus musculus RhoA in the presence of GMPPNP (a non-hydrolysable fluorescent GTP analogue) and in complex with RhoGDI, however, successfully captured the complete C-terminal region of RhoA (PDB 4F38) (Tnimov et al. 2012) (**Figure 19B**). The lipid modification seems to have a stabilizing effect on the otherwise flexible C-terminal region, therefore enabling the solution of its structure. Originally, the PDB 1A2B RhoA structure was chosen over the PDB 4F38 structure to display RhoA for multiple reasons. In 1A2B, the RhoA protein is of human origin, in absence of an interaction partner, and complexed with GTPγS rather than GMPPNP. Of the two GTP analogues, GTPγS has been suggested to be the more accurate mimic (Gasmi-Seabrook et al. 2010). Yet, considering that the C terminus of RhoA is ubiquitinated, the PDB 4F38 structure may be the better choice for visualisation.

3.3.1.4 GTP-RhoA is the preferred E6-E6AP substrate

When studying proteins like Rho GTPases whose conformation is subject to switches induced by distinct small molecules, the potential effect of the bound nucleoside di- or triphosphate on any phenomenon has to be considered. Therefore, we were interested whether the binding state affects the recognition of RhoA by E6AP alone and by the 16 E6-E6AP complex and thus ubiquitination of RhoA. One of the possible approaches is the introduction of distinct point mutations that result in an either predominantly GTP- or GDP-bound protein. As described in detail in the introductory part (1.4.4 ‘Frequently used Rho mutants’), the mutation of glycine at position 14 to a valine (G14V) converts RhoA into a dominantly active form (Chen et al. 2022). This mutation within the G1 domain affects the structural conformation of both switch regions and therefore abolishes the intrinsic and stimulated GTPase activity of RhoA (Ihara et al. 1998). The dominant-negative threonine to asparagine mutation at position 19 (T19N) renders the GTPase in an inactive state as its affinity for GDP is higher than for GTP (Farnsworth and Feig 1991).

In addition to the G14V mutant (see above), the T19N mutant was created and their ubiquitination over time was investigated in comparison to RhoA WT (**Figure 20A**). Although the results obtained look similar, the G14V mutant appears to be somewhat more efficiently ubiquitinated than RhoA WT, which in turn is a better substrate than the T19N mutant. Similarly, the intensity of the bands representing the respective unmodified RhoA variant shows differences, especially at 30 min. While there is hardly any unmodified RhoA G14V left, most of the T19N is not ubiquitinated yet (**Figure 20A**; asterisk). In the sample without additional ubiquitin, the 16 E6-E6AP complex and the ubiquitin that is present in the reticulocyte lysate used for the *in vitro* translation are sufficient for prominent RhoA G14V ubiquitination, already causing a reduction in the levels of unmodified protein. While literature (Ihara et al. 1998; Feig and Cooper 1988a) suggests the G14V and T19N mutants to predominantly bind GTP and GDP, respectively, the actual amount of bound nucleotide or the GTP/GDP ratio is unknown.

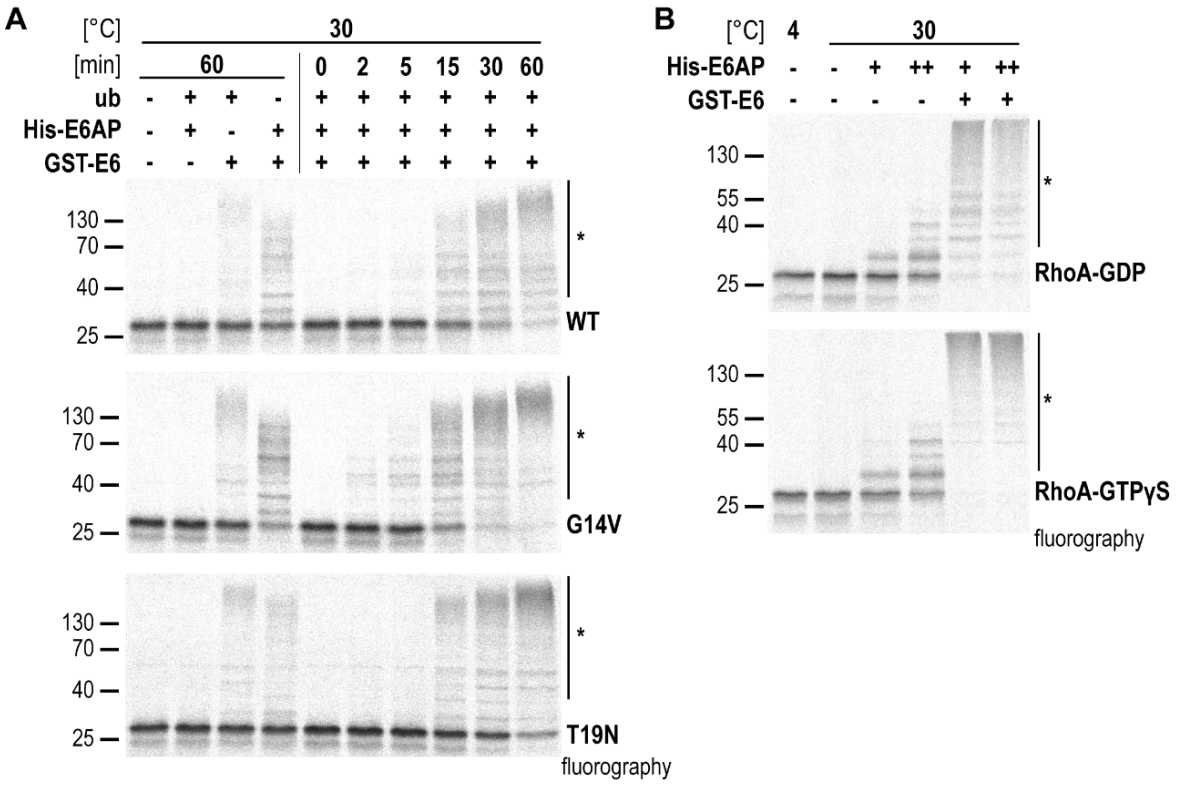

Figure 20. GTP-bound RhoA is the preferred 16 E6-E6AP substrate. A| *In vitro* translated, radiolabelled RhoA WT, G14V, or T19N were incubated with UBA1 and UbcH7 in the presence and absence of His-E6AP, GST-tagged 16 E6, and ubiquitin (ub) for different time points (0-60 min) at 30°C as indicated. The reactions were stopped with Laemmli buffer (see 0) and the samples were analysed by SDS-PAGE followed by fluorography. The running positions of the molecular mass markers (in kDa), the unmodified forms (WT, G14V, T19N), and the ubiquitinated forms (*) are indicated. **B**| *In vitro* translated, radiolabelled RhoA was subjected to guanine nucleotide exchange with either GDP or GTPγS. After the exchange, it was incubated with UBA1, UbcH7, and ubiquitin in the presence and absence of either 1 µM (+) or 5 µM (++) His-E6AP and GST-tagged 16 E6 for 90 min at 30°C as indicated. The reactions were stopped with Laemmli buffer (see 0) and the samples were analysed by SDS-PAGE followed by fluorography. The running positions of the molecular mass markers (in kDa), the unmodified forms (RhoA) and the ubiquitinated forms (*) are indicated.

With this in mind, the comparison of RhoA WT ubiquitination to that of RhoA G14V and T19N (**Figure 20A**) indicates that the WT protein resulting from the *in vitro* translation may be a mixture of GTP- and GDP-bound species. In addition to G14V and T19N, also the Q63L and G17A mutants were cloned. The Q63L mutant is often used analogous to G14V, as both share high structural similarities (Longenecker et al. 2003). In contrast to G14V, Q63L mainly affects the conformational integrity of the switch I region. In line with this, the ubiquitination of *in vitro* translated RhoA Q63L is highly similar to RhoA G14V (data not shown). The G17A mutation renders the GTPase unable to bind any guanine nucleotide, therefore mimicking the intermediate GEF-bound state of RhoA (García-Mata et al. 2006). In ubiquitination assays, RhoA G17A behaves similar to the T19N mutant (data not shown). Instead of using mutant RhoA proteins, it is also possible to actively exchange the existing GDP/GTP with GDP or GTPγS, a non-hydrolysable GTP analogue. The use of the GTP analogue is necessary, as unaltered GTP would be quickly hydrolysed to GDP. For the exchange,

the *in vitro* translated protein was incubated with GDP or GTPγS in presence of EDTA and $MgCl_2$ (see 5.2.4.4 'Guanine nucleotide exchange' for details). The actual binding state after the nucleotide exchange was not determined. A potential approach to do this in the future, could be the use of thin layer chromatography to resolve nucleotides on a cellulose resin (Grippo et al. 1965).

The 'exchanged' RhoA-GDP and RhoA-GTPγS proteins were subjected to ubiquitination assays in the presence or absence of GST-16 E6 with two different amounts of E6AP (**Figure 20B**, + = 1µM E6AP, ++ = 5 µM E6AP). A definite increase in 16 E6-E6AP-mediated polyubiquitination (**Figure 20**, asterisks) of RhoA-GTPγS can be observed in the lower panel in comparison to RhoA-GDP in the upper panel. This is indicated by the loss of the 'ubiquitination ladder' and the appearance of more high molecular mass RhoA species. The higher amount of E6AP does not further increase the polyubiquitination, indicating a saturation already with 1 µM of E6AP. In contrast to this, monoubiquitination and multi-monoubiquitination mediated by E6AP alone increase with the higher amount of E6AP, while the efficiency is not affected by the nucleotide exchange. This suggests that the actual nucleotide binding state has no impact on the recognition by E6AP alone, but GTP-bound RhoA is preferentially targeted by 16 E6-E6AP (**Figure 20B**). However, it has recently been suggested that GTP-bound RhoA G14V also exists in an additional inactive conformation (Lin et al. 2021). This might indicate that RhoA regulation is not quite as black and white as originally suggested with the GTP- or GDP-bound state.

3.3.1.5 Degradation of ectopic RhoA

To verify the effects observed in the *in vitro* ubiquitination assays, E6-E6AP-mediated degradation of the RhoA variants was investigated in transient transfection experiments. Expression constructs with N-terminally HA-tagged variants of the respective proteins were used for western blot analysis with an αHA.11 antibody. Degradation was tested in the non-small cell lung carcinoma cell line H1299 (which does not contain endogenous p53) and an H1299 E6APi cell line (containing a stable RNAi-mediated E6AP knockdown, **Supplementary Figure 1**). The fact that H1299 cells do not express endogenous p53 makes them a helpful cell line for the investigation of potential 16 E6-E6AP substrates, as p53 is the most prominent for 16 E6-E6AP and its presence could obscure any potential effects.

For the degradation assay, constructs encoding the respective RhoA variant, E6AP, and 16 E6 or 11 E6 were co-transfected in H1299 cells (**Figure 21A**). All three RhoA variants are degraded to some extent in the presence of 16 E6-E6AP, indicated by the reduction of the intensity of the input bands. In presence of 11 E6-E6AP, or E6AP alone, degradation cannot be observed. **Figure 21B** shows the quantification of the relative RhoA levels from **Figure 21A** in a bar graph, where the RhoA levels in absence of E6AP and E6 proteins serve as reference. In line with the *in vitro* data (**Figure 20**), the strongest degradation can be observed for the predominantly GTP-bound RhoA G14V mutant (**Figure 21A** and **B**, sample #10). Levels of RhoA T19N are overall lower for unknown reasons, even though twice the amount of plasmid DNA was transfected for RhoA T19N in comparison to RhoA WT and RhoA G14V. The degradation of HA-

RhoB and HA-RhoC variants in transient transfection experiments reveal similar results. The G14V mutants always show the strongest degradation and RhoB is overall only inefficiently degraded by 16 E6-E6AP (data not shown). This is in line with the RhoB data obtained from RhoB KR mutants, which indicates the importance of K194 within the proteolytically processed CAAX box for 16 E6-E6AP-mediated RhoB ubiquitination.

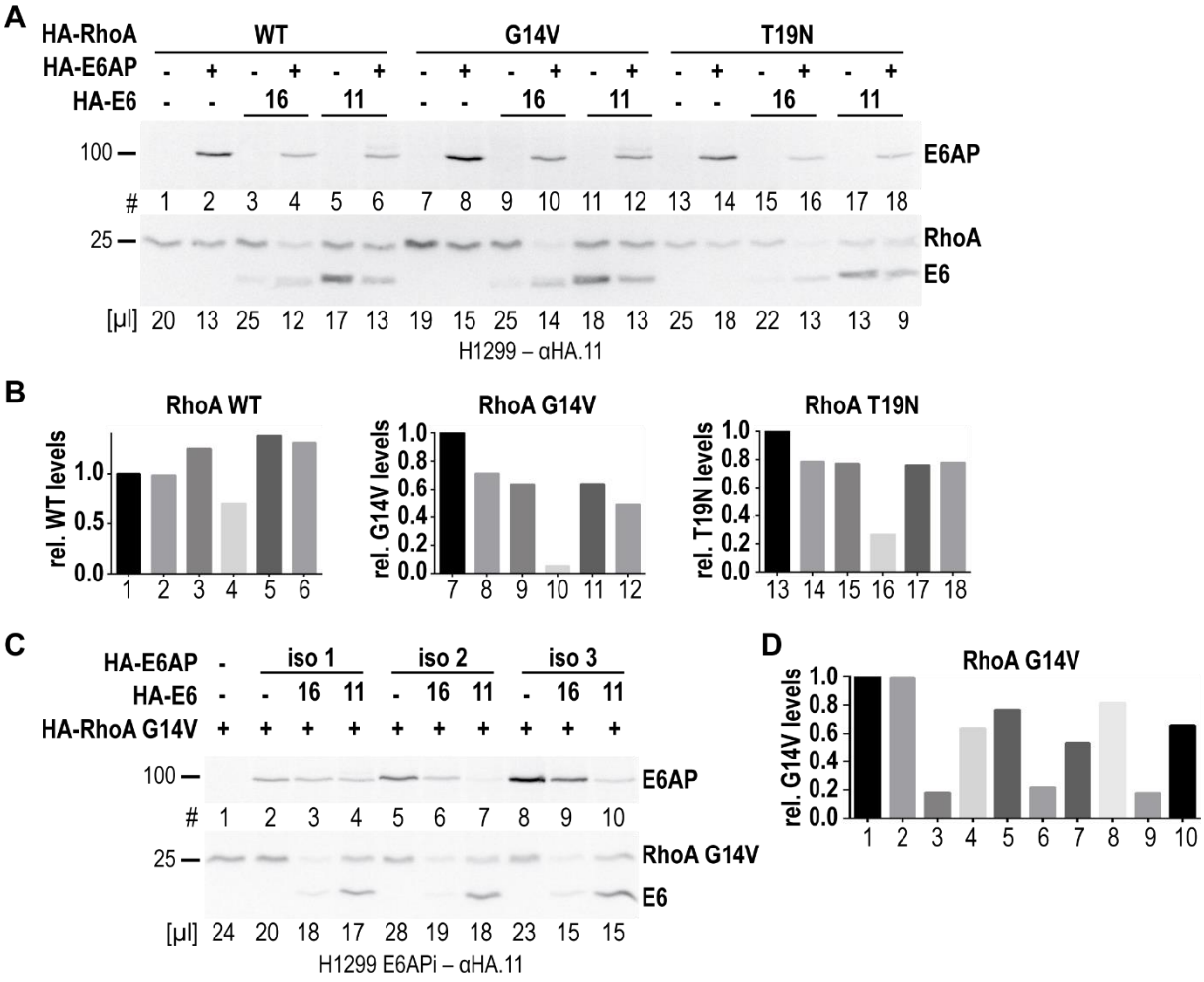

Figure 21. Ectopic RhoA is degraded by 16 E6-E6AP in H1299 cells. A│ H1299 cells were transfected with expression constructs encoding for HA-tagged RhoA variants, E6AP and E6 proteins as indicated. 24 h post-transfection, the lysates were prepared and adjusted according to the transfection efficiency (β-galactosidase activity). Samples were analysed by SDS-PAGE followed by western blot analysis and proteins were detected using an αHA.11 antibody. The running positions of the molecular mass markers (in kDa), the HA-tagged proteins, and the amount of lysate loaded of each sample (25 µl of the sample with the lowest β-gal assay value) are indicated. **B**│ Quantification of relative RhoA levels from (**A**), the sample #1 without 16 E6 and E6AP serves as reference. **C**│ H1299 E6APi (stable downregulation of E6AP by RNAi) cells were transfected with expression constructs encoding for HA-tagged RhoA G14V, 16 E6, and E6AP isoforms (iso) 1, 2, and 3 as indicated. 24 h post-transfection, the lysates were prepared and adjusted according to the transfection efficiency (β-galactosidase activity). Samples were analysed by SDS-PAGE followed by western blot analysis and proteins were detected using an αHA.11 antibody. The running positions of the molecular mass markers (in kDa), the HA-tagged proteins, and the amount of lysate loaded of each sample (28 µl of the sample with the lowest β-gal assay value) are indicated. **D**│ Quantification of relative RhoA levels from (**C**), the sample #1 without 16 E6 and E6AP serves as reference.

There are three different E6AP isoforms that differ in their N-terminal extension and are the result of alternative splicing of the *UBE3A* gene (Yamamoto, Huibregtse, and Howley 1997). In addition to the 852 amino acids of isoform 1 (in this study, 'E6AP' stands for isoform 1, unless stated otherwise), isoforms 2 and 3 contain 20 and 23 amino acids long N terminal extensions, respectively (Yamamoto, Huibregtse, and Howley 1997). The different isoforms show differential expression patterns in subcellular compartments, while the exact functional relevance of the extensions and the isoforms remains to be determined (Avagliano Trezza et al. 2019). To examine any potential E6AP isoform effects, the degradation of RhoA G14V was investigated in transient transfection experiments in H1299 cells with an RNAi-mediated E6AP knockdown (H1299 E6APi cells).

RhoA G14V is degraded by all three E6AP isoforms in presence of 16 E6 (**Figure 21C**). Quantification of the relative RhoA G14V levels confirms an identical effect of the E6AP isoforms on the RhoA G14V levels (**Figure 21D**). Furthermore, 11 E6 does not target RhoA G14V for degradation irrespective of the E6AP isoforms. In addition to 11 E6 and 16 E6, RhoA degradation was also tested in H1299 cells in presence of ectopic E6AP, the low-risk protein 6 E6, the high-risk 18 E6 oncoprotein, and 5 E6, which is derived from a beta-papillomavirus (de Villiers et al. 2004). While 18 E6 shows weak potential to stimulate RhoA degradation, 5 E6 and 6 E6 are like 11 E6 unable to target RhoA for degradation (**Supplementary Figure 2**). Transient transfection experiments including the catalytically inactive E6AP C820A mutant further reveal that RhoA degradation is dependent on an active E6AP enzyme (**Supplementary Figure 3**). Thus, RhoA appears to be targeted for proteasomal degradation in an E6AP-dependent manner.

In comparative transient transfection experiments, it is important that the amount of lysates analysed is adjusted according to transfection efficiency. To do so, a construct encoding β-galactosidase is consistently cotransfected. For unknown reasons, the values resulting from the β-galactosidase assay in almost all transient transfection experiments were the highest in samples where the expression constructs for HA-E6AP and HA-E6 are present and the lowest for the input samples where only the construct encoding the POI is present. Since the amount of lysate that is loaded onto the gels is adjusted according to these values, oftentimes the lowest signal on the western blot for a given protein is observed in the sample with E6AP and E6 (as the lowest amount of lysate is loaded), making interpretation of the results with respect to whether a protein is targeted for degradation or not difficult. The severity of the observed variations in β-galactosidase activity differs between different DNA preparations and cell passages, yet we have not been able to determine the exact underlying mechanism so far. As indicated in **Figure 21A** and **C**, the actual amount of lysate that was used for the western blot analysis varied after the adjustment according to the results of the β-galactosidase assay. Looking at **Figure 21A,** the loading variation seems to be acceptable, since the amount of lysate in e.g. lanes 10 and 12 is similar, while the levels of RhoA G14V differ notably. This indicates that the decrease in RhoA G14V levels is actually due to the 16 E6-E6AP-mediated degradation and not a loading artefact due to the β-galactosidase assay. Also in **Figure 21C**, comparable

amounts of lysate were loaded and thus, when comparing samples 3 to 4, 6 to 7, and 9 to 10, differences in RhoA G14V degradation can be observed in presence of 16 E6 or 11 E6. However, in some of the performed experiments, especially with some mutant Rho proteins, the loading differences are more severe (data not shown) and, thus, the data cannot easily be interpreted.

For this reason, as a second approach to investigate the degradation of transiently transfected proteins, the Rho mutants were cloned into a construct as a fusion with dihydrofolate reductase (DHFR) (Kühnle et al. 2013). In this construct, a C-terminally HA-tagged DHFR is followed by ubiquitin and the N-terminally HA-tagged POI – in this case RhoA. During translation, the fusion protein is cleaved after the C terminal glycine of ubiquitin by ubiquitin-specific proteases. This results in two separate and quantifiable proteins: DHFR-HA-ubiquitin and HA-RhoA. The ubiquitin within the fusion protein contains a K48R mutation, which prevents the formation of K48-linked ubiquitin chains and therefore the proteasomal degradation of the DHFR-HA-ubiquitin. This ensures stable levels of DHFR-HA-ubiquitin, which are then used as internal reference for any changes in HA-RhoA levels. For western blot analysis, equal amounts of the lysate were loaded and after detection, DHFR-HA-ubiquitin and HA-RhoA levels were quantified. The relative ratio of the HA-RhoA variants to DHFR-HA-ubiquitin was then calculated, with the ratio of HA-RhoA to DHFR-HA-ubiquitin in the absence of 16 E6-E6AP set to 100% for each RhoA variant. Multiple co-transfection experiments reveal highly variable and inconsistent results. While the relative ratio of the three different RhoA variants (WT, G14V, T19N) is decreased in the experiment to **Supplementary Figure 4A**, an increase in the ratio of relative RhoA levels can be observed in **Supplementary Figure 4B**. The fusion constructs were also cloned and tested with the DHFR N-terminally HA-tagged. This results in very low HA-DHFR-ubiquitin levels (data not shown) and was therefore not an alternative. Overall, it was not possible to obtain reproducible data from the DHFR-fusion construct co-transfection experiments.

One has to keep in mind that E6AP- and 16 E6-E6AP-mediated ubiquitination of RhoA might not only lead to proteasomal degradation of RhoA but could also be of regulatory nature. For this reason, the potential effect of 16 E6 and E6AP on the activity and localisation of RhoA should be evaluated next. The former could be achieved with a bioluminescence resonance energy transfer (BRET) construct, containing RhoA coupled to a fluorophore and a Rho binding domain (RBD) coupled to a luciferase. With this setup, only active RhoA would lead to BRET signals, as it is able to interact with the RBD. Additionally, the phosphorylation state of downstream RhoA targets can be exploited as a RhoA activity readout, like the phosphorylation of the myosin phosphatase target subunit 1 (MYPT1). MYPT1 is known to be phosphorylated by the RhoA effector kinase family ROCK (Hartmann, Ridley, and Lutz 2015), which in turn are activated by RhoA.

To circumvent the ‘sample loading problem’ arising from the adjustment according to the β-galactosidase assay, the degradation of endogenous RhoA could be evaluated. For this, cells would need to be transfected with constructs encoding for differentially fluorescently labelled 16 E6 and E6AP proteins. Untransfected cells and cells transfected with either 16 E6, E6AP, or both proteins could subsequently be separated

by cell sorting. After lysate adjustment via a BCA assay, the detection of endogenous RhoA via western blot analysis in samples containing equal amounts of cell lysate would give direct insight into 16 E6-E6AP mediated degradation of endogenous RhoA (and RhoB, RhoC).

3.3.2 RhoA as interaction partner of E6-E6AP – coprecipitation analyses

After establishing the GTPase RhoA and its family members RhoB and RhoC as ubiquitination targets of 16 E6-E6AP *in vitro* and as potential targets for proteasomal degradation *in cellula*, the next step was to check whether the formation of stable complexes is detectable in *in vitro* coprecipitation experiments.

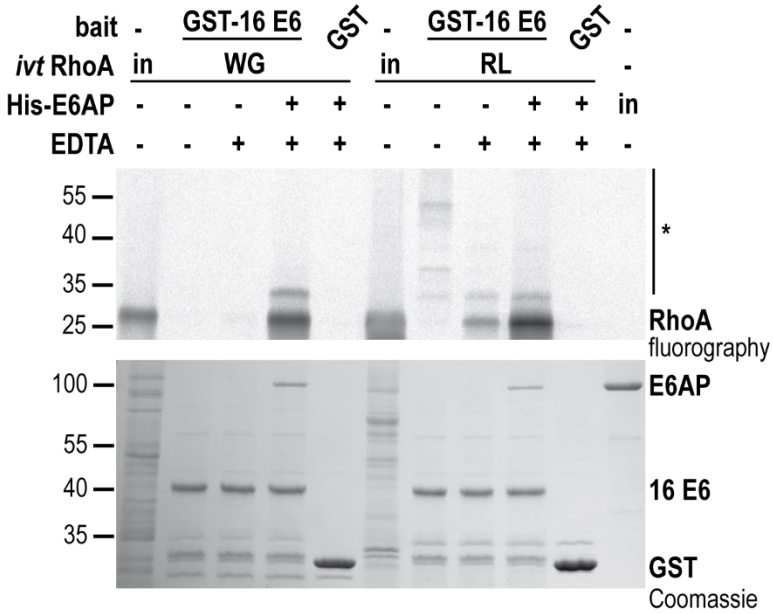

Figure 22. RhoA, E6AP and 16 E6 form a stable ternary complex. The GST-16 E6 fusion protein or GST alone bound to GSH beads were incubated with *in vitro* translated, radiolabelled RhoA for 90 min at 4°C in the presence or absence of His-E6AP and 20 mM EDTA as indicated. The *in vitro* translation was either performed in wheat germ extract (WG) or in rabbit reticulocyte lysate (RL). In contrast to RL, WG does not contain endogenous E6AP. Beads were washed after the binding reaction and the eluates were analysed by SDS-PAGE followed by Coomassie staining (GST bait input detection, lower panel) and fluorography (binding reaction, upper panel). The running positions of the molecular mass markers (in kDa), GST-16 E6 or GST, E6AP, RhoA, and ubiquitinated forms of RhoA (*) are indicated. in⎪ 10% of the RhoA and 100% of the His-E6AP used in the binding reaction.

GST or MBP coprecipitation experiments are a common method to determine the stable interaction of proteins. For this, the GST- or MBP-tagged bait protein is expressed in bacteria (see 5.2.2.1 ‘Expression and purification of recombinant proteins’) and subsequently purified and immobilized on glutathione or amylose resin. The bait protein is then incubated with the POI, which is either *in vitro* translated and radiolabelled (see 5.2.2.7 ‘*In vitro* translation’), or also bacterially expressed, but differentially tagged in comparison to the bait protein or untagged. The use of *in vitro* translated proteins enables a highly sensitive readout via fluorography (see 5.2.3.4 ‘Fluorography’), in which only the radioactively labelled protein is visualized. As source for *in vitro* protein transcription and translation, either rabbit reticulocyte lysate (RL) or

wheat germ extract (WG) can be used. In this thesis, we exploited the fact that, in contrast to RL, WG does not contain endogenous E6AP (Huibregtse, Scheffner, and Howley 1991).

In addition to the bait and prey proteins, the coprecipitation reaction contains an unrelated protein (either crude bacterial extract containing UbcH5b or BSA), as this was previously shown in our group to reduce background binding (data not shown). However, the additional presence of the E2 enzyme UbcH5b as blocking-protein leads to the ubiquitination of RhoA in the binding assays, resulting in a smear of bound ubiquitinated protein. To counteract this, 20 mM EDTA are added in order to chelate the Mg^{2+} required for the ATP-dependent step in the ubiquitination reaction. This enables the binding readout with a single band of the bound protein, instead of a smear (see **Figure 22** RL samples). As alternative to UbcH5b, BSA was also tested as blocking protein. The experiment shows that the use of BSA or UbcH5b+EDTA render equivalent results (data not shown).

To check for ternary complex formation, a GST coprecipitation assay was performed with GST-tagged 16 E6 or GST alone in presence of either WG or RL *in vitro* translated RhoA and E6AP (**Figure 22**). The coprecipitation assay shows a strong binding of both WG and RL RhoA to GST-16 E6 in presence of E6AP and EDTA and no background binding to GST alone (**Figure 22**, upper panel). In the reactions with RL RhoA, ubiquitinated RhoA forms (asterisk) can be observed in the absence of E6AP and EDTA, while in the presence of EDTA only one band representing unmodified RhoA is detected. Note that the addition of E6AP in absence of EDTA causes an increase in bound ubiquitinated RhoA forms (data not shown) and that E6AP-mediated monoubiquitination seems not to be affected by the addition of EDTA. The fact that in the absence of E6AP, there is binding with RL RhoA but not with WG RhoA indicates that even the low E6AP levels present in the RL are sufficient to mediate the interaction. The Coomassie stained gel in the lower panel shows the inputs of the GST, GST-16 E6 and E6AP and also the binding of E6AP to GST-16 E6. Taken together, RhoA, E6AP, and 16 E6 form a stable ternary complex *in vitro*. Furthermore, this complex formation can be observed, independent of which of the three proteins is used as bait protein, and neither E6AP nor E6 proteins are able to detectably interact with RhoA on their own, i.e. in the absence of the third interactor (see below).

3.3.2.1 High-risk and low-risk E6 proteins

So far, RhoA was shown to be ubiquitinated only by the 16 E6-E6AP complex (**Figure 15A**), and only the 16 E6-E6AP complex is able to target RhoA for proteasomal degradation (**Figure 21**). Any other tested E6 protein, in presence or absence of E6AP, is unable to promote RhoA ubiquitination or degradation (**Supplementary Figure 2**). As a next step, ternary complex formation was checked in GST coprecipitation experiments with GST-E6 proteins of the HPV types 11, 16, and 18 in combination with RL RhoA WT, RhoA G14V, and T19N (**Figure 23A**).

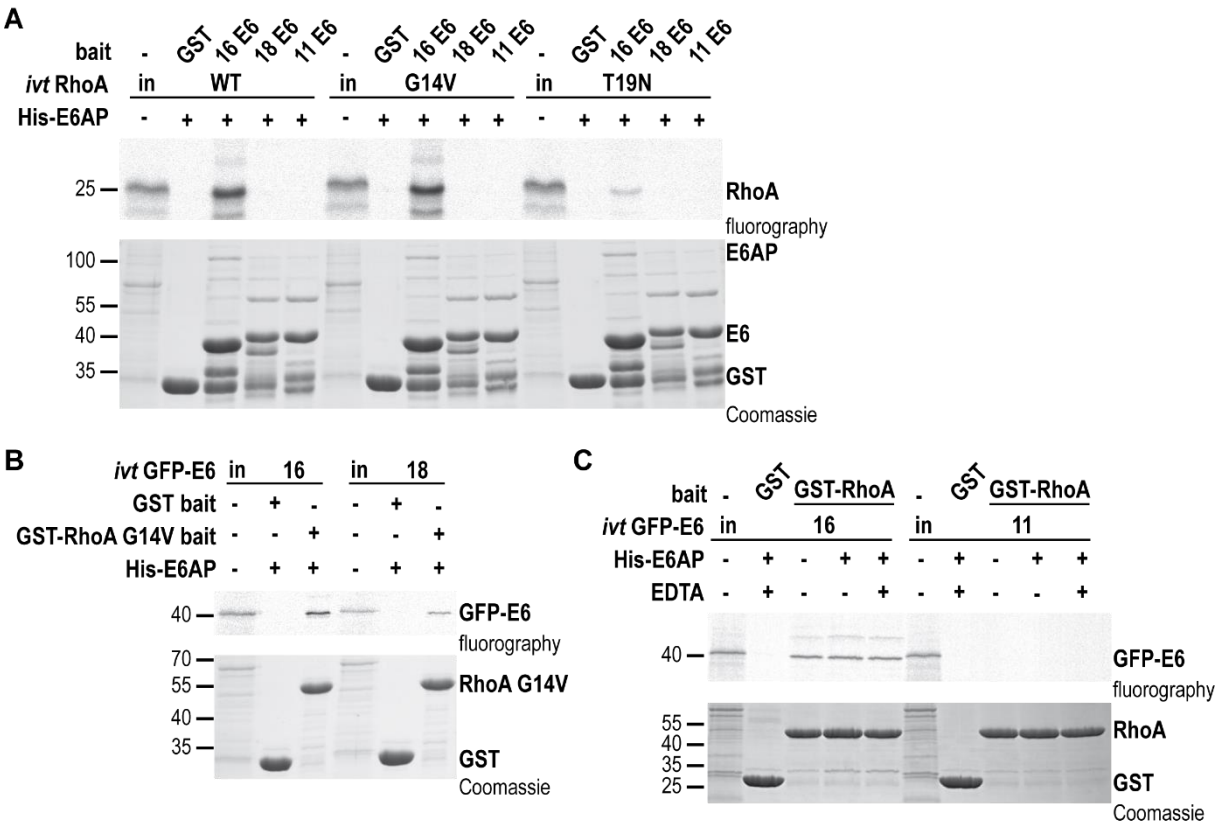

Figure 23. High-risk E6 proteins, E6AP, and RhoA form a stable ternary complex. A│ The GST-E6 fusion proteins or GST alone bound to GSH beads were incubated with *in vitro* translated, radiolabelled RhoA variants for 90 min at 4°C in the presence of His-E6AP as indicated and with 20 mM EDTA. Beads were washed after the binding reaction and the eluates were analysed by SDS-PAGE followed by Coomassie staining (GST bait input detection, lower panel) and fluorography (binding reaction, upper panel). The running positions of the molecular mass markers (in kDa), the GST-E6 fusion proteins or GST, RhoA, and E6AP are indicated. in│ 10% of the *in vitro* translated RhoA variants used in the binding reaction. **B**│ The GST-RhoA G14V fusion protein or GST alone bound to GSH beads was incubated with *in vitro* translated, radiolabelled GFP-E6 proteins for 90 min at 4°C in the presence of His-E6AP as indicated. Beads were washed after the binding reaction and the eluates were analysed by SDS-PAGE followed by Coomassie staining (GST bait input detection, lower panel) and fluorography (binding reaction, upper panel). The running positions of the molecular mass markers (in kDa), GST-RhoA G14V or GST, and GFP-E6 are indicated. in│ 10% of the GFP-E6 used in the binding reaction. **C**│ The GST-RhoA fusion protein or GST alone bound to GSH beads was incubated with *in vitro* translated, radiolabelled GFP-E6 proteins for 90 min at 4°C in the presence of His-E6AP and 20 mM EDTA as indicated. Beads were washed after the binding reaction and the eluates were analysed by SDS-PAGE followed by Coomassie staining (GST bait input detection, lower panel) and fluorography (binding reaction, upper panel). The running positions of the molecular mass markers (in kDa), the GST-RhoA fusion protein or GST, and GFP-E6 are indicated. in│ 10% of the GFP-E6 used in the binding reaction.

Both RhoA WT and G14V strongly interact with GST-16 E6, while RhoA T19N shows only a very weak interaction. In addition, none of the RhoA variants are able to form a stable complex with GST-11 E6 or GST-18 E6. This might correlate with the most efficient binding of E6AP to GST-16 E6 as visualised in the Coomassie stained gel (lower panel).

In *in vitro* translations, proteins are radioactively labelled by the use of S^{35} methionine. Therefore, proteins without methionine residues in addition to the initial methionine are

only poorly labelled with the system used in our laboratory. Since the 11 E6 and the 16 E6 proteins contain only one internal methionine residue and 18 E6 contains no internal methionine residue, GFP-E6 fusion proteins are used to enable proper radioactive labelling of the E6 proteins. Within the GFP protein, 5 internal methionine residues are present.

In order to further confirm the specificity of the ternary complex formation for 16 E6, the coprecipitation experiment was repeated with GST-RhoA G14V as bait protein and *in vitro* translated GFP-16 E6 or GFP-18 E6 (**Figure 23B**). The GST coprecipitation assay shows an interaction of GST-RhoA G14V with GFP-16 E6 and also, although weaker, an interaction with GFP-18 E6. It remains elusive, as to why the interaction between RhoA G14V and 18 E6 appears to depend on which protein is used as bait. In general, active protein preparations of GST-16 E6 have proven to be less complicated to produce than active GST-11 E6 or GST-18 E6 preparations (with active defined as the property to stimulate E6AP-mediated ubiquitination). It is therefore possible that GST-18 E6, in contrast to the GFP-18 E6, is e.g. not properly folded or lacks a necessary post-translational modification. Alternatively but not mutually exclusive, we speculate that the interaction between 16 E6 and RhoA is stronger than that of RhoA and 18 E6, and therefore lower RhoA amounts are sufficient to observe the 16 E6-RhoA interaction. In the coprecipitation experiment of GST-RhoA with GFP-11 E6, no interaction could be observed (**Figure 23C**). This shows that RhoA and 11 E6, in contrast to RhoA-18 E6, are unable to form a ternary complex with E6AP even with high RhoA amounts.

3.3.2.2 E6AP truncations and functional mutants

After having established the formation of a ternary complex between high-risk HPV E6 proteins, E6AP, and RhoA, we set out to determine which regions or domains of each of the proteins are required for the interaction. For this, we employed different N- or C-terminal truncations or functional point mutants of each of the participating proteins. Constructs for the bacterial expression of various E6AP truncations and mutants were already created in previous projects (F. Müller, AG Scheffner). Accordingly, the already existing E6AP variants were expressed and purified for the interaction studies. **Figure 24** shows a GST-16 E6 coprecipitation experiment with in WG *in vitro* translated RhoA, in the absence or presence of the different E6AP variants. The lower panel shows the input level of each of the E6AP variants. The middle panel shows the Coomassie staining of the coprecipitation assay, i.e. GST-16 E6 and any bound E6AP. The fluorographic readout in the top panel shows the formation of the different ternary complexes. As already confirmed in the degradation assays (**Figure 21C**), the E6AP isoforms 2 and 3 behave like isoform 1 in this regard. The loss of the N-terminal AZUL domain (ΔAZUL, residues 1-64), which is important for the interaction of E6AP with Rpn10 (Lemak et al. 2011; Kühnle et al. 2018), has no impact on the ternary complex formation. The deletion of the C-terminal six residues (ΔC6) diminishes the ligase activity of E6AP, which is visualised by the loss of the RhoA monoubiquitination in the coprecipitation experiment and a RhoA ubiquitination assay (**Supplementary Figure 5**) but is still able to promote complex formation.

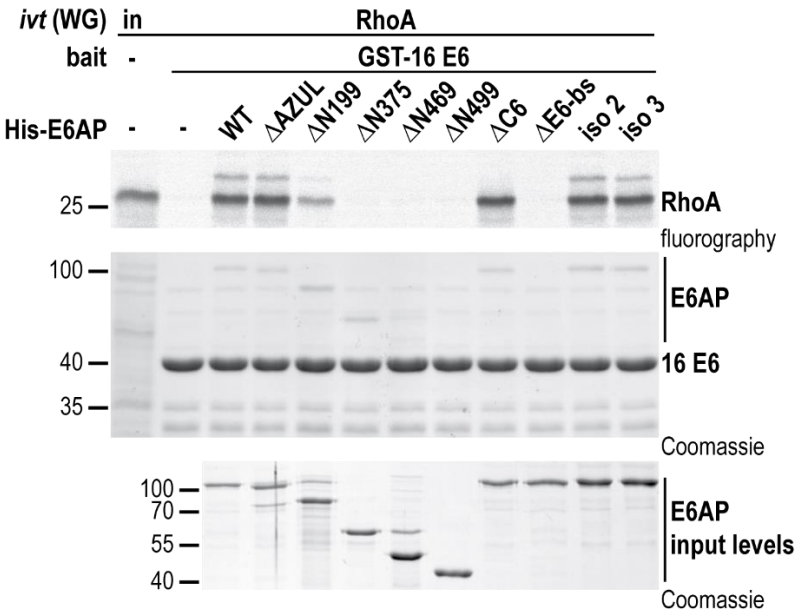

Figure 24. No specific region of E6AP could be identified as RhoA binding site. The GST-E6 fusion protein bound to GSH beads was incubated with *in vitro* translated, radiolabelled RhoA for 90 min at 4°C in the presence of His-E6AP variants as indicated and 20 mM EDTA. The *in vitro* translation was performed in wheat germ extract (WG), which does not contain endogenous E6AP. Beads were washed after the binding reaction and the eluates were analysed by SDS-PAGE followed by Coomassie staining (GST bait input detection, middle panel) and fluorography (binding reaction, upper panel). In the lower panel, the input levels of the E6AP variants are shown. The running positions of the molecular mass markers (in kDa), the GST-E6 fusion protein, RhoA, and E6AP variants are indicated. in | 10% of the RhoA used in the binding reaction.

An E6AP mutant lacking the binding site (bs) for 16 E6 (ΔE6-bs, E6AP residues 378-395 are missing; Huibregtse, Scheffner, and Howley (1993b)), on the other hand, is unable to promote the formation of the ternary complex, indicating that an undisturbed 16 E6-E6AP interaction is required for the formation of the ternary complex with RhoA. The E6-bs is also not present in the N-terminal truncations ΔN469 (residues 1-469 are missing) and ΔN499 (corresponds to the HECT domain of E6AP), explaining why the two truncations are unable to promote ternary complex formation. Similarly, mutants comprising residues 1-470 or 1-500, therefore lacking the HECT domain, were also unable to promote RhoA binding to GST-16E6 (data not shown).

Deletion of the N-terminal 199 (ΔN199) residues weakens the interaction, while the ΔN199 mutant is still able to promote ubiquitination of *in vitro* translated RhoA (**Supplementary Figure 5**) and to bind to GST-16 E6 (**Figure 24**, middle panel). The interaction between RhoA and GST-16 E6 is completely abolished in presence of the E6AP ΔN375 mutant. The region ranging from residue 199 to 375 may therefore be required for the interaction with RhoA. Alternatively, the expression of E6AP proteins with such large deletions may result in an incorrectly folded protein (in this context it should be noted that the structure of E6AP has not yet been solved, see 1.2.1 'Structural characteristics of E6AP' in the introductory part). The fact that E6AP ΔN375 is still able to bind to GST-16 E6 (**Figure 24**, middle panel) does not contradict the hypothesis of folding problems.

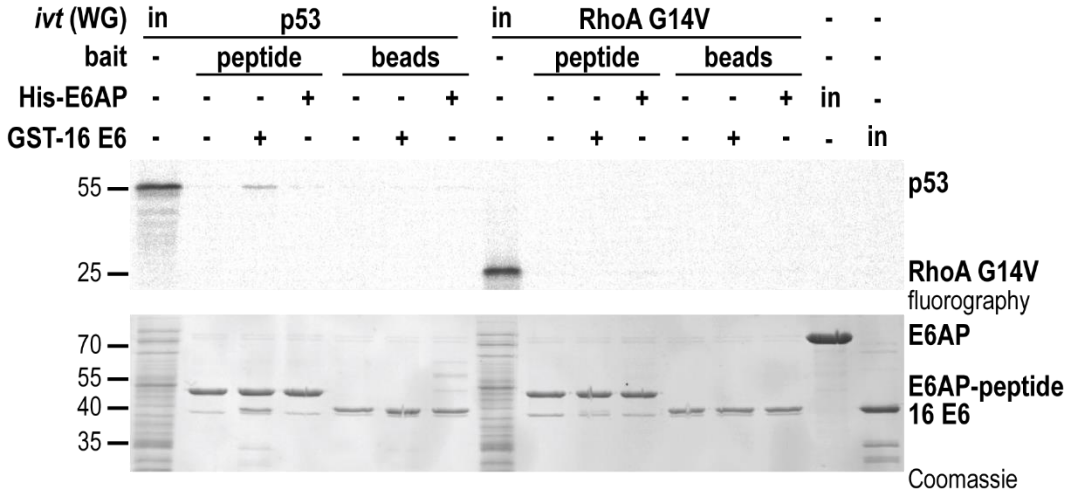

Figure 25. The E6-binding peptide of E6AP is insufficient to promote RhoA binding. The MBP-E6-binding peptide of E6AP (ELT-LQELL-GEER) fusion protein (peptide) bound to amylose beads or empty amylose beads (beads) were incubated with *in vitro* translated, radiolabelled p53 or RhoA G14V for 90 min at 4°C in the presence of GST-16 E6 or His-E6AP as indicated. The *in vitro* translation was performed in wheat germ extract (WG), which does not contain endogenous E6AP. Beads were washed after the binding reaction and the eluates were analysed by SDS-PAGE followed by Coomassie staining (MBP bait input detection, lower panel) and fluorography (binding reaction, upper panel). The running positions of the molecular mass markers (in kDa), the MBP-E6AP peptide fusion protein, p53, RhoA G14V, E6AP, and GST-16 E6 are indicated. in | 10% of the p53 or RhoA G14V and 100% of the His-E6AP or GST-16 E6 used in the binding reaction.

The region ranging from residues 150 to 200 of E6AP has been reported to be essential for the interaction between E6AP and HERC2 (Kühnle et al. 2011). In a coprecipitation assay with a GST-16 E6 bait and *in vitro* translated RhoA, the E6AP Δ150-200 mutant is able to promote the ternary complex formation with E6AP WT efficiency (data not shown), thereby excluding this region as primary RhoA binding site.

While an active E6AP is required to promote the ubiquitination and subsequent proteasomal degradation of p53 (Huibregtse, Scheffner, and Howley 1993b), the E6-binding peptide (LQELL) of E6AP has been described as sufficient to mediate the 16 E6-E6AP-p53 interaction (Zanier et al. 2013). An MBP coprecipitation experiment with the extended E6-binding peptide (ELT-LQELL-GEER) fused to the MBP tag (Zanier et al. 2013) and immobilized on amylose resin confirms GST-16 E6 to be able to promote the binding of p53 to the MBP-E6-binding peptide (**Figure 25**). Even though the binding is not strong, the control reaction with empty amylose resin indicates the interaction to be specific. However, it was not possible to coprecipitate the active RhoA G14V mutant with the MBP-E6-binding peptide in presence of GST-16 E6. This shows that although both RhoA and p53 bind to E6 only when E6AP or a part of it is present, RhoA and p53 have a different mode of binding to 16 E6-E6AP. **Table 2** summarizes results regarding the ability of different E6AP variants to promote ternary complex formation with 16 E6 and RhoA.

Table 2. Overview of E6AP variants used for ternary complex formation. Listed are the different E6AP variants that were tested regarding their ability to promote ternary complex formation with 16 E6 and RhoA.

	E6AP variant	ternary complex?	characteristics
isoform 1	WT	yes	-
	ΔAZUL	yes	lacks residues 1-64
	ΔN199	yes (weak)	-
	ΔC6	yes	catalytically impaired
	ΔHERC2 binding site	yes	lacks residues 150-200
	ΔN375	no	-
	ΔN469	no	lacks the E6-bs
	ΔN499	no	= HECT domain
	ΔE6 binding site	no	lacks residues 378-395
	E6-binding peptide	no	sufficient for E6-p53 interaction
	isoform 2	yes	20 aa N-terminal extension
	isoform 3	yes	23 aa N-terminal extension

3.3.2.3 16 E6 mutants and chimeric E6 proteins

The interaction between HPV E6 proteins and multiple other proteins has been extensively investigated (White et al. 2012; Thomas et al. 2016). Dlg1 and p53 are two of the best known and well established 16 E6 interactors (Talis, Huibregtse, and Howley 1998; Kiyono et al. 1997). To compare the binding of 16 E6 to RhoA, Dlg1, and p53, coprecipitation experiments with different GST-E6 variants were performed.

At its very C terminus, high-risk E6 proteins contain a PDZ-binding motif (E148 T149 Q150 L151 in 16 E6), which mediates the interaction with PDZ domain-containing proteins like Dlg1 (Kiyono et al. 1997; Gardiol et al. 1999). The threonine residue at position 149 of 16E6 is part of the PDZ-binding motif and essential for the interaction with PDZ domain-containing proteins. Additionally, phosphorylation of T149 (T156 in 18 E6) by protein kinase A (PKA) exhibits an inhibitory effect on the 16 E6-Dlg1 interaction (Kühne et al. 2000). Mutation of T149 to aspartic acid (T149D) can be used to mimic this phosphorylation state. While RhoA G14V is able to bind to GST-16 E6 T149D (**Figure 26A**), Dlg1 is unable to do so, as expected (**Figure 26B**). In line with this, deletion of the C-terminal 2 (ΔC2, partial PDZ-binding motif lost) or the C-terminal 5 (ΔC5, complete PDZ-binding motif lost) residues of E6 renders Dlg1 unable to interact with 16 E6, while the interaction between RhoA G14V and 16 E6 in presence of E6AP is not affected.

As described above (**Figure 23A** and **C**), RhoA is unable to form a ternary complex with the low-risk 11 E6 protein and E6AP. For this reason, chimeric E6 proteins as described in (Kuballa, Matentzoglu, and Scheffner 2007) were employed in the next step. This includes a 16 E6 variant (residues 1-139) fused C terminus of the 11 E6

protein (residues 141-150, 16C11), as well as an 11 E6 variant (residues 1-140) with the PDZ-binding motif containing C terminus of 16 E6 (residues 140-151, 11C16) (Kuballa 2004).

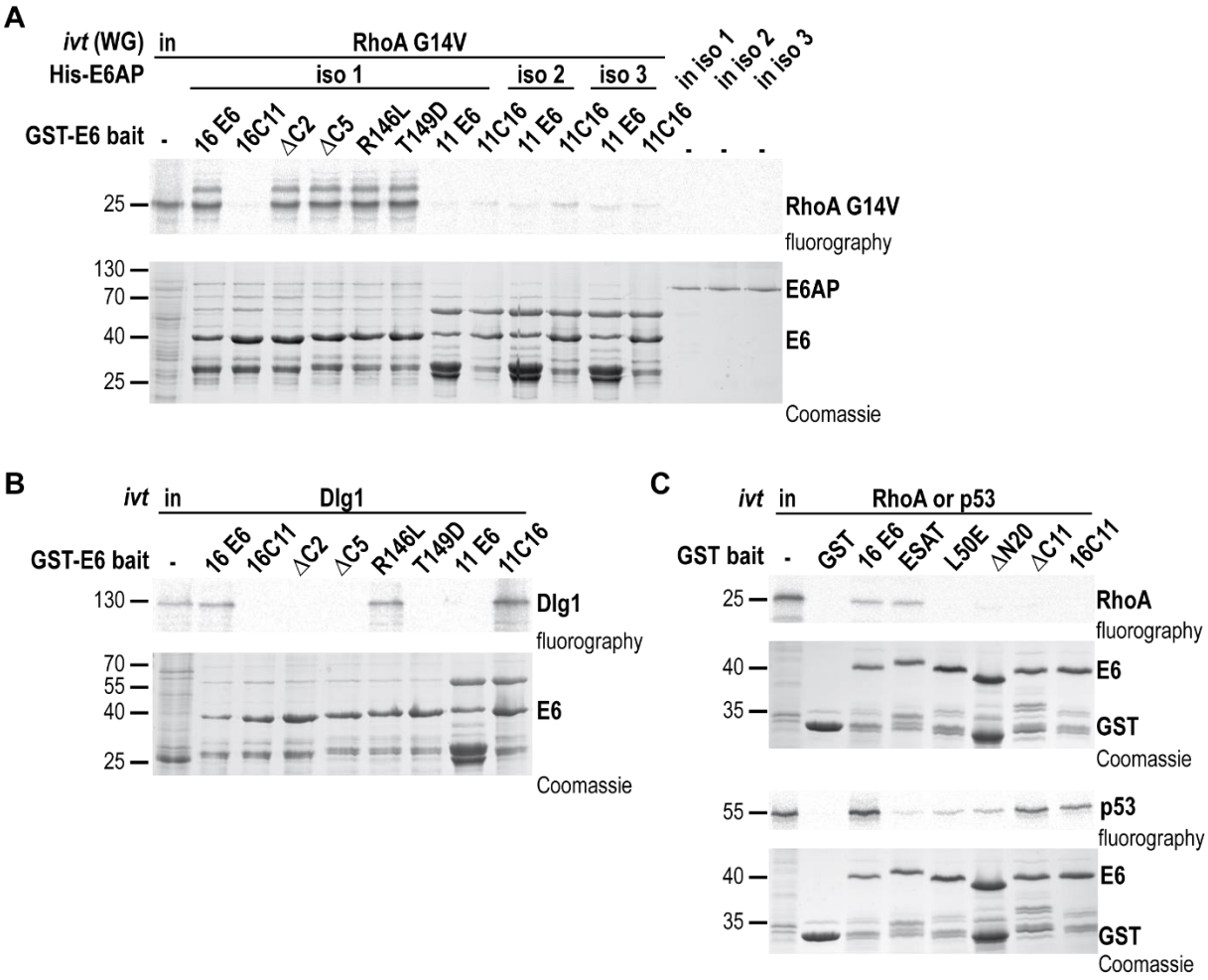

Figure 26. RhoA shows differential E6 binding properties in comparison to p53 and Dlg1. A| The GST-E6 fusion proteins bound to GSH beads were incubated with *in vitro* translated, radiolabelled RhoA G14V for 90 min at 4°C in the presence of different His-E6AP isoforms as indicated and 20 mM EDTA. The *in vitro* translation was performed in wheat germ extract (WG), which does not contain endogenous E6AP. Beads were washed after the binding reaction and the eluates were analysed by SDS-PAGE followed by Coomassie staining (GST bait input detection, lower panel) and fluorography (binding reaction, upper panel). The running positions of the molecular mass markers (in kDa), the GST-E6 fusion proteins, RhoA G14V, and the E6AP isoforms are indicated. in| 10% of the RhoA G14V and 100% of the His-E6AP variants used in the binding reaction. **B**| The GST-E6 fusion proteins bound to GSH beads were incubated with *in vitro* translated, radiolabelled Dlg1 for 90 min at 4°C. Beads were washed after the binding reaction and the eluates were analysed by SDS-PAGE followed by Coomassie staining (GST bait input detection, lower panel) and fluorography (binding reaction, upper panel). The running positions of the molecular mass markers (in kDa), the GST-E6 fusion proteins, and Dlg1 are indicated. in| 10% of the Dlg1 used in the binding reaction. **C**| The GST-E6 fusion proteins bound to GSH beads were incubated with *in vitro* translated, radiolabelled RhoA or p53 for 90 min at 4°C. Beads were washed after the binding reaction and the eluates were analysed by SDS-PAGE followed by Coomassie staining (GST bait input detection, lower panels) and fluorography (binding reaction, upper panels). The running positions of the molecular mass markers (in kDa), the GST-E6 fusion proteins, RhoA, and p53 are indicated. in| 10% of the RhoA or p53 used in the binding reaction.

The exchange of the 16 E6 C terminus for the 11 E6 C terminus (16C11) renders RhoA unable to interact with the GST-E6 protein, indicating an important role of the 16 E6 C terminus in the interaction (**Figure 26A** and **C**). The deletion of the C-terminal 11 residues of 16 E6 has the same effect (**Figure 26C**, upper fluorography panel). On the other hand, the presence of the 16 E6 C terminus in the 11 E6 chimeric protein (11C16) does not promote the formation of a ternary complex. The results obtained by the chimeric E6 proteins indicate the 16 E6 C terminus to be necessary but not sufficient to facilitate an interaction with RhoA. Control coprecipitation experiments with Dlg1 indicate the functional integrity of the mutants. 16C11 (no PDZ-binding motif) is unable to bind to Dlg1, but the 11 E6 chimera with the 16 E6 C terminus (including the PDZ-binding motif) is able to interact with Dlg1 (**Figure 26B**). The use of E6AP isoforms 2 or 3 does not rescue the binding deficit of RhoA G14V to GST-11 E6 or GST-11C16 (**Figure 26A**).

Table 3. Overview of E6 variants used for ternary complex formation. Listed are the different high-risk and low-risk E6 variants that were tested regarding their ability to promote ternary complex formation with E6AP and RhoA.

	E6 variant	ternary complex?	characteristics
16 E6	WT	yes	high-risk E6 protein
	ESAT	yes	p53 binding deficient
	ΔC2	yes	Dlg1 binding deficient
	ΔC5	yes	Dlg1 binding deficient
	T149D	yes	Dlg1 binding deficient
	L50E	no	E6AP binding deficient
	ΔN20	no	lacks residues 1-20
	16C11	no	chimeric protein with 11 E6 C terminus
	18 E6	not with E6 as bait	high-risk E6 protein
	11 E6	no	low-risk E6 protein
	11C16	no	chimeric protein with 16 E6 C terminus

The 16 E6 L50E mutant has been described to be E6AP-binding deficient (Zanier et al. 2013). The exchange of several N-terminal 16 E6 residues (R8, P9, R10) with the respective residues of the 11 E6 protein (R8S, P9A, and R10T), including an F2E mutation, renders the 16 E6 protein unable to interact with p53 (ESAT mutant) (Foster et al. 1994). In contrast to p53, RhoA G14V is still able to interact with 16 E6 ESAT (**Figure 26C**). Both RhoA and p53 are unable to interact with GST-16 E6 L50E, again indicating the importance of a functional E6-E6AP interaction for the formation of the ternary complex with RhoA. Unlike RhoA, p53 is able to bind efficiently to the C-terminally altered 16C11 and the 16 E6 ΔC11 variants. In conclusion, while it was not possible to determine a specific region or domain of 16 E6 required for the interaction with RhoA, the requirements of E6 to bind to RhoA and to Dlg1 and p53 were shown to be clearly different. A summary of the obtained results regarding the ability of

different E6 proteins to promote ternary complex formation with E6AP and RhoA is shown in **Table 3**.

3.3.2.4 RhoA activity mutants and truncations

Finally, RhoA variants were investigated for their ability to bind to 16 E6-E6AP. To this end, the preferentially GTP-bound G14V and Q63L mutants were compared to the fast-cycling F30L, the nucleotide unbound G17A, and the preferentially GDP-bound T19N mutant (Chen et al. 2022; Lin, Cerione, and Manor 1999; Feig and Cooper 1988a; García-Mata et al. 2006). A GST coprecipitation assay with GST-16 E6 as bait protein in presence of E6AP and the *in vitro* translated RhoA variants reveals that T19N and G17A show almost no interaction with the 16 E6-E6AP complex (for T19N see **Figure 23A**, for G17A: data not shown). In contrast, the G14V, F30L, and Q63L mutants strongly interact with GST-16 E6. This holds also true when GST-E6AP is used as bait in the presence of untagged 16 E6 and the *in vitro* translated RhoA variants (data not shown).

In cells, RhoA is post-translationally processed to enable the correct subcellular localisation of active RhoA at the cell membrane (Moissoglu and Schwartz 2014). This three-step mechanism involves the prenylation of the Cys within the CAAX box (CLVL), the removal of the C-terminal three residues (LVL), and finally the methylation of the Cys at the very C terminus (reviewed in Zhang and Casey (1996); Cox and Der (1992)). To be able to evaluate the characteristics of the processed RhoA forms in *in vitro* experiments, several so-called ‘processing mutants’ were generated: 1) RhoA C190A (prenylation not possible), 2) RhoA ΔLVL (mimics proteolysis), and 3) RhoA C190A ΔLVL (mimics proteolysis and prenylation not possible). In coprecipitation experiments with GST-16 E6 in the presence and absence of E6AP and EDTA, all processing mutants behave like the RhoA WT protein. In addition, they are ubiquitinated by 16 E6-E6AP with WT efficiency (data not shown). This suggests that the 16 E6-E6AP complex is probably able to interact with RhoA in its processed form. This would be in accordance with the data suggesting that the active GTP-bound form and therefore membrane-bound RhoA is the preferential target (**Figure 20** and **Figure 21A**). However, it is not possible to exclude any potential inhibitory effect of the prenylation in cells, which is not accounted for with the ‘processing mutants’ *in vitro*. The lack of prenylation could be the reason why the 16 E6-E6AP-mediated ubiquitination of *in vitro* translated RhoA is more pronounced than the 16 E6-E6AP-mediated degradation of ectopic RhoA in most transient transfection experiments. In this regard, the degradation of the prenylation deficient RhoA C190A mutant should be tested.

As with E6AP (Figure 24), multiple N-terminal (ΔN) and C-terminal (ΔC) RhoA truncation variants were created with the aim of identifying the RhoA regions that are required for ternary complex formation (Table 4). The truncations were designed such that they do not interrupt any known α-helices or β-sheets (according to Ihara et al. (1998)). This project was partly performed by Nadja Eulich during her bachelor thesis (2021) and continued by Sarah Lott during her advanced course (2021), under my supervision. Most of the mutants are still ubiquitinated, at least to some extent (data not shown), but in general, especially with the very short RhoA truncations (ΔN163 and

ΔC107), we have no means to determine whether they are still functional or correctly folded. Also, while RhoA contains five internal methionine residues, most of them are located towards the C terminus. S^{35} radioactive labelling in the *in vitro* translation reaction was therefore strongly impaired in C-terminal truncations, especially for ΔC107. Coprecipitation experiments with these weakly labelled RhoA truncations do not render clear results (data not shown). The ΔC12 mutant, which lacks the hypervariable region and the CAAX box, shows the most promising results. While this mutant is still able to form a ternary complex with E6-E6AP independent of the protein used as bait (**Supplementary Figure 6**, data not shown for GST-RhoA variants with *in vitro* translated GFP-16 E6), its ubiquitination by 16 E6-E6AP is strongly impaired (**Figure 35C**). This mutant will be further discussed in **3.3.5** '**Inhibitory effect on 16 E6 stimulation**'. Similar to the data obtained for the E6AP and E6 variants, the different truncations of RhoA did not help to reveal the E6-E6AP binding interface of RhoA.

Table 4. Overview of RhoA truncations. RhoA was N-terminally (ΔN) and C-terminally (ΔC) truncated at multiple positions. The corresponding ΔN and ΔC truncations at a certain amino acid residue of RhoA are listed in the same lane.

truncation at residue	ΔN	ΔC
86	ΔN85	ΔC107
110	ΔN109	ΔC83
122	-	ΔC71
139	ΔN138	ΔC54
164	ΔN163	ΔC29
181	-	ΔC12

3.3.3 RhoA subfamily members and other Rho GTPases as interaction partners of E6-E6AP

In addition to RhoA, potential ternary complex formation with 16 E6-E6AP was also investigated for RhoB, RhoC, Rac1, or Cdc42. To do so, GST coprecipitation assays were performed with either GST alone or GST-16 E6 as bait in the absence or presence of E6AP and EDTA (**Figure 27**). For RhoB, a weak interaction can be observed in the presence of E6AP. Even though no binding of ubiquitinated RhoB forms is detectable, the addition of EDTA strongly increases the signal for the binding of unmodified RhoB to GST-16 E6 (**Figure 27A**). RhoC, on the other hand, shows binding of ubiquitinated forms to GST-16 E6 already only with the E6AP present in the reticulocyte lysate. This is increased in the presence of additional E6AP and only unmodified RhoC is observed in the presence of EDTA (**Figure 27B**).

In contrast to this, *in vitro* translated Rac1 (**Figure 27C**) and Cdc42 (**Figure 27D**) are unable to form a ternary complex with GST-16 E6 in presence of E6AP. Based on the data obtained for ternary complex formation between RhoA and 18 E6 in presence of

E6AP, where an interaction could only be observed with the Rho protein as bait, a similar experiment was performed with Rac1 and Cdc42. Indeed, coprecipitation experiments with GST-Rac1 or GST-Cdc42 show that both proteins are able to interact with *in vitro* translated E6AP and to a lesser extent also with *in vitro* translated GFP-16 E6 (**Supplementary Figure 7**). This indicates that while all tested Rho GTPases are able to form ternary complexes with E6-E6AP to some extent, RhoA subfamily members have the highest affinity for 16 E6-E6AP.

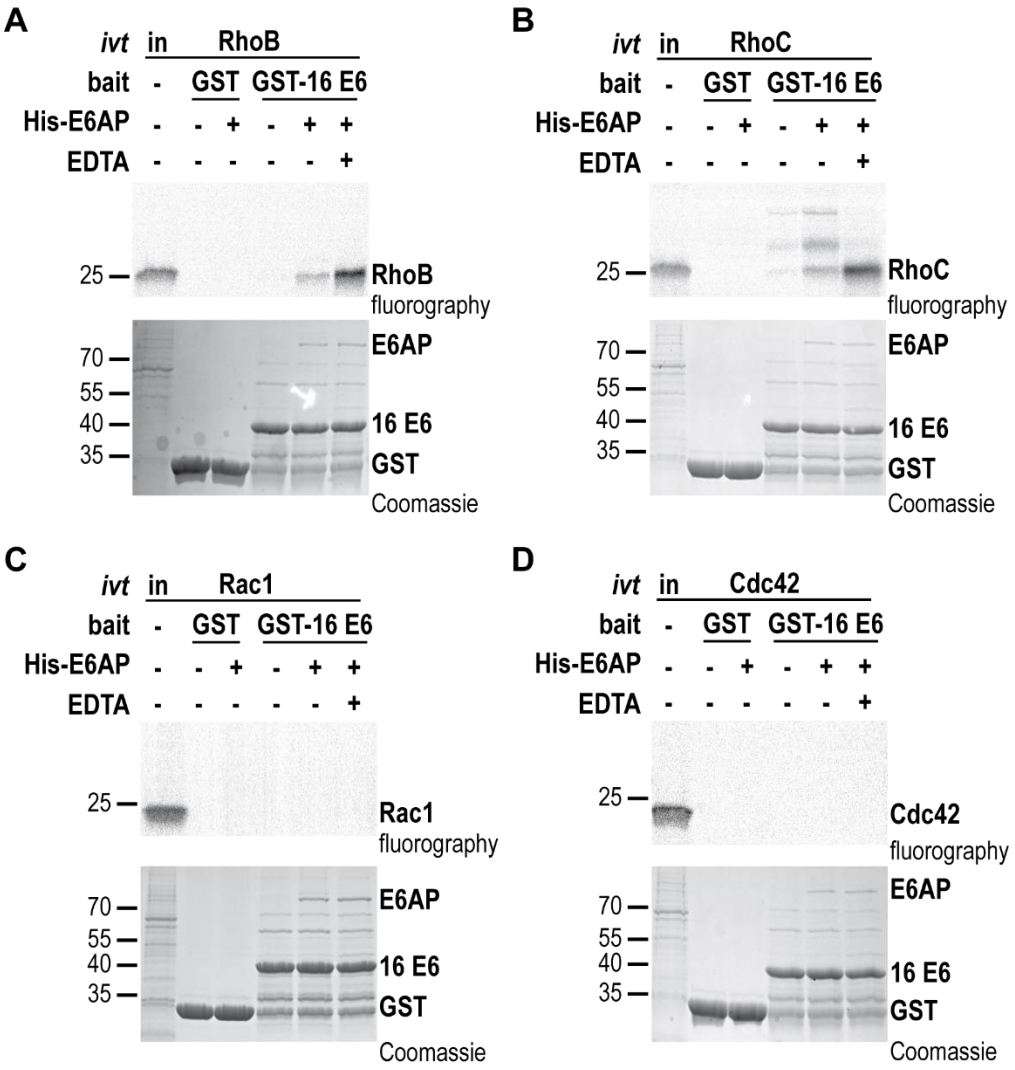

Figure 27. The ternary complex formation is restricted to RhoA subfamily members. The GST-16 E6 fusion protein or GST bound to GSH beads was incubated with *in vitro* translated, radiolabelled **A**| RhoB, **B**| RhoC, **C**| Rac1, or **D**| Cdc42 for 90 min at 4°C in the presence of His-E6AP and 20 mM EDTA as indicated. Beads were washed after the binding reaction and the eluates were analysed by SDS-PAGE followed by Coomassie staining (GST bait input detection, lower panels) and fluorography (binding reaction, upper panels). The running positions of the molecular mass markers (in kDa), GST-16 E6, GST, and the Rho proteins are indicated. in| 10% of the Rho proteins used in the binding reaction.

The Rho proteins mainly differ in their C-terminal regions, especially in the hypervariable region (**Figure 14**). Analogous to the chimeric E6 proteins and to evaluate the importance of the RhoA C terminus for ternary complex formation, a Rac1-RhoA chimeric protein was generated. The chimera consists of residues 1-176

of Rac1, fused to the C-terminal 14 residues of RhoA that contain the hypervariable region. In a GST-16 E6 coprecipitation assay in the presence of E6AP, this chimera is unable to rescue the binding deficit of Rac1 (data not shown). This indicates that the differential recognition of the Rho proteins by 16 E6-E6AP is probably not mediated solely by the C terminus, but involves additional regions. **Table 5** is a summary of the obtained results regarding the ability of different Rho proteins to form a ternary complex with 16 E6-E6AP.

Table 5. Overview of Rho proteins and mutants used for ternary complex formation. Listed are the different RhoA mutants and other Rho GTPases that were tested regarding their ability to form a ternary complex with 16 E6-E6AP.

	Rho GTPase	ternary complex?	characteristics
RhoA	WT	yes	-
	G14V	yes	preferentially GTP-bound
	F30L	yes	fast-cycling
	Q63L	yes	preferentially GTP-bound
	ΔC12	yes	lacks HVR and CAAX box (CLVL)
	C190A	yes	prenylation deficient
	ΔLVL	yes	mimics proteolysis
	C190A ΔLVL	yes	prenylation deficient and mimics proteolysis
	G17A	no	impaired nucleotide binding
	T19N	no	preferentially GDP-bound
	RhoB	yes	member of the RhoA subfamily of GTPases
	RhoC	yes	member of the RhoA subfamily of GTPases
	Rac1	not with E6 as bait	member of different Rho GTPase subfamily
	Cdc42	not with E6 as bait	member of different Rho GTPase subfamily
	Rac1-RhoA	no	chimeric protein with the C terminus of RhoA

3.3.4 Additional approaches to determine the primary RhoA interaction partner

While we were able to establish that specifically members of the RhoA subfamily, and these preferentially in a GTP-bound state, form a ternary complex with high-risk HPV E6 and E6AP, we could not determine the domains or regions involved in this interaction by the use of defined mutants. Furthermore, in the coprecipitation experiments, an interaction could only be observed in presence of all three proteins, but independently of which protein was immobilized as bait. A potential shortcoming of coprecipitation assays is that under the conditions used, weaker interactions (i.e. low affinity interactions) cannot be captured and, thus, a potential interaction between RhoA and E6AP alone or RhoA and E6 alone may be missed. Along this line, the presence of both, 16 E6 and E6AP, may have an enhancing and/ or stabilising effect, which enables the detection of the complex in coprecipitation assays. Therefore, an important next step was to employ other methods in order to determine if E6 and/or E6AP alone have the potential to interact with RhoA and, thus, represent the primary interaction partner of RhoA within the ternary complex.

Size-exclusion chromatography (SEC) is a useful tool to investigate the oligomerisation status or complex formation of proteins. Larger proteins, oligomers, or complexes pass the column faster than smaller proteins, as the small ones enter pores within the column resin, which prolongs their retention time. In other words, SEC separates proteins according to their size. With the use of proteins of defined mass as standards, it is possible to determine the mass of a given protein or protein complex (reviewed in Burgess (2018)). For SEC, His-tagged E6AP as well as untagged or GST-tagged 16 E6 and untagged or MBP-tagged RhoA were prepared (for column and sample preparation see 5.2.3.5 ‘Size exclusion chromatography’). His-E6AP, 16 E6, and RhoA were analysed on their own and together in all possible combinations: 1) E6AP, 2) 16 E6, 3) RhoA, 4) E6AP+16 E6, 5) E6AP+RhoA, 6) 16 E6+RhoA, and 7) E6AP+16 E6+RhoA. After SEC, the fractions obtained were analysed by SDS-PAGE followed by Coomassie staining. Serving as a positive control to validate the functionality of the method, E6AP together with 16 E6 was analysed. As expected, the SEC experiment shows a co-elution of E6AP and 16 E6 (data not shown). However, RhoA neither eluted together with E6AP alone nor with 16 E6 alone, but in presence of all three proteins, a co-elution can be observed (data not shown). While this confirms the data obtained in coprecipitation experiments, it does not further the understanding of the interactions within the ternary complex.

Isothermal titration calorimetry (iTC) is a sensitive tool for the determination of binding energies of e.g. protein-protein interactions. In brief, iTC is able to determine the temperature changes arising from any given interaction and to measure the amount of energy that is required to maintain the temperature at a constant level (25°C) (reviewed in Velázquez-Campoy et al. (2004)). It has the advantage to measure affinities with all binding partners in solution (no immobilization), but high protein concentrations, especially of the ‘ligand’ are required. For iTC, His-tagged E6AP, MBP-tagged RhoA G14V, MBP-tagged 16 E6, and GST-tagged 16 E6 were expressed and purified. Prior to the iTC measurement (iTC200, MicroCal; AG Wittmann, Dept. of Chemistry, University of Konstanz), all proteins were concentrated and dialysed overnight in

dialysis buffer (25 mM Tris pH7.5, 50 mM NaCl); some of the buffer was kept as reference for the measurement. To achieve the highest possible concentration, the proteins were concentrated until the onset of precipitation. For the first iTC measurements, MBP-RhoA was in the sample cell, and a ~1:5 mixture of His-E6AP:GST-16 E6 was titrated in as the ‘ligand’. As already observed with the other methods, an interaction with all three proteins can be detected by iTC. However, it is not possible to calculate a binding constant, since saturation of the MBP-RhoA G14V in the sample cell cannot be reached with the ligand mixture (data not shown). This indicates that the protein concentration in the sample cell is too high or vice versa the ligand concentration is too low. Next, the reversed experiment was performed, with His-E6AP and GST-16 E6 (~1:10) together in the sample cell and the active MBP-RhoA G14V mutant was titrated in as the ‘ligand’. Again, this enabled the detection of an interaction, but no saturation can be achieved and therefore no binding affinity can be calculated (data not shown). Even with a reduction of the protein concentration in the sample cell (E6AP and 16 E6), the ratio of the ‘ligand’ concentration (RhoA G14V) in regard to the protein concentration in the sample cell remains too low (data not shown). As it was not possible to establish the iTC method even in presence of all three proteins, the interaction of E6AP-RhoA or 16 E6-RhoA was not tested.

While the formation of a ternary complex of 16 E6-E6AP and RhoA could be verified with several different methods, it remained unclear, if RhoA can directly interact with E6AP or E6. It could be envisioned that to be able to detect a respective heterodimeric complex, coexpression of RhoA with E6 or E6AP is required. To approach this possibility, cDNAs encoding RhoA, E6 or E6AP with different tags were cloned into a bicistronic vector (pRSFDuet, Novagen) to enable the bacterial expression of two different proteins from a single transcript. With a His-tagged protein in multiple cloning site (MCS) 1 and an MBP-tagged protein in MCS2, differential purification and subsequent interaction analysis were possible. This project was started during the bachelor thesis of Julia Küpfer (2022) and continued in the master thesis of Sarah Lott (2023), under my supervision. The method per se is tested with the interaction between E6AP and 16 E6 as control, but the main drawback turns out to be unspecific binding of some MBP-tagged proteins to the Ni-NTA resin or of His-tagged proteins to the amylose resin (data not shown, see master thesis Sarah Lott, 2023), a problem that despite considerable efforts could not be solved. Therefore, also with this approach it was not possible to determine if E6 or E6AP represent the primary interaction partner for RhoA within the ternary complex.

3.3.4.1 Cross-linking coupled to mass spectrometry (XL-MS)

Chemical cross-linking coupled to mass spectrometry (XL-MS) represents a more recent approach for the analysis of protein complexes (Leitner, Walzthoeni, and Aebersold 2014). To do so, we teamed up with Jasmin Jansen from the AG Stengel. For XL-MS, a chemical molecule like disuccinimidyl suberate (DSS) is used which can covalently react with two amino acid side chains – a so called cross-linker (Leitner, Walzthoeni, and Aebersold 2014). DSS contains two N-hydroxysuccinimidyl (NHS)-activated carboxyl groups, which are separated by an alkyl arm of distinct length (Müller et al. 2001; Collins et al. 2003). At pH 7-9, this homo-bifunctional cross-linker primarily reacts with the free electron pair of primary amines, like the ε-amino group of lysines and of the N-terminal methionine of proteins (Mädler et al. 2009). Only lysine residues with a proximity of less than 30Å can be covalently connected by the DSS used (Merkley et al. 2014). Thus, any formed link therefore contains structural information in form of distance restraints determined by the length of the linker arm (Leitner et al. 2012). However, the surface accessibility as well as the reactivity of the given amino acid also contribute to a successful cross-link formation (Kai Kammer, unpublished data) (Ward, Kleinman, and Nomura 2017).

Prior to the addition of DSS, the POIs are incubated on ice for 30 min to enable protein-protein interactions to occur, before they are captured by the cross-linker. For evaluation, cross-links originating from different proteins are termed interlinks, while intralinks describe cross-links arising from the same protein. A ‘monolink’ describes that a lysine has reacted with one side of a cross-linker molecule and the other side was either hydrolysed or quenched with ammonium.

Several setups with differentially tagged proteins were tested in order to optimize the experimental conditions. First, His-E6AP, GST-16 E6, and GST-RhoA G14V were used. However, the use of two proteins with the same affinity tag results in cross-links that cannot be unambiguously assigned to a specific protein. In the second attempt, untagged RhoA G14V was used instead of GST-RhoA WT but the protein strongly precipitated during purification and concentration steps. After these two unsuccessful attempts, an MBP-tagged version of RhoA G14V was used in the third attempt, in order to enhance RhoA solubility in absence of the GST tag. However, the MBP-tag itself elicits a great number of links within itself and between all potential interaction partners. This indicates the MBP-tag to be unsuitable for XL-MS experiments.

Therefore, in the fourth attempt, we again resorted to untagged RhoA G14V, yet this time avoiding higher protein concentrations during purification to prevent precipitation. In the control complex consisting of His-E6AP and GST-16 E6, an amount of inter- and intralinks comparable to previous successful 16E6-E6AP cross-linking experiments (Sailer et al. 2018) can be identified (**Figure 28A**). This indicates that the cross-linking experiment per se was successful. No links can be detected between E6AP and RhoA G14V in absence of 16 E6 (**Figure 28B**), while links between E6AP and RhoA are detected in the presence of E6 (**Figure 28C**). Between RhoA and 16 E6, no links can be observed regardless of whether E6AP is present or not (**Figure 28D**). **Figure 28E-G** shows the cross-link pattern of each of the proteins alone as references.

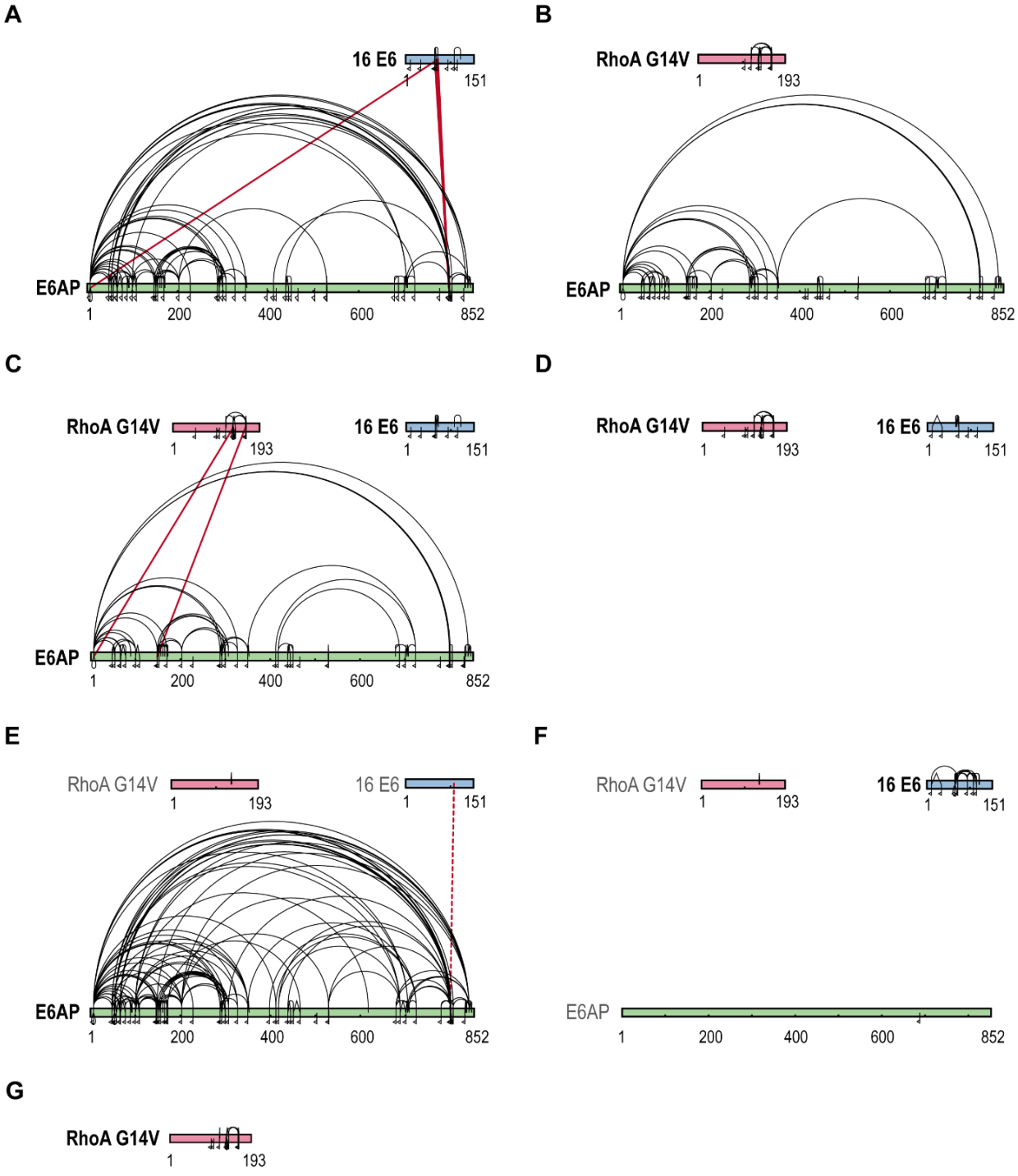

Figure 28. E6AP is indicated as the RhoA interaction partner in the ternary complex by XL-MS/MS. Pattern of the E6AP (light green) interlink and intralink distribution in **A**| presence and **E**| absence of 16 E6 (light blue), in presence of **B**| RhoA G14V (light red), or **C**| in presence of 16 E6 and RhoA. **E-G**| Intralink pattern of each of the proteins alone. Intralinks (indicated as curve above the protein) and monolinks (indicated as flag below the protein) are shown in black. Interlinks between two different proteins are indicated in red. The probably false positive link between E6AP and 16 E6 in the sample of E6AP alone is shown in a red dotted line. The links were found in two of three replicates with an ld-score of ≥ 25.

Overall, the cross-linking data represents a promising start in clarifying the identity of the primary interaction partner of RhoA in the ternary complex with high-confidence interlinks between RhoA and E6AP in presence of 16E6 (**Figure 28C**). E6AP lysine residues 7 and 148 were cross-linked to RhoA lysine residues 135 and 162, respectively. However, a direct interaction between RhoA and E6AP or RhoA and 16 E6 in the absence of the respective other protein could again not be shown. This may indicate that the interaction between RhoA and its primary interaction partner requires the presence of both E6 and E6AP. This could be a scenario similar to the E6-E6AP-p53 interaction, where E6AP stabilizes a conformation of E6 required for the interaction with p53. In this case, E6 might be required to stabilize E6AP for the interaction with RhoA, without E6 contacting RhoA directly, or vice versa. In any case, the cross-linking experiments need to be repeated and potentially adjusted to a cross-linker with a different side chain reactivity. A diazirine-based acid specific linker may be a good option, as the interaction sites of RhoA and E6AP suggested by the cross-linking experiment contain many acidic and only few lysine residues.

3.3.4.2 Interaction analysis with AlphaFold

After failing to identify the primary interaction partner of RhoA by the use of size exclusion chromatography, isothermal titration calorimetry, bacterial co-expression, and cross-linking coupled to mass spectrometry, we resorted to the protein structure prediction tool AlphaFold (Jumper et al. 2021; Varadi et al. 2021). Alpha Fold has been shown to accurately predict protein structures and model protein complexes (Bryant et al. 2022; Marcu, Tăbîrcă, and Tangney 2022). Thus, in cooperation with Maite Mißun (AG Marx), we supplied AlphaFold with the amino acid sequences for E6AP, HPV 16 E6, and RhoA.

A

mutated to alanine	
RhoA residue	16 E6 residue
V33	R141
E40	S138
N41	D44
Y66	C111
D76	H24
K186	Q20

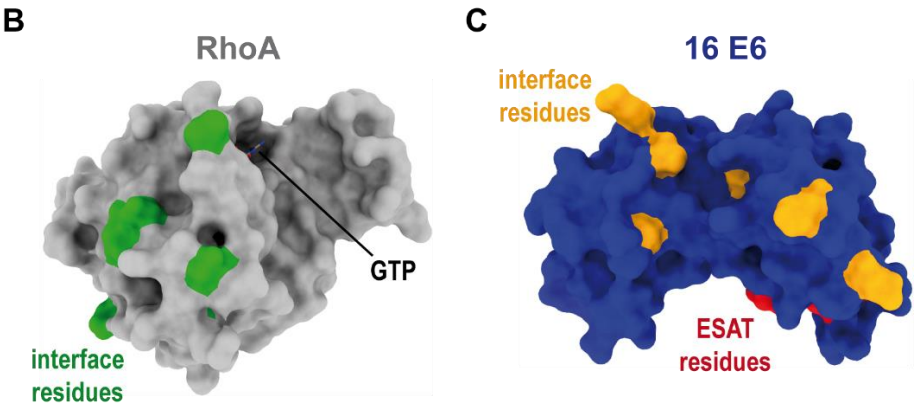

Figure 29. Interacting residues of RhoA and 16 E6 as suggested by AlphaFold. A│ List of residues of RhoA (left column) and of 16 E6 (right column) which were predicted to interact via H-bridges with each other by AlphaFold and were therefore each mutated to an alanine. **B**│ Structure of RhoA (PDB 1A2B) in grey with the RhoA interface residues highlighted in green, K186 is not present in the structure. The position of the GTP-binding pocket is indicated. **C**│ Structure of 16 E6 (PDB 4XR8) in dark blue with the 16 E6 interface residues highlighted in orange. In comparison, the residues which render 16 E6 unable to bind to p53 (ESAT) are highlighted in red. The structures were modified with UCSF ChimeraX (Goddard et al. 2018).

Various attempts by different groups to crystalise the full-length E6AP protein have failed over the years (M. Scheffner, personal communication), indicating the challenge of this endeavour. However, structures of isolated E6AP domains have been published, namely for the isolated HECT domain in complex with UbcH7 (Huang et al. 1999) and the N-terminal AZUL domain in complex with the Rpn10 RAZUL domain (Buel et al. 2020). It is therefore not surprising that AlphaFold also has difficulties in predicting a high-confidence structure of E6AP, in particular the structure of disordered regions within E6AP, which result in long stretches of very low confidence (see AlphaFold E6AP prediction, accessed in March 2023). Nevertheless, AlphaFold is able to model the 16 E6-E6AP interaction with high confidence (~85%), including the α-helix of E6AP known to contain the E6-binding peptide. For E6AP and RhoA, AlphaFold predicts a low confidence interaction (20-30%) between the E6AP HECT domain and RhoA (data not shown). However, that the HECT domain represents the RhoA interface appears unlikely, as in GST coprecipitation experiments (**Figure 24**), RhoA is unable to interact with E6AP ΔN499 (= E6AP HECT domain) in the presence of GST-16 E6. Between 16 E6 and RhoA, AlphaFold suggests an interaction site comprising six amino acid residues of both proteins with medium confidence (~50%). The residues predicted to form H-bonds with each other are listed in **Figure 29A**. All of these residues were mutated to alanine to prevent H-bond formation. The resulting RhoA and a 16 E6 mutants were termed 'interface mutants' (IFM). The positions of the 'interface residues' are highlighted on the RhoA surface (PDB 1A2B, Ihara et al. (1998)) in green (**Figure 29B**) and on the 16 E6 surface (PDB 4XR8, Martinez-Zapien et al. (2016)) in orange. As a reference, the ESAT residues of E6 (required for the interaction with p53, Foster et al. (1994)) are highlighted in red (**Figure 29C**).

First, the RhoA IFM was examined in coprecipitation experiments. For this, the *in vitro* translated RhoA IFM and RhoA WT were incubated with GST-tagged 16 E6 in the presence or absence of either His-tagged or MBP-tagged E6AP. E6AP and MBP-E6AP were both used, since they show rather different activity levels in ubiquitination experiments (data not shown). The binding of both E6AP variants to 16 E6 can be observed in the Coomassie stained gel (**Figure 30A**). Also, both E6AP variants show the same effect regarding RhoA binding. RhoA WT shows strong binding to GST-16 E6 in the presence of both E6AP variants. The binding of the RhoA IFM to GST-16 E6, on the other hand, is strongly impaired (**Figure 30A**). To confirm this result, the coprecipitation experiment was repeated with MBP-tagged 16 E6 immobilised on amylose resin in the presence or absence of E6AP. Again, the binding of the RhoA IFM is strongly impaired in comparison to RhoA WT (**Figure 30B**).

Using E6AP as bait, similar results were obtained. A GST coprecipitation assay reveals that RhoA IFM is unable to bind to GST-E6AP even in presence of MBP-16 E6 (**Figure 31A**). In contrast, the coprecipitation assay with MBP-E6AP reveals binding of the RhoA IFM to MBP-E6AP in the presence of GST-16 E6 (**Figure 31B**), though with little efficiency. Comparing the fluorographic readouts (**Figure 31A** and **B**), MBP-E6AP is able to mediate a stronger interaction with RhoA than GST-tagged E6AP.

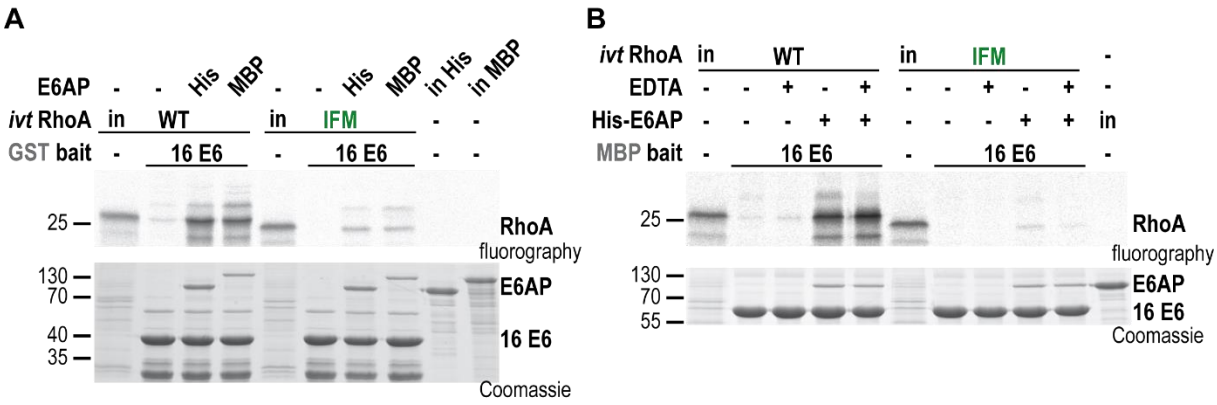

Figure 30. Mutation of the RhoA IFM residues impairs the RhoA-16 E6 interaction. **A**| The GST-16 E6 fusion protein bound to GSH beads was incubated with *in vitro* translated, radiolabelled RhoA variants for 90 min at 4°C in the presence of His-E6AP or MBP-E6AP as indicated. Beads were washed after the binding reaction and the eluates were analysed by SDS-PAGE followed by Coomassie staining (GST bait input detection, lower panel) and fluorography (binding reaction, upper panel). The running positions of the molecular mass markers (in kDa), the GST-16 E6 fusion protein, RhoA, and E6AP are indicated. in| 10% of the RhoA variants and 100% of the His-E6AP or MBP-E6AP used in the binding reaction. **B**| The MBP-16 E6 fusion protein bound to amylose beads was incubated with *in vitro* translated, radiolabelled RhoA variants for 90 min at 4°C in the presence of His-E6AP and 20 mM EDTA as indicated. Beads were washed after the binding reaction and the eluates were analysed by SDS-PAGE followed by Coomassie staining (GST bait input detection, lower panel) and fluorography (binding reaction, upper panel). The running positions of the molecular mass markers (in kDa), the MBP-16 E6 fusion protein, RhoA, and E6AP are indicated. in| 10% of the RhoA variants and 100% of the His-E6AP used in the binding reaction.

Nonetheless, overall, the coprecipitation experiments with the differently tagged E6AP forms show similar results, since the ratio of bound RhoA WT to bound RhoA IFM is very similar: when RhoA WT strongly interacts with MBP-E6AP, we can observe some binding of RhoA IFM, while there is no binding of RhoA IFM when RhoA WT shows a weaker interaction to the GST-tagged E6AP. As clearly visible in the Coomassie staining (**Figure 31A**, lower panel), there are many impurities in the GST-E6AP protein preparation that are also present in the binding assay. These may contribute to the decreased interaction strength in comparison to the purer MBP-E6AP protein preparation. Also, for the MBP-E6AP coprecipitation assay, more (GST-) 16 E6 is present, which might also add to the stronger interaction. In **Figure 30A** and **Figure 31A**, no EDTA was added since the binding of RhoA is readily observable in its absence. To rule out any potential EDTA effects, the experiment shown in **Figure 30A** was repeated in the presence and absence of EDTA and shows that EDTA has no impact on the interaction of RhoA with GST-16 E6-E6AP (data not shown). Furthermore, the reciprocal coprecipitation assay was performed with MBP-tagged RhoA WT of MBP-RhoA IFM as bait. The interaction was checked with either *in vitro* translated E6AP in combination with GST-tagged 16 E6 or with *in vitro* translated GFP-16 E6 in combination with His-E6AP. Both prey proteins show a strong interaction with MBP-RhoA WT and a very weak binding to MBP-RhoA IFM (data not shown).

To indirectly validate the structural integrity of the RhoA IFM, a ubiquitination assay with *in vitro* translated RhoA WT and RhoA IFM was performed in the presence or absence of E6AP and GST-16 E6. The assumption was that the 16 E6-E6AP complex does not recognize an incorrectly folded RhoA variant. This assay reveals that RhoA IFM is ubiquitinated with an efficiency similar to RhoA WT (**Supplementary Figure 8**). Therefore, the weak interaction observed in the coprecipitation assays (**Figure 30** and **Figure 31**) is apparently sufficient to enable efficient RhoA IFM ubiquitination.

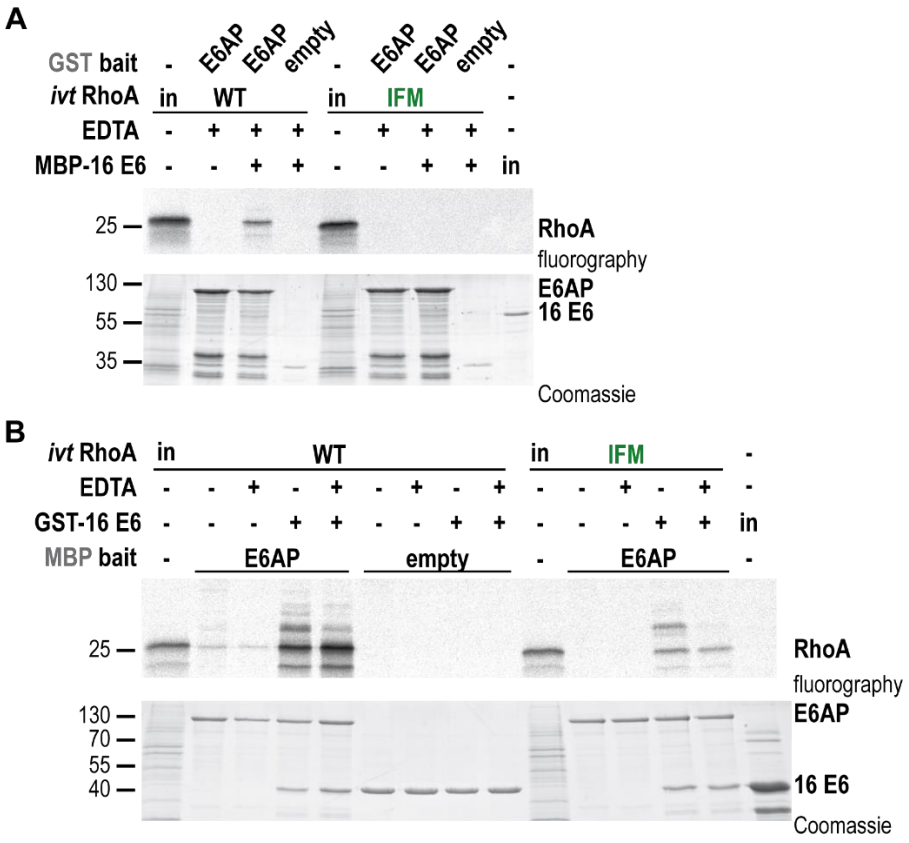

Figure 31. The RhoA IFM shows deficits in the interaction with E6AP. A│ The GST-E6AP fusion protein bound to GSH beads or empty GSH beads (empty) was incubated with *in vitro* translated, radiolabelled RhoA variants for 90 min at 4°C in the presence of MBP-16 E6 and 20 mM EDTA as indicated. **B**│ The MBP-E6AP fusion protein bound to amylose beads or empty amylose beads (empty) was incubated with *in vitro* translated, radiolabelled RhoA variants for 90 min at 4°C in the presence of GST-16 E6 and 20 mM EDTA as indicated. **A-B**│ Beads were washed after the binding reaction and the eluates were analysed by SDS-PAGE followed by Coomassie staining (GST or MBP bait input detection, lower panel) and fluorography (binding reaction, upper panel). The running positions of the molecular mass markers (in kDa), the GST-E6AP or MBP-E6AP fusion protein, RhoA, and 16 E6 are indicated. in│ 10% of the RhoA variants and 100% of the MBP-16 E6 or GST-16 E6 used in the binding reaction.

Finally, we compared in WG *in vitro* translated GFP-16 E6 WT and the GFP-16 E6 IFM in a coprecipitation assay with GST-RhoA WT or GST-RhoA G14V as bait. In the presence of E6AP, both 16 E6 proteins are able to interact with both GST-RhoA variants, but the GFP-16 E6 IFM shows a weaker interaction (data not shown). Since the ubiquitination of the *in vitro* translated RhoA IFM is unaffected by the mutations (**Supplementary Figure 8**), the 16 E6 IFM was used for the validation of the AlphaFold predictions in degradation assays in H1299 cells. The degradation of the known 16 E6-

E6AP substrate p53 was included as control. Rather unexpectedly, the degradation assay reveals that, while the 16 E6 IFM is still able to promote the degradation of RhoA G14V, it is unable to promote p53 degradation (**Figure 32**). In follow-up degradation experiments, the 16 E6 IFM was shown to exhibit the same effect as the 16 E6 ESAT mutant (data not shown).

In general, AlphaFold predictions should not be considered as facts, but rather as support for hypotheses regarding protein-protein interactions. The *in vitro* experiments with RhoA IFM show that not only the predicted binding to 16 E6, but also the binding to E6AP in presence of 16 E6 is impaired. AlphaFold predicts RhoA valine 33 to form an H-bond with arginine 141 of 16 E6. The non-polar amino acid valine, however, does not possess an oxygen atom besides the one in the amino acid backbone. A closer look into the suggested interaction reveals that AlphaFold actually predicts the H-bond to be formed between the amino acid backbone of valine and the side chain of arginine. This suggests that even though replacement of valine by alanine in RhoA IFM may indirectly impair the interaction via structural alterations, the H-bond between the two residues may still be formed. This also applies to the aspartate at position 76 of RhoA and the glutamine at position 20 of 16 E6. The data of the degradation assay (**Figure 32**) suggests that the 16 E6 IFM is as deficient in p53 degradation in cells as the 16 E6 ESAT mutant and not or less deficient in RhoA degradation. However, it should be noted that binding between p53 and 16 E6 IFM was not tested *in vitro*. The residues suggested by AlphaFold to be important for the p53-16 E6 interaction (data not shown) differ to those suggested for the RhoA-16 E6 interaction (**Figure 29A**). The AlphaFold prediction for the p53 structure includes, similar to the E6AP prediction, multiple loops of intrinsically disordered regions. the structure of which cannot be predicted (see AlphaFold p53 prediction, accessed in March 2023). The 16 E6 IFM cDNA was not cloned into a construct for bacterial expression, therefore the activity of the 16 E6 IFM could not be tested in *in vitro* ubiquitination assays. In conclusion, with the experiments resulting from the AlphaFold predictions, it is not possible to unravel the binding enigma of RhoA-16 E6-E6AP.

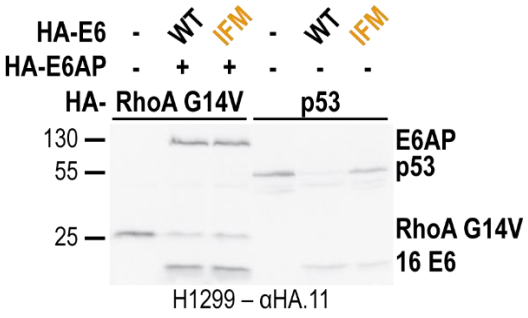

Figure 32. The 16 E6 IFM shows wild-type activity in RhoA degradation. H1299 cells were transfected with expression constructs encoding for HA-tagged RhoA, p53, E6AP and 16 E6 WT or 16 E6 IFM as indicated. 24 h post-transfection, the lysates were prepared and adjusted according to the transfection efficiency (β-galactosidase activity). Samples were analysed by SDS-PAGE followed by western blot analysis and proteins were detected using an αHA.11 antibody. The running positions of the molecular mass markers (in kDa) and the HA-tagged proteins are indicated.

All of the different approaches that were employed to analyse the complex formation between E6, E6AP, and RhoA confirmed the formation of the RhoA-E6AP-16 E6 ternary complex. However, it was not possible to determine whether there is a preferred interaction partner of RhoA within the complex. Similarly, no evidence for direct binding of RhoA to E6AP or of RhoA to 16 E6 in the absence of the respective other could be obtained. Yet, it cannot be excluded that RhoA is able to bind directly to E6AP and/or 16 E6 alone, albeit with an affinity that is too low to be detected by the means used. To obtain more insight into the E6-E6AP-RhoA complex, it would be necessary to solve the structure of the complex by X-ray crystallography or by Cryo-EM.

3.3.5 Inhibitory effect on 16 E6 stimulation

The phenomenon of reduced ubiquitin consumption by E6-E6AP in presence of RhoA was first noticed in GST-RhoA ubiquitination assays, as observed by Coomassie staining of free ubiquitin in the lower panel of **Figure 16A** and **C** and by quantification of free ubiquitin levels in **Figure 16B** and **D**. Furthermore, this reduction is observed only for E6-E6AP, but not for E6AP alone (**Figure 16**). In this context, it should be noted again that 16 E6 acts as an allosteric activator of E6AP and, thus, ubiquitin consumption by E6AP is expected to be increased in the presence of 16 E6 which is indeed observed in all our standard ubiquitination assays in the absence of RhoA (data not shown).

Based on this unexpected finding, the effect of GST-RhoA on the autoubiquitination of *in vitro* translated E6AP was investigated next. *In vitro* translated E6AP was used, as this allows for a clearer readout via fluorography in comparison to the Coomassie staining of bacterially expressed E6AP. For sufficient ubiquitination to occur also in the absence of 16 E6, *in vitro* translated E6AP was supplemented with additional low amounts of bacterially expressed E6AP (**Figure 33A**). In the absence of GST-16 E6, addition of increasing amounts of GST-RhoA has no effect on E6AP autoubiquitination. However, in the presence of GST-16 E6 addition of GST-RhoA results in a decreased E6AP autoubiquitination indicated by the reappearance of the non-modified E6AP and the reduction of the polyubiquitination smear (**Figure 33A**, asterisk).

The addition of GST-16 E6 alone also leads to a slight reduction in E6AP autoubiquitination, probably due to rate-limiting amounts of ubiquitin in the experiment. Next, the effect of GST-RhoA on substrate ubiquitination was evaluated in *in vitro* ubiquitination assays with different 16 E6-E6AP substrate proteins. In **Figure 33B**, ubiquitination assays with *in vitro* translated NHERF1 (upper panel) and p53 (lower panel) are shown. E6AP alone ubiquitinates NHERF1 and p53 only inefficiently. In line with the data of the E6AP autoubiquitination assay (**Figure 33A**), titration of GST-RhoA has no effect on this reaction. Upon addition of GST-16 E6, a strong increase in NHERF1 and p53 ubiquitination can be observed. This is blocked in the presence of increasing GST-RhoA amounts, regardless of the substrate protein (**Figure 33B**).

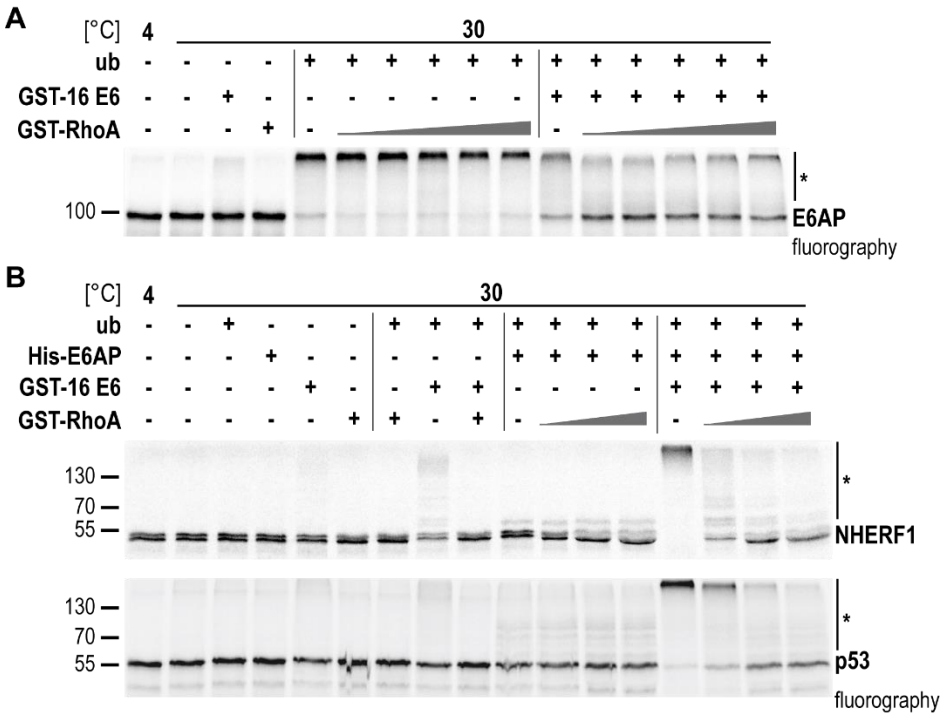

Figure 33. RhoA blocks the 16 E6 stimulatory effect on E6AP autoubiquitination and substrate ubiquitination. A| *In vitro* translated, radiolabelled E6AP was incubated with UBA1, UbcH7, and additional His-E6AP in the presence and absence of GST-tagged 16 E6, ubiquitin (ub), and increasing amounts of GST-tagged RhoA for 90 min at 30°C as indicated. The reactions were stopped with Laemmli buffer (see 0) and the samples were analysed by SDS-PAGE followed by fluorography. The running positions of the molecular mass markers (in kDa), the unmodified form (E6AP) and ubiquitinated forms of E6AP (*) are indicated. **B**| *In vitro* translated, radiolabelled NHERF1 (upper panel) and p53 (lower panel) was incubated with UBA1 and UbcH7 in the presence and absence of His-E6AP, ubiquitin (ub), GST-tagged 16 E6, and increasing amounts of GST-tagged RhoA for 90 min at 30°C as indicated. The reactions were stopped with Laemmli buffer (see 0) and the samples were analysed by SDS-PAGE followed by fluorography. The running positions of the molecular mass markers (in kDa), the unmodified forms (NHERF1 or p53) and ubiquitinated forms (*) are indicated.

In addition to NHERF1 and p53, ubiquitination assays with *in vitro* translated Ring1b and RhoA provided the same results (data not shown). The inhibiting effect of RhoA on the stimulatory effect of GST-16 E6 is therefore independent of the identity of the substrate protein. Preincubation of different assay components for 30 min on ice prior to the ubiquitination assay did not alter the results (**Supplementary Figure 9**).

As GST is known to dimerize (Maru et al. 1996), the inhibitory effect could be argued to arise from GST-16 E6-GST-RhoA oligomerisation rather than RhoA itself. However, tag free RhoA (**Figure 34A**) and MBP-tagged RhoA (data not shown) are also able to inhibit GST-16 E6-stimulated ubiquitination as well as GST-RhoA is able to inhibit MBP-16 E6-stimulated ubiquitination (**Figure 35A**) making this possibility unlikely. Since we have previously observed that the 16 E6-E6AP-Rho ternary complex is preferentially formed with the RhoA subfamily members (RhoA, RhoB, and RhoC, see **Figure 27**), we were also interested in testing the inhibitory potential of the different RhoA subfamily GTPases.

In a ubiquitination assay with *in vitro* translated p53, which was performed in presence of E6AP and GST-16 E6, different Rho variants were added (**Figure 34A**). The lower panel shows the Coomassie staining of the Rho proteins investigated. Besides GST-RhoA, untagged RhoA, GST-RhoB, and GST-RhoC show comparable inhibitory effects. While GST-RhoC shows the strongest effect in the assay shown, this tendency varies between different Rho protein preparations.

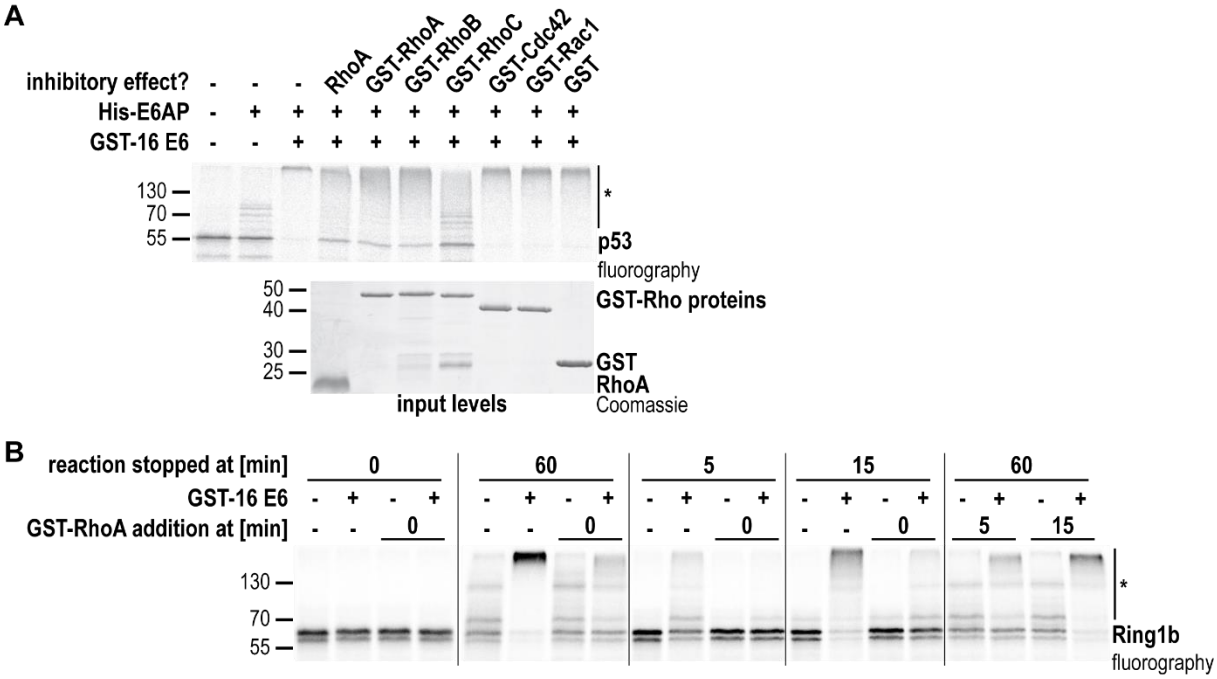

Figure 34. The inhibitory effect is restricted to RhoA family GTPases. A| *In vitro* translated, radiolabelled p53 was incubated with UBA1, UbcH7, and ubiquitin in the presence and absence of His-E6AP, GST-tagged 16 E6 and untagged RhoA or GST-Rho variants at 30°C as indicated. The reactions were stopped with Laemmli buffer (see 0) after the respective time points and the samples were analysed by SDS-PAGE followed by fluorography. The running positions of the molecular mass markers (in kDa), the unmodified form (p53) and ubiquitinated p53 forms (*) are indicated. **B**| *In vitro* translated, radiolabelled Ring1b I53S (catalytically inactive form of Ring1b) was incubated with UBA1, UbcH7, ubiquitin, and His-E6AP in the presence and absence of GST-tagged 16 E6 and RhoA at 30°C as indicated. GST-RhoA was added at different time points as indicated. The reactions were stopped with Laemmli buffer (see 0) after the respective time points and the samples were analysed by SDS-PAGE followed by fluorography. The running positions of the molecular mass markers (in kDa), the unmodified form (Ring1b) and ubiquitinated Ring1b forms (*) are indicated.

On the other hand, GST-Cdc42, GST-Rac1, and GST alone were unable to inhibit 16 E6-E6AP-mediated ubiquitination of p53. To further demonstrate that the inhibitory effect is specific for Rho proteins, the unrelated protein NHERF2 (GST-NHERF2) was tested but its presence does not have any effects on p53 ubiquitination (data not shown). Taken together, this data indicates that the potential to inhibit the 16 E6-mediated stimulation of E6AP is restricted to members of the RhoA subfamily.

To gain further insights into the inhibitory effect, inhibition of 16 E6-mediated ubiquitination of Ring1b I53S was monitored over time (0, 5, 15, 60 min) with addition of GST-RhoA at different time points of the reaction (0, 5, 15 min; **Figure 34B**). In case of RhoA addition at 0 min, the stimulatory effect of 16 E6 is completely blocked. This

is readily observable by comparing the reactions stopped at 60 min in the absence of RhoA to the reaction with addition of RhoA at 0 min. The reaction efficiency in the presence of both RhoA and 16 E6 is comparable to the reaction in their absence. The addition of RhoA after 15 min shows that when Ring1b polyubiquitination has already occurred, it cannot be reversed by RhoA, but further Ring1b ubiquitination is blocked. The inhibitory effect can also be observed in ubiquitination assays with the ubiquitin hydrophobic patch mutant LIA, GST-18 E6, or with the E6 mutants ESAT and the 16 E6 ΔPDZ binding motif mutants (data not shown). In addition to 16 E6, HERC2 is another known allosteric activator of E6AP (Kühnle et al. 2011). Due to its large size (~ 530 kDa), only the HERC2 fragment known to be required for E6AP activation (the isolated RLD2 domain; Kühnle et al. (2011)), was used for ubiquitination assays. The GST-tagged RLD2 is able to enhance E6AP autoubiquitination (albeit not as efficiently as GST-16 E6) and this stimulation is not impaired in the presence of GST-RhoA (**Supplementary Figure 10**). This indicates that the inhibitory effect of RhoA is specific for E6-mediated stimulation of E6AP.

In the presence of the RhoA subfamily members, which themselves are ubiquitination substrates of 16 E6-E6AP, 16 E6-E6AP-mediated ubiquitination of other substrate proteins is strongly impaired. Thus, rather than by an inhibitory effect, the decrease in ubiquitination could be due to competition of the substrates for ubiquitination by 16 E6-E6AP. In such a scenario, RhoA would have to be the preferred 16 E6-E6AP ubiquitination target.

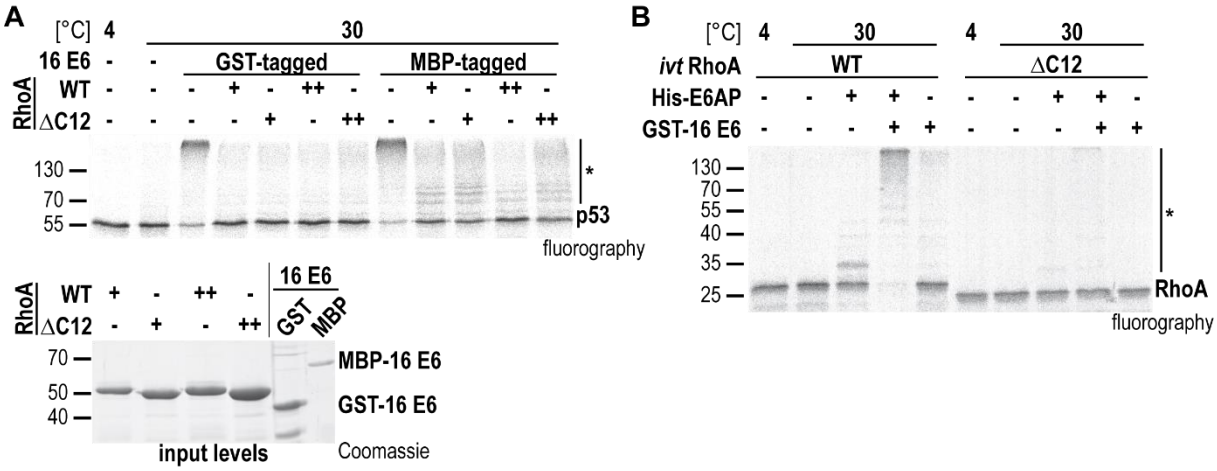

Figure 35. RhoA does not compete for ubiquitination with p53. A⎪ *In vitro* translated, radiolabelled p53 was incubated with UBA1, UbcH5b, ubiquitin, and His-E6AP in the presence and absence of GST-tagged or MBP-tagged 16 E6 and the GST-RhoA WT (WT) or GST-RhoA ΔC12 (ΔC12) for 90 min at 30°C as indicated. The reactions were stopped with Laemmli buffer (see 0) and the samples were analysed by SDS-PAGE followed by fluorography. The running positions of the molecular mass markers (in kDa), the unmodified form (p53), and ubiquitinated p53 forms (*) are indicated. **B**⎪ Coomassie staining of the inputs of the proteins used in (**A**). **C**⎪ *In vitro* translated, radiolabelled RhoA WT (WT) or RhoA ΔC12 (ΔC12) was incubated with UBA1, UbcH7, and ubiquitin in the presence and absence of His-E6AP and GST-tagged 16 E6 for 90 min at 30°C as indicated. The reactions were stopped with Laemmli buffer (see 0) and the samples were analysed by SDS-PAGE followed by fluorography. The running positions of the molecular mass markers (in kDa), the unmodified form (RhoA), and ubiquitinated RhoA forms (*) are indicated.

In case of p53, this seems unlikely, as p53 is more efficiently ubiquitinated than RhoA and the inhibitory effect was still observable in the presence of high, i.e. not rate-limiting amounts of ubiquitin in the ubiquitination assays (data not shown). Furthermore, in H1299 cells, the endogenous E6AP is sufficient for complete p53 degradation in presence of ectopic 16 E6 (**Figure 32**). For the degradation of RhoA, the endogenous E6AP is insufficient. RhoA is only degraded in presence of additional ectopic E6AP, and even then, to a lesser extent than p53 without additional E6AP (**Figure 32**). The above data indicate that at least for p53, the inhibitory effect mediated by RhoA is not due to substrate competition.

To further strengthen this hypothesis, we made use of the RhoA ΔC12 truncation, which was already introduced in 3.3.2.4 'RhoA activity mutants and truncations'. The truncated protein includes amino acid residues 1-181 of RhoA, thus lacking the C-terminal 12 residues including the hypervariable region and the CAAX box.

Bacterially expressed GST-tagged RhoA ΔC12 mutant was able to inhibit 16 E6-E6AP-mediated ubiquitination of *in vitro* translated p53 with GST-RhoA WT efficiency (**Figure 35A**, upper panel). In the experiment, two different amounts of RhoA proteins were used (see lower panel for input levels), and a complete block is already achieved with the lower concentration. Both GST-RhoA WT and GST-RhoA ΔC12 are able to inhibit GST-16 E6-mediated as well as MBP-16 E6-mediated stimulation of E6AP. The ability of RhoA ΔC12 mutant to serve as ubiquitination substrate for E6-E6AP was then determined (**Figure 35B**). In contrast to RhoA WT, *in vitro* translated RhoA ΔC12 is not ubiquitinated by 16 E6-E6AP. This is as expected, since the ΔC12 truncation lacks the lysines at position 185-187 that were shown to be the preferred ubiquitination sites for 16 E6-E6AP (**Figure 18**). In a GST coprecipitation experiment, the RhoA ΔC12 mutant is shown to bind to GST-16 E6 in presence of E6AP with similar efficiency as RhoA G14V (**Supplementary Figure 6**, left panel). The fact that the RhoA ΔC12 mutant cannot be ubiquitinated but is still able to inhibit 16 E6-mediated E6AP stimulation strengthens the notion that the inhibition is unrelated to substrate competition.

After characterization of the 'E6-inhibitory effect' of the RhoA subfamily members *in vitro*, the next step was to validate the data in cells. For this, we first used H1299 cells, which do not contain endogenous p53. Also, potential differences between Rho WT, the active G14V mutant, and the preferentially GDP-bound T19N mutant were of interest. Therefore, H1299 cells were transfected with HA-tagged constructs encoding p53, 16 E6, and the Rho variants. As mentioned before (e.g. **Figure 32**), endogenous E6AP in H1299 cells is sufficient for 16 E6-E6AP-mediated degradation of p53, thus no additional E6AP construct was transfected.

The Rho proteins and p53 were detected by western blot analysis with an αHA antibody. Levels of p53 were additionally determined with the p53-specific DO-I antibody. The degradation assay reveals that 16 E6-E6AP-mediated proteasomal degradation of p53 is blocked in the presence of RhoA, RhoB or RhoC (**Figure 36A-C**, middle and lower panels). In presence of the preferentially GTP-bound G14V mutants, p53 degradation is most strongly impaired, as judged by the intensity of the

p53 band. Rho WT has some inhibitory effect and the presence of Rho T19N has no impact on p53 degradation (for the quantification of p53 levels see **Figure 36D-F**). Even though the amounts of transfected DNA were adjusted based on the results of preliminary experiments, protein expression levels of the RhoA and RhoC T19N mutants are still lower than for WT and G14V, as indicated by quantification of Rho levels (**Figure 36G-I**). In case of RhoA and RhoC, the weaker T19N effects might therefore be due to the lower levels of these proteins.

For RhoB, however, levels of the T19N mutant are comparable to those of WT and G14V, yet there is no inhibitory effect of RhoB T19N on p53 degradation. This suggests that the lack of an inhibitory effect of RhoA T19N and RhoC T19N is probably not due to lower protein amounts but due to the T19N mutation. As discussed above (see 3.3.2.4 'RhoA activity mutants and truncations'), prenylation deficient mutants, e.g. RhoA C190A, should also be tested regarding their ability to block 16 E6-E6AP-mediated p53 degradation. This may offer information regarding the subcellular localisation, i.e. membrane-bound or cytosolic, of Rho proteins required to exhibit inhibitory effects.

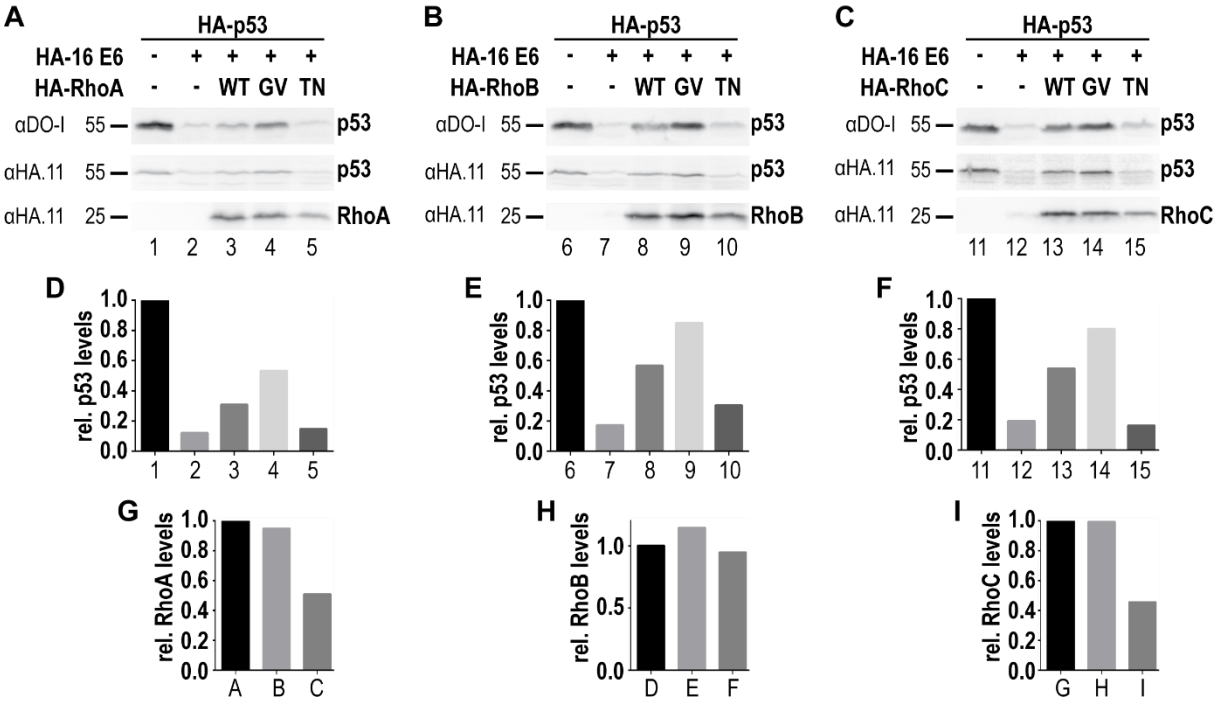

Figure 36. RhoA GTPases block the 16 E6-E6AP-mediated degradation of ectopic p53 in H1299 cells. H1299 cells were transfected with expression constructs encoding for HA-tagged p53, 16 E6 and **A**│ RhoA, **B**│ RhoB, or **C**│ RhoC as indicated. For each Rho protein, the wild-type (WT), the G14V mutant (GV), and the T19N mutant (TN), were compared. 24 h post-transfection, the lysates were prepared and adjusted according to the transfection efficiency (β-galactosidase activity). Samples were analysed by SDS-PAGE followed by western blot analysis and proteins were detected using an αHA.11 (Rho proteins and p53) and αDO-I (p53) antibody. The running positions of the molecular mass markers (in kDa) and the HA-tagged proteins are indicated. Levels of HA-16 E6 (200 ng) are too low for the detection via western blot. **D-F**│ The quantification of the relative p53 levels was performed from the αDO-I blots. **G-I**│ The quantification of the relative Rho levels was performed from the αHA.11 blot.

As mentioned before, the possibility of substrate competition is also unlikely in this scenario, since in contrast to p53, the Rho proteins are not degraded in the absence of ectopic E6AP. Additionally, the amount of 16 E6 construct transfected was reduced from 2000 ng (as in Rho degradation assays) to 200 ng in this experiment, to only have the amount of 16 E6 present that is required to promote efficient p53 degradation. Transfection of 2000 ng of the 16 E6 construct enables the detection of 16 E6 protein via western blot analysis. As this is not possible with 200 ng expression construct, a 16 E6 western blot is missing in **Figure 36**. Analogue to the experiment with RhoA/B/C, the effect of Rac1 and Cdc42 on p53 degradation was also investigated, but only with the WT variants. In line with the results obtained *in vitro* (**Figure 34A**), Rac1 and Cdc42 are unable to inhibit 16 E6-E6AP mediated degradation of p53 (**Supplementary Figure 11**).

3.3.6 Formation of quaternary complexes

A possible explanation for the inhibitory effect of the Rho proteins is that they compete with p53/Ring1b/NHERF1 for binding to E6-E6AP. To test this possibility, GST coprecipitation experiments were initially performed with WG *in vitro* translated p53 as prey protein and GST-tagged RhoA variants as bait, in the absence or presence of untagged 16 E6 and E6AP. The experiment shows that in the presence of 16 E6 and E6AP, p53 strongly interacts with GST-tagged RhoA WT, RhoA G14V, and RhoA Q63L (**Figure 37**). The presence of either 16 E6 or E6AP alone is insufficient for p53 to bind to RhoA (data not shown for E6AP alone).

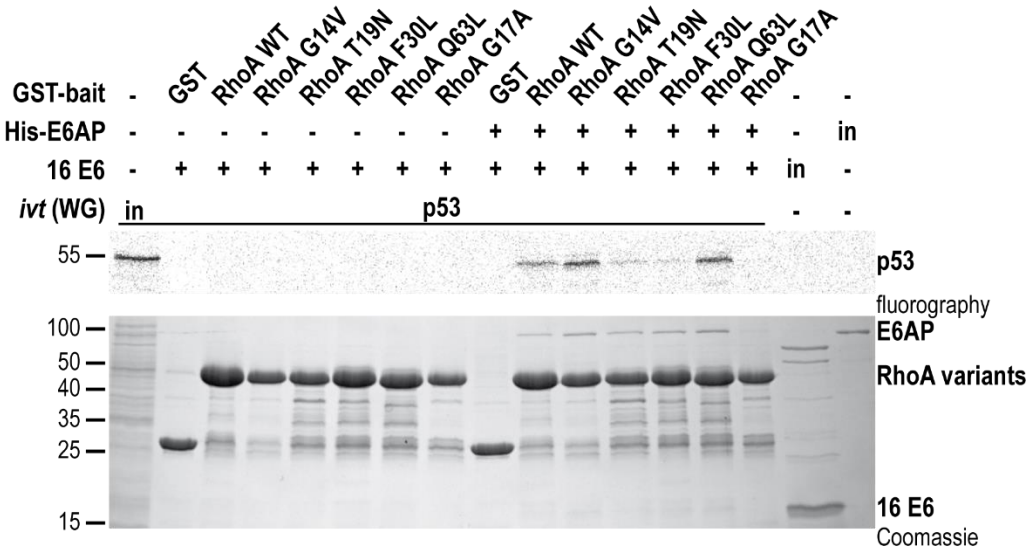

Figure 37.The quaternary complex is preferentially formed with GTP-bound, active RhoA. The GST-RhoA fusion variants bound to GSH beads were incubated with wheat germ *in vitro* translated, radiolabelled p53 for 90 min at 4°C in the presence of His-E6AP and untagged 16 E6 as indicated. Beads were washed after the binding reaction and the eluates were analysed by SDS-PAGE followed by Coomassie staining (GST bait input detection, lower panel) and fluorography (binding reaction, upper panel). The running positions of the molecular mass markers (in kDa), the GST-RhoA fusion proteins, p53, 16 E6, and E6AP are indicated. in | 10% of the p53 and 100% of the His-E6AP or untagged 16 E6 used in the binding reaction. The experiment was performed by Tom Pfleghaar during the VTK 2021 under my supervision.

This indicates the formation of a quaternary complex comprised of p53-RhoA-16E6-E6AP. Furthermore, p53 can be observed to preferentially interact with RhoA in its GTP-bound form (G14V and Q63L mutants), while hardly any interaction is observable with RhoA T19N and RhoA F30L. Considering the inhibitory effect of RhoA on 16 E6-E6AP-mediated p53 ubiquitination, this further strengthens the notion that RhoA and p53 do not compete for the interaction with 16 E6-E6AP, but rather are able to coexist in the same complex.

The use of MBP-tagged RhoA G14V instead of GST-tagged RhoA for the formation of the quaternary complex with p53 renders the same result. *In vitro* translated p53 is able to bind to MBP-RhoA G14V in presence of E6AP and 16 E6 (**Supplementary Figure 12**). In the next step, GST coprecipitation was performed in presence of different 16 E6 variants. In addition to 16 E6 WT, the 16 E6 ESAT mutant (deficient in p53 binding; Foster et al. (1994)) and the 16 E6 L50E mutant (deficient in E6AP binding; Zanier et al. (2013)), were employed (**Figure 38**).

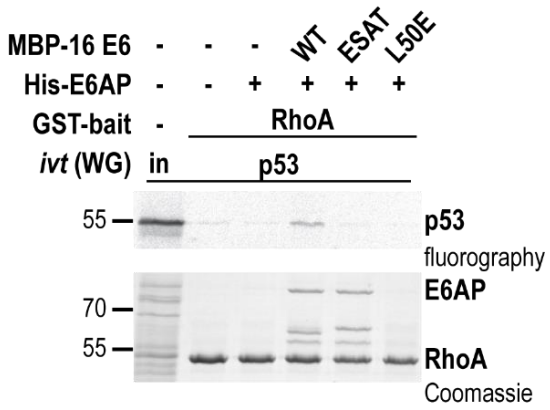

Figure 38. 16 E6 interaction with p53 and E6AP is required for quaternary complex formation. The GST-RhoA fusion protein bound to GSH beads was incubated with *in vitro* translated, radiolabelled p53 for 90 min at 4°C in the presence of His-E6AP and MBP-tagged 16 E6 variants as indicated. The *in vitro* translation was performed in wheat germ extract (WG), which does not contain endogenous E6AP. Beads were washed after the binding reaction and the eluates were analysed by SDS-PAGE followed by Coomassie staining (GST bait input detection, lower panel) and fluorography (binding reaction, upper panel). The running positions of the molecular mass markers (in kDa), the GST-RhoA fusion protein, p53, and E6AP are indicated. in⎪ 10% of the p53 used in the binding reaction.

This experiment confirmed the interaction between 16 E6 and p53, as well as 16 E6 and E6AP to be required for the successful formation of the quaternary complex. The functionality of the 16 E6 L50E mutant is additionally observed in the Coomassie readout, as no E6AP can be detected. Unexpectedly, reciprocal coprecipitation with Strep-tagged p53 immobilized on Strep-Tactin beads and *in vitro* translated RhoA in presence or absence of E6AP and GST-16 E6 shows an interaction so weak that it is hardly detectable (data not shown). This may be due to the same reasons discussed in context of the interaction with 18 E6 and Rac1/Cdc42 (see 3.3.2.1 ‘High-risk and low-risk E6 proteins’ and 0 ‘

RhoA subfamily members and other Rho GTPases as interaction partners of E6-E6AP’).

In addition to RhoA, the potential formation of a quaternary complex with RhoB, RhoC, Rac1, or Cdc42 was also of interest. The GST coprecipitation experiments were performed with the GST-tagged Rho proteins, *in vitro* translated p53, E6AP and untagged 16 E6. In comparison to RhoA, RhoB and RhoC show a weaker potential to form a quaternary complex with p53 (**Supplementary Figure 13**). Cdc42 shows a very weak interaction with p53, while Rac1 is able to interact with p53 almost as efficiently as the RhoA subfamily members, but in comparison to RhoA, RhoB, and RhoC more Rac1 protein was used as bait. Also in the Coomassie readout, the binding of E6AP to GST-Rac1 or GST-Cdc42 is decreased. Therefore, it seems like all tested GTPases were able to form a quaternary complex with E6, E6AP, and p53, with RhoA showing the strongest interaction.

Even though p53 is the best studied and most prominent interaction partner of 16 E6-E6AP, other known 16 E6 interacting proteins were also of interest. Dlg1 was tested as representative for proteins known to interact with 16 E6 via its PDZ domain-binding motif and independent of E6AP (Kiyono et al. 1997; Gardiol et al. 1999). NHERF1 was tested as representative for proteins known to interact with 16 E6 independent of its PDZ domain-binding motif but in an E6AP-dependent manner (Drews, Case, and Vande Pol 2019).

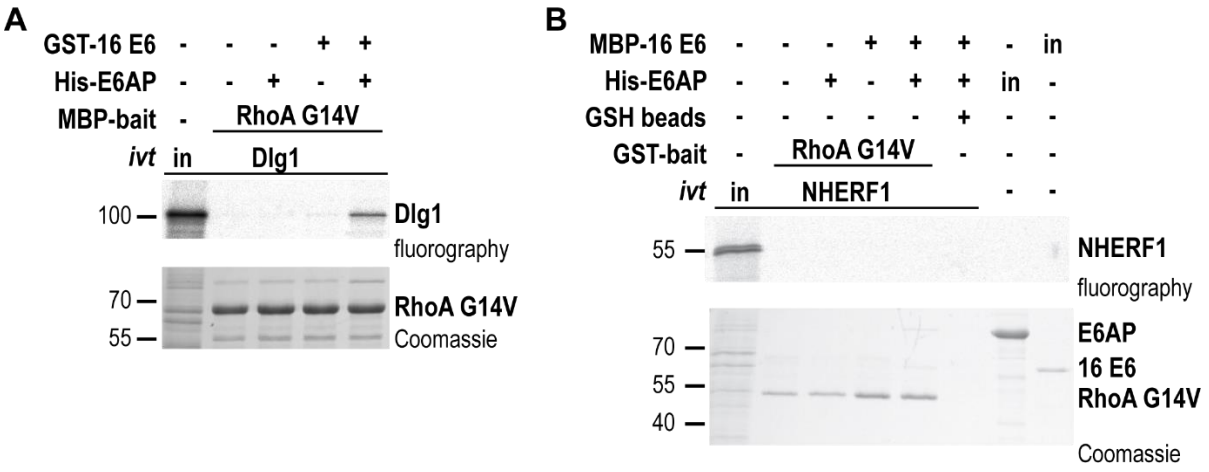

Figure 39. RhoA forms a quaternary complex with Dlg1 but not with NHERF1. A│ The MBP-RhoA G14V fusion protein bound to amylose beads was incubated with *in vitro* translated, radiolabelled Dlg1 for 90 min at 4°C in the presence of His-E6AP and GST-tagged 16 E6 as indicated and 20 mM EDTA. Beads were washed after the binding reaction and the eluates were analysed by SDS-PAGE followed by Coomassie staining (MBP bait input detection, lower panel) and fluorography (binding reaction, upper panel). The running positions of the molecular mass markers (in kDa), the MBP-RhoA G14V fusion protein and Dlg1 are indicated. in│ 10% of the Dlg1 used in the binding reaction. **B**│ The GST-RhoA G14V fusion protein bound to GSH beads, or GSH beads alone was incubated with *in vitro* translated, radiolabelled NHERF1 for 90 min at 4°C in the presence of His-E6AP and MBP-tagged 16 E6 as indicated. Beads were washed after the binding reaction and the eluates were analysed by SDS-PAGE followed by Coomassie staining (GST bait input detection, lower panel) and fluorography (binding reaction, upper panel). The running positions of the molecular mass markers (in kDa), the GST-RhoA G14V fusion protein and NHERF1 are indicated. in│ 10% of the NHERF1 and 100% of the His-E6AP or MBP-16 E6 used in the binding reaction. The experiment was performed by Nadja Eulich, under my supervision.

With coprecipitation experiments, the formation of a quaternary complex with Dlg1 (**Figure 39A**), but not with NHERF1 (**Figure 39B**) can be confirmed. Both proteins were independently tested in GST and MBP coprecipitation experiments with varying levels of bait proteins and all of them render similar results (data not shown). In a control coprecipitation experiment, the interaction between GST-16 E6 and NHERF1 is confirmed (data not shown), indicating that per se, binding with NHERF1 can be observed with our experimental setup.

In contrast to p53 and RhoA, NHERF1 and RhoA may compete for binding to 16 E6-E6AP, providing an obvious explanation for the inhibitory effect of the Rho proteins on E6-E6AP-mediated ubiquitination of NHERF1 *in vitro* (**Figure 33B**, upper panel). To further corroborate this possibility, GST-16 E6 coprecipitation experiments with either *in vitro* translated RhoA in the presence and absence of MBP-tagged NHERF1, or with *in vitro* translated NHERF1 in the presence and absence MBP-tagged RhoA, should be performed. In case of binding competition, the *in vitro* translated protein would be displaced from the complex. Furthermore, the inhibitory effect of RhoA on the degradation of NHERF1 in H1299 cells should be tested, analogous to the experiments performed with p53. E6AP levels in parental H1299 cells are sufficient to promote NHERF1 degradation in the presence of ectopic 16 E6 (data not shown).

The case of NHERF1 is intriguing, as NHERF1 has been suggested as an upstream activator of RhoA (Kuang et al. 2012), indicating a potentially more complex connection between the two proteins. This upregulation of RhoA entails the ROCK-mediated phosphorylation and therefore activation of Ezrin by releasing its auto-inhibited state (Favia et al. 2010). Ezrin, one of the ERM (Ezrin, Radixin, and Moesin) proteins, acts as a connector between actin filaments and the plasma membrane. It facilitates this connection by the use of scaffolding proteins like NHERF1, and only active and therefore membrane-associated Ezrin is able to interact with NHERF1 (Shaw et al. 1998). Overexpression of both, NHERF1 and RhoA G14V, was shown to cause an increase in active Ezrin levels and, additionally, activation of RhoA was shown to be NHERF1 dependent (Favia et al. 2010). Furthermore, the ERM proteins were shown to regulate Rho GTPases, suggesting a positive feedback loop. The binding of active ERM proteins to Rho-GDIs cause the displacement of the Rho-GDI from the Rho GTPase, thereby enabling the GTPase to bind GTP and become activated (reviewed in Ivetic and Ridley (2004)). In a clinical context, NHERF1 is known to play a major role in the regulation of cystic fibrosis transmembrane conductance regulator (CFTR) as part of the NHERF1/Ezrin/RhoA ‘signalosome’ (Guerra et al. 2005; Castellani et al. 2017) and is also able to rescue a CFTR mutant (ΔF508) which is known to cause cystic fibrosis (Bossard et al. 2007). In an E6-dependent context, NHERF1 was shown to be degraded by high-risk and low-risk E6 proteins in complex with E6AP (Drews, Case, and Vande Pol 2019). Overall, these insights show an intricate network around NHERF1 that has to be further unravelled in regard of the RhoA-E6-E6AP data obtained in this thesis.

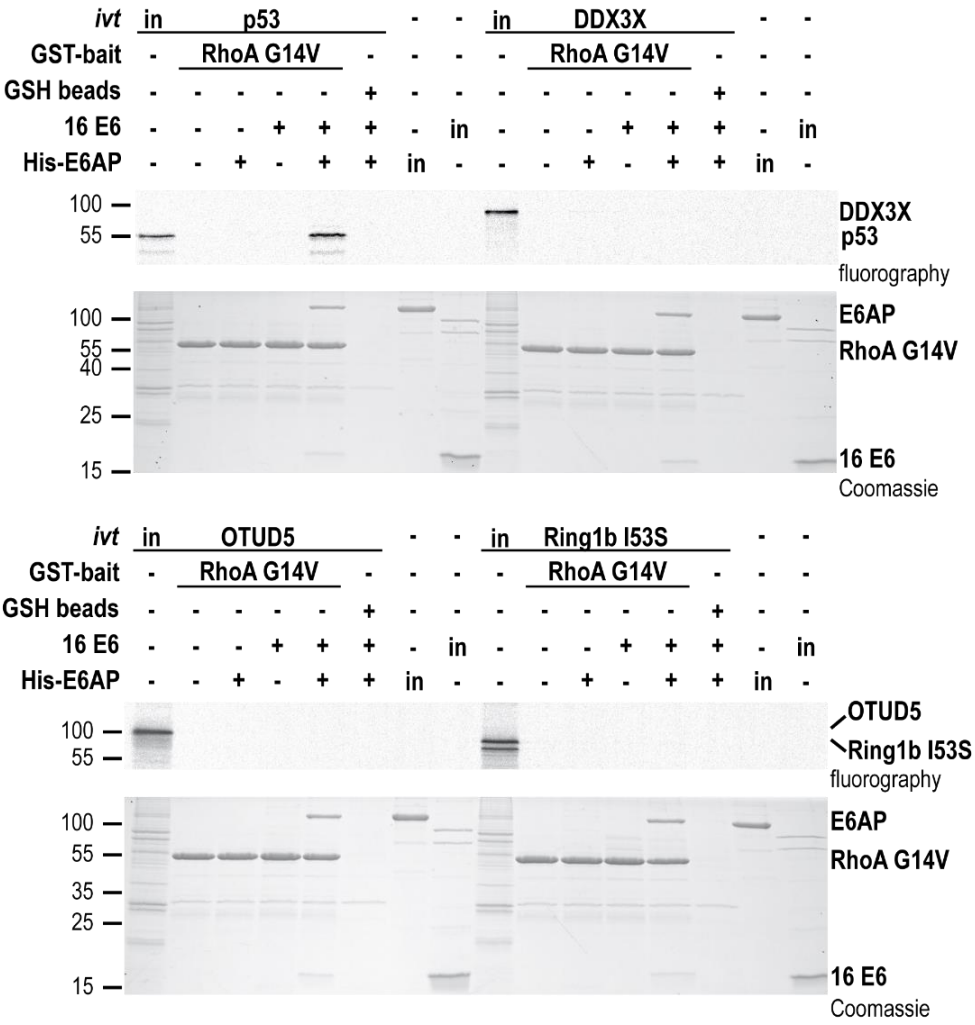

Figure 40. The ability to form a quaternary complex is restricted to certain proteins. The GST-RhoA G14V fusion protein or empty GSH beads were incubated with *in vitro* translated, radiolabelled p53, DDX3X, OTUD5, or Ring1b I53S (catalytically inactive Ring1b) with 20 mM EDTA for 90 min at 4°C in the presence or absence of His-E6AP and untagged 16 E6 as indicated. Beads were washed after the binding reaction and the eluates were analysed by SDS-PAGE followed by Coomassie Blue staining (GST bait input detection, lower panels) and fluorography (binding reaction, upper panels). The running positions of the molecular mass markers (in kDa), the GST-RhoA G14V, His-E6AP, and untagged 16E6 are indicated. in | 10% of the *in vitro* translated proteins and 100% of the His-E6AP or untagged 16 E6 used in the binding reaction. In contrast to p53, other known 16 E6-E6AP interactors (DDX3X, OTUD5 (Ebner et al. 2020)) and a known substrate of E6AP (Ring1b (Zaaroor-Regev et al. 2010)), were unable to form a quaternary complex with GST-RhoA G14V.

The extent of quaternary complex formation was further analysed with potential E6 substrates identified by Ebner et al. (2020) that do not contain a PDZ domain and which do not require additional E6AP for their interaction with E6 proteins. The DEAD box family of RNA helicases member DEAD box protein 3 X-chromosomal (DDX3X) and the deubiquitinating enzyme OTU domain-containing protein 5 (OTUD5) were previously shown to strongly interact with GST-16 E6 also in the absence of E6AP (Ebner et al. 2020). However, in contrast to p53, neither DDX3X nor OTUD5 are able to interact with GST-RhoA G14V in the presence or absence of 16 E6 and/or E6AP (**Figure 40**). Furthermore, a catalytically inactive variant of the known E6AP substrate

Ring1b (Zaaroor-Regev et al. 2010), Ring1b I53S, is also unable to form a quaternary complex with GST-RhoA G14V (**Figure 40**).

In conclusion, the data obtained indicate that the phenomenon of quaternary complex formation of E6-E6AP-RhoA is specific for certain proteins; however, the actual requirements have yet to be determined. An overview of the different tested combinations and their specifications is given in **Table 6**. However, the ability of RhoA to inhibit E6-E6AP-mediated ubiquitination of substrate proteins does not appear to correlate with the ability of the substrate proteins to form quaternary complexes. To further validate this assumption, the effect of RhoA on E6-E6AP-mediated ubiquitination of DDX3X or OTUD5 should be determined. In any case, the data obtained clearly indicate that the inhibitory effect of RhoA depends on the presence of 16 E6.

Table 6. Summary of the investigated RhoA-mediated quaternary complexes. Overview of the proteins that were tested in regard to their ability to form a quaternary complex with RhoA as bait protein. For DDX3X and OTUD5, the direct interactor is not known.

POI	direct interactor	E6AP required	16 E6 required	quaternary complex with RhoA
p53	16 E6	yes	-	yes
Dlg1	16 E6 (PDZ BM)	no	-	yes
NHERF1	16 E6	yes	-	no
Ring1b	E6AP	-	no	no
DDX3X	?	?	?	no
OTUD5	?	?	?	no

4. Summary and Outlook

The need for well-characterised E6AP substrates, and substrates of the HPV E6-E6AP complex in regard to human health has been extensively described in this thesis. With the data obtained by Ebner et al. (2020) as starting point, we were able to confirm several of the suggested (E6-)E6AP substrates, thereby also verifying the applied methodology.

The antagonistic p53 regulatory proteins iASPP and ASPP2 were both confirmed as 11 E6- and 16 E6-E6AP substrate proteins *in vitro*. In cellular degradation assays, iASPP was the first tested protein to be specifically degraded by low-risk 11 E6 in complex with E6AP, while ASPP2 was efficiently degraded by 11 E6-E6AP and 16 E6-E6AP. Future experiments should aim at the paradox as to why two antagonistic proteins are targeted and should account for the possibility that this could be regulated in a temporal manner. MRE11, a protein involved in DNA repair, was also verified as an E6-E6AP substrate *in vitro* and *in cellula.*

Furthermore, the small GTPase RhoA and its subfamily members RhoB and RhoC were successfully identified as E6-E6AP interactors. The ternary complex of Rho-E6-E6AP was preferentially formed with the high-risk HPV 16 E6 protein and the active, GTP-bound RhoA. Experiments with the high-risk E6 protein 18 E6, or with other Rho GTPases (e.g. Rac1, Cdc42) show that in cases of weaker interaction, ternary complex formation was dependent on correct ratios between the involved proteins. While the exact required ratio is unknown, an increase in Rho protein in comparison to E6-E6AP (i.e. Rho as bacterially expressed bait protein) was able to rescue any deficits in the ternary complex formation.

Additionally, members of the RhoA subfamily were efficiently ubiquitinated by 16 E6-E6AP *in vitro* and also served as substrates in cellular degradation assays. With the help of XL-MS/MS, it was possible to map the primary site of ubiquitination to the C terminus of the Rho proteins. In contrast to the polyubiquitination promoted by 16 E6-E6AP, E6AP alone was able to mostly catalyse monoubiquitination of *in vitro* translated or GST-tagged RhoA, which might have a regulatory function. The activation state of Rho GTPases is of constant interest, indicated also by the ever-evolving tools developed to monitor RhoA activation. This is demonstrated by this recently published fluorescent biosensor which is able to report on the activation state of multiple Rho GTPases at the same time (Pimenta et al. 2023). Potentially, tools like this could be used to observe any regulatory effects of E6AP (and 16 E6) on RhoA activation.

In comparison to other known E6-E6AP interactors like p53 or PDZ domain-containing proteins, the RhoA-16 E6-E6AP complex showed unique binding characteristics. However, even after several different experimental approaches, it was not possible to determine the primary RhoA interaction partner within the complex. It is possible that, analogous to the interaction with p53, E6AP is required to stabilize a certain 16 E6 conformation which then enables the ternary complex formation with RhoA, or vice versa.

Even though the data obtained from cross-linking experiments suggested E6AP as the primary interactor, these results have to be repeated. For this, also an alternative cross-linker (e.g. diazirine-based or photo-reactive on one side) should be considered, to not depend on the presence of reactive lysines. In line with the p53-16 E6-E6AP complex (Martinez-Zapien et al. 2016), it would be ideal to solve the structure of the RhoA-16 E6-E6AP complex by e.g. crystallography or by Cryo-EM. Also, the determination of the dissociation constant (K_D) of either RhoA-E6AP or RhoA-16 E6 with the MonolithX device from Nanotemper should be attempted. Here, preliminary experiments rendered promising results, and comparable to analyses with iTC, all proteins remain in solution during MonolithX measurements.

Furthermore, it was discovered that specifically members of the RhoA subfamily were able to block the 16 E6-mediated stimulatory effect on E6AP *in vitro* and *in cellula*. The effect could be observed independent of the targeted substrate while the allosteric activation of E6AP by HERC2 was unaffected. In the case of p53 as E6-E6AP substrate, with the help of a truncated RhoA variant (RhoA ΔC12), it was possible to show that the inhibitory effect on 16 E6 mediated by RhoA was independent of substrate competition. RhoA ΔC12 was able to block the ‘E6-effect’ but could not itself be ubiquitinated by 16 E6-E6AP, as it lacks the C-terminal 12 amino acid residues including the three lysine residues (K185-K187) that were shown to be preferentially used as ubiquitination targets by 16 E6-E6AP.

In addition to the RhoA-16 E6-E6AP ternary complex, the formation of a quaternary complex with p53 was confirmed. In presence of 16 E6-E6AP, p53 preferentially interacted with GTP-bound RhoA. The fact that RhoA and p53 were able to coexist in a complex further strengthens the notion that the RhoA-mediated inhibitory effect is indeed not based on substrate competition. However, while members of the RhoA subfamily were able to block the 16 E6-mediated stimulation of E6AP independent of the ubiquitination substrate, not all of the tested substrates were able to form a quaternary complex with RhoA-16 E6-E6AP. Exact requirements and the underlying mechanism have yet to be determined. Future experiments should address the potential effect of RhoA on the NHERF1-16E6-E6AP complex and investigate the RhoA-NHERF1 interaction, as NHERF1 was one of the tested interactors that was unable to form a quaternary complex with RhoA-16 E6-E6AP and is also known to participate in regulation of RhoA activation (Favia et al. 2010).

5. Experimental part

5.1 Materials

5.1.1 Chemicals and reagents

Name	Manufacturer
Acetic acid	VWR
Adenosine triphosphate (ATP)	Sigma-Aldrich
Ampicillin	Roth
Ammonium peroxydisulfate (APS)	Roth
Aprotinin	Sigma-Aldrich
Bovine serum albumin (BSA)	Roth
Bromphenol Blue	Serva
Chloramphenicol	Roth
Coomassie Brilliant Blue R250	Roth
Deoxynucleoside triphosphate (dNTP mix: 200 nM each of A, T, G, C)	Thermo Scientific
Dimethyl sulfoxide (DMSO)	Sigma-Aldrich
Disodium phosphate (Na_2HPO_4)	Merck
Dithiothreitol (DTT)	Roth
DNA Loading Dye (6X)	Thermo Scientific
Enlightning (Amplifier)	PerkinElmer
Ethanol	Roth
Ethylenediaminetetraacetic acid (EDTA)	Roth
Glutathione Sepharose 4 Fast Flow	GE Healthcare
Glycerol	Roth
Glycine	Roth
Guanidinium chloride	Roth
Hydrochloric Acid	Roth
Isopropanol	Sigma-Aldrich
Imidazole	Merck
Isopropyl-β-D-thiogalactopyranoside (IPTG)	Roth
Kanamycin	Roth
LB (Luria Broth)	Roth
Leupeptin	Roth

Name	Manufacturer
L-Glutathione reduced	Sigma-Aldrich
Lipofectamine 2000	Invitrogen
Magnesium chloride ($MgCl_2$)	Acros organics
Magnesium sulphate ($MgSO_4$)	Roth
β-Mercaptoethanol	Merck
Methanol	Sigma-Aldrich
Midori Green	Nippon Genetics
Milk powder	Roth
Monosodium phosphate (NaH_2PO_4)	Merck
Nonidet P40 substitute	Sigma-Aldrich
Ortho-Nitrophenyl-β-galactoside (ONPG)	Sigma-Aldrich (4 mg/ml in 100 mM Na_2HPO_4 pH 7.0)
Pefabloc	Boehringer Ingelheim
Phosphate-buffered saline (PBS)	Gibco
Pierce ECL Western Blotting Substrate	Thermo Scientific
Q Sepharose Fast Flow	GE Healthcare
RotiBlue	Roth
Rotiphorese Gel 30 (37.5:1) Acrylamide	Roth
S^{35}-methionine	PerkinElmer
Sodium chloride (NaCl)	Roth
Sodium dodecyl sulphate (SDS)	Roth
Sodium hydroxide (NaOH)	Sigma-Aldrich
Tetramethylethylenediamine (TEMED)	Roth
Triton X-100	Roth
Trizma Base (Tris)	Sigma-Aldrich
Tween20	Roth
Ubiquitin from bovine erythrocytes	Sigma-Aldrich
UltraPure agarose	Invitrogen

5.1.2 Buffers, solutions, and kits

Name	Composition
BufferZ	100 mM Na_2HPO_4 10 mM KCl 1 mM $MgSO_4$ 50 mM β-Mercaptoethanol pH 7.0
Coomassie destaining solution	50% MilliQ 40% Methanol 10% Acetic Acid
Coomassie staining solution	2 g/l Coomassie Brilliant Blue R250 in Coomassie destaining solution
GSH elution buffer	25 mM Glutathione 50 mM Tris-HCl pH 8.0
Laemmli SDS-PAGE running buffer	25 mM Tris-HCl pH 8.4 200 mM Glycine 0,1% (w/v) SDS
2x Laemmli buffer (SDS-PAGE sample buffer)	125 mM Tris-HCl pH 6.8 200 mM DTT 4% SDS 0.001 % Bromphenol blue
5x Laemmli buffer (SDS-PAGE sample buffer)	312,5 mM Tris-HCl pH 6.8 500 mM DTT 10% SDS 0.001% Bromphenol blue
PBS-T	1% Triton X-100 in PBS
PBS-T lysis buffer (bacteria)	1 µg/ml Aprotinin/Leupeptin 1 mM Pefabloc 1 mM DTT in PBS-T
Pulldown buffer	1 part TNN 4 parts $T_{25}N_{50}$ pH 7.5 1 mM DTT
SDS-PAGE separating gel buffer	1.5 M Tris-HCl pH 8.8 0.4% SDS
SDS-PAGE stacking gel buffer	0.5 M Tris-HCl pH 6.8 0.4% SDS 0.001% Bromphenol blue
SUMO protease buffer	50 mM Tris-HCl pH8 150 mM NaCl 1mM DTT 5% (v/v) glycerol

Name	Composition
T25N50	25 mM Tris-HCL pH7.5 50 mM NaCl
TAE buffer 50x	2 M Tris-HCl pH 8 950 mM Acetic acid 50 mM EDTA
TNE-T buffer	50 mM Tris-HCl pH7.6 50 mM NaCl 2.5 mM EDTA 0.1% (v/v) Tween20
TNN buffer	100 mM Tris-HCl pH 8 100 mM NaCl 1% (v/v) Nonidet P40 substitute
TNN lysis buffer (mammalian cells)	1 µg/ml Aprotinin/Leupeptin 1 mM Pefabloc 1 mM DTT, in TNN buffer
Transfer buffer 20x (western blot)	12.5 mM Tris-HCl pH 8.3 100 mM glycine

Kit	Manufacturer	Usage
Phusion High-Fidelity PCR kit	New England Biolabs	Cloning PCR
Pierce BCA Protein Assay kit	Thermo Scientific	Determination of protein concentration
PureYield Plasmid Midiprep System	Promega	DNA Midi prep
Q5 SDM kit	New England Biolabs	Site directed mutagenesis (point mutations, truncations, insertion)
QIAprep Spin Miniprep KIT	QIAGEN	DNA Mini prep
TnT T7-coupled Reticulocyte Lysate System	Promega	*in vitro* translation of proteins
TnT T7-coupled Wheat Germ Extract System	Promega	*in vitro* translation of proteins (in the absence of E6AP)

5.1.3 Enzymes and reaction buffers

All restriction enzymes were supplied by New England Biolabs (NEB) and used according to the manufacturer's instructions.

Name	Manufacturer	Usage
NEBuilder HiFi DNA Assembly Master Mix (NEB)	New England Biolabs	Gibson Assembly
TAQ Polymerase	AG Scheffner	Colony PCR
ThermoPol Reaction Buffer	New England Biolabs	Colony PCR

5.1.4 Bacterial strains (*E. coli*)

Name	Genotype	Usage
BL21 (DE3) gold	F^- dcm+ Hte ompT hsdS(r_B-m_B-) gal λ (DE3) endA Tet^r	protein expression
BL21 (DE3) Rosetta2	F^- dcm+ ompT hsdS(r_B- m_B-) gal λ (DE3) pRARE (Cam^R)	protein expression
XL-10 gold	TetrD (mcrA)183 Δ(mcrCB-hsdSMR-mrr)173 endA1 supE44 thi-1 recA1 gyrA96 relA1 lac Hte	DNA preparation

5.1.5 Mammalian cell lines

Name	Description	Passaging	#cells (6-well plate)
H1299	Non-small cell lung carcinoma cell line	1:6 or 1:12	300.000
H1299 K3	Single clone E6AP knockdown cell line (RNAi) derived from H1299 parental cells (Kuballa, Matentzoglu, and Scheffner 2007)	1:6 or 1:12	350.000
HeLa	Cervical cancer cell line (HPV 18 positive)	1:5 or 1:10	550.000
HEK293T	embryonic human kidney with the SV40 large T antigen	1:5 or 1:10	400.000

5.1.6 Plasmids

#DE	Backbone	Insert	Source
8	pcDNA3 HA	OTUD5	mutagenesis PCR
19	pRcCMV	β-Galactosidase	AG Scheffner
22	pcDNA3 HA	p53	AG Scheffner
24	pGEX 2TK GST	empty	AG Scheffner
25	pcDNA3 HA	empty	AG Scheffner
33	pcDNA3 HA	Ring1b I53S	AG Scheffner

#DE	Backbone	Insert	Source
35	pGEX 2TK GST	16 E6	AG Scheffner
40	pGEX 2TK GST	16 E6 ΔC11	AG Scheffner
42	pcDNA3 HA	16 E6	AG Scheffner
49	pcDNA3 HA	E6AP	AG Scheffner
53	pGEX 2TK GST	16 E6 C11	AG Scheffner
54	pGEX 2TK GST	11 E6 C16	AG Scheffner
59	pcDNA3.1	iASPP	kind gift of Antje Dickmanns
63	pcDNA3 HA	MRE11	mutagenesis PCR
64	pcDNA3 HA	16 E6 ESAT	AG Scheffner
65	pGEX 2TK GST	16 E6 ESAT	AG Scheffner
67	pcDNA3 HA	iASPP	mutagenesis PCR
72	pcDNA3 HA	11 E6	AG Scheffner
77	pcDNA3 HA	E6AP C820A	AG Scheffner
88	PHAGE CMV	ASPP2	kind gift of Gus Noel
98	pTZ E12 His	E6AP (codon optimized)	AG Scheffner
99	pGEX 2TK GST	RhoA	template: kind gift of AG Hauck
100	pcDNA3 HA	RhoA	template: kind gift of AG Hauck
101	pcDNA3 HA	ASPP2	mutagenesis PCR
107	pcDNA3 HA	NHERF1	template: addgene #28291
109	pGEX 2TK GST	RhoB	template: kind gift of AG Hauck
110	pcDNA3 HA	RhoB	template: kind gift of AG Hauck
111	pGEX 2TK GST	RhoC	template: kind gift of AG Hauck
112	pcDNA3 HA	RhoC	template: kind gift of AG Hauck
113	pGEX GST SUMO	16 E6	AG Scheffner
116	pGEX GST SUMO	empty	AG Scheffner
118	pcDNA3 HA	RhoA G14V	mutagenesis PCR
119	pGEX 2TK GST	RhoA G14V	mutagenesis PCR
120	pGEX GST SUMO	RhoA	mutagenesis PCR
121	pGEX 2TK GST	Cdc42	template: kind gift of AG Hauck
122	pcDNA3 HA	Cdc42	template: kind gift of AG Hauck
123	pGEX 2TK GST	Rac1	template: kind gift of AG Hauck
124	pcDNA3 HA	Rac1	template: kind gift of AG Hauck
125	pcDNA3 HA	GFP-16 E6	AG Scheffner
126	pcDNA3 HA	rat Dlg1	AG Scheffner
127	pGEX 2TK GST	RhoA T19N	mutagenesis PCR
128	pcDNA3 HA	RhoA T19N	mutagenesis PCR
130	pcDNA3 HA	GFP-11 E6	AG Scheffner
131	pET3a His	UbcH7	AG Scheffner
134	pGEX 2TK GST	16 E6 L50E	AG Scheffner
135	pTZ E12 His	E6AP (codon opt.) ΔAZUL	Franziska Müller
136	pTZ E12 His	E6AP (codon opt.) ΔN199	Franziska Müller

#DE	Backbone	Insert	Source
137	pTZ E12 His	E6AP (codon opt.) ΔN375	Franziska Müller
138	pTZ E12 His	E6AP (codon opt.) ΔN469	Franziska Müller
139	pTZ E12 His	E6AP (codon opt.) ΔN499	Franziska Müller
140	pTZ E12 His	E6AP (codon opt.) ΔC6	Franziska Müller
141	pTZ E12 His	E6AP (codon opt.) ΔE6 BS	Franziska Müller
142	pTZ E12 His	E6AP iso II	AG Scheffner
143	pTZ E12 His	E6AP iso III	AG Scheffner
147	pGEX 2TK GST	18 E6	AG Scheffner
148	pcDNA3 HA	18 E6	AG Scheffner
154	pcDNA3 HA	GFP-18 E6	AG Scheffner
155	pcDNA3 HA	E6AP iso II	AG Scheffner
156	pcDNA3 HA	E6AP iso III	AG Scheffner
158	pGEX 2TK GST	16 E6 ΔC2	AG Scheffner
160	pGEX 2TK GST	16 E6 ΔC5	AG Scheffner
167	pcDNA3 HA	RhoA F30L	mutagenesis PCR
168	pGEX 2TK GST	RhoA F30L	mutagenesis PCR
169	pcDNA3 HA	RhoA Q63L	mutagenesis PCR
170	pGEX 2TK GST	RhoA Q63L	mutagenesis PCR
173	pcDNA3 HA	RhoA C190A	mutagenesis PCR
180	pGEX 2TK GST	HERC2 fragment Rcc1b	AG Scheffner
181	pTZ E12 His	E6AP (codon opt.) aa 1-470	AG Scheffner
182	pTZ E12 His	E6AP (codon opt.) aa 1-500	AG Scheffner
185	pcDNA3 HA	16 E6 C11	AG Scheffner
186	pcDNA3 HA	11 E6 C16	AG Scheffner
206	pcDNA3 HA	E6AP Δ150-200	AG Scheffner
220	pcDNA3 HA	RhoA C190A ΔC3	mutagenesis PCR
221	pcDNA3 HA	RhoA G14V C190A ΔC3	mutagenesis PCR
234	pGEX GST SUMO	RBD of mouse Rhotekin	template: kind gift of AG Hauck
235	pcDNA3 HA	RhoA G17A	mutagenesis PCR
236	pGEX 2TK GST	RhoA G17A	mutagenesis PCR
255	pGEX 2TK GST	RhoA N-181 (ΔC12)	mutagenesis PCR
256	pcDNA3 HA	RhoA N-181 (ΔC12)	mutagenesis PCR
257	pGEX 2TK GST	RhoA G14V N-181 (ΔC12)	mutagenesis PCR
258	pcDNA3 HA	RhoA G14V N-181 (ΔC12)	mutagenesis PCR
265	pGEX 2TK GST	RhoA G14V N-164 (ΔC29)	mutagenesis PCR
266	pcDNA3 HA	RhoA G14V N-164 (ΔC29)	mutagenesis PCR
275	pTZ E12 His	E6AP (codon opt.) Δ150-200	mutagenesis PCR
278	pETM41 His MBP	E6AP iso I	kind gift of Gilles Travé
279	pETM41 His MBP	E6AP peptide for 16E6 binding	kind gift of Gilles Travé
280	pETM41 His MBP	16 E6 4C/4S	kind gift of Gilles Travé
284	pETM41 His MBP	16 E6 4C/4S ESAT	mutagenesis PCR

#DE	Backbone	Insert	Source
285	pETM41 His MBP	16 E6 4C/4S L50E	mutagenesis PCR
294	pETM41 His MBP	18 E6	mutagenesis PCR
298	pETM41 His MBP	11 E6 (codon optimized)	mutagenesis PCR
299	pETM41 His MBP	RhoA	mutagenesis PCR
300	pGEX 2TK GST	RhoA C-term RhoB	mutagenesis PCR
301	pcDNA3 HA	RhoA C-term RhoB	mutagenesis PCR
302	pGEX 2TK GST	RhoB C-term RhoA	mutagenesis PCR
303	pcDNA3 HA	RhoB C-term RhoA	mutagenesis PCR
305	pcDNA3 HA	Rac1 C-term RhoA	mutagenesis PCR
306	pGEX 2TK GST	16 E6 ESAT Δ5	mutagenesis PCR
307	pGEX 2TK GST	16 E6 ESAT Δ11	mutagenesis PCR
308	pGEX 2TK GST	RhoB N-180 (ΔC16)	mutagenesis PCR
309	pcDNA3 HA	RhoB N-180 (ΔC16)	mutagenesis PCR
310	pcDNA3 HA	16 E6 L50E	mutagenesis PCR
311	pcDNA3 HA	16 E6 ESAT	mutagenesis PCR
315	pGEX 2TK GST	RhoA N-180 (ΔC13)	mutagenesis PCR
318	pGEX 2TK GST	RhoB G14V	mutagenesis PCR
319	pcDNA3 HA	RhoB G14V (no initial M)	mutagenesis PCR
321	pGEX 2TK GST	RhoB T19N (no initial M)	mutagenesis PCR
329	pETM41 His MBP	16 E6 (not 4C/4S)	mutagenesis PCR
330	pcDNA3 HA	RhoB T19N	mutagenesis PCR
332	pETM41 His MBP	16 E6 ESAT Δ5	mutagenesis PCR
333	pETM41 His MBP	16 E6 WT Δ5	mutagenesis PCR
334	pETM41 His MBP	16 E6 WT Δ11	mutagenesis PCR
335	pETM41 His MBP	16 E6 ESAT Δ11	mutagenesis PCR
339	pETM41 His MBP	MBP alone	mutagenesis PCR
341	pETM41 His MBP	RhoA G17A	mutagenesis PCR
342	pETM41 His MBP	RhoA T19N	mutagenesis PCR
343	pETM41 His MBP	RhoA G14V	mutagenesis PCR
352	pGEX 2TK GST	E6AP (codon optimized)	mutagenesis PCR
359	pETM41 His MBP	p53	mutagenesis PCR
374	pcDNA3 HA	RhoA G14V K104R	mutagenesis PCR
375	pcDNA3 HA	RhoA G14V K118/119R	mutagenesis PCR
376	pcDNA3 HA	RhoA G14V K135R	mutagenesis PCR
377	pcDNA3 HA	RhoA G14V K185-187R	mutagenesis PCR
383	pcDNA3 HA	RhoA G14V K104 118/119R	mutagenesis PCR
384	pcDNA3 HA	RhoA G14V K118/119 135R	mutagenesis PCR
385	pcDNA3 HA	RhoA G14V K135 185-187R	mutagenesis PCR
386	pcDNA3 HA	RhoA G14V K104 135R	mutagenesis PCR
387	pcDNA3 HA	RhoA G14V K104 185-187R	mutagenesis PCR
390	pcDNA3 HA	RhoA GV K118/119 185-187R	mutagenesis PCR

#DE	Backbone	Insert	Source
392	pcDNA3 HA	RhoA G14V K6/7R	mutagenesis PCR
393	pcDNA3 HA	RhoA GV K104 135 185-187R	mutagenesis PCR
394	pcDNA3 HA	RhoA G14V K6/7 135R	mutagenesis PCR
395	pETM41 His MBP	RhoB	mutagenesis PCR
396	pETM41 His MBP	RhoC	mutagenesis PCR
397	pETM41 His MBP	Rac1	mutagenesis PCR
398	pcDNA3 HA	RhoA G14V KR 6/7 104 135 185-187	mutagenesis PCR
399	pcDNA3 HA	RhoA G14V KR 104 118/119 135 185-187	mutagenesis PCR
400	pcDNA3 HA	RhoA G14V KR 6/7 104 118/119 135 185-187	mutagenesis PCR
401	pcDNA3 HA	RhoA G14V K186R	mutagenesis PCR
404	pcDNA3 HA	RhoB K181R	mutagenesis PCR
405	pcDNA3 HA	RhoA G14V K185R	mutagenesis PCR
406	pcDNA3 HA	RhoA G14V K187R	mutagenesis PCR
407	pcDNA3 HA	RhoA G14V K140R	mutagenesis PCR
408	pcDNA3 HA	RhoA interface mut 1+2	mutagenesis PCR
409	pcDNA3 HA	RhoA WT K6_7_135R	mutagenesis PCR
410	pcDNA3 HA	RhoA WT K187R	mutagenesis PCR
413	pcDNA3 HA	RhoA G14V K162_164R	mutagenesis PCR
414	pcDNA3 HA	RhoB K194R	mutagenesis PCR
415	pcDNA3 HA	RhoB K162_164R	mutagenesis PCR
416	pcDNA3 HA	RhoA WT K186R	mutagenesis PCR
417	pcDNA3 HA	RhoA WT K185R	mutagenesis PCR
418	pcDNA3 HA	RhoA WT K187R	mutagenesis PCR
419	pcDNA3 HA	Rac1 K183/184/186/188R	mutagenesis PCR
420	pcDNA3 HA	RhoA WT K185-187A	mutagenesis PCR
421	pcDNA3 HA	RhoA WT K186/187R	mutagenesis PCR
422	pcDNA3 HA	RhoA WT K185-187R	mutagenesis PCR
424	pETM41 His MBP	RhoB G14V	mutagenesis PCR
425	pcDNA3 HA	RhoA WT K185/186R	mutagenesis PCR
426	pcDNA3 HA	RhoB C193A	mutagenesis PCR
433	pcDNA3 HA	RhoB (with initial M)	mutagenesis PCR
434	pcDNA3 HA	RhoC (with initial M)	mutagenesis PCR
435	pcDNA3 HA	Rac1 (with initial M)	mutagenesis PCR
436	pcDNA3 HA	Cdc42 (with initial M)	mutagenesis PCR
437	pET	His-UbcH5b	FO #2
440	pcDNA3 HA	RhoC (with initial M) G14V	mutagenesis PCR
441	pcDNA3 HA	RhoC G14V (no initial M)	mutagenesis PCR
443	pcDNA3 HA	RhoA IFM 1A+2A	mutagenesis PCR
445	pcDNA3 HA	RhoB G14V (with initial M)	mutagenesis PCR

#DE	Backbone	Insert	Source
446	pETM41 His MBP	RhoC G14V	mutagenesis PCR
447	pETM41 His MBP	RhoC T19N	mutagenesis PCR
449	pcDNA3 HA	RhoB (with initial M) T19N	mutagenesis PCR
450	pcDNA3 HA	RhoC (with initial M) T19N	mutagenesis PCR
454	pcDNA3 HA	GFP-16 E6 IFM1/2/3	mutagenesis PCR
460	pETM41 His MBP	RhoA IFM 1A2A	mutagenesis PCR
463	pcDNA3 HA	RhoC (w/ initial M) K183+185R	mutagenesis PCR
468	pETM41 His MBP	16 E6 IFM1/2/3	mutagenesis PCR
470	pcDNA3 HA	RhoA WT KR 6/7 104 118/119 135 185-187	mutagenesis PCR
473	pcDNA3 HA	RhoC (w/ initial M) K183R	mutagenesis PCR
474	pcDNA3 HA	RhoC (w/ initial M) K185R	mutagenesis PCR
475	pETM41 His MBP	RhoA N-181 (ΔC12)	mutagenesis PCR
480	pcDNA3 HA	RhoA K185/187R	mutagenesis PCR
483	pcDNA3 HA	RhoB K181/194R	mutagenesis PCR
484	pcDNA3 HA	DHFR HA ub HA	mutagenesis PCR
486	pcDNA3 HA	HA DHFR ub HA	mutagenesis PCR
499	pcDNA3 HA	DHFR HA ub HA-EcoRI	mutagenesis PCR
500	pcDNA3 HA	DHFR HA ub HA-RhoA WT	mutagenesis PCR
517	pcDNA3 HA	DHFR HA ub HA-RhoA G14V	mutagenesis PCR
521	pcDNA3 HA	DHFR HA ub HA-RhoA T19N	mutagenesis PCR

5.1.7 Oligonucleotides

Oligonucleotides were purchased at Integrated DNA Technologies (IDT; standard desalting, 25 nmol DNA). A list of all oligonucleotides used for cloning is provided on the local server in the AG Scheffner network. The oligonucleotides used for sequencing reactions are listed in **Table 7**.

Table 7. Oligonucleotides used for sequencing.

Name	Sequence (5’ → 3’)	Used for plasmid
pGEX5’ forward	GGGCTGGCAAGCCACGTTTGGTG	pGEX 2TK GST
pGEX3’ reverse	CCGGGAGCTGCATGTGTCAGAGG	pGEX 2TK GST
CMV forward	CGCAAATGGGCGGTAGGCGTG	pcDNA3 HA
T7 forward	TAATACGACTCACTATAGGG	pcDNA3 HA
BGH reverse	TAGAAGGCACAGTCGAGG	pcDNA3 HA
T7 terminator	GCTAGTTATTGCTCAGCGG	pETM41 His MBP
MBP-F forward	GATGAAGCCCTGAAAGACGCGCAG	pETM41 His MBP

5.1.8 Primary antibodies

All primary antibodies were diluted in TNE-T buffer (see 5.1.2 ‘Buffers, solutions, and kits’) and incubated with gentle agitation either for 90 min at room temperature or overnight at 4°C as indicated in the following.

Protein	Antibody	Species	Dilution	Incubation	Manufacturer
HA-tag	HA.11 (Clone 16B12)	mouse	1:2500	90 min	BioLegend Covance
p53	DO-I	mouse	1:750	90 min	Calbiochem
E6AP	α-E6AP	mouse	1:1000	90 min	AG Scheffner
RhoA	RhoA (67B9) mAb	rabbit	1:1000	overnight	Cell Signaling #2117
RhoB	RhoB	rabbit	1:1000	overnight	Cell Signaling #2098
RhoC	RhoC (D40E4) mAb	rabbit	1:1000	overnight	Cell Signaling #3430

5.1.9 Secondary antibodies

The secondary antibodies were diluted 1:30.000 in TNE-T buffer (see 5.1.2 ‘Buffers, solutions, and kits’) and incubated for 60 min at room temperature with gentle agitation.

Name	species	Manufacturer
HRP-coupled α-mouse	goat	Dianova
HRP-coupled α-rabbit	goat	Dianova

5.1.10 DNA and protein markers

Name	Manufacturer
Unstained Protein Ladder	Thermo Scientific
Prestained Protein Ladder	Thermo Scientific
1 kb Plus DNA Ladder	Thermo Scientific

5.1.11 Equipment

Equipment	Manufacturer
Amersham Hybond PVDF membrane (0.22 or 0.45 µm)	Cytiva
Amicon (ultra centrifugal units)	Merck-Millipore
Cell culture dished	Sarstedt
COUNTess Automated Cell counter	Invitrogen
Dialysis tubing (MWCO 3.000 to 12.000 Da)	Roth
Falcon tube (15 ml and 50 ml)	Sarstedt
FLA-5000	Fujifilm
FPLC Äkta Pure	GE Healthcare/Cytiva
FPLC columns	GE Healthcare/Cytiva
Gravity Flow Columns (10 ml)	Bio-Rad
iTC200	MicroCal
LAS-3000	Fujifilm
Nanophotometer	IMPLEN
pH Meter 765, Calimatic	Knick
Reaction tube (1.5 ml and 2 ml)	Sarstedt
Syringe filter (0.22 µm)	Roth
Whatman paper	Roth

5.2 Methods

5.2.1 DNA analysis and cloning

5.2.1.1 Site directed mutagenesis and deletions (Q5 kit)

The Q5 Site-Directed Mutagenesis Kit (NEB, E0554S) was used for the creation of point mutations and deletions within a protein, according to the manufacturer's instructions. Primers were designed using the NEBase Changer online tool (NEB, https://nebasechanger.neb.com/).

5.2.1.2 Exchange of vector backbone

To exchange the backbone of a given insert, the insert amplification was performed with Phusion High-Fidelity Polymerase (NEB, M0530), according to the manufacturer's instructions. Depending on available restriction sites, the desired vector was either enzymatically digested (pcDNA3-HA and pGEX2TK-GST with BamHI-HF) or PCR amplified with Phusion Polymerase (pETM41-MBP) and the primers designed accordingly with the NEBuilder online tool (https://nebuilder.neb.com/). For an enzymatic digest, 4 µg of plasmid DNA were incubated with 2 µl enzyme in 10X CutSmart buffer (NEB, B7204) and nuclease free water in a total volume of 50 µl for 1,5 h at 37°C. The digest was analysed on a 1% agarose gel (5.2.1.4 'Agarose gel electrophoresis') and the digested plasmid retrieved using the NucleoSpin Gel and PCR Clean-up kit (Macherey-Nagel), according to manufacturer's instructions. The 2X NEBuilder HiFi DNA Assembly Master Mix (NEB, E2621) was used to unite insert and backbone in a 2-fold insert to vector molar ratio in a total of 4 µl. The reaction was incubated for 20 min at 50°C and subsequently transformed into chemically competent bacteria (see 5.2.1.3 'Transformation of chemically competent *E. coli* cells').

5.2.1.3 Transformation of chemically competent *E. coli* cells

50 µl of chemically competent bacteria (5.1.4) were mixed with either 100 ng plasmid DNA, the Gibson Assembly product, or 5 µl of the KLD reaction mix. The mixture was incubated for 30 min on ice, followed by a heat-shock for 90 sec at 42°C. Bacteria containing DNA with an ampicillin resistance were further incubated for 10 min on ice. After the transformation with DNA conveying a kanamycin resistance, the bacteria were incubated in SOB medium for 60 – 90 min at 37°C and 300 rpm. The bacterial cells were then harvested at 5000 rpm for 5 min, the supernatant discarded, and the pellet resuspended in the remaining supernatant. Bacteria with either antibiotic resistance were subsequently plated on an LB-plate or used to inoculate 50 – 200 ml LB medium (containing 50 µg/ml ampicillin or 25 µg/ml kanamycin).

5.2.1.4 Agarose gel electrophoresis

DNA samples were supplemented with 6X DNA Loading Dye (Thermo Scientific) and separated by agarose gel electrophoresis using 0,5% – 2% (w/v) 100 ml TAE agarose gels supplemented with 3 µl Midori Green (Nippon Genetics). Gels were run at constant 100 V for 30 – 50 min. The DNA was visualized using UV light (254 nm).

5.2.1.5 Colony PCR

The reaction master mix contained 10X ThermoPol buffer (NEB), 0,5 mM dNTP mix, 0,5 µM forward and 0,5 µM reverse primer (**Fehler! Verweisquelle konnte nicht gefunden werden.** '**Fehler! Verweisquelle konnte nicht gefunden werden.**') and 1 µl of TAQ polymerase (AG Scheffner) in a total volume of 20 µl. Standard PCR conditions were adjusted to 1 min extension per kilobase with an annealing temperature of 55°C.

5.2.1.6 Sanger sequencing

Sequencing analysis of DNA samples was carried out by Genewiz/Azenta Life Sciences. Premixed samples were sent containing 5 µl of a 5 µM primer and 5 µl of 100 ng/µl DNA.

5.2.1.7 Isolation and quantification of plasmid DNA

Plasmid DNA isolation from *E. coli* was either performed in a small scale (QIAprep Spin Miniprep KIT, QIAGEN) using 4 ml or in a large scale (PureYield Plasmid Midiprep System; Promega) using 100 ml of transformed XL10-gold bacteria grown over night at 37°C at 180 rpm in LB medium. Plasmid DNA extraction was performed according to the manufacturer's instructions. The DNA was eluted in nuclease free water and the concentration measured photometrically (λ=260 nm) in triplicates using a NanoPhotometer (IMPLEN).

5.2.2 Protein preparation

5.2.2.1 Expression and purification of recombinant proteins

The expression of recombinant proteins was performed at varying conditions (for details see **Table 8**). In general, bacteria were transformed (5.2.1.3 'Transformation of chemically competent *E. coli* cells') with the plasmid encoding the tagged POI and a single clone was picked to inoculate a pre-culture of 100 – 200 ml LB medium (containing the respective antibiotic) and incubated over night at 37°C, 180 rpm. The pre-culture was then used to inoculate the expression-culture to an OD_{600} = 0,15, which was grown at 37°C, 180 rpm until OD_{600} = 0,6 was reached. At this point, the protein expression was induced by the addition of 400 µM IPTG and the cultures were incubated as listed in **Table 8**. MBP-tagged proteins were expressed in the presence of 0,2 % (v/v) glucose. The bacterial cultures were harvested by centrifugation at 4°C, 5000 rpm for 20 min and the resulting pellets were either directly used for purification or stored at -80°C.

Table 8. Parameters for the bacterial expression of recombinant proteins.

Tag	Protein	resistance	Bacterial strain	°C	h
GST	16 E6 variants	ampicillin	BL21 (DE3) gold	37	4
GST	Rho variants	ampicillin	BL21 (DE3) gold	37	4
His	E6AP variants	kanamycin	Rosetta2	20	16

Tag	Protein	resistance	Bacterial strain	°C	h
His	UbcH5b	ampicillin	BL21 (DE3) gold	37	4
His	UbcH7	ampicillin	BL21 (DE3) gold	30	16
His-MBP	Rho variants	kanamycin	BL21 (DE3) gold	16	18 – 24
His-MBP	16 E6 variants	kanamycin	BL21 (DE3) gold	16	18 – 24
-	ubiquitin LIA	ampicillin	BL21 (DE3) gold	37	4

5.2.2.2 Lysis of bacterial cells

Bacterial pellets resulting from 1000 ml expression-culture were lysed in 30 ml PBS-T lysis buffer (500 ml – 20 ml/250 ml – 10 ml). The lysates were homogenized using a sonifier (Branson, 3 x 30 sec, duty cycle 40%, output control 4) and cleared by centrifugation (13.000 rpm, 30 min, 4°C). The supernatant was used for the following purification steps.

5.2.2.3 Purification of GST-tagged proteins

In PBS-T lysis buffer equilibrated (3x) Glutathione (GSH) beads (1:1 mixture of Glutathione Sepharose 4B and Sepharose CL48, both GE Healthcare) were incubated with the cleared bacterial lysate (5.2.2.2 ‘Lysis of bacterial cells’) for 90 min at 4°C under constant rotation in a v/v ratio of beads slurry:culture = 1:1500. After the binding reaction, the beads were washed three times with PBS-T lysis buffer (2000 rpm, 3 min, 4°C). For the elution of GST-tagged proteins, the beads were incubated multiple times (3-5 x) with GSH elution buffer under constant rotation, followed by centrifugation for 3 min at 4°C, 2000 rpm. Each elution was transferred into a fresh tube.

5.2.2.4 Purification of tag free proteins for size exclusion

For the purification of tag free variants of 16 E6 and RhoA, the proteins were expressed as 1 l cultures in a pGEX GST SUMO construct. At the same time, GST-tagged Ulp1 protease was expressed as 1 l culture. The preparation and binding reaction function as described in 5.2.2.3 ‘Purification of GST-tagged proteins’. After the binding step, the POI-beads were transferred into 1 ml PolyPrep Chromatography columns (Biorad). Via gravity flow, the beads were washed three times with 10 ml PBS-T and once with 10 ml SUMO-protease buffer. The GST-Ulp1 beads were washed three times with PBS-T and once with SUMO-protease buffer in a 1,5 ml reaction tube. After the last washing step, the PolyPrep column was closed at the bottom and the GST-Ulp1 beads slurry was equally divided and was added onto the columns (600 µl 16 E6 or RhoA beads slurry, 300 µl Ulp1 beads slurry). For the cleavage, the column was closed and incubated over night at 4°C under constant rotation. The flow through is the first elution and the remaining cleaved protein was eluted in five additional 1 ml elution steps with

SUMO-protease buffer. Eluates were analysed by SDS-PAGE and concentrated using Amicon Ultra centrifugal filter units according to the manufacturer's instructions.

5.2.2.5 Purification of His-tagged/His-MBP tagged proteins

His-tagged proteins were purified using Nickel-NTA-chromatography columns (1 ml, 5 ml or 2x 5 ml in a row HisTrap HP or FF, GE Healthcare) with an Äkta purifier FPLC system (GE Healthcare). The method settings were adjusted according to **Table 9**. $T_{25}N_{50}$ pH7,5 with 1 mM DTT was used as buffer A and $T_{25}N_{50}$ pH7,5 with 1 mM DTT and 0,5 M Imidazole was used as buffer B. His-E6AP and His-MBP tagged proteins were further purified with anion exchange (1 ml or 5ml HiTrapQ HP columns, GE Healthcare) or cation exchange (HiTrapSP HP columns, GE Healthcare) chromatography. See **Table 10** for ion exchange FPLC settings. Unless stated otherwise, $T_{25}N_{50}$ pH7,5 with 1 mM DTT was used as buffer A and $T_{25}N_{1000}$ pH7,5 with 1 mM DTT was used as buffer B.

Table 9. FPLC settings (HisTrap). *A: buffer A; B: buffer B; CV: column volume*

		His-E6AP	His-MBP-RhoA	UbcH5b/UbcH7-His
	equilibration	2 CV A	2 CV A	5 CV A
	sample application (using air sensor)			
	column wash	2 CV A	2 CV A	2 CV A
elution	**step**	5 CV 4% B	5 CV 4% B	8 CV 4% B
	gradient	8 CV to 100% B	10 CV to 80% B	8 CV to 80% B
	step	5 CV 100% B	5 CV 100% B	5 CV 100% B
	equilibration	4 CV A	4 CV A	5 CV A

Table 10. FPLC settings (ion exchange). A: buffer A; B: buffer B; column volume

		His-E6AP pI 4,9	**His-MBP-RhoA** pI 5,4
	equilibration	5 CV A	5 CV A
	sample application (using air sensor)		
	column wash	5 CV A	5 CV A
elution	**step**	2 CV 4% B	-
	gradient	25 CV to 100% B	25 CV to 35% B
	step	5 CV 100% B	5 CV 100% B
	equilibration	5 CV A	4 CV A

5.2.2.6 Purification of the ubiquitin mutant LIA

The obtained cleared lysate (5.2.2.2 ‘Lysis of bacterial cells’) was incubated at 70°C for 25 min at 600 rpm. To remove the denatured proteins, the lysate was subsequently centrifuged for 10 min at 16.000 x g at 4°C and the supernatant containing the ubiquitin mutant LIA was aliquoted and stored at - 20°C.

5.2.2.7 *In vitro* translation

Radio-labelled proteins were expressed from T7 promotor-containing plasmids with the TnT T7-coupled System (Promega) in combination with ^{35}S-methionine (PerkinElmer) using T7 Polymerase, according to the manufacturer’s instructions. For the protein synthesis, either Reticulocyte Lysate (containing E6AP), or Wheat Germ Extract (without E6AP) was used.

5.2.3 Protein analysis

5.2.3.1 SDS-PAGE

Proteins were separated according to size with SDS-PAGE according to the protocol of Laemmli (Laemmli 1970). The percentage of the resolving gel (7-15%) was chosen depending on the size of the POI. Samples were mixed with Laemmli sample buffer, boiled for 1-5 min, and the gel was run at constant 65 mA. Proteins were detected by Coomassie staining (see 5.2.3.2 ‘Coomassie staining’), western blot analysis (5.2.3.3 ‘Western blot’) or fluorography (5.2.3.4 ‘Fluorography’).

5.2.3.2 Coomassie staining

SDS-PA gels were either stained for 20 min in fresh Coomassie staining solution or overnight in 1X used staining solution to visualize protein bands. The gels were incubated multiple times for 20 min in Coomassie destaining solution until the background was colourless. Gels with expected low amounts of protein were stained overnight with RotiBlue colloidal Coomassie staining solution (Roth) and destained in 40% (v/v) methanol in Milli-Q water.

5.2.3.3 Western blot

For western blot analysis, a 0,22 µm or 0,45 µm PVDF membrane (Amersham Hybond, Cytiva) was activated in methanol and equilibrated in transfer buffer together with the SDS-PA gel. The wet transfer was carried out in a Trans-Blot transfer cell (Bio-Rad) for 90 min at constant 60V. The membrane was subsequently washed in Milli-Q water and blocked for either 60 min at room temperature or overnight at 4°C. See section (5.1.8 ‘Primary antibodies’) for details regarding primary antibodies and section (5.1.9 ‘Secondary antibodies’) for secondary antibodies.

5.2.3.4 Fluorography

For the visualization of ^{35}S radio-labelled proteins (5.2.2.7 ‘*In vitro* translation’), the SDS-PA gels were first fixed in Coomassie destaining solution for 5-10 min and then incubated in Enlightning (Amplifier, PerkinElmer) for 10-30 min. The gels were dried onto Whatman paper at 80°C under vacuum for 30-90 min (depending on gel size and

percentage). After exposure for 1-24 h on a BAS imaging plate, the fluorography was detected using a FLA5000 (Fujifilm).

5.2.3.5 Size exclusion chromatography

The storage buffer (20% ethanol in milliQ) of a Superdex 200 Increase 10│300 GL column (GE Healthcare, lot 10271168/28-9909-44) was first replaced by milliQ (1 CV), which was subsequently replaced by the running buffer (1 CV), containing 25 mM Tris pH7.5, 150 mM NaCl, 1 mM DTT. The buffer of the proteins was exchanged to the SEC running buffer. The proteins of interest were then incubated together (100 µM) for 60 min on ice (input sample retrieved), centrifuged for 10 min at 4°C at full speed (input sample retrieved), and the supernatant transferred into a new tube. 230 µl were injected onto the column and analysed at a flow rate of 0,4 ml/min.

5.2.3.6 In-gel digestion for mass spectrometric analysis

In all following steps, the solutions were applied in appropriate volumes to sufficiently cover the gel pieces. To destain the excised gel pieces, they were covered with (~100 µl) 100 mM ammonium bicarbonate (ABI) and acetonitrile (ACN) (1:1 ratio v/v) at 37°C for 10 min at 300 rpm. The liquid was removed and the pieces were re-swollen with 100 mM ABI for 10 min. The liquid was removed and the steps repeated until the gel was fully destained, the incubation steps were increased to 30 min. After the last destaining step, the liquid was removed and 500 µl of neat ACN was added to dehydrate the gel pieces. The gel pieces were incubated at 37°C at 300 rpm until they became white and shrank. After a short spin down, the ACN was removed (storage at -20°C for several weeks is possible at this point). Next, the gel pieces were reduced and alkylated. For this, they were incubated in 10 mM DTT in 100 mM ABI and incubated for 30 min at 56°C at 300 rpm. The liquid was then removed and the pieces cooled down to room temperature. Next, 500 µl ACN were added and the white and dehydrated gel pieces spun down, the liquid was removed. 30-50 µl of iodoacetamide (IA) solution (55 mM IA in 100 mM ABI, light-sensitive) were added and incubated for 20 min at 22°C at 300 rpm in the dark. The gel pieces were then dehydrated with 500 µl ACN, spun down, and the liquid removed. For the tryptic digest, the dry gel pieces were covered with trypsin buffer (10 mM ABI, 10% ACN, 13 ng/µl trypsin in milliQ, ~50 µl) and incubated at 4°C. After 30 min, more trypsin buffer was added, in case the pieces were not covered completely anymore. Samples were incubated for additional 90 min at 4°C for saturation with trypsin. The addition of 10-20 µl of ABI ensures the gel pieces to stay wet during the digest. Incubate the samples at 37°C at 350 rpm for 18-20 h (check if pieces are covered after 5 min incubation at 37°C). The next day, add 300 µl of extraction buffer (1:2 5% formic acid/ACN (vol/vol)) and incubate for 15 min at 37°C at 300 rpm. Spin the tubes down, collect the liquid in a fresh tube and repeat the extraction with 150 µl extraction buffer for 15 min at 37°C at 300 rpm and combine the extracts. Dry the peptides in a vacuum centrifuge at 45°C and store it at -20°C. The samples were subsequently desalted with C18 spin tips and subjected to LC-MS/MS analysis (Jasmin Jansen, AG Stengel).

5.2.3.7 Cross-linking coupled to mass spectrometry (XL-MS)

The cross-linking experiment as well as the subsequent measurements and the evaluation were performed by Jasmin Jansen (AG Stengel) as described in (Sailer et al. 2018). In short, after the cross-linking in biological triplicates, the cysteine residues were reduced and alkylated, and the cross-linked samples were subsequently subjected to a tryptic digest. The digested samples were desalted (C18 columns), enriched via SEC, and detected via LC-MS/MS and identified utilizing the xQuest/xProphet software pipeline (Leitner, Walzthoeni, and Aebersold 2014). The samples were measured in technical duplicates and the high-confidence cross-links (ld-score ≥ 25) were quantified and analysed.

5.2.4 *In vitro* experiments

5.2.4.1 Ubiquitination assays

Ubiquitination assays were performed in a total volume of 20 µl for 90 min at 30°C, unless stated otherwise. The reactions contained UBA1 (E1, ~150 ng), UbcH5b or UbcH7 (E2, ~150 ng), E6AP (E3, 50 – 1500 ng), ubiquitin (10 µg) and 16 E6 (100 – 1000 ng) in $T_{25}N_{50}$ pH7,5 supplemented with 2 mM ATP, 2 mM $MgCl_2$ and 1 mM DTT. Substrate ubiquitination assays additionally contained 1 µl of *in vitro* translated protein (5.2.2.7 *In vitro* translation) and were visualized by fluorography (5.2.3.4 ‘Fluorography’). Alternatively, the assay contained a bacterially expressed substrate protein (~500 ng, visualization by Coomassie staining (5.2.3.2 ‘Coomassie staining’) or western blot analysis (5.2.3.3 ‘Western blot’)).

5.2.4.2 GST coprecipitation assay

The GSH resin (1:1 mixture of Glutathione Sepharose 4B and Sepharose CL48, both GE Healthcare) was equilibrated three times in PBS-T lysis buffer and subsequently incubated with the cleared bacterial lysate (5.2.2.2 ‘Lysis of bacterial cells’) containing the GST-tagged POI (5.2.2.1 ‘Expression and purification of recombinant proteins’) for 90 min at 4°C under constant rotation in a v/v ratio of beads slurry:culture = 1:1500. After the binding reaction, the beads were washed three times with PBS-T lysis buffer and once with pulldown buffer (2000 rpm, 3 min, 4°C). To detect the beads-bound protein levels, 10 µl of the slurry were analyzed on a preliminary SDS-PA gel and the protein levels were visualized with Coomassie staining (5.2.3.2 ‘Coomassie staining’). According to the actual protein levels, the beads slurry was diluted with equilibrated empty beads slurry to obtain comparable levels, that are readily detectable in the Coomassie staining (2-5 µg of protein bound to the resin).

The co-precipitation assay (GST and MBP) was performed in a total volume of 200 µl in pulldown buffer with 20 µl beads slurry, 10 µl of the in *vitro* translated protein (5.2.2.7 ‘*In vitro* translation’), and other components of interest which are indicated in the respective figure legends in the results part. The assay was incubated for 90 min at 4°C under constant rotation and unbound protein was removed in three subsequent washing steps with TNN buffer supplemented with 1 mM DTT. The washed beads were boiled in 15 µl 2x Laemmli buffer and subjected to Coomassie staining (5.2.3.2

‘Coomassie staining’, input level determination) and subsequently analyzed by fluorography (5.2.3.4 ‘Fluorography’) to verify the binding reaction.

5.2.4.3 MBP coprecipitation assay

The amylose resin (NEB, E8021S) was equilibrated three times in 1 ml pulldown buffer (centrifugation for 3 min, 2000 rpm, 4°C, aspirate supernatant, repeat) and subsequently incubated with the purified MBP-tagged bait protein (3 µg per reaction) in a 1:1 beads:buffer slurry (20 µl slurry per reaction) for 90 min at 4°C under constant rotation. Beads were washed three times with pulldown buffer and the obtained slurry used for the coprecipitation assay. The coprecipitation assay was performed as described above for the GST-tagged proteins.

5.2.4.4 Guanine nucleotide exchange

For the exchange of the present guanine nucleotide with either GDP (Sigma, G7127) or GTPγS (non-hydrolysable GTP analogue, Jena Bioscience, NU-412-10), the *in vitro* translated RhoA (5.2.2.7 ‘*In vitro* translation’) was incubated with 10 mM EDTA, 5 mM $MgCl_2$ and either 5 mM GDP or 5 mM GTPγS for 3 h at 25°C with 400 rpm. After the exchange, the proteins were directly used for ubiquitination assays.

5.2.5 Cell biology

5.2.5.1 Cultivation

Human cells (for details see 5.1.5) were cultivated at 37°C, 95 % humidity and 5 % CO_2 in DMEM (Gibco) containing 10 % (v/v) FCS in 10 cm dishes in a total volume of 10 ml. For passaging or seeding, the following steps were performed: 1) aspirate medium 2) wash with PBS 3) remove PBS 4) add 2 ml Trypsin/EDTA (Gibco) 5) incubate for 2-5 min 6) stop trypsinisation with medium 7) count cells for seeding according to manufacturer’s instructions (Countess Automated Cell Counter, Invitrogen).

5.2.5.2 Storage

For cryopreservation, cells of a confluent 10 cm dish were treated as described above (5.2.5.1 ‘Cultivation’) including step 6). Cells were then harvested at 300 x g for 5 min, the supernatant aspirated, and the pellet resuspended in 2 ml FCS supplemented with 10 % (v/v) DMSO. The cells were frozen in 1 ml aliquots in cryogenic storage vials in an isopropanol bath (Mr. Frosty, Thermo Scientific) and transferred into a liquid nitrogen tank the next day. For re-cultivation, cells of one cryogenic vial were thawed at 37°C and directly transferred into a 10 cm dish containing 9 ml DMEM supplemented with 10 % FCS.

5.2.5.3 Transient transfection

For transient transfection experiments, mammalian cells (H1299 300.000, HeLa 550.000) were seeded in 6-well plates (Sarstedt) in a total volume of 2 ml. 16 – 20 h after seeding and at a confluency of 70 – 90 %, the transfection was performed using Lipofectamine 2000 (Invitrogen) according to the manufacturer’s instructions. All samples were adjusted with pcDNA3 empty vector (DE #25) to contain the same

amount of total DNA in each transfection sample. To determine the transfection efficiency within each well, as 10% of the total DNA amount an expression construct for β-galactosidase (pRcCMV, DE #19) was co-transfected and subsequently used for a β-galactosidase assay (5.2.5.5 ‘β-galactosidase assay’).

5.2.5.4 Whole cell lysate preparation

Cells of one well (6-well plate) were scraped (Cell lifter, Corning Inc.) in 700 µl ice-cold PBS, the well subsequently washed with additional 700 µl ice-cold PBS and the cell suspensions transferred into the same 1,5 ml reaction tube on ice. Cells were harvested at 1000 x g for 10 min at 4°C and the supernatant aspirated. Cell pellets were either stored at -20°C or directly resuspended in 80 µl TNN lysis buffer and incubated for 30 min on ice. The lysate was cleared by centrifugation for 30 min at 13.000 rpm at 4°C and the supernatant transferred into a fresh tube.

5.2.5.5 β-galactosidase assay

To determine the transfection efficiency within each well, a β-galactosidase assay was performed with the lysates. In duplicates, 6 µl of lysate were incubated with 120 µl buffer Z and 5 µl ONPG in a transparent flat-bottom 96 well plate (Sarstedt). TNN lysis buffer was used as a blank. The samples were incubated at 37°C for 5 – 15 min and the absorbance measured at 405 nm in a micro-plate reader (Victor3 Multilabel plate reader, Perkin Elmer). Sample volumes for SDS-PA gels were adjusted to the sample with the lowest value, of which 20 – 30 µl were loaded.

6. References

Adhikary, S., F. Marinoni, A. Hock, E. Hulleman, N. Popov, R. Beier, S. Bernard, M. Quarto, M. Capra, S. Goettig, U. Kogel, M. Scheffner, K. Helin, and M. Eilers. 2005. 'The ubiquitin ligase HectH9 regulates transcriptional activation by Myc and is essential for tumor cell proliferation', *Cell*, 123: 409-21.

Adra, Chaker N., Danny Manor, Jon L. Ko, Shaochun Zhu, Tadashi Horiuchi, Linda Van Aelst, Richard A. Cerione, and Bing Lim. 1997. 'RhoGDIγ: A GDP-dissociation inhibitor for Rho proteins with preferential expression in brain and pancreas', *Proceedings of the National Academy of Sciences*, 94: 4279-84.

Amano, Mutsuki, Masaaki Ito, Kazushi Kimura, Yuko Fukata, Kazuyasu Chihara, Takeshi Nakano, Yoshiharu Matsuura, and Kozo Kaibuchi. 1996. 'Phosphorylation and Activation of Myosin by Rho-associated Kinase (Rho-kinase)*', *Journal of Biological Chemistry*, 271: 20246-49.

Amerik, Alexander Y., and Mark Hochstrasser. 2004. 'Mechanism and function of deubiquitinating enzymes', *Biochimica et Biophysica Acta (BBA) - Molecular Cell Research*, 1695: 189-207.

Amin, E., M. Jaiswal, U. Derewenda, K. Reis, K. Nouri, K. T. Koessmeier, P. Aspenström, A. V. Somlyo, R. Dvorsky, and M. R. Ahmadian. 2016. 'Deciphering the Molecular and Functional Basis of RHOGAP Family Proteins: A SYSTEMATIC APPROACH TOWARD SELECTIVE INACTIVATION OF RHO FAMILY PROTEINS', *J Biol Chem*, 291: 20353-71.

Angelman, Harry. 1965. ''Puppet' Children A Report on Three Cases', *Developmental Medicine & Child Neurology*, 7: 681-88.

Arendt, C. S., and M. Hochstrasser. 1997. 'Identification of the yeast 20S proteasome catalytic centers and subunit interactions required for active-site formation', *Proc Natl Acad Sci U S A*, 94: 7156-61.

Armstrong, Scott A., Voe C. Hannah, Joseph L. Goldstein, and Michael S. Brown. 1995. 'CAAX Geranylgeranyl Transferase Transfers Farnesyl as Efficiently as Geranylgeranyl to RhoB (∗)', *Journal of Biological Chemistry*, 270: 7864-68.

Arrazola Sastre, A., M. Luque Montoro, P. Gálvez-Martín, H. M. Lacerda, A. M. Lucia, F. Llavero, and J. L. Zugaza. 2020. 'Small GTPases of the Ras and Rho Families Switch on/off Signaling Pathways in Neurodegenerative Diseases', *Int J Mol Sci*, 21.

Avagliano Trezza, Rossella, Monica Sonzogni, Stijn N. V. Bossuyt, F. Isabella Zampeta, A. Mattijs Punt, Marlene van den Berg, Diana C. Rotaru, Linda M. C. Koene, Shashini T. Munshi, Jeffrey Stedehouder, Johan M. Kros, Mark Williams, Helen Heussler, Femke M. S. de Vrij, Edwin J. Mientjes, Geeske M. van Woerden, Steven A. Kushner, Ben Distel, and Ype Elgersma. 2019. 'Loss of nuclear UBE3A causes electrophysiological and behavioral deficits in mice and is associated with Angelman syndrome', *Nature Neuroscience*, 22: 1235-47.

Avraham, H., and R. A. Weinberg. 1989. 'Characterization and expression of the human rhoH12 gene product', *Mol Cell Biol*, 9: 2058-66.

Banks, L., S. C. Barnett, and T. Crook. 1990. 'HPV-16 E7 functions at the G1 to S phase transition in the cell cycle', *Oncogene*, 5: 833-7.

Bar-Sagi, D., and A. Hall. 2000. 'Ras and Rho GTPases: a family reunion', *Cell*, 103: 227-38.

Beal, R. E., D. Toscano-Cantaffa, P. Young, M. Rechsteiner, and C. M. Pickart. 1998. 'The hydrophobic effect contributes to polyubiquitin chain recognition', *Biochemistry*, 37: 2925-34.

Bedell, M. A., J. B. Hudson, T. R. Golub, M. E. Turyk, M. Hosken, G. D. Wilbanks, and L. A. Laimins. 1991. 'Amplification of human papillomavirus genomes in vitro is dependent on epithelial differentiation', *J Virol*, 65: 2254-60.

Ben-Saadon, R., D. Zaaroor, T. Ziv, and A. Ciechanover. 2006. 'The polycomb protein Ring1B generates self atypical mixed ubiquitin chains required for its in vitro histone H2A ligase activity', *Mol Cell*, 24: 701-11.

Bergamaschi, D., Y. Samuels, N. J. O'Neil, G. Trigiante, T. Crook, J. K. Hsieh, D. J. O'Connor, S. Zhong, I. Campargue, M. L. Tomlinson, P. E. Kuwabara, and X. Lu. 2003. 'iASPP oncoprotein is a key inhibitor of p53 conserved from worm to human', *Nat Genet*, 33: 162-7.

Bernard, B. A., C. Bailly, M. C. Lenoir, M. Darmon, F. Thierry, and M. Yaniv. 1989. 'The human papillomavirus type 18 (HPV18) E2 gene product is a repressor of the HPV18 regulatory region in human keratinocytes', *J Virol*, 63: 4317-24.

Bishop, A. L., and A. Hall. 2000. 'Rho GTPases and their effector proteins', *The Biochemical journal*, 348 Pt 2: 241-55.

Borden, K. L., and P. S. Freemont. 1996. 'The RING finger domain: a recent example of a sequence-structure family', *Curr Opin Struct Biol*, 6: 395-401.

Bossard, F., A. Robay, G. Toumaniantz, S. Dahimene, F. Becq, J. Merot, and C. Gauthier. 2007. 'NHE-RF1 protein rescues DeltaF508-CFTR function', *Am J Physiol Lung Cell Mol Physiol*, 292: L1085-94.

Bouvard, V., A. Storey, D. Pim, and L. Banks. 1994. 'Characterization of the human papillomavirus E2 protein: evidence of trans-activation and trans-repression in cervical keratinocytes', *Embo j*, 13: 5451-9.

Braaten, K. P., and M. R. Laufer. 2008. 'Human Papillomavirus (HPV), HPV-Related Disease, and the HPV Vaccine', *Rev Obstet Gynecol*, 1: 2-10.

Brakebusch, C. 2021. 'Rho GTPase Signaling in Health and Disease: A Complex Signaling Network', *Cells*, 10.

Brimer, N., C. Lyons, and S. B. Vande Pol. 2007. 'Association of E6AP (UBE3A) with human papillomavirus type 11 E6 protein', *Virology*, 358: 303-10.

Bryant, Patrick, Gabriele Pozzati, Wensi Zhu, Aditi Shenoy, Petras Kundrotas, and Arne Elofsson. 2022. 'Predicting the structure of large protein complexes using AlphaFold and Monte Carlo tree search', *Nature Communications*, 13: 6028.

Buchsbaum, Rachel J. 2007. 'Rho activation at a glance', *Journal of Cell Science*, 120: 1149-52.

Buel, Gwen R., Xiang Chen, Raj Chari, Maura J. O'Neill, Danielle L. Ebelle, Conor Jenkins, Vinidhra Sridharan, Sergey G. Tarasov, Nadya I. Tarasova, Thorkell Andresson, and Kylie J. Walters. 2020. 'Structure of E3 ligase E6AP with a proteasome-binding site provided by substrate receptor hRpn10', *Nature Communications*, 11: 1291.

Buiting, K, V Greger, B H Brownstein, R M Mohr, I Voiculescu, A Winterpacht, B Zabel, and B Horsthemke. 1992. 'A putative gene family in 15q11-13 and 16p11.2: possible implications for Prader-Willi and Angelman syndromes', *Proceedings of the National Academy of Sciences*, 89: 5457-61.

Buiting, K., C. Williams, and B. Horsthemke. 2016. 'Angelman syndrome - insights into a rare neurogenetic disorder', *Nat Rev Neurol*, 12: 584-93.

Burgess, Richard R. 2018. 'A brief practical review of size exclusion chromatography: Rules of thumb, limitations, and troubleshooting', *Protein Expression and Purification*, 150: 81-85.

Bzhalava, D., P. Guan, S. Franceschi, J. Dillner, and G. Clifford. 2013. 'A systematic review of the prevalence of mucosal and cutaneous human papillomavirus types', *Virology*, 445: 224-31.

Canguilhem, Bruno, Anne Pradines, Caroline Baudouin, Céline Boby, Isabelle Lajoie-Mazenc, Marie Charveron, and Gilles Favre. 2005. 'RhoB Protects Human Keratinocytes from UVB-induced Apoptosis through Epidermal Growth Factor Receptor Signaling *', *Journal of Biological Chemistry*, 280: 43257-63.

Cannizzaro, Linda A., Pascal Madaule, Frederick Hecht, Richard Axel, Carlo M. Croce, and Kay Huebner. 1990. 'Chromosome localization of human ARH genes, a ras-related gene family', *Genomics*, 6: 197-203.

Casey, P. J., J. A. Thissen, and J. F. Moomaw. 1991. 'Enzymatic modification of proteins with a geranylgeranyl isoprenoid', *Proc Natl Acad Sci U S A*, 88: 8631-5.

Castellani, S., M. Favia, L. Guerra, A. Carbone, A. C. Abbattiscianni, S. Di Gioia, V. Casavola, and M. Conese. 2017. 'Emerging relationship between CFTR, actin and tight junction organization in cystic fibrosis airway epithelium', *Histol Histopathol*, 32: 445-59.

Chan, Ai-Leen, Tamar Grossman, Valentina Zuckerman, Dafne Campigli Di Giammartino, Ofra Moshel, Martin Scheffner, Brendon Monahan, Pat Pilling, Yong-Hui Jiang, Sue Haupt, Ora Schueler-Furman, and Ygal Haupt. 2013. 'c-Abl Phosphorylates E6AP and Regulates Its E3 Ubiquitin Ligase Activity', *Biochemistry*, 52: 3119-29.

Chen, S., Z. Zhang, Y. Zhang, T. Choi, and Y. Zhao. 2022. 'Activation Mechanism of RhoA Caused by Constitutively Activating Mutations G14V and Q63L', *Int J Mol Sci*, 23.

Chen, Yuezhou, Zhenxiao Yang, Min Meng, Yue Zhao, Na Dong, Hongming Yan, Liping Liu, Mingxiao Ding, H. Benjamin Peng, and Feng Shao. 2009. 'Cullin Mediates Degradation of RhoA through Evolutionarily Conserved BTB Adaptors to Control Actin Cytoskeleton Structure and Cell Movement', *Molecular Cell*, 35: 841-55.

Chesson, H. W., E. F. Dunne, S. Hariri, and L. E. Markowitz. 2014. 'The estimated lifetime probability of acquiring human papillomavirus in the United States', *Sex Transm Dis*, 41: 660-4.

Chrzanowska-Wodnicka, M, and K Burridge. 1996. 'Rho-stimulated contractility drives the formation of stress fibers and focal adhesions', *Journal of Cell Biology*, 133: 1403-15.

Ciechanover, A., and R. Ben-Saadon. 2004. 'N-terminal ubiquitination: more protein substrates join in', *Trends Cell Biol*, 14: 103-6.

Ciechanover, A., and A. L. Schwartz. 1998. 'The ubiquitin-proteasome pathway: the complexity and myriad functions of proteins death', *Proc Natl Acad Sci U S A*, 95: 2727-30.

Ciehanover, A., Y. Hod, and A. Hershko. 1978. 'A heat-stable polypeptide component of an ATP-dependent proteolytic system from reticulocytes', *Biochem Biophys Res Commun*, 81: 1100-5.

Clayton, Natasha S., and Anne J. Ridley. 2020. 'Targeting Rho GTPase Signaling Networks in Cancer', *Frontiers in Cell and Developmental Biology*, 8.

Cobrinik, D. 2005. 'Pocket proteins and cell cycle control', *Oncogene*, 24: 2796-809.

Collins, Christopher J., Birgit Schilling, Malin Young, Gavin Dollinger, and R. Kiplin Guy. 2003. 'Isotopically labeled crosslinking reagents: resolution of mass degeneracy in the identification of crosslinked peptides', *Bioorganic & Medicinal Chemistry Letters*, 13: 4023-26.

Cook, D. R., K. L. Rossman, and C. J. Der. 2014. 'Rho guanine nucleotide exchange factors: regulators of Rho GTPase activity in development and disease', *Oncogene*, 33: 4021-35.

Côté, J. F., and K. Vuori. 2002. 'Identification of an evolutionarily conserved superfamily of DOCK180-related proteins with guanine nucleotide exchange activity', *J Cell Sci*, 115: 4901-13.

———. 2006. 'In vitro guanine nucleotide exchange activity of DHR-2/DOCKER/CZH2 domains', *Methods Enzymol*, 406: 41-57.

Coux, O., K. Tanaka, and A. L. Goldberg. 1996. 'Structure and functions of the 20S and 26S proteasomes', *Annu Rev Biochem*, 65: 801-47.

Cox, A. D., and C. J. Der. 1992. 'Protein prenylation: more than just glue?', *Curr Opin Cell Biol*, 4: 1008-16.

Cripe, T. P., T. H. Haugen, J. P. Turk, F. Tabatabai, P. G. Schmid, 3rd, M. Dürst, L. Gissmann, A. Roman, and L. P. Turek. 1987. 'Transcriptional regulation of the human papillomavirus-16 E6-E7 promoter by a keratinocyte-dependent enhancer, and by viral E2 trans-activator and repressor gene products: implications for cervical carcinogenesis', *Embo j*, 6: 3745-53.

de Bie, P., and A. Ciechanover. 2011. 'Ubiquitination of E3 ligases: self-regulation of the ubiquitin system via proteolytic and non-proteolytic mechanisms', *Cell Death & Differentiation*, 18: 1393-402.

de Villiers, E. M., C. Fauquet, T. R. Broker, H. U. Bernard, and H. zur Hausen. 2004. 'Classification of papillomaviruses', *Virology*, 324: 17-27.

DeGeer, Jonathan, and Nathalie Lamarche-Vane. 2013. 'Rho GTPases in neurodegeneration diseases', *Experimental Cell Research*, 319: 2384-94.

DerMardirossian, Céline, and Gary M. Bokoch. 2005. 'GDIs: central regulatory molecules in Rho GTPase activation', *Trends in Cell Biology*, 15: 356-63.

Deshaies, R. J., and C. A. Joazeiro. 2009. 'RING domain E3 ubiquitin ligases', *Annu Rev Biochem*, 78: 399-434.

Deveraux, Q., V. Ustrell, C. Pickart, and M. Rechsteiner. 1994. 'A 26 S protease subunit that binds ubiquitin conjugates', *J Biol Chem*, 269: 7059-61.

Dietrich, L. E., and C. Ungermann. 2004. 'On the mechanism of protein palmitoylation', *EMBO Rep*, 5: 1053-7.

Donlon, T A, M Lalande, A Wyman, G Bruns, and S A Latt. 1986. 'Isolation of molecular probes associated with the chromosome 15 instability in the Prader-Willi syndrome', *Proceedings of the National Academy of Sciences*, 83: 4408-12.

Doorbar, J. 2005. 'The papillomavirus life cycle', *J Clin Virol*, 32 Suppl 1: S7-15.

———. 2006. 'Molecular biology of human papillomavirus infection and cervical cancer', *Clin Sci (Lond)*, 110: 525-41.

Doorbar, J., W. Quint, L. Banks, I. G. Bravo, M. Stoler, T. R. Broker, and M. A. Stanley. 2012. 'The biology and life-cycle of human papillomaviruses', *Vaccine*, 30 Suppl 5: F55-70.

Dove, Katja K, and Rachel E Klevit. 2012. 'RING-between-RINGs—keeping the safety on loaded guns', *The EMBO Journal*, 31: 3792-94.

Drews, C. M., S. Case, and S. B. Vande Pol. 2019. 'E6 proteins from high-risk HPV, low-risk HPV, and animal papillomaviruses activate the Wnt/beta-catenin pathway through E6AP-dependent degradation of NHERF1', *PLoS Pathog*, 15: e1007575.

Driscoll, D. J., J. L. Miller, S. Schwartz, and S. B. Cassidy. 1993. 'Prader-Willi Syndrome.' in M. P. Adam, D. B. Everman, G. M. Mirzaa, R. A. Pagon, S. E. Wallace, L. J. H. Bean, K. W. Gripp and A. Amemiya (eds.), *GeneReviews(®)* (University of Washington, Seattle

Copyright © 1993-2023, University of Washington, Seattle. GeneReviews is a registered trademark of the University of Washington, Seattle. All rights reserved.: Seattle (WA)).

Dubash, Adi D., Christophe Guilluy, Melissa C. Srougi, Etienne Boulter, Keith Burridge, and Rafael García-Mata. 2011. 'The Small GTPase RhoA Localizes to the Nucleus and Is Activated by Net1 and DNA Damage Signals', *PLOS ONE*, 6: e17380.

Duensing, S., and K. Münger. 2002. 'The human papillomavirus type 16 E6 and E7 oncoproteins independently induce numerical and structural chromosome instability', *Cancer Res*, 62: 7075-82.

Dupraz, S., B. J. Hilton, A. Husch, T. E. Santos, C. H. Coles, S. Stern, C. Brakebusch, and F. Bradke. 2019. 'RhoA Controls Axon Extension Independent of Specification in the Developing Brain', *Curr Biol*, 29: 3874-86.e9.

Dvorsky, Radovan, Lars Blumenstein, Ingrid R. Vetter, and Mohammad Reza Ahmadian. 2004. 'Structural Insights into the Interaction of ROCKI with the Switch Regions of RhoA *', *Journal of Biological Chemistry*, 279: 7098-104.

Dyson, N. 1998. 'The regulation of E2F by pRB-family proteins', *Genes Dev*, 12: 2245-62.

Ebner, F. A., C. Sailer, D. Eichbichler, J. Jansen, A. Sladewska-Marquardt, F. Stengel, and M. Scheffner. 2020. 'A ubiquitin variant-based affinity approach selectively identifies substrates of the ubiquitin ligase E6AP in complex with HPV-11 E6 or HPV-16 E6', *J Biol Chem*.

Egawa, K. 2003. 'Do human papillomaviruses target epidermal stem cells?', *Dermatology*, 207: 251-4.

Eletr, Z. M., and B. Kuhlman. 2007. 'Sequence determinants of E2-E6AP binding affinity and specificity', *J Mol Biol*, 369: 419-28.

Eskeland, R., M. Leeb, G. R. Grimes, C. Kress, S. Boyle, D. Sproul, N. Gilbert, Y. Fan, A. I. Skoultchi, A. Wutz, and W. A. Bickmore. 2010. 'Ring1B compacts chromatin structure and represses gene expression independent of histone ubiquitination', *Mol Cell*, 38: 452-64.

Etienne-Manneville, Sandrine, and Alan Hall. 2002. 'Rho GTPases in cell biology', *Nature*, 420: 629-35.

Farnsworth, C. L., and L. A. Feig. 1991. 'Dominant inhibitory mutations in the Mg(2+)-binding site of RasH prevent its activation by GTP', *Mol Cell Biol*, 11: 4822-9.

Favia, Maria, Lorenzo Guerra, Teresa Fanelli, Rosa Angela Cardone, Stefania Monterisi, Francesca Di Sole, Stefano Castellani, Mingmin Chen, Ursula Seidler, Stephan Joel Reshkin, Massimo Conese, and Valeria Casavola. 2010. 'Na+/H+ Exchanger Regulatory Factor 1 Overexpression-dependent Increase of Cytoskeleton Organization Is Fundamental in the Rescue of F508del Cystic Fibrosis Transmembrane Conductance Regulator in Human Airway CFBE41o- Cells', *Molecular Biology of the Cell*, 21: 73-86.

Feig, L. A., and G. M. Cooper. 1988a. 'Inhibition of NIH 3T3 cell proliferation by a mutant ras protein with preferential affinity for GDP', *Mol Cell Biol*, 8: 3235-43.

———. 1988b. 'Relationship among guanine nucleotide exchange, GTP hydrolysis, and transforming potential of mutated ras proteins', *Mol Cell Biol*, 8: 2472-8.

Feng, J., M. Ito, K. Ichikawa, N. Isaka, M. Nishikawa, D. J. Hartshorne, and T. Nakano. 1999. 'Inhibitory phosphorylation site for Rho-associated kinase on smooth muscle myosin phosphatase', *J Biol Chem*, 274: 37385-90.

Fiesel, F. C., and W. Springer. 2015. 'Disease relevance of phosphorylated ubiquitin (p-S65-Ub)', *Autophagy*, 11: 2125-26.

Finley, D. 2009. 'Recognition and processing of ubiquitin-protein conjugates by the proteasome', *Annu Rev Biochem*, 78: 477-513.

Forget, Marie-Annick, Richard R. Desrosiers, Rolanda F. Del Maestro, Robert Moumdjian, Daniel Shedid, France Berthelet, and Richard Béliveau. 2002. 'The expression of Rho proteins decreases with human brain tumor progression: Potential tumor markers', *Clinical & Experimental Metastasis*, 19: 9-15.

Foster, S. A., G. W. Demers, B. G. Etscheid, and D. A. Galloway. 1994. 'The ability of human papillomavirus E6 proteins to target p53 for degradation in vivo correlates with their ability to abrogate actinomycin D-induced growth arrest', *J Virol*, 68: 5698-705.

Froyen, G., M. Corbett, J. Vandewalle, I. Jarvela, O. Lawrence, C. Meldrum, M. Bauters, K. Govaerts, L. Vandeleur, H. Van Esch, J. Chelly, D. Sanlaville, H. van Bokhoven, H. H. Ropers, F. Laumonnier, E. Ranieri, C. E. Schwartz, F. Abidi, P. S. Tarpey, P. A. Futreal, A. Whibley, F. L. Raymond, M. R. Stratton, J. P. Fryns, R. Scott, M. Peippo, M. Sipponen, M. Partington, D. Mowat, M. Field, A. Hackett, P. Marynen, G. Turner, and J. Gécz. 2008. 'Submicroscopic duplications of the hydroxysteroid dehydrogenase HSD17B10 and the E3 ubiquitin ligase HUWE1 are associated with mental retardation', *Am J Hum Genet*, 82: 432-43.

Fujisawa, K., A. Fujita, T. Ishizaki, Y. Saito, and S. Narumiya. 1996. 'Identification of the Rho-binding domain of p160ROCK, a Rho-associated coiled-coil containing protein kinase', *J Biol Chem*, 271: 23022-8.

Fukumoto, Y., K. Kaibuchi, Y. Hori, H. Fujioka, S. Araki, T. Ueda, A. Kikuchi, and Y. Takai. 1990. 'Molecular cloning and characterization of a novel type of regulatory protein (GDI) for the rho proteins, ras p21-like small GTP-binding proteins', *Oncogene*, 5: 1321-8.

Gao, J., J. Liao, and G. Y. Yang. 2009. 'CAAX-box protein, prenylation process and carcinogenesis', *Am J Transl Res*, 1: 312-25.

García-Mata, Rafael, Krister Wennerberg, William T. Arthur, Nicole K. Noren, Shawn M. Ellerbroek, and Keith Burridge. 2006. 'Analysis of Activated GAPs and GEFs in Cell Lysates.' in, *Methods in Enzymology* (Academic Press).

Gardiol, D., C. Kühne, B. Glaunsinger, S. S. Lee, R. Javier, and L. Banks. 1999. 'Oncogenic human papillomavirus E6 proteins target the discs large tumour suppressor for proteasome-mediated degradation', *Oncogene*, 18: 5487-96.

Gasmi-Seabrook, Geneviève M. C., Christopher B. Marshall, Melissa Cheung, Bryan Kim, Feng Wang, Ying Ju Jang, Tak W. Mak, Vuk Stambolic, and Mitsuhiko Ikura. 2010. 'Real-time NMR Study of Guanine Nucleotide Exchange and Activation of RhoA by PDZ-RhoGEF*', *Journal of Biological Chemistry*, 285: 5137-45.

Gatti, Marco, Sabrina Pinato, Alessio Maiolica, Francesca Rocchio, Maria Giulia Prato, Ruedi Aebersold, and Lorenza Penengo. 2015. 'RNF168 Promotes Noncanonical K27 Ubiquitination to Signal DNA Damage', *Cell Reports*, 10: 226-38.

Gerwert, Klaus, Daniel Mann, and Carsten Kötting. 2017. 'Common mechanisms of catalysis in small and heterotrimeric GTPases and their respective GAPs', 398: 523-33.

Gillison, M. L., W. M. Koch, R. B. Capone, M. Spafford, W. H. Westra, L. Wu, M. L. Zahurak, R. W. Daniel, M. Viglione, D. E. Symer, K. V. Shah, and D. Sidransky. 2000. 'Evidence for a causal association between human papillomavirus and a subset of head and neck cancers', *J Natl Cancer Inst*, 92: 709-20.

Glaunsinger, Britt A., Siu Sylvia Lee, Miranda Thomas, Lawrence Banks, and Ronald Javier. 2000. 'Interactions of the PDZ-protein MAGI-1 with adenovirus E4-ORF1 and high-risk papillomavirus E6 oncoproteins', *Oncogene*, 19: 5270-80.

Goddard, T. D., C. C. Huang, E. C. Meng, E. F. Pettersen, G. S. Couch, J. H. Morris, and T. E. Ferrin. 2018. 'UCSF ChimeraX: Meeting modern challenges in visualization and analysis', *Protein Sci*, 27: 14-25.

Goldstein, G., M. Scheid, U. Hammerling, D. H. Schlesinger, H. D. Niall, and E. A. Boyse. 1975. 'Isolation of a polypeptide that has lymphocyte-differentiating properties and is probably represented universally in living cells', *Proc Natl Acad Sci U S A*, 72: 11-5.

González-Mariscal, L., A. Betanzos, and A. Avila-Flores. 2000. 'MAGUK proteins: structure and role in the tight junction', *Semin Cell Dev Biol*, 11: 315-24.

Govek, Eve-Ellen, Sarah E. Newey, and Linda Van Aelst. 2005. 'The role of the Rho GTPases in neuronal development', *Genes & Development*, 19: 1-49.

Graham, D. L., J. F. Eccleston, and P. N. Lowe. 1999. 'The conserved arginine in rho-GTPase-activating protein is essential for efficient catalysis but not for complex formation with Rho.GDP and aluminum fluoride', *Biochemistry*, 38: 985-91.

Graham, S. V. 2010. 'Human papillomavirus: gene expression, regulation and prospects for novel diagnostic methods and antiviral therapies', *Future Microbiol*, 5: 1493-506.

Grayson, W., H. A. Rhemtula, L. F. Taylor, U. Allard, and A. J. Tiltman. 2002. 'Detection of human papillomavirus in large cell neuroendocrine carcinoma of the uterine cervix: a study of 12 cases', *J Clin Pathol*, 55: 108-14.

Griffin, T. A., D. Nandi, M. Cruz, H. J. Fehling, L. V. Kaer, J. J. Monaco, and R. A. Colbert. 1998. 'Immunoproteasome assembly: cooperative incorporation of interferon gamma (IFN-gamma)-inducible subunits', *J Exp Med*, 187: 97-104.

Grippo, P., M. Iaccarino, M. Rossi, and E. Scarano. 1965. 'Thin-layer chromatography of nucleotides, nucleosides and nucleic acid bases', *Biochimica et Biophysica Acta (BBA) - Nucleic Acids and Protein Synthesis*, 95: 1-7.

Groll, M., M. Bajorek, A. Köhler, L. Moroder, D. M. Rubin, R. Huber, M. H. Glickman, and D. Finley. 2000. 'A gated channel into the proteasome core particle', *Nat Struct Biol*, 7: 1062-7.

Groll, M., L. Ditzel, J. Löwe, D. Stock, M. Bochtler, H. D. Bartunik, and R. Huber. 1997. 'Structure of 20S proteasome from yeast at 2.4 A resolution', *Nature*, 386: 463-71.

Grossman, Steven R., Maria E. Deato, Chrystelle Brignone, Ho Man Chan, Andrew L. Kung, Hideaki Tagami, Yoshihiro Nakatani, and David M. Livingston. 2003. 'Polyubiquitination of p53 by a Ubiquitin Ligase Activity of p300', *Science*, 300: 342-44.

Grou, Cláudia P., Manuel P. Pinto, Andreia V. Mendes, Pedro Domingues, and Jorge E. Azevedo. 2015. 'The de novo synthesis of ubiquitin: identification of deubiquitinases acting on ubiquitin precursors', *Scientific Reports*, 5: 12836.

Guerra, Lorenzo, Teresa Fanelli, Maria Favia, Stefania M. Riccardi, Giovanni Busco, Rosa Angela Cardone, Salvatore Carrabino, Edward J. Weinman, Stephan Joel Reshkin, Massimo Conese, and Valeria Casavola. 2005. 'Na+/H+ Exchanger Regulatory Factor Isoform 1 Overexpression Modulates Cystic Fibrosis Transmembrane Conductance Regulator (CFTR) Expression and Activity in Human Airway 16HBE14o- Cells and Rescues ΔF508 CFTR Functional Expression in Cystic Fibrosis Cells*', *Journal of Biological Chemistry*, 280: 40925-33.

Ha, B. H., and E. E. Kim. 2008. 'Structures of proteases for ubiqutin and ubiquitin-like modifiers', *BMB Rep*, 41: 435-43.

Haas, A. L., J. V. Warms, and I. A. Rose. 1983. 'Ubiquitin adenylate: structure and role in ubiquitin activation', *Biochemistry*, 22: 4388-94.

Hakoshima, Toshio, Toshiyuki Shimizu, and Ryoko Maesaki. 2003. 'Structural Basis of the Rho GTPase Signaling', *The Journal of Biochemistry*, 134: 327-31.

Hancock, J. F., A. I. Magee, J. E. Childs, and C. J. Marshall. 1989. 'All ras proteins are polyisoprenylated but only some are palmitoylated', *Cell*, 57: 1167-77.

Hart, Matthew J., Yoshiro Maru, David Leonard, Owen N. Witte, Tony Evans, and Richard A. Cerione. 1992. 'A GDP Dissociation Inhibitor That Serves as a GTPase Inhibitor for the Ras-Like Protein CDC42Hs', *Science*, 258: 812-15.

Hartmann, Svenja, Anne J. Ridley, and Susanne Lutz. 2015. 'The Function of Rho-Associated Kinases ROCK1 and ROCK2 in the Pathogenesis of Cardiovascular Disease', *Frontiers in Pharmacology*, 6.

Hasche, D., S. Stephan, I. Braspenning-Wesch, J. Mikulec, M. Niebler, H. J. Gröne, C. Flechtenmacher, B. Akgül, F. Rösl, and S. E. Vinzón. 2017. 'The interplay of UV and cutaneous papillomavirus infection in skin cancer development', *PLoS Pathog*, 13: e1006723.

Hawley-Nelson, P., K. H. Vousden, N. L. Hubbert, D. R. Lowy, and J. T. Schiller. 1989. 'HPV16 E6 and E7 proteins cooperate to immortalize human foreskin keratinocytes', *Embo j*, 8: 3905-10.

Heink, S., D. Ludwig, P. M. Kloetzel, and E. Krüger. 2005. 'IFN-gamma-induced immune adaptation of the proteasome system is an accelerated and transient response', *Proc Natl Acad Sci U S A*, 102: 9241-6.

Hershko, A., and A. Ciechanover. 1992. 'The ubiquitin system for protein degradation', *Annu Rev Biochem*, 61: 761-807.

———. 1998. 'The ubiquitin system', *Annu Rev Biochem*, 67: 425-79.

Hershko, A., and I. A. Rose. 1987. 'Ubiquitin-aldehyde: a general inhibitor of ubiquitin-recycling processes', *Proc Natl Acad Sci U S A*, 84: 1829-33.

Hicke, Linda, Heidi L. Schubert, and Christopher P. Hill. 2005. 'Ubiquitin-binding domains', *Nature Reviews Molecular Cell Biology*, 6: 610-21.

Hines, C. S., C. Meghoo, S. Shetty, M. Biburger, M. Brenowitz, and R. S. Hegde. 1998. 'DNA structure and flexibility in the sequence-specific binding of papillomavirus E2 proteins', *J Mol Biol*, 276: 809-18.

Hjerpe, R., F. Aillet, F. Lopitz-Otsoa, V. Lang, P. England, and M. S. Rodriguez. 2009. 'Efficient protection and isolation of ubiquitylated proteins using tandem ubiquitin-binding entities', *EMBO Rep*, 10: 1250-8.

Hodge, Richard G., and Anne J. Ridley. 2016. 'Regulating Rho GTPases and their regulators', *Nature Reviews Molecular Cell Biology*, 17: 496-510.

Hoffman, Gregory R., and Richard A. Cerione. 2002. 'Signaling to the Rho GTPases: networking with the DH domain', *FEBS Letters*, 513: 85-91.

Houben, Klaartje, Cyril Dominguez, Frederik M. A. van Schaik, H. Th Marc Timmers, Alexandre M. J. J. Bonvin, and Rolf Boelens. 2004. 'Solution Structure of the Ubiquitin-conjugating Enzyme UbcH5B', *Journal of Molecular Biology*, 344: 513-26.

Howie, Heather L., Rachel A. Katzenellenbogen, and Denise A. Galloway. 2009. 'Papillomavirus E6 proteins', *Virology*, 384: 324-34.

Huang, L., E. Kinnucan, G. Wang, S. Beaudenon, P. M. Howley, J. M. Huibregtse, and N. P. Pavletich. 1999. 'Structure of an E6AP-UbcH7 complex: insights into ubiquitination by the E2-E3 enzyme cascade', *Science*, 286: 1321-6.

Huang, M., and G. C. Prendergast. 2006. 'RhoB in cancer suppression', *Histol Histopathol*, 21: 213-8.

Huh, K., X. Zhou, H. Hayakawa, J. Y. Cho, T. A. Libermann, J. Jin, J. W. Harper, and K. Munger. 2007. 'Human papillomavirus type 16 E7 oncoprotein associates with the cullin

2 ubiquitin ligase complex, which contributes to degradation of the retinoblastoma tumor suppressor', *J Virol*, 81: 9737-47.

Huibregtse, J. M., M. Scheffner, S. Beaudenon, and P. M. Howley. 1995. 'A family of proteins structurally and functionally related to the E6-AP ubiquitin-protein ligase', *Proc Natl Acad Sci U S A*, 92: 2563-7.

Huibregtse, J. M., M. Scheffner, and P. M. Howley. 1991. 'A cellular protein mediates association of p53 with the E6 oncoprotein of human papillomavirus types 16 or 18', *Embo j*, 10: 4129-35.

———. 1993a. 'Cloning and expression of the cDNA for E6-AP, a protein that mediates the interaction of the human papillomavirus E6 oncoprotein with p53', *Mol Cell Biol*, 13: 775-84.

———. 1993b. 'Localization of the E6-AP regions that direct human papillomavirus E6 binding, association with p53, and ubiquitination of associated proteins', *Mol Cell Biol*, 13: 4918-27.

Humphries, B. A., Z. Wang, and C. Yang. 2020. 'MicroRNA Regulation of the Small Rho GTPase Regulators-Complexities and Opportunities in Targeting Cancer Metastasis', *Cancers (Basel)*, 12.

Hurst, M., D. J. McGarry, and M. F. Olson. 2022. 'Rho GTPases: Non-canonical regulation by cysteine oxidation', *Bioessays*, 44: e2100152.

Husnjak, K., S. Elsasser, N. Zhang, X. Chen, L. Randles, Y. Shi, K. Hofmann, K. J. Walters, D. Finley, and I. Dikic. 2008. 'Proteasome subunit Rpn13 is a novel ubiquitin receptor', *Nature*, 453: 481-8.

Husnjak, Koraljka, and Ivan Dikic. 2012. 'Ubiquitin-Binding Proteins: Decoders of Ubiquitin-Mediated Cellular Functions', *Annual Review of Biochemistry*, 81: 291-322.

Ibeawuchi, Stella-Rita C., Larry N. Agbor, Frederick W. Quelle, and Curt D. Sigmund. 2015. 'Hypertension-causing Mutations in Cullin3 Protein Impair RhoA Protein Ubiquitination and Augment the Association with Substrate Adaptors*', *Journal of Biological Chemistry*, 290: 19208-17.

Ihara, K., S. Muraguchi, M. Kato, T. Shimizu, M. Shirakawa, S. Kuroda, K. Kaibuchi, and T. Hakoshima. 1998. 'Crystal structure of human RhoA in a dominantly active form complexed with a GTP analogue', *J Biol Chem*, 273: 9656-66.

Itoh, Kazuyuki, Kiyoko Yoshioka, Hitoshi Akedo, Masayoshi Uehata, Toshimasa Ishizaki, and Shuh Narumiya. 1999. 'An essential part for Rho–associated kinase in the transcellular invasion of tumor cells', *Nature Medicine*, 5: 221-25.

Ivetic, A., and A. J. Ridley. 2004. 'Ezrin/radixin/moesin proteins and Rho GTPase signalling in leucocytes', *Immunology*, 112: 165-76.

Iwabuchi, K, P L Bartel, B Li, R Marraccino, and S Fields. 1994. 'Two cellular proteins that bind to wild-type but not mutant p53', *Proceedings of the National Academy of Sciences*, 91: 6098-102.

Iwai, K., H. Fujita, and Y. Sasaki. 2014. 'Linear ubiquitin chains: NF-κB signalling, cell death and beyond', *Nat Rev Mol Cell Biol*, 15: 503-8.

Johnson, Bryan A., Heather L. Aloor, and Cary A. Moody. 2017. 'The Rb binding domain of HPV31 E7 is required to maintain high levels of DNA repair factors in infected cells', *Virology*, 500: 22-34.

Jumper, John, Richard Evans, Alexander Pritzel, Tim Green, Michael Figurnov, Olaf Ronneberger, Kathryn Tunyasuvunakool, Russ Bates, Augustin Žídek, Anna Potapenko, Alex Bridgland, Clemens Meyer, Simon A. A. Kohl, Andrew J. Ballard, Andrew Cowie, Bernardino Romera-Paredes, Stanislav Nikolov, Rishub Jain, Jonas

Adler, Trevor Back, Stig Petersen, David Reiman, Ellen Clancy, Michal Zielinski, Martin Steinegger, Michalina Pacholska, Tamas Berghammer, Sebastian Bodenstein, David Silver, Oriol Vinyals, Andrew W. Senior, Koray Kavukcuoglu, Pushmeet Kohli, and Demis Hassabis. 2021. 'Highly accurate protein structure prediction with AlphaFold', *Nature*, 596: 583-89.

Kabsch, K., and A. Alonso. 2002. 'The human papillomavirus type 16 E5 protein impairs TRAIL- and FasL-mediated apoptosis in HaCaT cells by different mechanisms', *J Virol*, 76: 12162-72.

Kajitani, N., A. Satsuka, A. Kawate, and H. Sakai. 2012. 'Productive Lifecycle of Human Papillomaviruses that Depends Upon Squamous Epithelial Differentiation', *Front Microbiol*, 3: 152.

Kalsner, L., and S. J. Chamberlain. 2015. 'Prader-Willi, Angelman, and 15q11-q13 Duplication Syndromes', *Pediatr Clin North Am*, 62: 587-606.

Kamadurai, Hari B., Judith Souphron, Daniel C. Scott, David M. Duda, Darcie J. Miller, Daniel Stringer, Robert C. Piper, and Brenda A. Schulman. 2009. 'Insights into Ubiquitin Transfer Cascades from a Structure of a UbcH5B~Ubiquitin-HECTNEDD4L Complex', *Molecular Cell*, 36: 1095-102.

Kao, W. H., S. L. Beaudenon, A. L. Talis, J. M. Huibregtse, and P. M. Howley. 2000. 'Human papillomavirus type 16 E6 induces self-ubiquitination of the E6AP ubiquitin-protein ligase', *J Virol*, 74: 6408-17.

Khan, Alamzeb, Weiming Ni, Francesc Lopez-Giraldez, Martin S. Kluger, Jordan S. Pober, and Richard W. Pierce. 2021. 'Tumor necrosis factor-induced ArhGEF10 selectively activates RhoB contributing to human microvascular endothelial cell tight junction disruption', *The FASEB Journal*, 35: e21627.

Khatri, N., and H. Y. Man. 2019. 'The Autism and Angelman Syndrome Protein Ube3A/E6AP: The Gene, E3 Ligase Ubiquitination Targets and Neurobiological Functions', *Front Mol Neurosci*, 12: 109.

Kholmanskikh, Stanislav, Shawn Singh, and M. Elizabeth Ross. 2022. 'Activation of RhoC by regulatory ubiquitination is mediated by LNX1 and suppressed by LIS1', *Scientific Reports*, 12: 16493.

Kienle, Simon Maria, Tobias Schneider, Katrin Stuber, Christoph Globisch, Jasmin Jansen, Florian Stengel, Christine Peter, Andreas Marx, Michael Kovermann, and Martin Scheffner. 2022. 'Electrostatic and steric effects underlie acetylation-induced changes in ubiquitin structure and function', *Nature Communications*, 13: 5435.

Kim, Hyung Cheol, and Jon M. Huibregtse. 2009. 'Polyubiquitination by HECT E3s and the Determinants of Chain Type Specificity', *Molecular and Cellular Biology*, 29: 3307-18.

Kim, J. W., S. H. Song, C. H. Jin, J. K. Lee, N. W. Lee, and K. W. Lee. 2012. 'Factors affecting the clearance of high-risk human papillomavirus infection and the progression of cervical intraepithelial neoplasia', *J Int Med Res*, 40: 486-96.

Kimura, Kazushi, Masaaki Ito, Mutsuki Amano, Kazuyasu Chihara, Yuko Fukata, Masato Nakafuku, Bunpei Yamamori, Jianhua Feng, Takeshi Nakano, Katsuya Okawa, Akihiro Iwamatsu, and Kozo Kaibuchi. 1996. 'Regulation of Myosin Phosphatase by Rho and Rho-Associated Kinase (Rho-Kinase)', *Science*, 273: 245-48.

Kirisako, T., K. Kamei, S. Murata, M. Kato, H. Fukumoto, M. Kanie, S. Sano, F. Tokunaga, K. Tanaka, and K. Iwai. 2006. 'A ubiquitin ligase complex assembles linear polyubiquitin chains', *Embo j*, 25: 4877-87.

Kiyono, T., A. Hiraiwa, M. Fujita, Y. Hayashi, T. Akiyama, and M. Ishibashi. 1997. 'Binding of high-risk human papillomavirus E6 oncoproteins to the human homologue of the

Drosophila discs large tumor suppressor protein', *Proc Natl Acad Sci U S A*, 94: 11612-6.

Klingelhutz, Aloysius J., Scott A. Foster, and James K. McDougall. 1996. 'Telomerase activation by the E6 gene product of human papillomavirus type 16', *Nature*, 380: 79-82.

Knoll, J. H. M., R. D. Nicholls, R. E. Magenis, J. M. Graham Jr., M. Lalande, S. A. Latt, John M. Opitz, and James F. Reynolds. 1989. 'Angelman and Prader-Willi syndromes share a common chromosome 15 deletion but differ in parental origin of the deletion', *American Journal of Medical Genetics*, 32: 285-90.

Koegl, M., T. Hoppe, S. Schlenker, H. D. Ulrich, T. U. Mayer, and S. Jentsch. 1999. 'A novel ubiquitination factor, E4, is involved in multiubiquitin chain assembly', *Cell*, 96: 635-44.

Komander, D., M. J. Clague, and S. Urbé. 2009. 'Breaking the chains: structure and function of the deubiquitinases', *Nat Rev Mol Cell Biol*, 10: 550-63.

Komander, D., and M. Rape. 2012. 'The ubiquitin code', *Annu Rev Biochem*, 81: 203-29.

Kovačević, I., T. Sakaue, J. Majoleé, M. C. Pronk, M. Maekawa, D. Geerts, M. Fernandez-Borja, S. Higashiyama, and P. L. Hordijk. 2018. 'The Cullin-3-Rbx1-KCTD10 complex controls endothelial barrier function via K63 ubiquitination of RhoB', *J Cell Biol*, 217: 1015-32.

Kozlova, Maria I., Daria N. Shalaeva, Daria V. Dibrova, and Armen Y. Mulkidjanian. 2022. 'Common Patterns of Hydrolysis Initiation in P-loop Fold Nucleoside Triphosphatases', *Biomolecules*, 12: 1345.

Kozma, R., S. Sarner, S. Ahmed, and L. Lim. 1997. 'Rho family GTPases and neuronal growth cone remodelling: relationship between increased complexity induced by Cdc42Hs, Rac1, and acetylcholine and collapse induced by RhoA and lysophosphatidic acid', *Mol Cell Biol*, 17: 1201-11.

Kuang, Yi-Qun, Wei Pang, Yong-Tang Zheng, and Denis J. Dupré. 2012. 'NHERF1 regulates gp120-induced internalization and signaling by CCR5, and HIV-1 production', *European Journal of Immunology*, 42: 299-310.

Kuballa, P., K. Matentzoglu, and M. Scheffner. 2007. 'The role of the ubiquitin ligase E6-AP in human papillomavirus E6-mediated degradation of PDZ domain-containing proteins', *J Biol Chem*, 282: 65-71.

Kuballa, Petric. 2004. 'Das E6-Onkoprotein humaner Papillomviren und seine Wechselwirkung mit E6AP als Zielstruktur für eine molekulare Therapie zervikaler Karzinome', Dissertation, Universität zu Köln.

Kühne, Christian, Daniela Gardiol, Corrado Guarnaccia, Heinz Amenitsch, and Lawrence Banks. 2000. 'Differential regulation of human papillomavirus E6 by protein kinase A: conditional degradation of human discs large protein by oncogenic E6', *Oncogene*, 19: 5884-91.

Kühnle, S., U. Kogel, S. Glockzin, A. Marquardt, A. Ciechanover, K. Matentzoglu, and M. Scheffner. 2011. 'Physical and functional interaction of the HECT ubiquitin-protein ligases E6AP and HERC2', *J Biol Chem*, 286: 19410-6.

Kühnle, S., G. Martínez-Noël, F. Leclere, S. D. Hayes, J. W. Harper, and P. M. Howley. 2018. 'Angelman syndrome-associated point mutations in the Zn(2+)-binding N-terminal (AZUL) domain of UBE3A ubiquitin ligase inhibit binding to the proteasome', *J Biol Chem*, 293: 18387-99.

Kühnle, Simone, Benedikt Mothes, Konstantin Matentzoglu, and Martin Scheffner. 2013. 'Role of the ubiquitin ligase E6AP/UBE3A in controlling levels of the synaptic protein Arc', *Proceedings of the National Academy of Sciences*, 110: 8888-93.

Kumar, S., A. L. Talis, and P. M. Howley. 1999. 'Identification of HHR23A as a substrate for E6-associated protein-mediated ubiquitination', *J Biol Chem*, 274: 18785-92.

Laemmli, U. K. 1970. 'Cleavage of structural proteins during the assembly of the head of bacteriophage T4', *Nature*, 227: 680-5.

Lamothe, B., A. Besse, A. D. Campos, W. K. Webster, H. Wu, and B. G. Darnay. 2007. 'Site-specific Lys-63-linked tumor necrosis factor receptor-associated factor 6 auto-ubiquitination is a critical determinant of I kappa B kinase activation', *J Biol Chem*, 282: 4102-12.

Larson, A. M., J. E. Shinnick, E. A. Shaaya, E. A. Thiele, and R. L. Thibert. 2015. 'Angelman syndrome in adulthood', *Am J Med Genet A*, 167a: 331-44.

LaSalle, J. M., L. T. Reiter, and S. J. Chamberlain. 2015. 'Epigenetic regulation of UBE3A and roles in human neurodevelopmental disorders', *Epigenomics*, 7: 1213-28.

Laurin, M., and J. F. Côté. 2014. 'Insights into the biological functions of Dock family guanine nucleotide exchange factors', *Genes Dev*, 28: 533-47.

Leeuwen, F. N., H. E. Kain, R. A. Kammen, F. Michiels, O. W. Kranenburg, and J. G. Collard. 1997. 'The guanine nucleotide exchange factor Tiam1 affects neuronal morphology; opposing roles for the small GTPases Rac and Rho', *J Cell Biol*, 139: 797-807.

Lehman, C. W., and M. R. Botchan. 1998. 'Segregation of viral plasmids depends on tethering to chromosomes and is regulated by phosphorylation', *Proc Natl Acad Sci U S A*, 95: 4338-43.

Leitner, A., T. Walzthoeni, and R. Aebersold. 2014. 'Lysine-specific chemical cross-linking of protein complexes and identification of cross-linking sites using LC-MS/MS and the xQuest/xProphet software pipeline', *Nat Protoc*, 9: 120-37.

Leitner, Alexander, Lukasz A Joachimiak, Andreas Bracher, Leonie Mönkemeyer, Thomas Walzthoeni, Bryan Chen, Sebastian Pechmann, Susan Holmes, Yao Cong, Boxue Ma, Steve Ludtke, Wah Chiu, F. Ulrich Hartl, Ruedi Aebersold, and Judith Frydman. 2012. 'The Molecular Architecture of the Eukaryotic Chaperonin TRiC/CCT', *Structure*, 20: 814-25.

Lelias, J. M., C. N. Adra, G. M. Wulf, J. C. Guillemot, M. Khagad, D. Caput, and B. Lim. 1993. 'cDNA cloning of a human mRNA preferentially expressed in hematopoietic cells and with homology to a GDP-dissociation inhibitor for the rho GTP-binding proteins', *Proceedings of the National Academy of Sciences*, 90: 1479-83.

Lemak, Alexander, Adelinda Yee, Irina Bezsonova, Sirano Dhe-Paganon, and Cheryl H. Arrowsmith. 2011. 'Zn-binding AZUL domain of human ubiquitin protein ligase Ube3A', *Journal of Biomolecular NMR*, 51: 185.

Li, Guangpu, and Xuejun C. Zhang. 2004. 'GTP Hydrolysis Mechanism of Ras-like GTPases', *Journal of Molecular Biology*, 340: 921-32.

Li, Zheng, Carlos D. Aizenman, and Hollis T. Cline. 2002. 'Regulation of Rho GTPases by Crosstalk and Neuronal Activity In Vivo', *Neuron*, 33: 741-50.

Lin, Rui, Richard A. Cerione, and Danny Manor. 1999. 'Specific Contributions of the Small GTPases Rho, Rac, and Cdc42 to Dbl Transformation*', *Journal of Biological Chemistry*, 274: 23633-41.

Lin, Yuan, Shaoyong Lu, Jian Zhang, and Yi Zheng. 2021. 'Structure of an inactive conformation of GTP-bound RhoA GTPase', *Structure*, 29: 553-63.e5.

Liu, Ax, G. J. Cerniglia, E. J. Bernhard, and G. C. Prendergast. 2001. 'RhoB is required to mediate apoptosis in neoplastically transformed cells after DNA damage', *Proc Natl Acad Sci U S A*, 98: 6192-7.

Liu, M., F. Bi, X. Zhou, and Y. Zheng. 2012. 'Rho GTPase regulation by miRNAs and covalent modifications', *Trends Cell Biol*, 22: 365-73.

Liu, Yue, Wenjuan Zhang, Shiwen Wang, Lili Cai, Yanyu Jiang, Yongfu Pan, Yupei Liang, Jingrong Xian, Lijun Jia, Lihui Li, Hu Zhao, and Yanmei Zhang. 2021. 'Cullin3-TNFAIP1 E3 Ligase Controls Inflammatory Response in Hepatocellular Carcinoma Cells via Ubiquitination of RhoB', *Frontiers in Cell and Developmental Biology*, 9.

Longenecker, K., P. Read, S. K. Lin, A. P. Somlyo, R. K. Nakamoto, and Z. S. Derewenda. 2003. 'Structure of a constitutively activated RhoA mutant (Q63L) at 1.55 A resolution', *Acta Crystallogr D Biol Crystallogr*, 59: 876-80.

Lopez, S. J., D. J. Segal, and J. M. LaSalle. 2018. 'UBE3A: An E3 Ubiquitin Ligase With Genome-Wide Impact in Neurodevelopmental Disease', *Front Mol Neurosci*, 11: 476.

Lorenz, Sonja. 2018. 'Structural mechanisms of HECT-type ubiquitin ligases', *Biological Chemistry*, 399: 127-45.

Lou, Yingyue, Yuhan Jiang, Zhen Liang, Bingzhang Liu, Tian Li, and Duo Zhang. 2021. 'Role of RhoC in cancer cell migration', *Cancer Cell International*, 21: 527.

Lusk, L., V. Vogel-Farley, C. DiStefano, and S. Jeste. 1993. 'Maternal 15q Duplication Syndrome.' in M. P. Adam, D. B. Everman, G. M. Mirzaa, R. A. Pagon, S. E. Wallace, L. J. H. Bean, K. W. Gripp and A. Amemiya (eds.), *GeneReviews(®)* (University of Washington, Seattle

Copyright © 1993-2023, University of Washington, Seattle. GeneReviews is a registered trademark of the University of Washington, Seattle. All rights reserved.: Seattle (WA)).

Maciejowski, J., and T. de Lange. 2017. 'Telomeres in cancer: tumour suppression and genome instability', *Nat Rev Mol Cell Biol*, 18: 175-86.

Madaule, P., and R. Axel. 1985. 'A novel ras-related gene family', *Cell*, 41: 31-40.

Mädler, Stefanie, Claudia Bich, David Touboul, and Renato Zenobi. 2009. 'Chemical cross-linking with NHS esters: a systematic study on amino acid reactivities', *Journal of Mass Spectrometry*, 44: 694-706.

Maesaki, R., K. Ihara, T. Shimizu, S. Kuroda, K. Kaibuchi, and T. Hakoshima. 1999. 'The structural basis of Rho effector recognition revealed by the crystal structure of human RhoA complexed with the effector domain of PKN/PRK1', *Mol Cell*, 4: 793-803.

Marcu, Ştefan-Bogdan, Sabin Tăbîrcă, and Mark Tangney. 2022. 'An Overview of Alphafold's Breakthrough', *Frontiers in Artificial Intelligence*, 5.

Margolis, S. S., J. Salogiannis, D. M. Lipton, C. Mandel-Brehm, Z. P. Wills, A. R. Mardinly, L. Hu, P. L. Greer, J. B. Bikoff, H. Y. Ho, M. J. Soskis, M. Sahin, and M. E. Greenberg. 2010. 'EphB-mediated degradation of the RhoA GEF Ephexin5 relieves a developmental brake on excitatory synapse formation', *Cell*, 143: 442-55.

Margolis, S. S., G. L. Sell, M. A. Zbinden, and L. M. Bird. 2015. 'Angelman Syndrome', *Neurotherapeutics*, 12: 641-50.

Marín, I., and A. Ferrús. 2002. 'Comparative genomics of the RBR family, including the Parkinson's disease-related gene parkin and the genes of the ariadne subfamily', *Mol Biol Evol*, 19: 2039-50.

Martínez-Noël, G., K. Luck, S. Kühnle, A. Desbuleux, P. Szajner, J. T. Galligan, D. Rodriguez, L. Zheng, K. Boyland, F. Leclere, Q. Zhong, D. E. Hill, M. Vidal, and P. M. Howley. 2018. 'Network Analysis of UBE3A/E6AP-Associated Proteins Provides Connections to Several Distinct Cellular Processes', *J Mol Biol*, 430: 1024-50.

Martinez-Zapien, Denise, Francesc Xavier Ruiz, Juline Poirson, André Mitschler, Juan Ramirez, Anne Forster, Alexandra Cousido-Siah, Murielle Masson, Scott Vande Pol,

Alberto Podjarny, Gilles Travé, and Katia Zanier. 2016. 'Structure of the E6/E6AP/p53 complex required for HPV-mediated degradation of p53', *Nature*, 529: 541-45.

Maru, Y., D. E. Afar, O. N. Witte, and M. Shibuya. 1996. 'The dimerization property of glutathione S-transferase partially reactivates Bcr-Abl lacking the oligomerization domain', *J Biol Chem*, 271: 15353-7.

Masutani, C., K. Sugasawa, J. Yanagisawa, T. Sonoyama, M. Ui, T. Enomoto, K. Takio, K. Tanaka, P.J. van der Spek, and D. Bootsma. 1994. 'Purification and cloning of a nucleotide excision repair complex involving the xeroderma pigmentosum group C protein and a human homologue of yeast RAD23', *The EMBO Journal*, 13: 1831-43.

Matsushita, Tomonaga, Kyota Ashikawa, Koji Yonemoto, Yoichiro Hirakawa, Jun Hata, Hanae Amitani, Yasufumi Doi, Toshiharu Ninomiya, Takanari Kitazono, Setsuro Ibayashi, Mitsuo Iida, Yusuke Nakamura, Yutaka Kiyohara, and Michiaki Kubo. 2009. 'Functional SNP of ARHGEF10 confers risk of atherothrombotic stroke', *Human Molecular Genetics*, 19: 1137-46.

Mattiroli, F., and T. K. Sixma. 2014. 'Lysine-targeting specificity in ubiquitin and ubiquitin-like modification pathways', *Nat Struct Mol Biol*, 21: 308-16.

Mayer, T., M. Meyer, A. Janning, A. C. Schiedel, and A. Barnekow. 1999. 'A mutant form of the rho protein can restore stress fibers and adhesion plaques in v-src transformed fibroblasts', *Oncogene*, 18: 2117-28.

McIntyre, M. C., M. G. Frattini, S. R. Grossman, and L. A. Laimins. 1993. 'Human papillomavirus type 18 E7 protein requires intact Cys-X-X-Cys motifs for zinc binding, dimerization, and transformation but not for Rb binding', *J Virol*, 67: 3142-50.

Mendes, M. L., M. R. Fougeras, and G. Dittmar. 2020. 'Analysis of ubiquitin signaling and chain topology cross-talk', *J Proteomics*, 215: 103634.

Merkley, Eric D., Steven Rysavy, Abdullah Kahraman, Ryan P. Hafen, Valerie Daggett, and Joshua N. Adkins. 2014. 'Distance restraints from crosslinking mass spectrometry: Mining a molecular dynamics simulation database to evaluate lysine–lysine distances', *Protein Science*, 23: 747-59.

Metzger, Meredith B., Jonathan N. Pruneda, Rachel E. Klevit, and Allan M. Weissman. 2014. 'RING-type E3 ligases: Master manipulators of E2 ubiquitin-conjugating enzymes and ubiquitination', *Biochimica et Biophysica Acta (BBA) - Molecular Cell Research*, 1843: 47-60.

Michaelson, D., J. Silletti, G. Murphy, P. D'Eustachio, M. Rush, and M. R. Philips. 2001. 'Differential localization of Rho GTPases in live cells: regulation by hypervariable regions and RhoGDI binding', *J Cell Biol*, 152: 111-26.

Miller, Raymond D., Louise Prakash, and Satya Prakash. 1982. 'Defective excision of pyrimidine dimers and interstrand DNA crosslinks in rad7 and rad23 mutants of Saccharomyces cerevisiae', *Molecular and General Genetics MGG*, 188: 235-39.

Mistry, N., C. Wibom, and M. Evander. 2008. 'Cutaneous and mucosal human papillomaviruses differ in net surface charge, potential impact on tropism', *Virol J*, 5: 118.

Mittnacht, Sibylle. 1998. 'Control of pRB phosphorylation', *Current Opinion in Genetics & Development*, 8: 21-27.

Moissoglu, K., and M. A. Schwartz. 2014. 'Spatial and temporal control of Rho GTPase functions', *Cell Logist*, 4: e943618.

Moody, C. A., and L. A. Laimins. 2010. 'Human papillomavirus oncoproteins: pathways to transformation', *Nat Rev Cancer*, 10: 550-60.

Moorman, J. P., D. Luu, J. Wickham, D. A. Bobak, and C. S. Hahn. 1999. 'A balance of signaling by Rho family small GTPases RhoA, Rac1 and Cdc42 coordinates cytoskeletal morphology but not cell survival', *Oncogene*, 18: 47-57.

Morris, S. W., M. B. Valentine, M. N. Kirstein, and K. Huebner. 1993. 'Reassignment of the human ARH9 RAS-related gene to chromosome 1p13-p21', *Genomics*, 15: 677-9.

Mortensen, F., D. Schneider, T. Barbic, A. Sladewska-Marquardt, S. Kühnle, A. Marx, and M. Scheffner. 2015. 'Role of ubiquitin and the HPV E6 oncoprotein in E6AP-mediated ubiquitination', *Proc Natl Acad Sci U S A*, 112: 9872-7.

Mosaddeghzadeh, N., and M. R. Ahmadian. 2021. 'The RHO Family GTPases: Mechanisms of Regulation and Signaling', *Cells*, 10.

Mukhopadhyay, D., and M. Dasso. 2007. 'Modification in reverse: the SUMO proteases', *Trends Biochem Sci*, 32: 286-95.

Müller, D. R., P. Schindler, H. Towbin, U. Wirth, H. Voshol, S. Hoving, and M. O. Steinmetz. 2001. 'Isotope-Tagged Cross-Linking Reagents. A New Tool in Mass Spectrometric Protein Interaction Analysis', *Analytical Chemistry*, 73: 1927-34.

Münger, K., B. A. Werness, N. Dyson, W. C. Phelps, E. Harlow, and P. M. Howley. 1989. 'Complex formation of human papillomavirus E7 proteins with the retinoblastoma tumor suppressor gene product', *Embo j*, 8: 4099-105.

Nakagawa, S., and J. M. Huibregtse. 2000. 'Human scribble (Vartul) is targeted for ubiquitin-mediated degradation by the high-risk papillomavirus E6 proteins and the E6AP ubiquitin-protein ligase', *Mol Cell Biol*, 20: 8244-53.

Nakahara, Tomomi, and Tohru Kiyono. 2016. 'Interplay between NF-κB/interferon signaling and the genome replication of HPV', *Future Virology*, 11: 141-55.

Nawaz, Zafar, David M. Lonard, Carolyn L. Smith, Efrat Lev-Lehman, Sophia Y. Tsai, Ming-Jer Tsai, and Bert W. O'Malley. 1999. 'The Angelman Syndrome-Associated Protein, E6-AP, Is a Coactivator for the Nuclear Hormone Receptor Superfamily', *Molecular and Cellular Biology*, 19: 1182-89.

Nguyen, L. K., B. N. Kholodenko, and A. von Kriegsheim. 2018. 'Rac1 and RhoA: Networks, loops and bistability', *Small GTPases*, 9: 316-21.

Niggli, Verena. 1999. 'Rho-kinase in human neutrophils: a role in signalling for myosin light chain phosphorylation and cell migration', *FEBS Letters*, 445: 69-72.

Nuber, U., S. Schwarz, P. Kaiser, R. Schneider, and M. Scheffner. 1996. 'Cloning of human ubiquitin-conjugating enzymes UbcH6 and UbcH7 (E2-F1) and characterization of their interaction with E6-AP and RSP5', *J Biol Chem*, 271: 2795-800.

Nuber, Ulrike, Sylvia E. Schwarz, and Martin Scheffner. 1998. 'The ubiquitin-protein ligase E6-associated protein (E6-AP) serves as its own substrate', *European Journal of Biochemistry*, 254: 643-49.

Nusser, N., E. Gosmanova, N. Makarova, Y. Fujiwara, L. Yang, F. Guo, Y. Luo, Y. Zheng, and G. Tigyi. 2006. 'Serine phosphorylation differentially affects RhoA binding to effectors: implications to NGF-induced neurite outgrowth', *Cell Signal*, 18: 704-14.

Ohga, N., A. Kikuchi, T. Ueda, J. Yamamoto, and Y. Takai. 1989. 'Rabbit intestine contains a protein that inhibits the dissociation of GDP from and the subsequent binding of GTP to rhoB p20, a ras p21-like GTP-binding protein', *Biochem Biophys Res Commun*, 163: 1523-33.

Ohtake, F., Y. Saeki, K. Sakamoto, K. Ohtake, H. Nishikawa, H. Tsuchiya, T. Ohta, K. Tanaka, and J. Kanno. 2015. 'Ubiquitin acetylation inhibits polyubiquitin chain elongation', *EMBO Rep*, 16: 192-201.

Olenik, Claudia, Holger Barth, Ingo Just, Klaus Aktories, and Dieter K. Meyer. 1997. 'Gene expression of the small GTP-binding proteins RhoA, RhoB, Rac1, and Cdc42 in adult rat brain', *Molecular Brain Research*, 52: 263-69.

Olsen, Jesper V., Shao-En Ong, and Matthias Mann. 2004. 'Trypsin Cleaves Exclusively C-terminal to Arginine and Lysine Residues*', *Molecular & Cellular Proteomics*, 3: 608-14.

Olson, M. F. 2018. 'Rho GTPases, their post-translational modifications, disease-associated mutations and pharmacological inhibitors', *Small GTPases*, 9: 203-15.

Ordureau, Alban, Jin-Mi Heo, David M. Duda, Joao A. Paulo, Jennifer L. Olszewski, David Yanishevski, Jesse Rinehart, Brenda A. Schulman, and J. Wade Harper. 2015. 'Defining roles of PARKIN and ubiquitin phosphorylation by PINK1 in mitochondrial quality control using a ubiquitin replacement strategy', *Proceedings of the National Academy of Sciences*, 112: 6637-42.

Orgaz, Jose L., Cecilia Herraiz, and Victoria Sanz-Moreno. 2014. 'Rho GTPases modulate malignant transformation of tumor cells', *Small GTPases*, 5: e983867.

Owais, A., R. K. Mishra, and H. Kiyokawa. 2020. 'The HECT E3 Ligase E6AP/UBE3A as a Therapeutic Target in Cancer and Neurological Disorders', *Cancers (Basel)*, 12.

Ozbun, M. A., and C. Meyers. 1998. 'Human papillomavirus type 31b E1 and E2 transcript expression correlates with vegetative viral genome amplification', *Virology*, 248: 218-30.

Ozdamar, Barish, Rohit Bose, Miriam Barrios-Rodiles, Hong-Rui Wang, Yue Zhang, and Jeffrey L. Wrana. 2005. 'Regulation of the Polarity Protein Par6 by TGFß Receptors Controls Epithelial Cell Plasticity', *Science*, 307: 1603-09.

Pandya, Nikhil J., Sonja Meier, Stefka Tyanova, Marco Terrigno, Congwei Wang, A. Mattijs Punt, E. J. Mientjes, Audrey Vautheny, Ben Distel, Thomas Kremer, Ype Elgersma, and Ravi Jagasia. 2022. 'A cross-species spatiotemporal proteomic analysis identifies UBE3A-dependent signaling pathways and targets', *Molecular Psychiatry*, 27: 2590-601.

Pedroza-Saavedra, A., E. W. Lam, F. Esquivel-Guadarrama, and L. Gutierrez-Xicotencatl. 2010. 'The human papillomavirus type 16 E5 oncoprotein synergizes with EGF-receptor signaling to enhance cell cycle progression and the down-regulation of p27(Kip1)', *Virology*, 400: 44-52.

Peng, J., D. Schwartz, J. E. Elias, C. C. Thoreen, D. Cheng, G. Marsischky, J. Roelofs, D. Finley, and S. P. Gygi. 2003. 'A proteomics approach to understanding protein ubiquitination', *Nat Biotechnol*, 21: 921-6.

Petit, Alain-Pierre, Christel Garcia-Petit, Juan A. Bueren-Calabuig, Laurent M. Vuillard, Gilles Ferry, and Jean A. Boutin. 2018. 'A structural study of the complex between neuroepithelial cell transforming gene 1 (Net1) and RhoA reveals a potential anticancer drug hot spot', *Journal of Biological Chemistry*, 293: 9064-77.

Pfister, H., and J. Ter Schegget. 1997. 'Role of HPV in cutaneous premalignant and malignant tumors', *Clin Dermatol*, 15: 335-47.

Phelps, W. C., and P. M. Howley. 1987. 'Transcriptional trans-activation by the human papillomavirus type 16 E2 gene product', *J Virol*, 61: 1630-8.

Pickart, Cecile M., and Michael J. Eddins. 2004. 'Ubiquitin: structures, functions, mechanisms', *Biochimica et Biophysica Acta (BBA) - Molecular Cell Research*, 1695: 55-72.

Pimenta, F. M., J. Huh, B. Guzman, D. Amanah, D. J. Marston, N. K. Pinkin, G. Danuser, and K. M. Hahn. 2023. 'Rho MultiBinder, a fluorescent biosensor that reports the activity of multiple GTPases', *Biophys J*.

Porter, A. P., A. Papaioannou, and A. Malliri. 2016a. 'Deregulation of Rho GTPases in cancer', *Small GTPases*, 7: 123-38.

Porter, Andrew P., Alexandra Papaioannou, and Angeliki Malliri. 2016b. 'Deregulation of Rho GTPases in cancer', *Small GTPases*, 7: 123-38.

Redman, K. L., and M. Rechsteiner. 1989. 'Identification of the long ubiquitin extension as ribosomal protein S27a', *Nature*, 338: 438-40.

Reid, T., T. Furuyashiki, T. Ishizaki, G. Watanabe, N. Watanabe, K. Fujisawa, N. Morii, P. Madaule, and S. Narumiya. 1996. 'Rhotekin, a new putative target for Rho bearing homology to a serine/threonine kinase, PKN, and rhophilin in the rho-binding domain', *J Biol Chem*, 271: 13556-60.

Reiss, Y., J. L. Goldstein, M. C. Seabra, P. J. Casey, and M. S. Brown. 1990. 'Inhibition of purified p21ras farnesyl:protein transferase by Cys-AAX tetrapeptides', *Cell*, 62: 81-8.

Reyes-Turcu, Francisca E., and Keith D. Wilkinson. 2009. 'Polyubiquitin Binding and Disassembly By Deubiquitinating Enzymes', *Chemical Reviews*, 109: 1495-508.

Ridley, A. J. 2013. 'RhoA, RhoB and RhoC have different roles in cancer cell migration', *J Microsc*, 251: 242-9.

Robinson, R. A., X. Lu, E. Y. Jones, and C. Siebold. 2008. 'Biochemical and structural studies of ASPP proteins reveal differential binding to p53, p63, and p73', *Structure*, 16: 259-68.

Romanczuk, H., and P. M. Howley. 1992. 'Disruption of either the E1 or the E2 regulatory gene of human papillomavirus type 16 increases viral immortalization capacity', *Proc Natl Acad Sci U S A*, 89: 3159-63.

Ronchi, V. P., J. M. Klein, D. J. Edwards, and A. L. Haas. 2014. 'The active form of E6-associated protein (E6AP)/UBE3A ubiquitin ligase is an oligomer', *J Biol Chem*, 289: 1033-48.

Rose, R., M. Weyand, M. Lammers, T. Ishizaki, M. R. Ahmadian, and A. Wittinghofer. 2005. 'Structural and mechanistic insights into the interaction between Rho and mammalian Dia', *Nature*, 435: 513-8.

Rossman, Kent L., Channing J. Der, and John Sondek. 2005. 'GEF means go: turning on RHO GTPases with guanine nucleotide-exchange factors', *Nature Reviews Molecular Cell Biology*, 6: 167-80.

Rotin, Daniela, and Sharad Kumar. 2009. 'Physiological functions of the HECT family of ubiquitin ligases', *Nature Reviews Molecular Cell Biology*, 10: 398-409.

Rougeulle, C., H. Glatt, and M. Lalande. 1997. 'The Angelman syndrome candidate gene, UBE3A/E6-AP, is imprinted in brain', *Nat Genet*, 17: 14-5.

Rousseau, Adrien, and Anne Bertolotti. 2018. 'Regulation of proteasome assembly and activity in health and disease', *Nature Reviews Molecular Cell Biology*, 19: 697-712.

Runte, Maren, Alexander Hüttenhofer, Stephanie Groß, Martin Kiefmann, Bernhard Horsthemke, and Karin Buiting. 2001. 'The IC-SNURF–SNRPN transcript serves as a host for multiple small nucleolar RNA species and as an antisense RNA for UBE3A', *Human Molecular Genetics*, 10: 2687-700.

Sadikovic, B., P. Fernandes, V. W. Zhang, P. A. Ward, I. Miloslavskaya, W. Rhead, R. Rosenbaum, R. Gin, B. Roa, and P. Fang. 2014. 'Mutation Update for UBE3A variants in Angelman syndrome', *Hum Mutat*, 35: 1407-17.

Sahoo, T., C. A. Bacino, J. R. German, C. A. Shaw, L. M. Bird, V. Kimonis, I. Anselm, S. Waisbren, A. L. Beaudet, and S. U. Peters. 2007. 'Identification of novel deletions of 15q11q13 in Angelman syndrome by array-CGH: molecular characterization and genotype-phenotype correlations', *Eur J Hum Genet*, 15: 943-9.

Sailer, C., F. Offensperger, A. Julier, K. M. Kammer, R. Walker-Gray, M. G. Gold, M. Scheffner, and F. Stengel. 2018. 'Structural dynamics of the E6AP/UBE3A-E6-p53 enzyme-substrate complex', *Nat Commun*, 9: 4441.

Sakakibara, Nozomi, Ruchira Mitra, and Alison A. McBride. 2011. 'The Papillomavirus E1 Helicase Activates a Cellular DNA Damage Response in Viral Replication Foci', *Journal of Virology*, 85: 8981-95.

Samuels-Lev, Y., D. J. O'Connor, D. Bergamaschi, G. Trigiante, J. K. Hsieh, S. Zhong, I. Campargue, L. Naumovski, T. Crook, and X. Lu. 2001. 'ASPP proteins specifically stimulate the apoptotic function of p53', *Mol Cell*, 8: 781-94.

Sanders, C. M., and A. Stenlund. 1998. 'Recruitment and loading of the E1 initiator protein: an ATP-dependent process catalysed by a transcription factor', *Embo j*, 17: 7044-55.

Saric, T., C. I. Graef, and A. L. Goldberg. 2004. 'Pathway for degradation of peptides generated by proteasomes: a key role for thimet oligopeptidase and other metallopeptidases', *J Biol Chem*, 279: 46723-32.

Scheffner, M, J M Huibregtse, and P M Howley. 1994. 'Identification of a human ubiquitin-conjugating enzyme that mediates the E6-AP-dependent ubiquitination of p53', *Proceedings of the National Academy of Sciences*, 91: 8797-801.

Scheffner, M., J. M. Huibregtse, R. D. Vierstra, and P. M. Howley. 1993. 'The HPV-16 E6 and E6-AP complex functions as a ubiquitin-protein ligase in the ubiquitination of p53', *Cell*, 75: 495-505.

Scheffner, M., and S. Kumar. 2014. 'Mammalian HECT ubiquitin-protein ligases: biological and pathophysiological aspects', *Biochim Biophys Acta*, 1843: 61-74.

Scheffner, M., B. A. Werness, J. M. Huibregtse, A. J. Levine, and P. M. Howley. 1990. 'The E6 oncoprotein encoded by human papillomavirus types 16 and 18 promotes the degradation of p53', *Cell*, 63: 1129-36.

Scheffner, Martin, and Olivier Staub. 2007. 'HECT E3s and human disease', *BMC Biochemistry*, 8: S6.

Scherle, P., T. Behrens, and L. M. Staudt. 1993. 'Ly-GDI, a GDP-dissociation inhibitor of the RhoA GTP-binding protein, is expressed preferentially in lymphocytes', *Proc Natl Acad Sci U S A*, 90: 7568-72.

Schiffman, M., P. E. Castle, J. Jeronimo, A. C. Rodriguez, and S. Wacholder. 2007. 'Human papillomavirus and cervical cancer', *Lancet*, 370: 890-907.

Schmidt, S. I., M. Blaabjerg, K. Freude, and M. Meyer. 2022. 'RhoA Signaling in Neurodegenerative Diseases', *Cells*, 11.

Schreiner, P., X. Chen, K. Husnjak, L. Randles, N. Zhang, S. Elsasser, D. Finley, I. Dikic, K. J. Walters, and M. Groll. 2008. 'Ubiquitin docking at the proteasome through a novel pleckstrin-homology domain interaction', *Nature*, 453: 548-52.

Schwarz, E., U. K. Freese, L. Gissmann, W. Mayer, B. Roggenbuck, A. Stremlau, and H. zur Hausen. 1985. 'Structure and transcription of human papillomavirus sequences in cervical carcinoma cells', *Nature*, 314: 111-4.

Sedman, J., and A. Stenlund. 1998. 'The papillomavirus E1 protein forms a DNA-dependent hexameric complex with ATPase and DNA helicase activities', *J Virol*, 72: 6893-7.

Shaw, R. J., M. Henry, F. Solomon, and T. Jacks. 1998. 'RhoA-dependent phosphorylation and relocalization of ERM proteins into apical membrane/actin protrusions in fibroblasts', *Mol Biol Cell*, 9: 403-19.

Shutes, Adam, and Channing J. Der. 2004. 'Small GTPases.' in William J. Lennarz and M. Daniel Lane (eds.), *Encyclopedia of Biological Chemistry* (Elsevier: New York).

Snyder, J. T., D. K. Worthylake, K. L. Rossman, L. Betts, W. M. Pruitt, D. P. Siderovski, C. J. Der, and J. Sondek. 2002. 'Structural basis for the selective activation of Rho GTPases by Dbl exchange factors', *Nat Struct Biol*, 9: 468-75.

Soundararajan, M., and J. Eswaran. 2012. 'Atypical GTPases as drug targets', *Anticancer Agents Med Chem*, 12: 19-28.

Spratt, D. E., H. Walden, and G. S. Shaw. 2014. 'RBR E3 ubiquitin ligases: new structures, new insights, new questions', *The Biochemical journal*, 458: 421-37.

Srougi, Melissa C., and Keith Burridge. 2011. 'The Nuclear Guanine Nucleotide Exchange Factors Ect2 and Net1 Regulate RhoB-Mediated Cell Death after DNA Damage', *PLOS ONE*, 6: e17108.

Steger, G., and S. Corbach. 1997. 'Dose-dependent regulation of the early promoter of human papillomavirus type 18 by the viral E2 protein', *J Virol*, 71: 50-8.

Stevaux, O., and N. J. Dyson. 2002. 'A revised picture of the E2F transcriptional network and RB function', *Curr Opin Cell Biol*, 14: 684-91.

Stewart, Mikaela D., Tobias Ritterhoff, Rachel E. Klevit, and Peter S. Brzovic. 2016. 'E2 enzymes: more than just middle men', *Cell Research*, 26: 423-40.

Sullivan, A., and X. Lu. 2007. 'ASPP: a new family of oncogenes and tumour suppressor genes', *Br J Cancer*, 96: 196-200.

Suraweera, A., C. Münch, A. Hanssum, and A. Bertolotti. 2012. 'Failure of amino acid homeostasis causes cell death following proteasome inhibition', *Mol Cell*, 48: 242-53.

Sutcliffe, J. S., Y. H. Jiang, R. J. Galijaard, T. Matsuura, P. Fang, T. Kubota, S. L. Christian, J. Bressler, B. Cattanach, D. H. Ledbetter, and A. L. Beaudet. 1997. 'The E6-Ap ubiquitin-protein ligase (UBE3A) gene is localized within a narrowed Angelman syndrome critical region', *Genome Res*, 7: 368-77.

Svensmark, Julius H., and Cord Brakebusch. 2019. 'Rho GTPases in cancer: friend or foe?', *Oncogene*, 38: 7447-56.

Swaney, Danielle L, Ricard A Rodríguez-Mias, and Judit Villén. 2015. 'Phosphorylation of ubiquitin at Ser65 affects its polymerization, targets, and proteome-wide turnover', *EMBO reports*, 16: 1131-44.

Swatek, Kirby N., and David Komander. 2016. 'Ubiquitin modifications', *Cell Research*, 26: 399-422.

Taherbhoy, A. M., B. A. Schulman, and S. E. Kaiser. 2012. 'Ubiquitin-like modifiers', *Essays Biochem*, 52: 51-63.

Takai, Y., K. Kaibuchi, A. Kikuchi, T. Sasaki, and H. Shirataki. 1993. 'Regulators of small GTPases', *Ciba Found Symp*, 176: 128-38; discussion 38-46.

Talis, A. L., J. M. Huibregtse, and P. M. Howley. 1998. 'The role of E6AP in the regulation of p53 protein levels in human papillomavirus (HPV)-positive and HPV-negative cells', *J Biol Chem*, 273: 6439-45.

Taylor, J. S., T. S. Reid, K. L. Terry, P. J. Casey, and L. S. Beese. 2003. 'Structure of mammalian protein geranylgeranyltransferase type-I', *Embo j*, 22: 5963-74.

Thomas, Miranda, Michael P. Myers, Paola Massimi, Corrado Guarnaccia, and Lawrence Banks. 2016. 'Analysis of Multiple HPV E6 PDZ Interactions Defines Type-Specific PDZ Fingerprints That Predict Oncogenic Potential', *PLOS Pathogens*, 12: e1005766.

Tkachenko, E., M. Sabouri-Ghomi, O. Pertz, C. Kim, E. Gutierrez, M. Machacek, A. Groisman, G. Danuser, and M. H. Ginsberg. 2011. 'Protein kinase A governs a RhoA-RhoGDI protrusion-retraction pacemaker in migrating cells', *Nat Cell Biol*, 13: 660-7.

Tnimov, Zakir, Zhong Guo, Yann Gambin, Uyen T. T. Nguyen, Yao-Wen Wu, Daniel Abankwa, Anouk Stigter, Brett M. Collins, Herbert Waldmann, Roger S. Goody, and Kirill Alexandrov. 2012. 'Quantitative Analysis of Prenylated RhoA Interaction with Its Chaperone, RhoGDI *', *Journal of Biological Chemistry*, 287: 26549-62.

Tomaic, V., D. Pim, M. Thomas, P. Massimi, M. P. Myers, and L. Banks. 2011. 'Regulation of the human papillomavirus type 18 E6/E6AP ubiquitin ligase complex by the HECT domain-containing protein EDD', *J Virol*, 85: 3120-7.

Ueda, T., A. Kikuchi, N. Ohga, J. Yamamoto, and Y. Takai. 1990. 'Purification and characterization from bovine brain cytosol of a novel regulatory protein inhibiting the dissociation of GDP from and the subsequent binding of GTP to rhoB p20, a ras p21-like GTP-binding protein', *J Biol Chem*, 265: 9373-80.

Uehata, Masayoshi, Toshimasa Ishizaki, Hiroyuki Satoh, Takashi Ono, Toshio Kawahara, Tamami Morishita, Hiroki Tamakawa, Keiji Yamagami, Jun Inui, Midori Maekawa, and Shuh Narumiya. 1997. 'Calcium sensitization of smooth muscle mediated by a Rho-associated protein kinase in hypertension', *Nature*, 389: 990-94.

Urraca, N., K. Hope, A. K. Victor, T. G. Belgard, R. Memon, S. Goorha, C. Valdez, Q. T. Tran, S. Sanchez, J. Ramirez, M. Donaldson, D. Bridges, and L. T. Reiter. 2018. 'Significant transcriptional changes in 15q duplication but not Angelman syndrome deletion stem cell-derived neurons', *Mol Autism*, 9: 6.

van Buul, J. D., D. Geerts, and S. Huveneers. 2014. 'Rho GAPs and GEFs: controling switches in endothelial cell adhesion', *Cell Adh Migr*, 8: 108-24.

Varadi, Mihaly, Stephen Anyango, Mandar Deshpande, Sreenath Nair, Cindy Natassia, Galabina Yordanova, David Yuan, Oana Stroe, Gemma Wood, Agata Laydon, Augustin Žídek, Tim Green, Kathryn Tunyasuvunakool, Stig Petersen, John Jumper, Ellen Clancy, Richard Green, Ankur Vora, Mira Lutfi, Michael Figurnov, Andrew Cowie, Nicole Hobbs, Pushmeet Kohli, Gerard Kleywegt, Ewan Birney, Demis Hassabis, and Sameer Velankar. 2021. 'AlphaFold Protein Structure Database: massively expanding the structural coverage of protein-sequence space with high-accuracy models', *Nucleic Acids Research*, 50: D439-D44.

Vega, F. M., and A. J. Ridley. 2008. 'Rho GTPases in cancer cell biology', *FEBS Lett*, 582: 2093-101.

Velázquez-Campoy, Adrián, Hiroyasu Ohtaka, Azin Nezami, Salman Muzammil, and Ernesto Freire. 2004. 'Isothermal Titration Calorimetry', *Current Protocols in Cell Biology*, 23: 17.8.1-17.8.24.

Venuti, A., F. Paolini, L. Nasir, A. Corteggio, S. Roperto, M. S. Campo, and G. Borzacchiello. 2011. 'Papillomavirus E5: the smallest oncoprotein with many functions', *Mol Cancer*, 10: 140.

Verma, R., L. Aravind, R. Oania, W. H. McDonald, J. R. Yates, 3rd, E. V. Koonin, and R. J. Deshaies. 2002. 'Role of Rpn11 metalloprotease in deubiquitination and degradation by the 26S proteasome', *Science*, 298: 611-5.

Vetter, Ingrid R., and Alfred Wittinghofer. 2001. 'The Guanine Nucleotide-Binding Switch in Three Dimensions', *Science*, 294: 1299-304.

Vijay-Kumar, S., C. E. Bugg, and W. J. Cook. 1987. 'Structure of ubiquitin refined at 1.8 A resolution', *J Mol Biol*, 194: 531-44.

Vousden, K. H., and C. Prives. 2009. 'Blinded by the Light: The Growing Complexity of p53', *Cell*, 137: 413-31.

Walboomers, J. M., M. V. Jacobs, M. M. Manos, F. X. Bosch, J. A. Kummer, K. V. Shah, P. J. Snijders, J. Peto, C. J. Meijer, and N. Muñoz. 1999. 'Human papillomavirus is a necessary cause of invasive cervical cancer worldwide', *J Pathol*, 189: 12-9.

Walz, J., A. Erdmann, M. Kania, D. Typke, A. J. Koster, and W. Baumeister. 1998. '26S proteasome structure revealed by three-dimensional electron microscopy', *J Struct Biol*, 121: 19-29.

Wang, De-An, and Said M. Sebti. 2005. 'Palmitoylated Cysteine 192 Is Required for RhoB Tumor-suppressive and Apoptotic Activities*', *Journal of Biological Chemistry*, 280: 19243-49.

Wang, H. R., Y. Zhang, B. Ozdamar, A. A. Ogunjimi, E. Alexandrova, G. H. Thomsen, and J. L. Wrana. 2003. 'Regulation of cell polarity and protrusion formation by targeting RhoA for degradation', *Science*, 302: 1775-9.

Wang, M., L. Guo, Q. Wu, T. Zeng, Q. Lin, Y. Qiao, Q. Wang, M. Liu, X. Zhang, L. Ren, S. Zhang, Y. Pei, Z. Yin, F. Ding, and H. R. Wang. 2014. 'ATR/Chk1/Smurf1 pathway determines cell fate after DNA damage by controlling RhoB abundance', *Nat Commun*, 5: 4901.

Wang, Min, and Cecile M Pickart. 2005. 'Different HECT domain ubiquitin ligases employ distinct mechanisms of polyubiquitin chain synthesis', *The EMBO Journal*, 24: 4324-33.

Ward, Carl C., Jordan I. Kleinman, and Daniel K. Nomura. 2017. 'NHS-Esters As Versatile Reactivity-Based Probes for Mapping Proteome-Wide Ligandable Hotspots', *ACS Chemical Biology*, 12: 1478-83.

Watanabe, Naoki, Takayuki Kato, Akiko Fujita, Toshimasa Ishizaki, and Shuh Narumiya. 1999. 'Cooperation between mDia1 and ROCK in Rho-induced actin reorganization', *Nature Cell Biology*, 1: 136-43.

Wauer, Tobias, Kirby N Swatek, Jane L Wagstaff, Christina Gladkova, Jonathan N Pruneda, Martin A Michel, Malte Gersch, Christopher M Johnson, Stefan MV Freund, and David Komander. 2015. 'Ubiquitin Ser65 phosphorylation affects ubiquitin structure, chain assembly and hydrolysis', *The EMBO Journal*, 34: 307-25.

Webb, G. C., R. T. Baker, M. Coggan, and P. G. Board. 1994. 'Localization of the human UBA52 ubiquitin fusion gene to chromosome band 19p13.1-p12', *Genomics*, 19: 567-9.

Wei, J., R. K. Mialki, S. Dong, A. Khoo, R. K. Mallampalli, Y. Zhao, and J. Zhao. 2013. 'A new mechanism of RhoA ubiquitination and degradation: roles of SCF(FBXL19) E3 ligase and Erk2', *Biochim Biophys Acta*, 1833: 2757-64.

Wei, Yunyi, Yan Zhang, Urszula Derewenda, Xiaopu Liu, Wladek Minor, Robert K. Nakamoto, Avril V. Somlyo, Andrew P. Somlyo, and Zygmunt S. Derewenda. 1997. 'Crystal structure of RhoA–GDP and its functional implications', *Nature Structural Biology*, 4: 699-703.

Wennerberg, Krister, and Channing J. Der. 2004. 'Rho-family GTPases: it's not only Rac and Rho (and I like it)', *Journal of Cell Science*, 117: 1301-12.

Wevrick, R., and U. Francke. 1996. 'Diagnostic test for the Prader-Willi syndrome by SNRPN expression in blood', *Lancet*, 348: 1068-9.

Wheeler, A. P., and A. J. Ridley. 2004. 'Why three Rho proteins? RhoA, RhoB, RhoC, and cell motility', *Exp Cell Res*, 301: 43-9.

White, E. A., R. E. Kramer, M. J. Tan, S. D. Hayes, J. W. Harper, and P. M. Howley. 2012. 'Comprehensive analysis of host cellular interactions with human papillomavirus E6 proteins identifies new E6 binding partners and reflects viral diversity', *J Virol*, 86: 13174-86.

Wiborg, O., M. S. Pedersen, A. Wind, L. E. Berglund, K. A. Marcker, and J. Vuust. 1985. 'The human ubiquitin multigene family: some genes contain multiple directly repeated ubiquitin coding sequences', *Embo j*, 4: 755-9.

Wickliffe, K., A. Williamson, L. Jin, and M. Rape. 2009. 'The multiple layers of ubiquitin-dependent cell cycle control', *Chem Rev*, 109: 1537-48.

Williams, R. S., J. S. Williams, and J. A. Tainer. 2007. 'Mre11-Rad50-Nbs1 is a keystone complex connecting DNA repair machinery, double-strand break signaling, and the chromatin template', *Biochem Cell Biol*, 85: 509-20.

Winget, Jason M., and Thibault Mayor. 2010. 'The Diversity of Ubiquitin Recognition: Hot Spots and Varied Specificity', *Molecular Cell*, 38: 627-35.

Wittinghofer, A., and I. R. Vetter. 2011. 'Structure-function relationships of the G domain, a canonical switch motif', *Annu Rev Biochem*, 80: 943-71.

Wu, Zizhen, Huifang Liu, Weilin Sun, Yingxin Du, Wenting He, Shiwei Guo, Liqiao Chen, Zhenzhen Zhao, Pengliang Wang, Han Liang, and Jingyu Deng. 2020. 'RNF180 mediates STAT3 activity by regulating the expression of RhoC via the proteasomal pathway in gastric cancer cells', *Cell Death & Disease*, 11: 881.

Xu, Y., Y. Feng, Z. Sun, and Q. Li. 2021. 'RNF168 promotes RHOC degradation by ubiquitination to restrain gastric cancer progression via decreasing HDAC1 expression', *Biochem Biophys Res Commun*, 557: 135-42.

Yamamoto, Y., J. M. Huibregtse, and P. M. Howley. 1997. 'The human E6-AP gene (UBE3A) encodes three potential protein isoforms generated by differential splicing', *Genomics*, 41: 263-6.

Yang, J. P., M. Hori, T. Sanda, and T. Okamoto. 1999. 'Identification of a novel inhibitor of nuclear factor-kappaB, RelA-associated inhibitor', *J Biol Chem*, 274: 15662-70.

Yang, Quan, Jinyao Zhao, Dan Chen, and Yang Wang. 2021. 'E3 ubiquitin ligases: styles, structures and functions', *Molecular Biomedicine*, 2: 23.

Ye, Yihong, and Michael Rape. 2009. 'Building ubiquitin chains: E2 enzymes at work', *Nature Reviews Molecular Cell Biology*, 10: 755-64.

Yi, J. J., J. Berrios, J. M. Newbern, W. D. Snider, B. D. Philpot, K. M. Hahn, and M. J. Zylka. 2015. 'An Autism-Linked Mutation Disables Phosphorylation Control of UBE3A', *Cell*, 162: 795-807.

Yokoyama, K., G. W. Goodwin, F. Ghomashchi, J. A. Glomset, and M. H. Gelb. 1991. 'A protein geranylgeranyltransferase from bovine brain: implications for protein prenylation specificity', *Proc Natl Acad Sci U S A*, 88: 5302-6.

Yuan, W. C., Y. R. Lee, S. Y. Lin, L. Y. Chang, Y. P. Tan, C. C. Hung, J. C. Kuo, C. H. Liu, M. Y. Lin, M. Xu, Z. J. Chen, and R. H. Chen. 2014. 'K33-Linked Polyubiquitination of Coronin 7 by Cul3-KLHL20 Ubiquitin E3 Ligase Regulates Protein Trafficking', *Mol Cell*, 54: 586-600.

Zaaroor-Regev, D., P. de Bie, M. Scheffner, T. Noy, R. Shemer, M. Heled, I. Stein, E. Pikarsky, and A. Ciechanover. 2010. 'Regulation of the polycomb protein Ring1B by self-ubiquitination or by E6-AP may have implications to the pathogenesis of Angelman syndrome', *Proc Natl Acad Sci U S A*, 107: 6788-93.

Zalcman, G., V. Closson, G. Linarès-Cruz, F. Lerebours, N. Honoré, A. Tavitian, and B. Olofsson. 1995. 'Regulation of Ras-related RhoB protein expression during the cell cycle', *Oncogene*, 10: 1935-45.

Zalcman, Gérard, Violaine Closson, Jacques Camonis, Nicole Honoré, Marie-Françoise Rousseau-Merck, Armand Tavitian, and Birgitta Olofsson. 1996. 'RhoGDI-3 Is a New GDP Dissociation Inhibitor (GDI): IDENTIFICATION OF A NON-CYTOSOLIC GDI

PROTEIN INTERACTING WITH THE SMALL GTP-BINDING PROTEINS RhoB AND RhoG*', *Journal of Biological Chemistry*, 271: 30366-74.

Zanella, S., M. Barthelemy, F. Muscatelli, and G. Hilaire. 2008. 'Necdin gene, respiratory disturbances and Prader-Willi syndrome', *Adv Exp Med Biol*, 605: 159-64.

Zanier, K., S. Charbonnier, A. O. Sidi, A. G. McEwen, M. G. Ferrario, P. Poussin-Courmontagne, V. Cura, N. Brimer, K. O. Babah, T. Ansari, I. Muller, R. H. Stote, J. Cavarelli, S. Vande Pol, and G. Travé. 2013. 'Structural basis for hijacking of cellular LxxLL motifs by papillomavirus E6 oncoproteins', *Science*, 339: 694-8.

Zaoui, Kossay, and Stéphanie Duhamel. 2023. 'RhoB as a tumor suppressor: It's all about localization', *European Journal of Cell Biology*, 102: 151313.

Zhang, B., W. Chen, and A. Roman. 2006. 'The E7 proteins of low- and high-risk human papillomaviruses share the ability to target the pRB family member p130 for degradation', *Proc Natl Acad Sci U S A*, 103: 437-42.

Zhang, B., Y. Zhang, Z. Wang, and Y. Zheng. 2000. 'The role of Mg2+ cofactor in the guanine nucleotide exchange and GTP hydrolysis reactions of Rho family GTP-binding proteins', *J Biol Chem*, 275: 25299-307.

Zhang, F. L., and P. J. Casey. 1996. 'Protein prenylation: molecular mechanisms and functional consequences', *Annu Rev Biochem*, 65: 241-69.

Zhao, Xudong, Julian Ik-Tsen Heng, Daniele Guardavaccaro, Richeng Jiang, Michele Pagano, Francois Guillemot, Antonio Iavarone, and Anna Lasorella. 2008. 'The HECT-domain ubiquitin ligase Huwe1 controls neural differentiation and proliferation by destabilizing the N-Myc oncoprotein', *Nature Cell Biology*, 10: 643-53.

zur Hausen, H. 2002. 'Papillomaviruses and cancer: from basic studies to clinical application', *Nat Rev Cancer*, 2: 342-50.

7. Supplementary Data

7.1 Supplementary figures

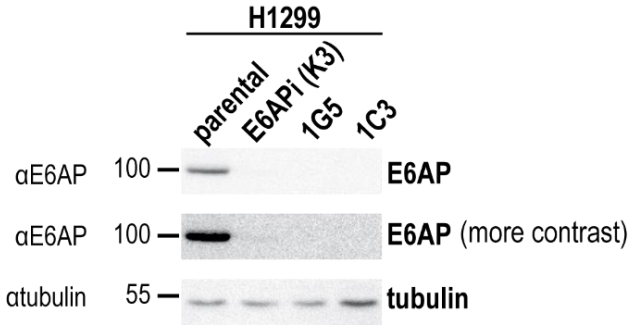

Supplementary Figure 1. Endogenous E6AP levels in different H1299 cell lines. The lysates of parental H1299, H1299 E6APi (stable RNAi-mediated knockdown of E6AP) and two different cell lines with a CRISPR/Cas9-mediated knockout of E6AP (1G5, 1C3), were analysed regarding their endogenous E6AP levels. The lysates were subjected to a BCA to determine the total amount of protein present and adjusted accordingly to load equal amounts of protein of each cell line. The samples were analysed by SDS-PAGE followed by western blotting and E6AP levels were determined using an αE6AP antibody. The membranes were stripped and blotted against αtubulin. In the E6AP blot with higher contrast, some remaining E6AP can be detected in the E6APi cell line.

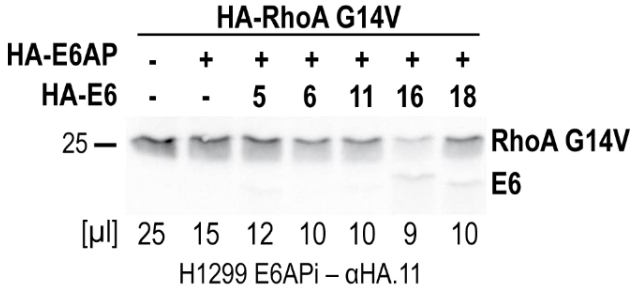

Supplementary Figure 2. RhoA is only degraded in presence of the high-risk HPV type 16 E6 protein. H1299 E6APi cells (RNAi mediated knockdown of E6AP) were transfected with expression constructs encoding for HA-tagged RhoA G14V, E6AP, and the HPV E6 variants as indicated. 24 h post-transfection, the lysates were prepared and adjusted according to the transfection efficiency (β-galactosidase activity). Samples were analysed by SDS-PAGE followed by western blot analysis and proteins were detected using an αHA.11 antibody. The running positions of the molecular mass markers (in kDa), the HA-tagged proteins, and the amount of lysate loaded of each sample (25 µl of the sample with the lowest β-gal assay value) are indicated.

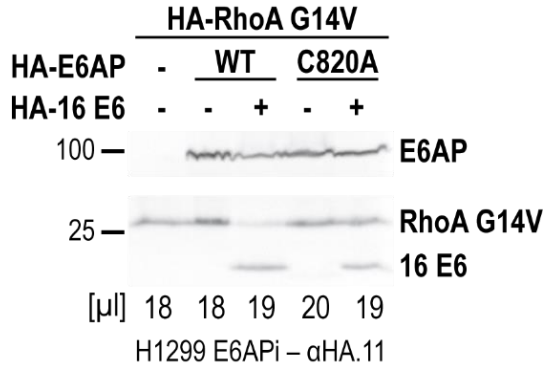

Supplementary Figure 3. The degradation of ectopic RhoA is dependent on a catalytically active E6AP. H1299 E6APi cells (RNAi mediated knockdown of E6AP) were transfected with expression constructs encoding for HA-tagged RhoA G14V, 16 E6, and E6AP variants as indicated. 24 h post-transfection, the lysates were prepared and adjusted according to the transfection efficiency (β-galactosidase activity). Samples were analysed by SDS-PAGE followed by western blot analysis and proteins were detected using an αHA.11 antibody. The running positions of the molecular mass markers (in kDa), the HA-tagged proteins, and the amount of lysate loaded of each sample (20 µl of the sample with the lowest β-gal assay value) are indicated. In presence of 16 E6 and the catalytically inactive E6AP (C820A), RhoA G14V levels remain stable, indicating that a functional E6AP is required for the degradation of RhoA G14V. The experiment was performed by Nadja Eulich, under my supervision.

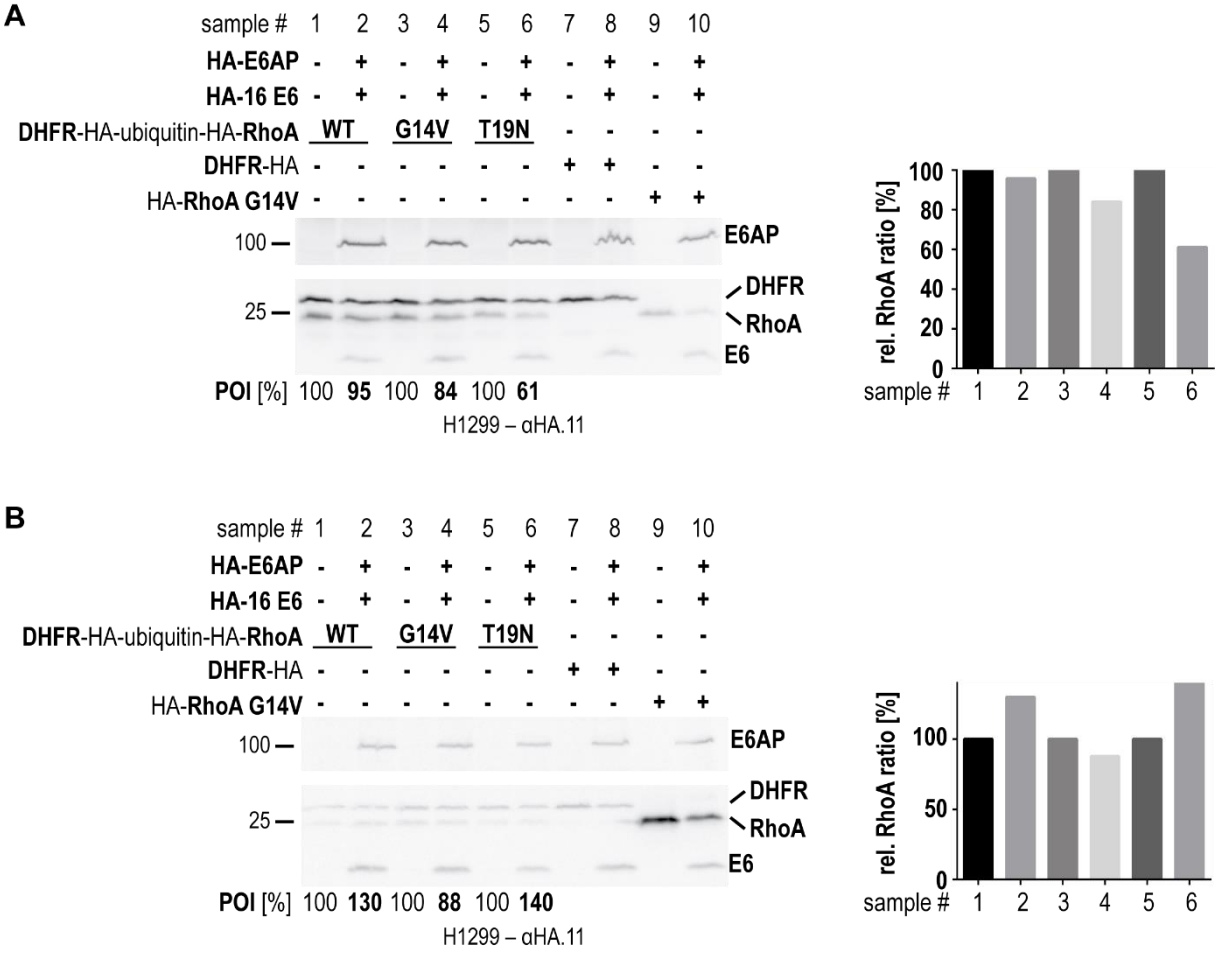

Supplementary Figure 4. The degradation of RhoA as part of a DHFR-ubiquitin fusion construct is impaired. A-B H1299 cells were transfected with expression constructs encoding for HA-tagged 16 E6 and E6AP, as well as DHFR-HA-ubiquitin fusion proteins of HA-RhoA variants as indicated. 24 h post-transfection, the lysates were prepared and 25 µl of each sample were analysed by SDS-PAGE and western blot. The proteins were detected using an αHA.11 antibody and the DHFR-HA-ubiquitin and HA-RhoA levels quantified. The relative ratio of the HA-RhoA variants to DHFR-HA-ubiquitin is indicated (POI [%]), with the ratio of HA-RhoA to DHFR-HA-ubiquitin in the absence of 16 E6-E6AP set to 100% for each RhoA variant. The running positions of the molecular mass markers (in kDa) and of the HA-tagged proteins are indicated. For better visualisation, the relative ratio is additionally displayed in the bar graph in the right panel. The experiments in **A** and **B** represent two independent transfection experiments to display the problem of the high variability between DHFR experiments. The experiment in **A** was performed by Nadja Eulich, under my supervision. The principle of the DHFR-fusion construct is described in (Kühnle et al. 2013). As running controls, DHFR-HA and HA-RhoA G14V were additionally transfected.

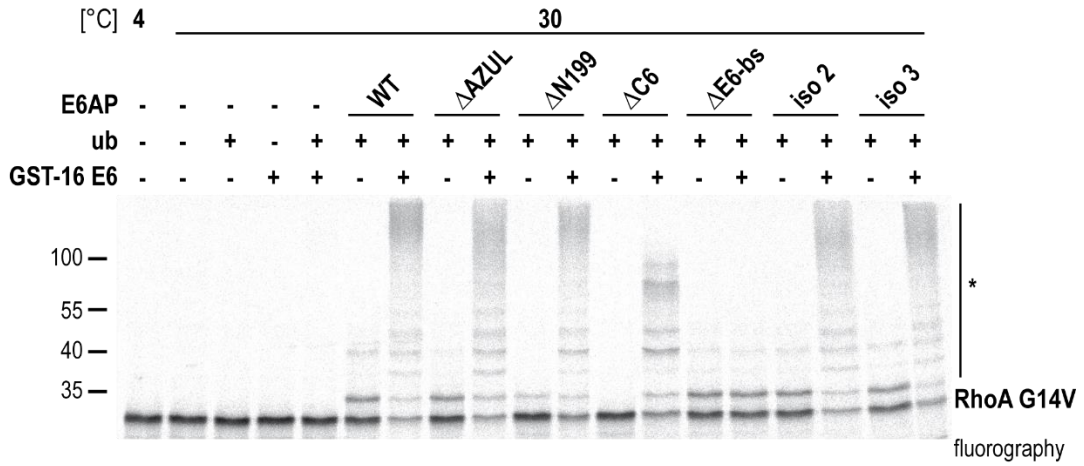

Supplementary Figure 5. RhoA G14V ubiquitination with E6AP mutants and isoforms. In wheat germ extract *in vitro* translated, radiolabelled RhoA G14V was incubated with UBA1 and UbcH7 in the presence and absence of GST-tagged 16 E6, ubiquitin (ub), and the bacterially expressed His-E6AP variants, for 90 min at 30°C as indicated. The reactions were stopped with Laemmli buffer (see 0) and the samples were analysed by SDS-PAGE followed by fluorography. The running positions of the molecular mass markers (in kDa), the unmodified forms (G14V), and the ubiquitinated RhoA G14V forms (*) are indicated. E6AP variants capable of ternary complex formation are able to catalyse RhoA G14V poly-ubiquitination in presence of GST-16 E6.

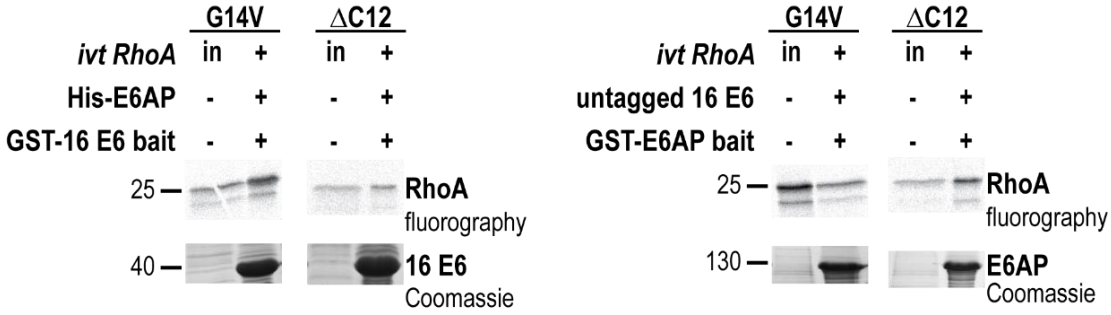

Supplementary Figure 6. The RhoA truncation ΔC12 is able to form ternary complexes. The GST-16 E6 (left panel) or the GST-E6AP (right panel) fusion proteins were incubated with *in vitro* translated, radiolabelled RhoA G14V or RhoA ΔC12 for 90 min at 4°C in the presence of either His-E6AP or untagged 16 E6 as indicated and in presence of 20 mM EDTA. Beads were washed after the binding reaction and the eluates were analysed by SDS-PAGE followed by Coomassie Blue staining (GST bait input detection, lower panel) and fluorography (binding reaction, upper panel). The running positions of the molecular mass markers (in kDa), the GST- fusion proteins, and the RhoA variants are indicated. in⎸ 10% of the RhoA used in the binding reaction. The experiment was performed by Sarah Lott, under my supervision.

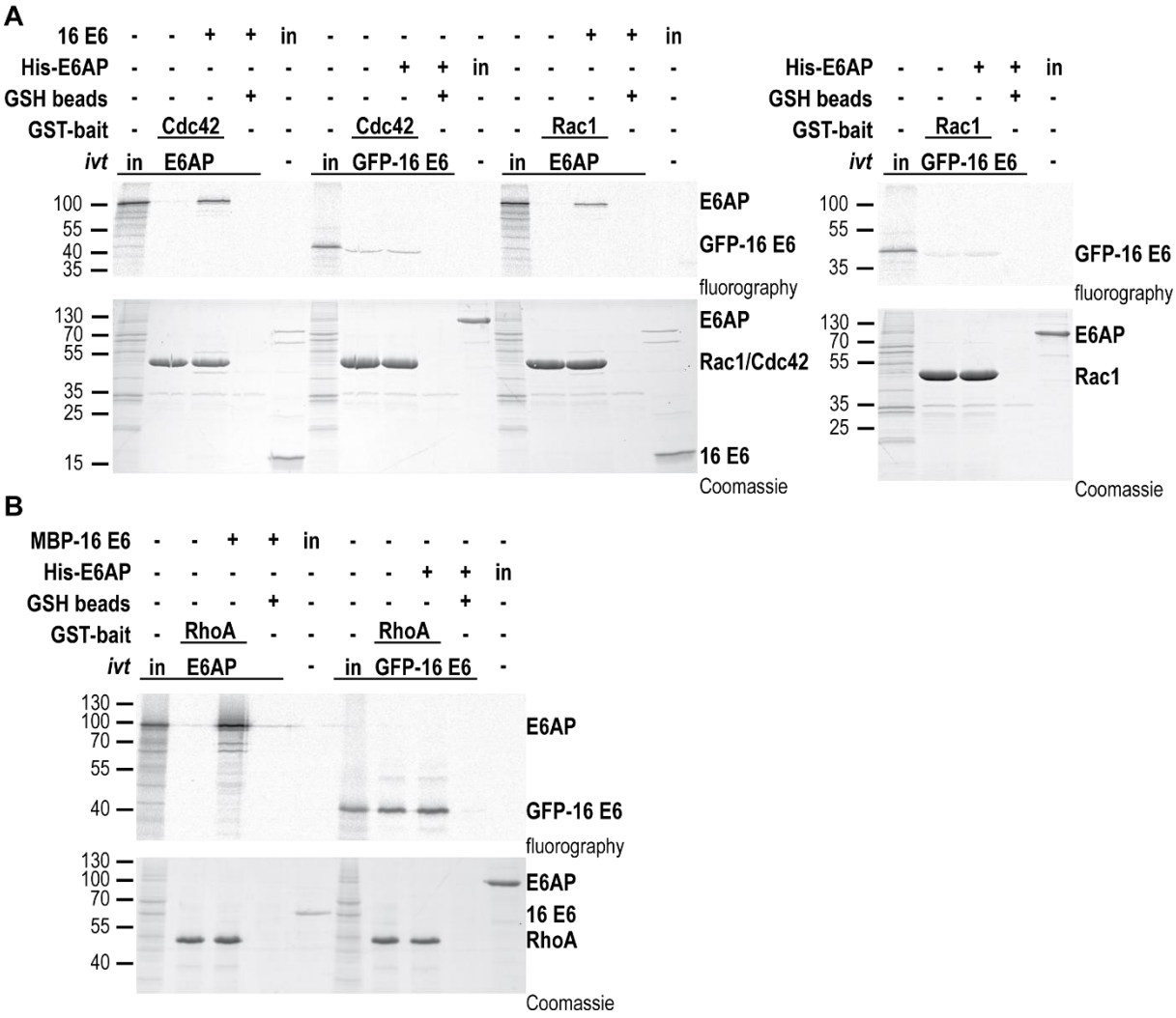

Supplementary Figure 7. The ternary complex formation of Rac1 and Cdc42 is impaired. A│ The GST-Rac1 or GST-Cdc42 fusion proteins or empty GSH beads were incubated with *in vitro* translated, radiolabelled E6AP or GFP-16 E6 for 90 min at 4°C in the presence of either untagged 16 E6 or His-E6AP as indicated and in presence of 20 mM EDTA. Beads were washed after the binding reaction and the eluates were analysed by SDS-PAGE followed by Coomassie Blue staining (GST bait input detection, lower panel) and fluorography (binding reaction, upper panel). The running positions of the molecular mass markers (in kDa), the GST-Rac1 or GST-Cdc42 fusion proteins, E6AP, and 16E6 are indicated. in│ 10% of the *in vitro* translated E6AP or GFP-16 E6 and 100% of the His-E6AP or untagged 16 E6 used in the binding reaction. **B**│ The GST-RhoA fusion protein or empty GSH beads were incubated with *in vitro* translated, radiolabelled E6AP or GFP-16 E6 for 90 min at 4°C in the presence of either MBP-16 E6 or His-E6AP as indicated and in presence of 20 mM EDTA. Beads were washed after the binding reaction and the eluates were analysed by SDS-PAGE followed by Coomassie Blue staining (GST bait input detection, lower panel) and fluorography (binding reaction, upper panel). The running positions of the molecular mass markers (in kDa), the GST-RhoA fusion protein, E6AP, and 16E6 are indicated. in│ 10% of the *in vitro* translated E6AP or GFP-16 E6 and 100% of the His-E6AP or MBP-16 E6 used in the binding reaction.

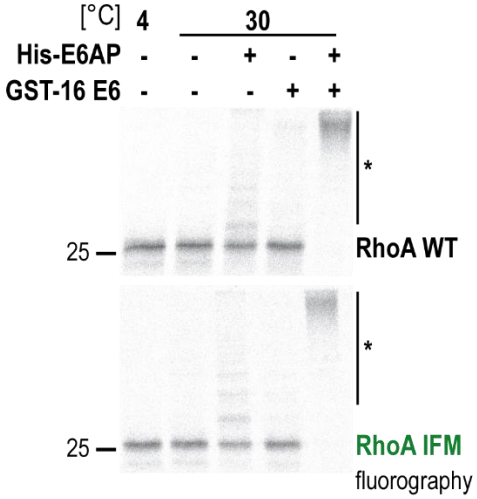

Supplementary Figure 8. The RhoA IFM is ubiquitinated like RhoA WT. *In vitro* translated, radiolabelled RhoA WT or the RhoA IFM was incubated with UBA1, UbcH7, and ubiquitin in the presence and absence of His-E6AP and GST-tagged 16 E6, for 90 min at 30°C as indicated. The reactions were stopped with Laemmli buffer (see 0) and the samples were analysed by SDS-PAGE followed by fluorography. The running positions of the molecular mass markers (in kDa), the unmodified forms (RhoA WT, RhoA IFM), and the ubiquitinated RhoA forms (*) are indicated.

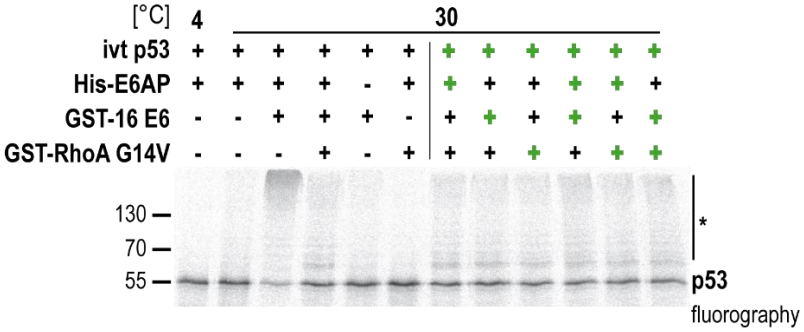

Supplementary Figure 9. p53 ubiquitination is inhibited independent of differential preincubation steps. *In vitro* translated, radiolabelled p53 was incubated with UBA1, UbcH7, and ubiquitin in the presence and absence of GST-tagged 16 E6, GST-tagged RhoA G14V, and His-E6AP for 90 min at 30°C as indicated. For each reaction, the components indicated in green were preincubated for 30 min on ice, prior to the addition of the remaining assay components. The reactions were stopped with Laemmli buffer (see 0) and the samples were analysed by SDS-PAGE followed by fluorography. The running positions of the molecular mass markers (in kDa), the unmodified forms (p53), and the ubiquitinated p53 forms (*) are indicated. GST-RhoA G14V is able to block the GST-16 E6 mediated stimulatory effect independent of any preincubation. The experiment was performed by Nadja Eulich, under my supervision.

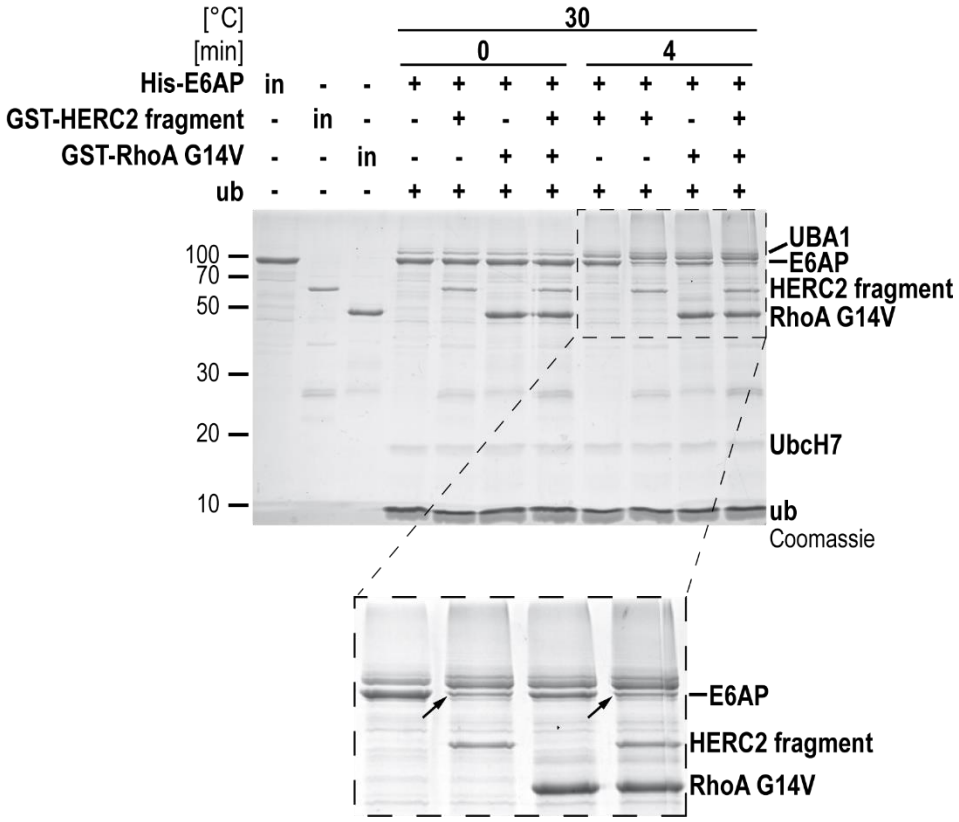

Supplementary Figure 10. HERC2-mediated stimulation of E6AP is not impaired by RhoA. His-tagged E6AP was incubated with UBA1, UbcH7, and ubiquitin (ub) in the presence and absence of GST-tagged RLD2 (HERC2 fragment: the isolated RLD2 domain of HERC2 is known to activates E6AP on its own (Kühnle et al. 2011)) and GST-tagged RhoA G14V at 30°C as indicated. The reactions were stopped at 0 min or 4 min with Laemmli buffer (see 0) and the samples were analysed by SDS-PAGE followed by Coomassie staining. The running positions of the molecular mass markers (in kDa) and of the different assay components are indicated. HERC2 stimulates E6AP autoubiquitination. The arrows in the enlarged sector mark the reduced E6AP levels, indicating that RhoA G14V has no effect on the HERC2-mediated stimulation of E6AP. The experiment was performed by Daniel Lingott, under my supervision.

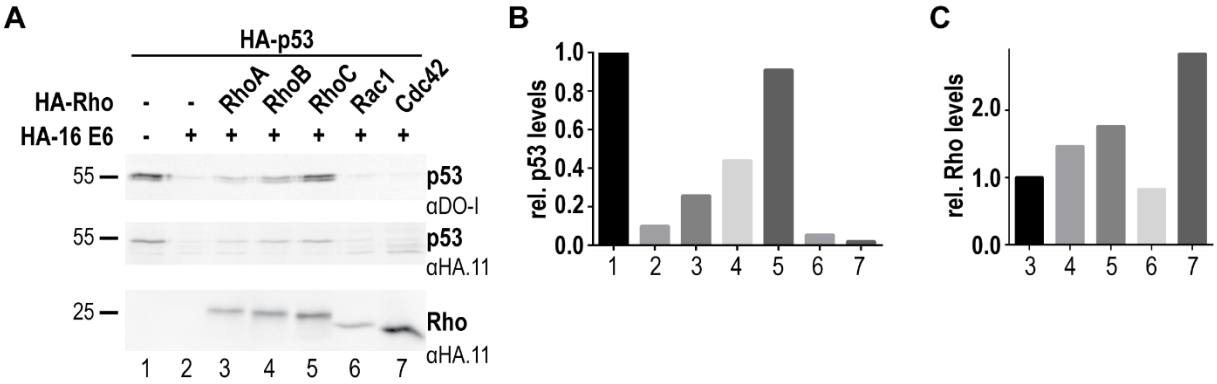

Supplementary Figure 11. The inhibitory effect on p53 degradation is restricted to RhoA family members. A| H1299 cells were transfected with expression constructs encoding for HA-tagged p53, 16 E6 and RhoA, RhoB, RhoC, Rac1, and Cdc42 as indicated. 24 h post-transfection, the lysates were prepared and adjusted according to the transfection efficiency (β-galactosidase activity). Samples were analysed by SDS-PAGE followed by western blot analysis and proteins were detected using an αHA.11 (Rho proteins and p53) and αDO-I (p53) antibody. The running positions of the molecular mass markers (in kDa) and the HA-tagged proteins are indicated. Levels of HA-16 E6 (200 ng) are too low for the detection via western blot. **B**| The quantification of the relative p53 levels was performed from the αDO-I blot. **C**| The quantification of the relative Rho levels was performed from the αHA.11 blot. In presence of Rac1 and Cdc42, the 16 E6-mediated degradation of p53 is unaffected.

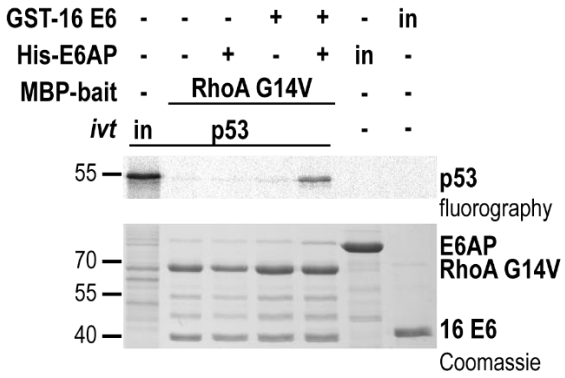

Supplementary Figure 12. MBP-RhoA is as efficient as GST-RhoA in the formation of the quaternary complex with p53. The MBP-RhoA G14V fusion protein bound to amylose beads was incubated with *in vitro* translated, radiolabelled p53 for 90 min at 4°C in the presence of His-E6AP and GST-tagged 16 E6 as indicated and 20 mM EDTA. Beads were washed after the binding reaction and the eluates were analysed by SDS-PAGE followed by Coomassie Blue staining (MBP bait input detection, lower panel) and fluorography (binding reaction, upper panel). The running positions of the molecular mass markers (in kDa), the MBP-RhoA G14V fusion protein, p53, E6AP, and 16 E6 are indicated. in| 10% of the p53 and 100% of the His-E6AP or GST-16 E6 used in the binding reaction.

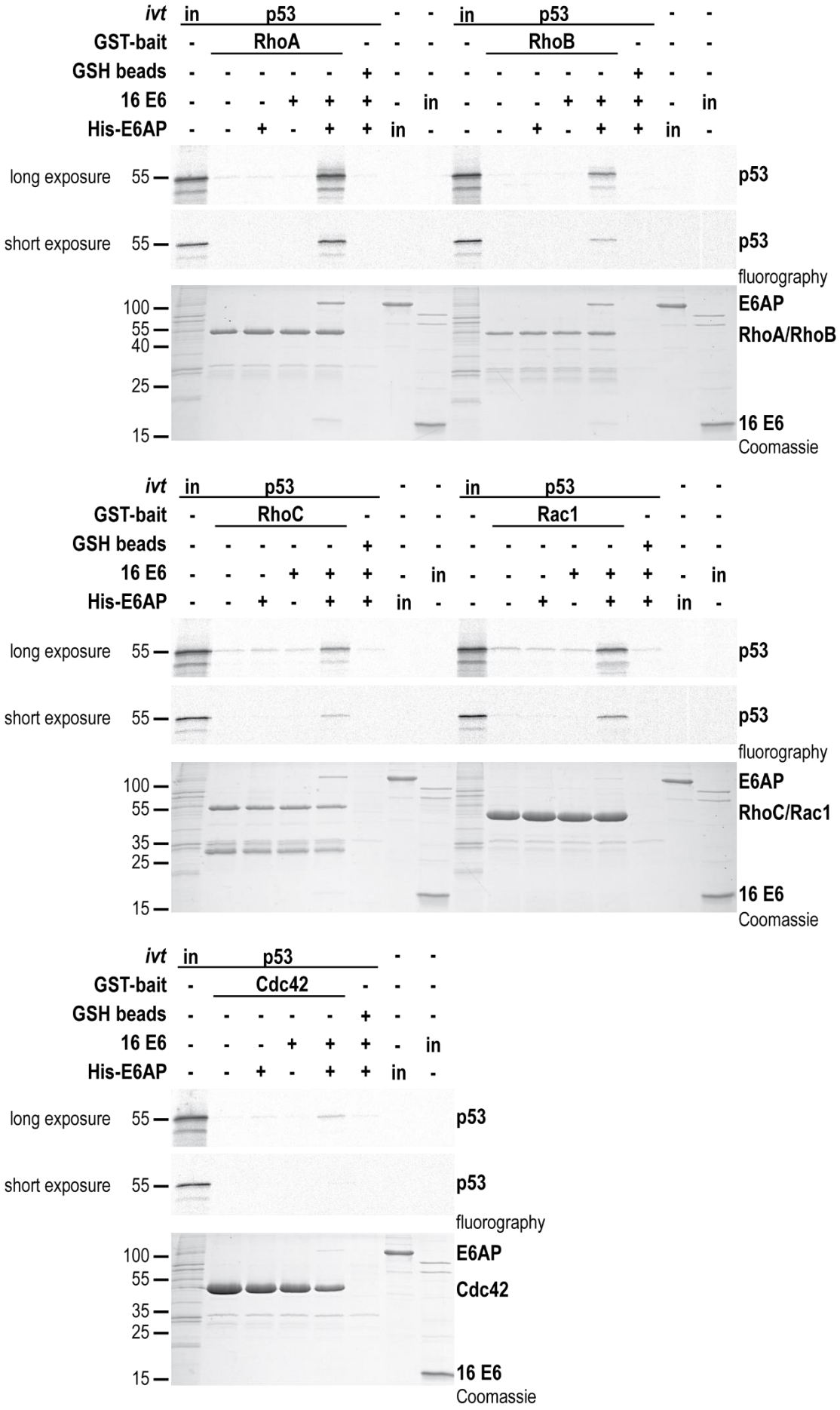
ivt in p53 - - in p53 - -
GST-bait - RhoA - - - - RhoB - - -
GSH beads - - - - - + - - - - - - - + - -
16 E6 - - - + + + - in - - - + + + - in
His-E6AP - - + - + + in - - - + - + + in -
long exposure 55
p53
short exposure 55
p53
fluorography
100
55
40
25
15
E6AP
RhoA/RhoB
16 E6
Coomassie
ivt in p53 - - in p53 - -
GST-bait - RhoC - - - - Rac1 - - -
GSH beads - - - - - + - - - - - - - + - -
16 E6 - - - + + + - in - - - + + + - in
His-E6AP - - + - + + in - - - + - + + in -
long exposure 55
p53
short exposure 55
p53
fluorography
100
55
35
25
15
E6AP
RhoC/Rac1
16 E6
Coomassie
ivt in p53 - -
GST-bait - Cdc42 - - -
GSH beads - - - - - + - -
16 E6 - - - + + + - in
His-E6AP - - + - + + in -
long exposure 55
p53
short exposure 55
p53
fluorography
100
55
35
25
15
E6AP
Cdc42
16 E6
Coomassie

Supplementary Figure 13. All tested Rho GTPases are able to form a quaternary complex with p53 to some extent. The GST-Rho fusion proteins or empty GSH beads were incubated with *in vitro* translated, radiolabelled p53 with 20 mM EDTA for 90 min at 4°C in the presence or absence of His-E6AP and untagged 16 E6 as indicated. Beads were washed after the binding reaction and the eluates were analysed by SDS-PAGE followed by Coomassie Blue staining (GST bait input detection, lower panel) and fluorography (binding reaction, upper panel). The running positions of the molecular mass markers (in kDa), the GST-fusion proteins, His-E6AP, and untagged 16E6 are indicated. in│ 10% of the p53 and 100% of the His-E6AP or untagged 16 E6 used in the binding reaction. All tested GTPases are able to form a quaternary complex with RhoA. However, the interaction is weaker with GST-Cdc42. In addition to the interaction with p53, the Coomassie readout shows that E6AP and 16 E6 have a higher affinity for members of the RhoA subfamily. Due to the differential amounts of GST-bait proteins, a quantitative analysis is not possible.

7.2 Raw data

Supplementary Table 1. Detailed results for the identified RhoA peptides with a diGly motif in replicate a. The sequence of the identified peptide, the number of found peptide spectrum matches (PSM), the position of the GG modification within the respective peptide and the position of the GG modification in RhoA are listed.

sample	Sequence	#PSM	Modifications	Position in RhoA
RhoA a_I	**HFCPNVPIILVGNKK**	**8**	**1xGG [K]**	**118 and 119**
	KLVIVGDGACGK	6	1xGG [K1]	7
	HFCPNVPIILVGNK	6	1xGG [K14]	118
RhoA a_II	**KLVIVGDGACGK**	**6**	**1xGG [K1]**	**7**
	HFCPNVPIILVGNK	5	1xGG [K14]	118
	HFCPNVPIILVGNKK	4	1xGG [K]	118 and 119
	MAAIRKK	4	1xGG [K]	6 and 7
RhoA a_III	**HFCPNVPIILVGNKK**	**9**	**1xGG [K]**	**118 and 119**
	MKQEPVKPEEGR	6	1xGG [K2]	135
	KLVIVGDGACGK	5	1xGG [K1]	7
	KKLVIVGDGACGK	3	1xGG [K]	6 and 7
	KKSGCLVL	3	1xGG [K]	186 and 187
RhoA a_IV	**HFCPNVPIILVGNKK**	**5**	**1xGG [K]**	**118 and 119**
	KLVIVGDGACGK	4	1xGG [K1]	7
RhoA a_V	**KLVIVGDGACGK**	**6**	**1xGG [K1]**	**7**
	MKQEPVKPEEGR	6	1xGG [K2]	135
	HFCPNVPIILVGNKK	4	1xGG [K]	118 and 119
	WTPEVKHFCPNVPIILVGNK	4	1xGG [K6]	104
RhoA a_VI	**MKQEPVKPEEGR**	**6**	**1xGG [K2]**	**135**
RhoA a_VII	**HFCPNVPIILVGNKK**	**2**	**1xGG [K]**	**118 and 119**
RhoA a_III	**KLVIVGDGACGK**	**3**	**1xGG [K1]**	**7**
	HFCPNVPIILVGNKK	2	1xGG [K14]	118 and 119

Supplementary Table 2. Detailed results for the identified RhoA peptides with a diGly motif in replicate b. The sequence of the identified peptide, the number of found peptide spectrum matches (PSM), the position of the GG modification within the respective peptide and the position of the GG modification in RhoA are listed.

sample	Sequence	#PSM	Modifications	Position in RhoA
RhoA b_I	**HFCPNVPIILVGNKK**	**5**	**1xGG [K]**	**118 and 119**
	HFCPNVPIILVGNK	3	1xGG [K14]	118
	KKLVIVGDGACGK	2	1xGG [K1]	6 and 7
RhoA b_II	**HFCPNVPIILVGNKK**	**4**	**1xGG [K]**	**118 and 119**
	HFCPNVPIILVGNK	4	1xGG [K14]	118
	KLVIVGDGACGK	3	1xGG [K1]	7
RhoA b_III	**HFCPNVPIILVGNKK**	**3**	**1xGG [K]**	**118 and 119**
	WTPEVKHFCPNVPIILVGNK	3	1xGG [K6]	104
	KSGCLVL	3	1xGG [K1]	187
	KKSGCLVL	3	1xGG [K]	186 and 187
RhoA b_IV	**KLVIVGDGACGK**	**4**	**1xGG [K1]**	**7**
	HFCPNVPIILVGNK	4	1xGG [K14]	118
	HFCPNVPIILVGNKK	2	1xGG [K15]	119
	IGAFGYMECSAK	2	1xGG [K12]	162
	QEPVKPEEGR	2	1xGG [K5]	140
RhoA b_V	**KKSGCLVL**	**3**	**1xGG [K2]**	**187**
	KSGCLVL	3	1xGG [K1]	186
	MKQEPVKPEEGR	3	1xGG [K]	135 and 140
RhoA b_VI	KKSGCLVL	2	2xGG [K1; K2]	**186 and 187**
	MKQEPVKPEEGR	2	1xGG [K2]	135
RhoA b_VII	**WTPEVKHFCPNVPIILVGNK**	**2**	**1xGG [K6]**	**104**
RhoA b_VIII	**DMANRIGAFGYMECSAKTK**	**4**	**1xGG [K]**	**162 and 164**

7.3 List of figures and supplementary figures

List of tables

8. Danksagung

Ich danke allen.